Biotransformations of fungal phytotoxins in plants and indolyl-3-acetaldoxime in fungi

A Thesis Submitted to the College

of Graduate Studies and Research

in Partial Fulfillment of the Requirements

for the Degree of Doctor of Philosophy

Department of Chemistry

University of Saskatchewan

Saskatoon

By

Iman Khallaf

© Copyright Iman Khallaf, April 2013. All rights reserved.

PERMISSION TO USE

In presenting this thesis in partial fulfillment of the requirements for a Postgraduate degree from the University of Saskatchewan, I agree that the Libraries of this University may make it freely available for inspection. I further agree that permission for copying of this thesis in any manner, in whole or in part, for scholarly purposes may be granted by the professor who supervised this thesis work, or in her absence, by the Head of the Department of Chemistry, or the Dean of the College of Graduate Studies and Research. It is understood that any copying, publication, or use of this thesis or parts thereof for financial gain shall not be allowed without my written permission. It is also understood that due recognition shall be given to me and to the University of Saskatchewan in any scholarly use which may be made of any material in my thesis.

Requests for permission to copy or to make other use of material in this thesis in whole or part should be addressed to:

The Head of the Department of Chemistry

University of Saskatchewan

Saskatoon, Saskatchewan, S7N 5C9

.

ABSTRACT

In the first part of this thesis the metabolism of the phytotoxins destruxin B (**1**) and sirodesmin PL (**13**) in crucifers and non-crucifers was studied using HPLC-ESI-MS^n. Destruxin B (**1**) and sirodesmin PL (**13**) are phytotoxins produced by the phytopathogenic fungi *Alternaria brassicae* (Berk.) Sacc. (causative agent of blackspot disease) and *Leptosphaeria maculans* (Desm) Ces. et de Not.[asexual stage *Phoma lingam* (Tode ex Fr) Desm.] (causative agent of blackleg disease). Five cruciferous species were used in this study: *Arabidopsis thaliana* L., *Brassica rapa* L., *B. napus* L., *Thellungiella salsuginea* Pallas and *Erucastrum gallicum* O.E. Schulz. In addition, the cereals *Avena sativa* L. and *Triticum aestivum* L. were studied similarly. Destruxin B (**1**) was metabolized by all crucifers to hydroxydestruxin B (**32**), a transformation similar to previously reported reactions in other crucifers. In addition, destruxin B (**1**) elicited production of phytoalexins in *A. thaliana*, *T. salsuginea* and *E. gallicum*, while no phytoalexins were detected in case of *B. rapa* and *B. napus*. In cereals destruxin B (**1**) was transformed differently. Several metabolites were detected and identified by HPLC-ESI-MS^n analyses: hydroxydestruxin B (**32**), two isomers of dehydrodestruxin B (**178**, **179**) and desmethyldestruxin B (**180**). On the other hand, no metabolites related to transformation of sirodesmin PL (**13**) were detected in crucifers; however, in cereals sirodesmin PL (**13**) was transformed to deacetylsirodesmin PL (**14**). In all crucifers sirodesmin PL (**13**) was found to be a stronger elicitor of phytoalexin production than destruxin B (**1**).

In the second part of this thesis, mycelia from different pathogenic fungi were screened for indolyl-3-acetaldoxime dehydratase. *L. maculans* isolate Laird 2 was chosen for isolation, characterization and substrate specificity of aldoxime dehydratase, as it showed the highest specific activity among the tested pathogens. The enzyme was partially purified using three chromatographic steps. It showed Michaelis–Menten kinetics and an apparent molecular mass of about 40 kDa. Based on its substrate specificity, the enzyme appears to be an indolyl-3-acetaldoxime dehydratase.

ACKNOWLEDGEMENTS

First, I would like to express my sincere gratitude to my supervisor, Professor M. Soledade C. Pedras, Department of Chemistry, University of Saskatchewan for her excellent guidance and continuous support throughout the program.

I am also grateful to the members of my Advisory Committee members: Prof. M. Majewski and Dr. D. Sanders, Department of Chemistry, University of Saskatchewan and Prof. R. Chibbar, Department of Plant Sciences, University of Saskatchewan. Their valuable advice and help during my Ph.D. work is greatly acknowledged. I also thank my external examiner, Dr. D. Y. Suh, Department of Biochemistry, University of Regina, for his review of my thesis, suggestion and advice.

I would like to acknowledge the support and encouragement from all past and present members of Prof. Pedras group: Dr. Z. Minic, Dr. A. Adio, Dr. A. Vogt, Dr. P. B. Chumala, Dr. Q-A. Zheng, Dr. O. Okeola, Dr. D. Okinyo, Dr. P. Saha, Dr. P. D. Thongbam, Dr. V. K. Sarma-Mamillapalle, Dr. Y. Yu, Dr. S. Hossain, Dr. M. Hossain, Dr. Md. G. Sarwar and my fellow graduate students E. Yaya, A. Abdoli, M. R. Park, T. Chintamani and M. Alavi.

I would like to thank Egyptian Government and University of Saskatchewan for their financial support.

Finally, I would like to thank my parents and sisters for their support, constant encouragement and patience.

DEDICATION

To my parents

TABLE OF CONTENTS

LIST OF FIGURES

LIST OF SCHEME

LIST OF TABLES

LIST OF ABBREVIATIONS

ABA	abscisic acid
A. brassicae	*Alternaria brassicae*
A. brassicicola	*Alternaria brassicicola*
Ac	acetyl
Ac_2O	acetic anhydride
AcOH	acetic acid
ADON	acetyl nivalenol
A. denitrificans	*Alcaligenes denitrificans*
Ala	alanine
A. niger	*Aspergillus niger*
Arg	arginine
A. sativa	*Avena sativa*
Asp	asparagine
A. thaliana	*Arabidopsis thaliana*
B.	*Brassica*
Ben	benzyl
br	broad
Butt	2,3-butanedione
BSA	bovine serum albumin
calc.	calculated
C. carbonum	*Cochliobolus carbonum*
C. bursa-pastoris	*Capsella bursa-pastoris*
CFE	cell-free extract
CHAPS	3-[(3-cholamidopropyl)dimethylammonium]-1-propanesulfonate
CHAPSO	3-[(3-cholamidopropyl)dimethylammonium]-2-hydroxy-1-propanesulfonate
CID	collision-induced dissociation
C. lemon	*Citrus lemon*
C4H	4-hydroxycinnamic acid hydroxylase
^{13}C NMR	carbon-13 nuclear magnetic resonance
C. rosea	*Clonostachy rosea*
C. sativa	*Camelina sativa*
C. sinensis	*Citrus sinensis*
Cys	cysteine
Da	Dalton
DBH	destruxin B hydroxylase
DEAE-Sephacel	diethylaminoethyl-Sephacel
DIBAL-H	diisobutylaluminium hydride
DMF	dimethylformamide
DMSO	dimethylsulfoxide
DON	4-deoxynivalenol
DOGT1	deoxynivalenol-glucosyl transferase

DPEC	diethyl pyrocarbonate
DTT	dithiothreitol
DTNB	dithiobis(2-nitrobenzoic acid)
EAM	ethyl acetimidate
E. coli	*Escherichia coli*
EDC	1-ethyl-3-(3-dimethylaminopropyl)carbodiimide
EDTA	ethylenediaminetetraacetic acid
E. gallicum	*Erucastrum gallicum*
EI	electron impact
E. lata	*Eutypa lata*
ERE	eutypine reductase enzyme
ESI-MS^n	electrospray ionization-mass spectrometry
Et_2O	diethyl ether
EtOAc	ethyl acetate
EtOH	ethanol
F.	*Fusarium*
FAD	flavin adenine dinucleotide
FCC	flash column chromatography
FMN	flavin mononucleotide
GC	gas chromatography
GC-MS	gas chromatography-mass spectrometry
G. graminis	*Gaeumannomyces graminis*
G. fujikuroi	*Gibberellins fujikuroi*
Glc	glucose
Glu	glutamine
GST	glutathione-S-transferase
h	hour(s)
HCTR	HC-toxin reductase
His	histidine
HMW	high molecular weight
^{1}H NMR	proton nuclear magnetic resonance
HPLC	high performance liquid chromatography
HR-EIMS	mass spectrometry-high-resolution-electron ionization
HST	Host-selective toxin
Hz	hertz
IAA	indolyl-3-acetic acid
IAD	indolyl-3-acetaldoxime dehydratase
IACA	iodoacetamide
IAOx	indolyl-3-acetaldoxime
Ile	isoleucine
J	coupling constant
K. oxytoca	*Klebsiella oxytoca*
L. maculans	*Leptosphaeria maculans*
L. biglobosa	*Leptosphaeria biglobosa*
LC-MS-ESI	liquid chromatography-mass spectrometry-electrospray ionization
LeA	isoleucinic acid

Lys	lysine
MALDI	matrix assisted laser desorption/ionization
MHz	megahertz
min	minute
MM	minimal media
mmol	millimole
m/z	mass/charge ratio
NADPH	nicotinamide adenine dinucleotide phosphate
NAI	*N*-acetylimidazole
NEM	*N*-ethylmaleimide
NIV	nivalenol
N. haematococca	*Nectria haematococca*
PAL	phenylalanine ammonia lyase
PAOx	phenylacetaldoxime
PBE resin	polybuffer exchanger resin
PDA	potato dextrose agar
Pda	pisatin demethylase
PDB	potato dextrose broth
P. dispersa	*Pontoea dispersa*
Phe	phenylalanine
PHMB	*p*-hydroxymercuribenzoate
p*I*	isoelectric point
P. infestans	*Phytophthora infestans*
PLP	pyridoxal-5'-phosphate
PMSF	phenylmethanesulfonyl fluoride
3-PPAH	3-phenylpropionaldehyde
PPN	3-phenylpropionitrile
Pro	proline
P. chlororaphis	*Pseudomonas chlororaphis*
psi	pound per square inch
PTC	phenylthiocyanate
PVPP	polyvinylpolypyrrolidone
ppm	parts per million
PTLC	preparative thin layer chromatography
PyOx	pyridine-3-carboxaldehyde oxime
QQ/MM	quantum mechanics coupled with molecular mechanics
Quant.	quantitative
R. globerulus A-4	*Rhodococcus globerulus* A-4
RR	resonance Raman
R. sp N-771	*Rhodococcus* sp N-771
RP-FCC	reversed phase flash column chromatography
R. solani	*Rhizoctonia solani*
rpm	revolutions per minute
r.t.	room temperature
S. acidiscabies	*Streptomyces acidiscabies*
S. alba	*Sinapis alba*

S. bicolor	*Sorghum bicolor*
S. cerevisiae	*Saccharomyces cerevisiae*
Ser	serine
SGF	spore germination fluid
S. ipomoeae	*Streptomyces ipomoeae*
S. scabies	*Streptomyces scabies*
S. sclerotiorum	*Sclerotinia sclerotiorum*
STD	standard deviation
T. salsuginea	*Thellungiella salsuginea*
T. aestivum	*Triticum aestivum*
THF	tetrahydrofuran
THFA	tetrahydrofolic acid
TIC	total ion current
TLC	thin layer chromatography
t_R	retention time
Tris-HCl	tris(hydroxymethyl)aminomethane HCl
T. urticae	*Tetranychus urticae*
Tyr	tyrosine
v	volume
Val	valine
V. berlandieri	*Vitis berlandieri*
UV	ultraviolet
X. albilineans	*Xanthomonas albilineans*
ZAA	zearalanone
α-ZAOL	zearalanol
ZEA	zearalenone
ZOL	zearalenol

1. Chapter 1: Introduction

1.1 General objectives

Part 1

Phytotoxins are secondary metabolites produced by plant pathogens to facilitate their invasion and colonization of plant tissues. As a defense strategy, some plants are able to detoxify fungal phytotoxins and/or produce concomitantly several antimicrobial defense metabolites, e.g. phytoalexins. Cruciferous plants are exposed to diseases mediated by different phytotoxins. Among them, blackleg and blackspot are major diseases caused by *Leptosphaeria maculans* (Desm) Ces. et de Not. [asexual stage *Phoma lingam* (Tode ex Fr) Desm.] and *Alternaria brassicae* (Berkeley) Sacc. and *A. brassicicola* (Schwein) Wiltshire, respectively. Destruxin B (**1**) and sirodesmin PL (**13**) are major phytotoxins produced by *A. brassicae* (Pedras and Smith, 1997) and *L. maculans*, respectively and are suggested to be involved in pathogenesis (Elliott, Gardiner et al., 2007). Previous work showed that resistance of crucifers to blackspot disease is correlated with their ability to detoxify destruxin B (**1**) to hydroxydestruxin B (**32**) (Pedras, Montaut et al., 2003; Pedras, Zaharia et al., 2001; Pedras, Zaharia et al., 1999), as well as the production of phytoalexins in a blackspot resistant crucifer, *Sinapis alba* Ochre (Pedras and Smith, 1997). Sirodesmin PL (**13**) elicited production of phytoalexins in blackleg resistant *Brassica juncea* (Pedras and Yu, 2008a). However, no metabolites of sirodesmin PL (**13**) have been reported in plants. My research investigates the metabolism of and phytoalexin elicitation by destruxin B (**1**) and sirodesmin PL (**13**) in crucifers and non-crucifers. The following aspects are investigated in the first part of this thesis:

1. Determination of destruxin B (**1**) transformation and phytoalexin elicitation in crucifers and non-crucifers species: leaves of thale cress (*Arabidopsis thaliana* L.), leaves of salt cress (*Thellungiella salsuginea* Pallas.), leaves of dog mustard (*Erucastrum gallicum* O.E. Schulz.), roots of turnip (*B. rapa* L.), roots of rutabaga (*B. napus* L.), leaves of oat (*Avena sativa* L.) and leaves of wheat (*Triticum aestivum* L.).
2. Determination of the chemical structures of destruxin B metabolites.

3. Determination of sirodesmin PL (**13**) transformation, chemical structures of sirodesmin PL (**13**) metabolites and phytoalexin elicitation in crucifers and non-crucifers plants: leaves of thale cress (*Arabidopsis thaliana* L.), leaves of salt cress (*Thellungiella. salsuginea* Pallas.), leaves of dog mustard (*Erucastrum gallicum* O.E. Schulz.), roots of turnip (*B. rapa* L.), roots of rutabaga (*B. napus* L.), leaves of oat (*Avena sativa* L.) and leaves of wheat (*Triticum aestivum* L.).

Part 2

Indolyl-3-acetaldoxime (IAOx, **142**) is an important intermediate in the biosynthesis of several plant secondary metabolites. IAOx (**142**) was metabolized in both crucifers and their pathogens to indolyl-3-acetonitrile (IAC, **115**) (Pedras and Montaut, 2003a). The metabolism of IAOx (**142**) into IAC (**115**) was catalyzed by indolyl-3-acetaldoxime dehydratase (IAD, EC 4.99.1.6). For better understanding of the potential role of indolyl-3-acetaldoxime dehydratases in the interaction of plants with their fungal pathogens, it is important to study IAD in different crucifer pathogenic fungi. The objectives of this study are:

1. Screening indolyl-3-acetaldoxime dehydratase activity in plant pathogenic fungal species.
2. Isolation, characterization, substrate specificity and identification of indolyl-3-acetaldoxime dehydratase from *L. maculans* isolate Laird 2.

1.2 Plant pathogens

Plant fungal diseases cause major global crop losses. The ability of plant pathogenic fungi to colonize plant cells depends on several factors including: production of cell wall hydrolytic enzymes, production of phytotoxins and detoxification of plant secondary metabolites involved in defense mechanism (phytoalexins and phytoanticipins) (Schäfer, 1994). Phytotoxins are secondary metabolites produced by plant pathogens that allow them to successfully invade and colonize plant tissues. Phytotoxins have a role in plant disease either as pathogenicity factors (the ability to cause disease) or as virulence factors (the severity of disease). Based on the reaction of host plants to these phytotoxins, they are classified in two main classes: host selective

toxins (HSTs) affecting host plants and non-HSTs that can damage a much wider range of hosts than the microbe does (Graniti, 1991; Strange, 2007; Strobel, 1982). Since HSTs are essential for pathogenicity, isolates of the pathogen that have lost the capacity to produce toxins are unable to infect and cause disease. On the other hand, non-HSTs are not essential for pathogenicity but may contribute to the virulence of the pathogen (Ballio, 1991).

Crucifers are economically important plants as sources of vegetables, oils, food and fuel. However, crucifers are subjected to various fungal diseases resulting in annual serious economical losses. Blackleg and blackspot diseases are two of the most important devastating diseases affecting crucifer crops. Blackleg disease is caused by the phytopathogenic fungi *L. maculans* and *L. biglobosa* while blackspot disease is caused by the phytopathogenic fungi *A. brassicae* and *A. brassicicola* (Saharan, 1993). Both diseases seem to be toxin mediated as several phytotoxins were isolated from fungal cultures and some were detected in the infected plants (Buchwaldt and Jensen, 1991; Pedras and Smith, 1997; Pedras and Yu, 2009). In the following sections phytotoxins produced by the phytopathogenic fungi *A. brassicae* and *L. maculans* are reviewed.

1.2.1 Phytotoxins from *Alternaria brassicae*

A. brassicae together with *A. brassicicola* are the causative agents of blackspot disease, one of the most devastating diseases of rapeseed (*B. rapa* and *B. napus*), canola (*B. rapa* and *B. napus*) and brown mustard (*B. juncea*) (Fitt, Brun, et al., 2006; Howlett, Idnurm, et al, 2001; Saharan, 1993). Destruxins (Ayer and Pena-Rodriguez, 1987a; Buchwaldt and Jensen, 1991) and ABR-toxin (Parada, Sakuno, et. al, 2008) are phytotoxins produced by *A. brassicae* so far.

Destruxins are cyclic hexadepsipeptides composed of an α-hydroxy acid and five amino acid residues (Pedras, Zaharia et al., 2002). Four destruxins were isolated from *A. brassicae* cultures: destruxin B (**1**), homodestruxin B (**2**), desmethyldestruxin B (**3**) and destruxin B_2 (**4**) (Ayer and Pena-Rodriguez, 1987a; Buchwaldt and Jensen, 1991) (Fig.1-1).

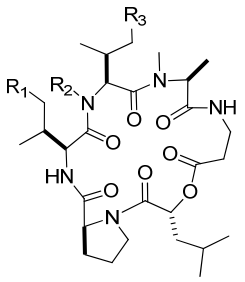

	R_1	R_2	R_3
1	CH_3	CH_3	H
2	CH_3	CH_3	CH_3
3	CH_3	H	H
4	H	CH_3	H

Figure 1-1: Chemical structures of destruxins produced by *Alternaria brassicae*: destruxin B (**1**), homodestruxin B (**2**), desmethyldestruxin B (**3**) and destruxin B_2 (**4**) (Ayer and Pena-Rodriguez, 1987a; Buchwaldt and Jensen, 1991).

Destruxins were reported to cause disease symptoms on different plants. Phytotoxic assays using destruxin B (**1**) on leaf assays (Bains and Tewari, 1987) as well as pollen germination and pollen tube growth assays (Shivanna, and Sawhney, 1993) indicated that it is a HST. Destruxin B (**1**) mimics the pathogenicity range of the fungus. The degree of sensitivity of different *Brassica* species to destruxin B (**1**) was correlated to their degree of susceptibility to *A. brassicae*. Moreover, the damage caused by the toxin was similar to that caused by the pathogenic fungus (Bains and Tewari, 1987, Shivanna, and Sawhney, 1993). Destruxin B (**1**), homodestruxin B (**2**) and desmethyldestruxin B (**3**) were tested in cell suspension cultures of the disease resistant species *S. alba*. Homodestruxin B (**2**) appeared to be more phytotoxic than destruxin B (**1**) while desmethyldestruxin B (**3**) was less phytotoxic (Pedras, Biesenthal et al. 2000). Homodestruxin B (**2**) caused symptoms similar to destruxin B (**1**) on *B. napus* leaves, in addition, it affected leaves of both host and non-host plants of *A. brassicae* and it was suggested to be non-HST (Bains, Tewari, et al. 1993). However, based on its metabolic biotransformation by blackspot resistant and susceptible species (presented in section 1.3.1.4) it was classified as HST (Zaharia, 2001).

Another phytotoxin isolated from *A. brassicae* is ABR-toxin. ABR-toxin is a protein isolated from the high molecular weight (HMW) fractions of the fungus spore germination fluid (SGF) inoculated on the leaves of cabbage (*B. oleracea*) (Parada, Oka et al. 2007). It has molecular weight of 27.5 KDa. The complete amino acid sequence of ABR-toxin was not determined. ABR-toxin was suggested to be a HST as it induced water-soaked symptoms and chlorosis on host leaves, but not on non-host leaves. Inoculation of the ABR-toxin with the non-pathogenic fungus *A. alternaria* allowed the fungus to colonize the leaves and to induce disease symptoms similar to symptoms developed on *Brassica* leaves infected by *A. brassicae* (Parada,

Sakuno, et. al, 2008); however, mutants of *A. brassicae* deficient in the production of ABR-toxin must be tested before conclusion can be drawn.

In conclusion, both destruxin B (**1**) and homodestruxin B (**2**) were suggested to play a role in pathogencity. First, both toxins were detected in extracts of *B. napus* leaves (Buchwaldt and Jensen, 1991) and *S. alba* leaves (Pedras and Smith, 1997) infected with *A. brassicae*. Second, the resistance of crucifers to blackspot disease was correlated with their ability to detoxify destruxin B (**1**) and homodestruxin B (**2**) to hydroxy derivatives at faster rates than blackspot susceptible crucifers (presented in section 1.3.1.4) (Pedras, Montaut et al., 2003; Pedras, Zaharia et al., 1999; Pedras, Zaharia et al., 2001). In addition, hydroxydestruxin B (**32**) elicited the production of the phytoalexins sinalexin (**103**) and sinalbin A (**100**) in resistant *S. alba* leaves but not in susceptible species (Pedras, Zaharia et al., 2001). Lastly, destruxin B (**1**) was detected in SGF of *A. brassicae* inoculated on different plant tissues (Buchwaldt, Green, 1992; Parada, Oka et al. 2007). Although Parada et al. (Parada, Oka et al. 2007) proposed that destruxin B (**1**) is not involved in pathogenicity of fungus; this proposal was based on testing the effect of destruxin B (**1**) on *A. alternate* not *A. brassicae*. Mutants deficient in the production of destruxin B (**1**) will be important to confirm the role of destruxin B (**1**) in pathogenicity of the fungus.

In addition to destruxins and ABR toxin, several plant growth factors were isolated from *A. brassicae* liquid culture: abscisic acid (ABA, **5**) (Dahiya, Tewari et al. 1991), *N*-methyl-2,5-dimethyl-*N*'-cinnamoylpiperazine (**6**), 2-hydroxy-l'-methylzeatin (**7**) and 3-carboxy-2-methylene-4-pentenyl-4-butenolide (**8**) (Fig. 1-2) (Dahiya and Tewari, 1991). Both **6** and **8** induced necrosis in canola and rapeseed cotyledons and reduced the growth of canola/rapeseed seedling. In contrast, **7**, a cytokinin derivative, increased the growth of seedlings and the chlorophyll content in canola and rapeseeds cotyledons (Dahiya and Tewari, 1991). However, these compounds were not detected by any other groups working with the fungus (Ayer and Pena-Rodriguez, 1987a; Buchwaldt and Jensen, 1991, Buchwaldt, Green, 1992).

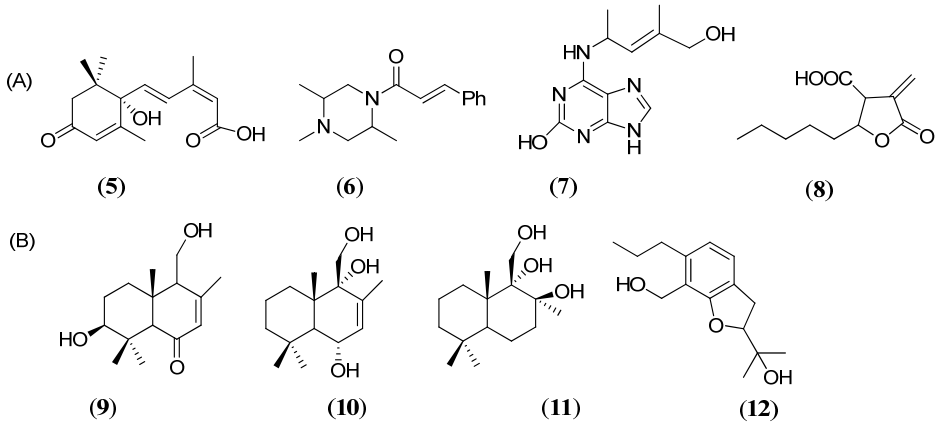

Figure 1-2: Chemical structures of metabolites produced by *Alternaria brassicae*: (A) compounds with plant growth effect: abscisic acid (ABA, **5**) (Dahiya, Tewari et al.1991), *N*-methyl-2,5-dimethyl-*N*'-cinnamoylpiperazine (**6**), 2-hydroxy-l'-methylzeatin (**7**) and 3-carboxy-2-methylene-4-pentenyl-4-butenolide (**8**) (Dahiya and Tewari, 1991); (B) sesquiterpenoids: deoxyuvidin (**9**), albrassitriol (**10**), isoalbrassitriol (**11**) and brassicadiol (**12**) (Ayer and Pena-Rodriguez, 1987b).

Several drimane type sesquiterpenoids were isolated from the liquid culture of *A. brassicae*: deoxyuvidin (**9**), albrassitriol (**10**), isoalbrassitriol (**11**) and brassicadiol (**12**). None of these metabolites showed phytotoxic activity towards canola (Fig. 1-2) (Ayer and Pena-Rodriguez, 1987b).

1.2.2 Phytotoxins from *Leptosphaeria maculans*

L. maculans and *L. biglobosa* are the causative agents of blackleg disease in rapeseed (*B. rapa*, *B. napus*) and canola (*B. rapa*, *B. napus*) worldwide (Fitt, Brun, et al., 2006; Howlett, Idnurm, et al, 2001). Three distinct groups of blackleg fungi were proposed based on their molecular and chemotaxonomic analysis (Pedras and Yu, 2009). One group of *L. maculans* is virulent on canola and rapeseed. Isolates of this group are chemically characterized by producing sirodesmins (**13**, **14-17**) (Férézou, Riche et al., 1977; Pedras, Abrams et al., 1988; Pedras, Séguin-Swartz et al., 1990), phomalide (**18**) (Pedras and Taylor, 1993a) and maculansins (**19**, **20**) (Pedras and Yu, 2008b) (Fig. 1-3). Sirodesmins are non-HSTs isolated from cultures of *L. maculans*. Several sirodesmins were separated and identified: sirodesmin PL (**13**) and deacetyl sirodesmin PL (**14**) (Férézou, Riche et al., 1977), sirodesmin J (**15**), sirodesmin K (**16**) and sirodesmin H (**17**) (Pedras, Abrams et al., 1988; Pedras, Séguin-Swartz et al., 1990) (Fig. 1-3).

Sirodesmin PL (**13**) is the major phytotoxin produced in a chemically defined liquid media. Its production in fungal cultures was suppressed by the phytoalexin brassinin (**117**) (Pedras and Taylor, 1993b). Recently, sirodesmin PL (**13**) was detected in the cotyledons and stem extracts of *B. napus* infected by *L. maculans* (Elliott, Gardiner et al., 2007). Sirodesmin PL (**13**) deficient mutants of *L. maculans* showed less damaging effect on canola (susceptible to blackleg) stems in comparison to the wild-type suggesting the role of sirodesmin PL (**13**) in pathogenesis of the fungus (Elliott, Gardiner et al., 2007). In addition, sirodesmin PL (**13**) elicited the production of the phytoalexins brassilexin (**104**), cyclobrassinin (**102**), rutalexin (**121**) and spirobrassinin (**114**) in *B. juncea* (blackleg resistant plant) (Pedras and Yu, 2008a). On the other hand, phomalide (**18**) is a depsipeptide HST produced in liquid cultures of virulent isolates of *L. maculans* (Pedras and Taylor, 1993a) and detected in the extracts of infected canola leaves, suggesting its role in the development of blackleg disease (Pedras and Biesenthal, 1998).

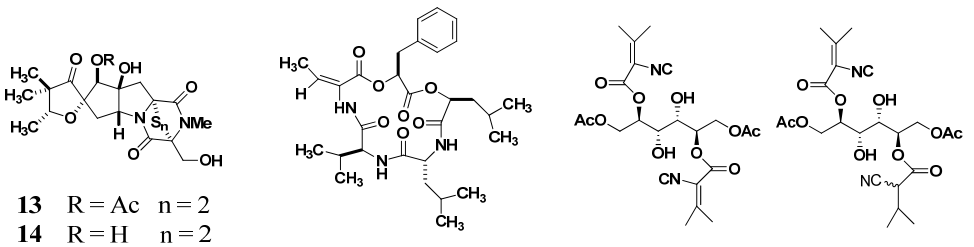

13 R = Ac n = 2
14 R = H n = 2
15 R = Ac n = 3
16 R = Ac n = 4
17 R = Ac n = 1

18 **19** **20**

Figure 1-3: Chemical structures of phytotoxins from *Leptosphaeria maculans* (virulent on canola): sirodesmin PL (**13**), deacetylsirodesmin PL (**14**), sirodesmin J (**15**), sirodesmin K (**16**), sirodesmin H (**17**) (Férézou, Riche et al., 1977; Pedras, Abrams et al., 1988; Pedras, Séguin-Swartz et al., 1990); phomalide (**18**) (Pedras and Taylor, 1993a); maculansin A (**19**) and maculansin B (**20**) (Pedras and Yu, 2008b).

In addition to sirodesmins (**13**-**17**) and phomalide (**18**), *L. maculans* isolates virulent on canola produce phytotoxins with mannitol skeleton: maculansin A (**19**) and maculansin B (**20**) (Fig. 1-3) (Pedras and Yu, 2008b). Maculansins were detected in fungal cultures grown in potato dextrose (PDB) media and at higher incubation temperature, in contrast to sirodesmins and phomalide that were not detected. Maculansin A (**19**) is a selective phytotoxin that showed higher phytotoxicity on the leaves of resistant plants (brown mustard) than on susceptible plants (canola) (Fig. 1-3) (Pedras and Yu, 2008b).

The second group of *L. maculans* includes isolates with reversed pathogenicity i.e. not virulent on canola, but virulent on brown mustard (*B. juncea*). It was suggested that this new group could include Polish isolates and Canadian Laird 2 and Mayfair 2 isolates. They are characterized by the production of polanrazines (Pedras and Chumala, 2005; Pedras, Smith et al., 1998), phomapyrones (Pedras and Chumala, 2005; Pedras and Biesenthal, 2001; Pedras, Erosa-López et al., 1999) and phomalairdenones (Pedras, Chumala et al., 2005; Pedras, Erosa-López et al., 1999). Among these metabolites, polanrazine C (**21**), phomalairdenone A (**22**), D (**23**), phomalairdenol A (**24**), lairdenol (**25**) showed phytotoxicity on brown mustard leaves but not on canola (Pedras, Chumala et al., 2005). In addition, Laird 2 and Mayfair 2 isolates produced a depsipeptide phytotoxin, depsilairdin (**26**) (Pedras, Chumala et al., 2004). Both phomalairdenone A (**22**) and depsilairdin (**26**) are host selective toxins that showed phytotoxicity on brown mustard but not on canola (Fig. 1-4). Interestingly, maculansin A (**19**) was also produced by *L. maculans* isolate Laird 2 grown in PDB media (Pedras and Chumala, 2011). The production of the same metabolites in different groups suggests the presence of common genes.

L. biglobosa is the third group of blackleg fungi. Isolates of this species are weakly virulent on canola and rapeseed and are characterized by the production of phomapyrones, phomaligadiones and phomaligols in PDB media (Pedras, 1996; Pedras, Morales et al., 1993; Pedras, Taylor et al., 1995).

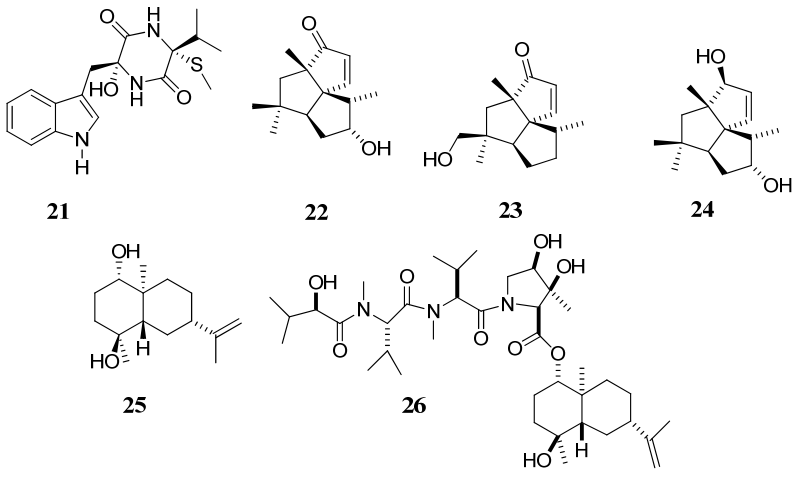

Figure 1-4: Phytotoxins from *Leptosphaeria maculans* Laird 2 and Mayfair 2 isolates: polanrazine C (**21**), phomalairdenone A (**22**), phomalairdenone D (**23**), phomalairdenol A (**24**), lairdenol (**25**) and depsilairdin (**26**) (Pedras, Chumala et al., 2004; Pedras, Chumala et al., 2005).

1.3 Chemical defense mechanisms of plants against phytopathogenic fungi

Plants have developed physical barriers together with chemical and biochemical defense mechanisms against their pathogens. Plant secondary metabolites play an important role in plant chemical defense mechanisms. Plants can produce antimicrobial secondary metabolites, which are either constitutive (phytoanticipins) or elicited (phytoalexins) (Mansfield and Bailey, 1982; VanEtten, Mansfield et al., 1994). In addition to the production of antimicrobial compounds, some plants can detoxify phytotoxins produced by invading pathogens, which can impart resistance (Karlovsky, 1999; Maor and Shirasu, 2005). Studying the mechanisms of resistance and susceptibility of plants to their pathogens can lead to the identification and cloning of resistance genes, which in turn could be used to generate disease resistant plants. Development of plant genotypes that are resistant to their pathogens has become an important goal to reduce crop losses and use of chemical pesticides (Karlovsky, 1999; Möbius and Hertweck, 2009; Strange, 2007). In the following sections, some of the chemical mechanisms involved in plant defense against their pathogens are reviewed.

1.3.1 Metabolism of phytotoxins

Some plants are able to overcome pathogens through detoxification of phytotoxins, i.e. they are able to convert phytotoxins to non-toxic metabolites (Karlovsky, 1999; Strange, 2007; Walton and Panaccione, 1993). The ability of plants to detoxify phytotoxins is attributed to the presence of enzyme(s) responsible for phytotoxin transformation (Karlovsky, 1999; Strange, 2007). Although only a few examples of phytotoxin detoxification have been reported so far, the current examples indicate that important plant defense mechanisms remain largely unexplored.

1.3.1.1 HC- toxin (27)

The role of HC-toxin (*Helminthosporium carbonum* toxin) in pathogenesis is the most thoroughly investigated so far (Walton, 2006). HC-toxin (**27**) is a HST produced by *Cochliobolus carbonum* race 1 (asexual stage *Helminthosporium carbonum*), the causative agent of leaf spot and ear mold disease of maize. HC-toxin (**27**) is a cyclotetrapeptide containing an α,β-

epoxyketone required for its activity (Walton and Earle, 1983). The pathogenicity of *C. carbonium* race 1 is controlled by single genetic locus *TOX2* which encodes the enzymes required for the biosynthesis of HC-toxin (**27**) (Ahn, Cheng et al., 2002; Panaccione, Scott-Craig et al., 1992; Scheffer, Nelson et al., 1967; Scheffer and Ullstrup, 1965). Two enzymes involved in the biosynthesis of HC-toxin (**27**) were isolated from *C. carbonium* race 1. The activities of these enzymes were not detected in race 2 and race 3, which do not produce HC-toxin (**27**) and are weakly pathogenic to maize (Walton, 1987). In addition, genetic variants that do not produce HC-toxin (**27**) are unable to colonize much beyond the site of penetration (Comstock and Scheffer, 1973; Panaccione, Scott-Craig et al., 1992). Maize genotypes that have the dominant gene *Hm* (either *Hm1* or *Hm2*) were found to be resistant to leaf spot and ear mold disease; however, *Hm1* is weaker and more prominent to older tissues.

To establish the biochemical basis of resistance of maize to leaf spot disease, the metabolism of tritiated HC-toxin (**27**) was studied in susceptible and resistant maize in *vivo* and in *vitro* (Meeley, Johal et al., 1992; Meeley and Walton, 1991). Initially, administration of radiolabeled HC-toxin (**27**) to segments of the mature green leaves of both susceptible and resistant maize indicated that HC-toxin (**27**) was converted to a single hydroxyderivative **28** that resulted from reduction of the carbonyl group on the side chain of one of the constituents amino acid residues (Fig. 1-5). This derivative was shown to have no phytotoxicity. This result excluded the role of HC-toxin detoxification in imparting resistance to maize (no relationship between the detoxification process and host selectivity) (Meeley and Walton, 1991). However, administration of radiolabeled HC-toxin (**27**) to intact resistant and susceptible etiolated maize seedlings showed conversion of HC-toxin (**27**) to the corresponding hydroxyderivative **28** by resistant genotypes but not by susceptible genotypes. Similar results were obtained using cell-free preparations of both resistant and susceptible genotypes (Meeley, Johal et al., 1992). The reduction of HC-toxin (**27**) to the corresponding 8-hydroxy derivative (**28**) is controlled by the enzyme HC-toxin reductase (HCTR) that requires NADPH as cofactor for its activity. HCTR was partially purified from resistant genotypes (Meeley and Walton, 1991), while no HCTR activity was detected in cell-free extracts (CFE) of susceptible genotype (Meeley, Johal et al., 1992). The gene *Hm1*, which was cloned and represents the first example of a plant disease resistance gene encoding a detoxifying enzyme (Johal and Briggs, 1992; Meeley, Johal et al., 1992), encodes HCTR. *Hm1* gene was found to be conserved in monocot plants. HCTR activity was detected in other

monocots (barley, sorghum, oat and wheat), while no activity was detected in dicots (Walton, 2006). In addition, homologs of *Hm1* were found in barely, rice and sorghum with high amino acid sequence similarity with *Hm1* from maize (Han, Kleinhofs et al., 1997; Multani, Meeley et al., 1998).

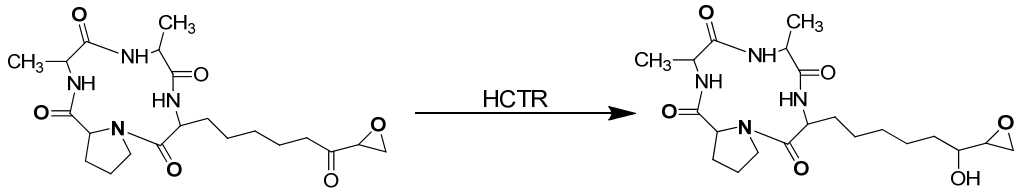

27 **28**

Figure 1-5: Detoxification of HC-toxin (**27**) by resistant maize genotype to the corresponding 8-hydroxy HC-toxin (**28**) by HC-toxin reductase enzyme (HCTR) (Meeley and Walton, 1991).

1.3.1.2 Eutypine (29)

In some cases, the tolerance of a plant to a pathogen is attributed to detoxification of a non-HST. For example, eutypine (**29**) is a non-HST produced by the fungus *Eutypa lata*, which is responsible for eutypa dieback disease of grapevines (Tey-Rulh, Philippe et al., 1991). Resistant genotypes are able to detoxify eutypine (**29**) to its corresponding alcohol (eutypinol, **30**) (Fig.1-6) which lacks phytotoxicity (Afifi, Monje et al., 2004; Fallot, Deswarte et al., 1997; Guillén, Guis et al., 1998). However, several plant species other than grapevine were found to convert eutypine (**29**) to eutypinol (**30**), among which *Vigna radiata* exhibited the highest activity. The reaction is catalyzed by eutypine reductase enzyme (ERE) that required NADPH for its activity (Colrat, Deswarte et al., 1999; Colrat, Latché et al., 1999). The gene encoding this detoxification activity was cloned and the calli of grapevine were transformed with that gene. These calli were found to be far less sensitive to eutypine (**29**) than the wild type (Guillén, Guis et al., 1998). The growth of the transgenic plants from grapevine rootstock 110 Richter *Vitis berlandieri* × *V. rupestris* that express the *Vr-ERE* gene were not affected by the toxin eutypine (**29**), whereas the toxin inhibited the growth of control plants (Legrand, Dalmayrac et al., 2003). An additional metabolic pathway was detected in fungi that can metabolize eutypine (**29**) to eutypinol (**30**) as in case of grapevine and to eutypinic acid (**31**) (Fig. 1-6). Similar to eutypinol (**30**), eutypinic acid (**31**) showed no phytotoxicity on grapevines (Christen, Tharin et al., 2005).

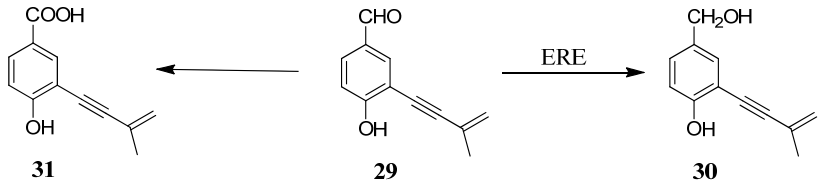

31 **29** **30**

Figure 1-6: Detoxification of non-HST eutypine (**29**) by resistant grapevine into eutypinol (**30**) by eutypine reductase enzyme (ERE) (Afifi, Monje et al., 2004) and by different fungi to eutypic acid (**31**) (Christen, Tharin et al., 2005).

1.3.1.3 Albicidins

Albicidins are family of phytotoxins produced by the sugar cane leaf scald bacterial pathogen *Xanthomonas albilineans* (Birch and Patil, 1985b). Albicidins were proposed to induce chlorosis in infected plants (Birch, 1987; Birch and Patil, 1987). Inoculation of *X. albilineans* mutants not producing albicidins on sugarcane leaves did not cause disease symptoms (Birch, 1987). In addition to their role in inducing disease in sugar cane, they are of interest as potential antibiotics (Birch and Patil, 1985a). Albicidins inhibit the DNA replication in bacteria (Birch and Patil, 1985b), as well as they inhibit the growth of broad spectrum of microorganisms pathogenic to human. However, the exact chemical structure of albicidins was not solved so far. ^{1}H- and ^{13}C-NMR and mass analysis of the major albicidin produced in the culture of *X. albilineans* indicated a compound of molecular weight of 842 with a carboxylate group (Birch and Patil, 1985a). Two genes are involved in the biosynthesis of albicidin, *xabA* and *xabB*. *xabB* encodes a multifunctional enzyme with polyketide synthase part fused to non-ribosomal peptide synthase (Huang and Zhang et al., 2001). On the other hand, *oxdA* is required for the post translation activation of the enzyme encoded by *oxdA* (Huang, Zhang et al., 2000). The cloning of albicidin resistance genes can provide an opportunity to biocontrol sugar cane leaf scald disease by producing recombinant albicidin-resistance sugarcane cultivars. Three bacteria were found to be resistant to albicidins: *Klebsiella oxytoca* (Walker, Birch et al., 1988), *Alcaligenes denitrificans* (Basnayake and Birch, 1995) and *Pontoea dispersa* strain SB 1403 (Zhang and Birch, 1997a). Albicidin resistance gene (*albA*) from *K. oxytoca* was cloned in *Escherichia coli* 294 and albA protein was purified (25 kDa) and found to inactivate albicidin. The inactivation mechanism did not involve biotransformation of albicidin to less toxic compound but involved the binding of albicidin with the protein (Walker, Birch et al., 1988). The second example is albicidin-resistance gene (*albB*) from the soil bacteria *A. denitrificans*. Similar to *albA* from *K. oxytoca*,

albB was cloned in *E. coli* and found to encode a protein of 23 kDa that inactivate albicidin via irreversible binding with the toxin (Basnayake and Birch, 1995).

The third example is *albD* gene isolated from *P. dispersa* strain SB 1403. *P. dispersa* strain SB 1403 was isolated from leaf scald diseased sugarcane leaves and was proposed to be used as biocontrol agent for sugar cane leaf scald disease. Inoculation of sugarcane leaves with *P. dispersa* strain SB 1403 in presence *X. albilineans* protected against infection and did not affect the growth of the plants (Zhang and Birch, 1996). The gene *albD* was cloned and sequenced and was found to encode detoxifying enzyme. The incubation of *albD* protein (albicidin detoxifying enzyme) with albicidin resulted in formation of degradation products with less phytotoxic activity. The chemical structures of these products were not identified. The enzyme involved in the biotransformation of albicidin was proposed to be an albicidin hydrolase as it showed esterase activity on 4-phenylbutyrate and was inhibited by the serine hydrolase inhibitor phenylmethanesulfonyl fluoride (PMSF, **208**) (Zhang and Birch, 1996; Zhang and Birch, 1997b). *P. dispersa* mutated at *albD* was not able to detoxify albicidin and was less efficient in biocontroling the disease (Zhang and Birch, 1997a). The expression of *albD* in *X. albilineans* abolished their ability to produce albicidin. In addition, transgenic sugarcane that expressed albicidin detoxifying enzyme was resistant to the pathogen (Zhang, Xu et al., 1999).

1.3.1.4 Destruxin B (1) and homodestruxin B (2)

Destruxin B (**1**) and homodestruxtin B (**2**) are HST isolated from the phytopathogenic fungus *A. brassicae* (Ayer and Pena-Rodriguez, 1987a; Buchwaldt and Jensen, 1991; Pedras, Zaharia et al., 2002). Both destruxins (**1**, **2**) were detected in planta infected with *A. brassicae* (Buchwaldt and Jensen, 1991; Pedras and Smith, 1997) indicating their role in pathogenesis (presented in section 1.2.1). The metabolism of destruxin B (**1**) and homodestruxin B (**2**) were studied in both susceptible and resistant plants using ^{14}C-labeled derivatives. Administration of ^{14}C- labelled destruxin B (**1**) to leaves of both resistant plants (*S. alba* cv. Ochre, Pennant and Sabre; *Camelina sativa* and *Capsella bursa-pastoris*) and susceptible plants (*B. napus* cv., Westar and *B. juncea* cv. Cutlass, Varuna and SWP083) showed that destruxin B (**1**) was biotransformed to hydroxydestruxin B (**32**) in both resistant and susceptible plants. Similarly, homodestruxin B (**2**) was metabolized to hydroxyhomodestruxin B (**33**) in both susceptible and resistant plants (Pedras, Montaut et al., 2003; Pedras, Zaharia et al., 1999; Pedras, Zaharia et al., 2001). However,

no metabolism of destruxins was observed in susceptible plants: *B. napus* cv. Quantum and Cresor as well as *B. rapa* cultivar GrGc1-6. The transformation of destruxin B (**1**) and homodestruxin B (**2**) to the corresponding hydroxyderivatives was a detoxification process. Hydroxydestruxin B (**32**) and hydroxyhomodestruxin B (**33**) were less phytotoxic than destruxin B (**1**) to *S. alba* and *B. napus* as evaluated from phytotoxic bioassays using leaf puncture, leaf uptake and cell suspension cultures biassays (Pedras, Zaharia et al., 1999; Pedras, Zaharia et al., 2001). The fate of hydroxydestruxin B (**32**) was further studied by administration of ^{14}C-labeled hydroxydestruxin B to susceptible and resistant plants. Hydoxydestruxin B (**32**) was metabolized to non-toxic metabolite hydroxydestruxin B β-D–glucopyranoside (**34**) and finally to 6-*O*-malonylhydroxydestruxin β–D-glucopyranoside (**35**) in both resistant and susceptible plants (Fig. 1-7) (Montaut et al., 2003; Pedras; Pedras, Zaharia et al., 2001). Although the detoxification of destruxins was reported in both susceptible and resistant plants, the hydroxylation process was the slow step in case of resistant plants, while the glucosylation was the slow step in case of resistant plants (Pedras, Montaut et al., 2003; Pedras, Zaharia et al., 2001).

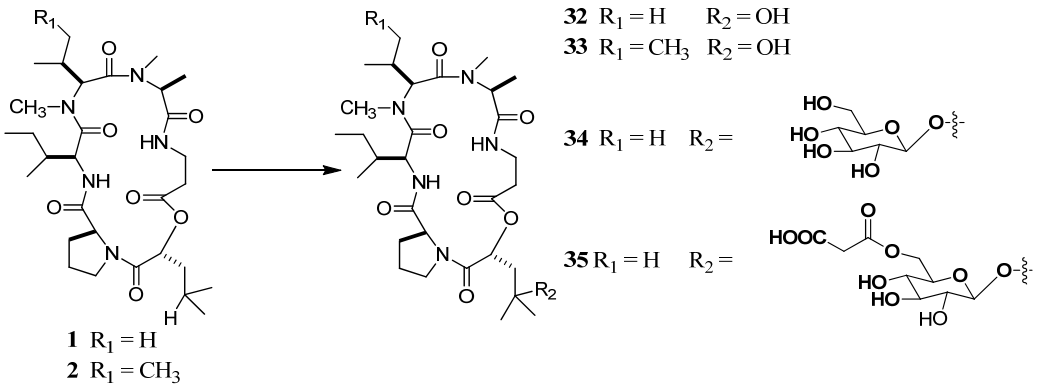

Figure 1-7: Metabolism of the host selective toxins: destruxin B (**1)** and homodestruxin B (**2**) (Pedras, Montaut et al., 2003; Pedras, Zaharia et al., 1999; Pedras, Zaharia et al., 2001).

In addition to the ability of resistant plant species to detoxify destruxins at faster rates than susceptible species, phytoalexin elicitation seemed to play role in their resistant mechanisms. Destruxin B (**1**) elicited the production of the phytoalexin sinalexin (**103**) in resistant plant *S. alba* leaves (Pedras and Smith, 1997) while hydroxydestruxin B (**32**) elicited the production of the phytoalexins sinalexin (**103**) and sinalbin A (**100**) in resistant *S. alba* leaves but not in susceptible

species (Pedras, Zaharia et al., 2001). Enzymes and genes involved in detoxification of destruxin (**1**) have not been reported.

1.3.1.5 Thaxtomins

Thaxtomins are dipeptide phytotoxins with 4-nitroindol-3-yl-2-5-dioxopiperazine skeletons produced by different pathogenic *Streptomyces species* (King and Calhoun, 2009). Thaxtomins A (**36**) and B (**39**) were the first thaxtomins isolated from potato tubers infected with *S. scabies* and from extracts of liquid cultures of *S. scabies* (King, Lawrence et al., 1989). Later different thaxtomins (**37**, **38**, **40-45**) (Fig. 1-8) were isolated from liquid cultures of *S. scabies*, *S. acidiscabies*, the causative agents of common scab disease of potato, radish and turnip, as well as *S. ipomoeae* the causative agent of soil rot disease of sweet potato (King and Lawrence, 1996; King, Lawrence et al., 1992; King, Lawrence et al., 1994; King, Lawrence et al., 1989; Loria, Bukhalid et al., 1995). The biosynthesis of thaxtomin A (**36**) was studied in *S. acidiscabies*. Three genes *txtA*, *txtB* and *txtC* were involved in the biosynthesis of thaxtomin A (**36**). *TxtA* and *txtB* were found to encode peptide synthases responsible for the formation of cyclic dipeptide backbone of thaxtomin (Healy, Wach et al., 2000). While *txtC* encodes cytochrome P450 monooxygenase responsible for the hydroxylation steps (Healy, Krasnoff et al., 2002). The production of these phytotoxins plays an important role in the pathogenesis of these microorganisms. Thaxtomins A (**36**) and B (**39**) were isolated from diseased potato tubers and were found to cause scab disease symptoms when inoculated with aseptically healthy tubers (Lawrence, Clark et al., 1990). *S. scabies* mutants producing less amount of thaxtomin A (**36**) were less or not pathogenic than wild type (Goyer, Vachon et al., 1998). In addition, the disruption of the gene included in the biosynthesis of thaxtomin A (**36**) (*txtA* gene) in *S. acidiscabies* resulted in the loss of production of thaxtomin A (**36**) and loss of pathogenicity on potato tubers (Healy, Wach et al., 2000). Thaxtomins was proposed to facilitate the penetration of host tissues. Thaxtomin A (**36**) inhibited cellulose biosynthesis (Bischoff, Cookson et al., 2009; Scheible, Fry et al., 2003). In addition, mutants of *S. ipomoeae* mutated in the production of thaxtomin C (**38**) were unable to penetrate intact roots of sweet potato (Guan, Grau et al., 2012).

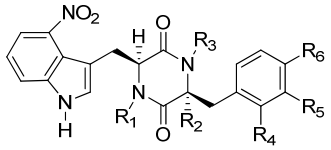

Compound	R_1	R_2	R_3	R_4	R_5	R_6
36	Me	OH	Me	H	OH	H
37	Me	OH	Me	OH	H	H
38	Me	H	H	H	H	H
39	Me	OH	Me	H	H	H
40	Me	H	Me	H	H	H
41	Me	OH	H	H	H	H
42	Me	OH	Me	H	H	OH
43	Me	OH	Me	H	OH	OH
44	Me	OH	H	H	OH	H
45	H	OH	Me	H	OH	H

Figure 1-8: Chemical structures of thaxtomins produced by different *Streptomyces* species (King and Lawrence, 1996; King, Lawrence et al., 1992; King, Lawrence et al., 1994; King, Lawrence et al., 1989; Loria, Bukhalid et al., 1995).

Thaxtomin A (**36**) and thaxtomin B (**39**) were biotransformed by *Bacillus mycoides* to the corresponding glucoside derivatives **46** and **47,** respectively (Fig. 1-9). This biotransformation process was considered as a partial detoxification as the resulting compounds were less toxic than the parent compounds (King, Lawrence et al., 2000). However, enzymes and genes involved in this process have not been reported.

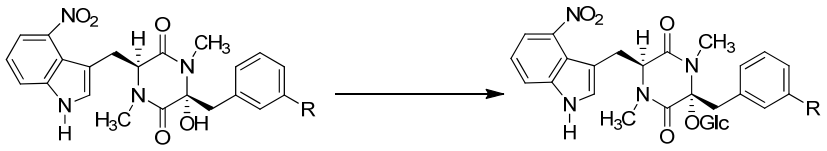

Compound	R
36	OH
39	H

Compound	R
46	OH
47	H

Figure 1-9: Biotransformation of thaxtomin A (**36**) and thaxtomin B (**39**) by the culture of *Bacillus mycoides* (King, Lawrence et al., 2000).

In addition, thaxtomin A (**36**) was detoxified by the fungal culture of *Aspergillus niger* van Tiegham var. *niger* to five metabolites that showed less phytotoxicity than thaxtomin A (**36**). The detoxification process involved either alkylation of the hydroxyl group at C-14 giving metabolites **48** and **49** or dehydration resulting in metabolites **50**, **51** and **52** (Lazarovits, Hill et al., 2004) (Fig. 1-10).

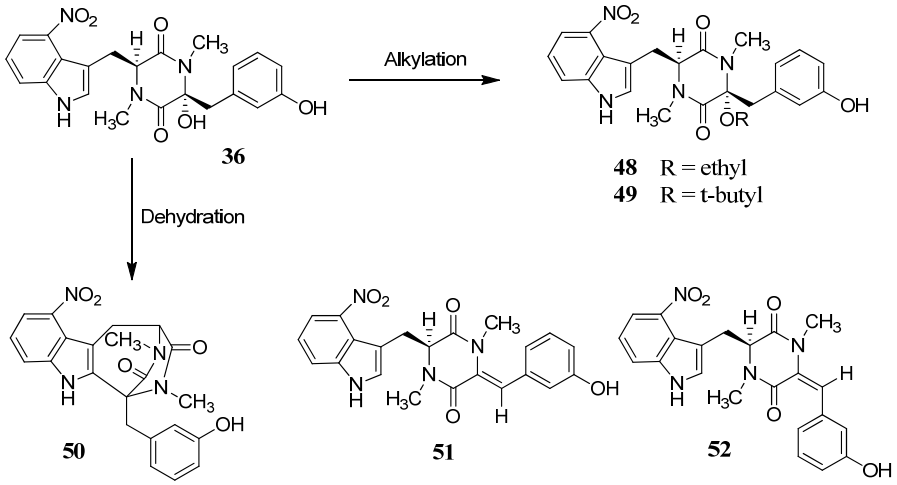

Figure 1-10: Biotransformation of thaxtomin A (**36**) by fungal culture of *Aspergillus niger* van Tiegham var. *niger* (Lazarovits, Hill et al., 2004).

Thaxtomin detoxification is important for breeding plants resistant to pathogenic *Streptomyces* species. However, enzymes and genes involved in thaxtomin detoxification were not reported. An *Arabidopsis* mutant (*txrt1* mutant) showed resistance to thaxtomin A. The resistance was attributed to the reduction in the uptake of thaxtomin A (**36**) not to its metabolism (Scheible, Fry et al., 2003).

1.3.1.6 Fusarium phytotoxins and mycotoxins

Fusarium head blight (FHB) is a significant disease of small grain cereals (e.g. wheat, barley and maize). FHB is caused by several species of the fungal pathogen *Fusarium*. The most important species are *F. graminearum* and *F. culmorum* that result in the most yield loss (Parry, Jenkinson et al., 1995). *Fusarium* spp. produce numerous toxic secondary metabolites that facilitate their colonization of plant tissues resulting in disease symptoms and yield loss (i.e. phytotoxins). In addition, these toxins are accumulated in *Fusarium*-infected grains causing health problems in humans and other mammalians (i.e. mycotoxins) (Parry, Jenkinson et al., 1995). Fusarium species produce a wide spectrum of toxic secondary metabolites as: trichothecenes, zearelenones, fumonisins, moniliformin, butenolide, fusarins, equisetin and enniatins (Desjardins and Proctor, 2007). However, most of these toxins have been studied with respect to the human and animal health problems. In this review the major toxins (trichothecenes and zearelenones) produced by *Fusarium* species will be presented.

Trichothecenes

Trichothecenes are sesquiterpenoids epoxides with tricyclic skeleton named trichothecene. The epoxide and double bond of cyclohexene are essential for their activities. Trichothecenes comprise a large family of compounds, over 150 trichothecenes and trichothecene derivatives have been isolated and characterized. They are non-HSTs that produce necrosis, chlorosis and wilting to a wide variety of plants (Rocha, Ansari et al., 2005). *Fusarium* mutants deficient in the production of trichothecenes are less virulent to wheat than wild types (Harris, Desjardins et al., 1999; Langevin, Eudes et al., 2004). In addition to their phytotoxic effect on plants, trichothecene contaminated food has negative impact on human and animal health (Awad, Ghareeb et al., 2010; Foroud and Eudes, 2009).

The main trichothecenes tested for their phytotoxic effects on plants are: T-2 toxin (**53**), HT-2 toxin (**54**), nivalenol (NIV, **55**), 4-deoxynivalenol (DON, vomitoxin, **56**), 3-*O*-acetyl DON (3-ADON, **57**), and 15-*O*-acetyl DON (15-ADON, **58**) (Fig. 1-11) (Foroud and Eudes, 2009; Rocha, Ansari et al., 2005).

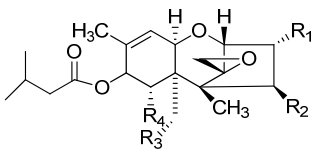

Toxin	R_1	R_2	R_3	R_4
53	OH	OAc	OAc	H
54	OH	OH	OAc	H

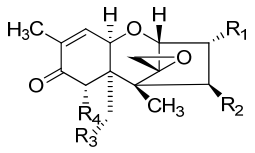

Toxin	R_1	R_2	R_3	R_4
55	OH	OH	OH	OH
56	OH	H	OH	OH
57	OAc	H	OH	OH
58	OH	H	OAc	OH

Figure 1-11: Chemical structures of some trichothecene structures including: T-2 toxin (**53**), HT-2 toxin (**54**), nivalenol (NIV, **55**), 4-deoxynivalenol (DON, **56**), 3-*O*-acetyl DON (3-ADON, **57**), and 15-*O*-acetyl DON (15-ADON, **58**), Ac = acetyl function.

Among these toxins DON (**56**) and 3-ADON (**57)** showed more phytotoxic effect on wheat than T-2 and HT-2 toxin (Bruins, Karsaï et al., 1993; Rocha, Ansari et al., 2005; Wang and Miller, 1988). DON (**56**) was proposed to be included in FHB pathogenicity. A correlation between aggressiveness of *Fusarium* species and their ability to produce DON (**56**) was observed (Proctor, Hohn et al., 1995). Resistance to DON (**56**) is correlated to the wheat resistance to FHB disease induced by *Fusarium* species. DON (**56**) significantly decreased the growth of wheat coleoptiles at 10^{-6} M. Resistant cultivars were less affected (10 -10^3 more tolerant) by DON (**56**)

(Wang and Miller, 1988). The application of DON (**56**) to the flowering wheat ears of both susceptible and resistant phenotypes induced symptoms similar to that caused by fungus infection only in susceptible species. While, resistant wheat phenotypes were not affected by DON (**56**) (Lemmens, Scholz et al., 2005). The resistance of some wheat phenotypes was correlated to their ability to convert DON (**56**) to the corresponding glucoside derivative **59** (Fig. 1-12) (Lemmens, Scholz et al., 2005). The same metabolic pathway was detected in cell suspension cultures of maize (Sewald, von Gleissenthall et al., 1992). The metabolism of DON (**56**) to its glucosyl derivative **59** seems to occur in both resistant and susceptible genotypes (Lemmens, Scholz et al., 2005). However, the rate of the conversion is higher in resistant phenotypes than susceptible ones. The enzyme involved in this biotransformation was not studied (Lemmens, Scholz et al., 2005). This biotransformation seems to occur in maize as DON-3-β-D-glucopyranoside **59** was detected and isolated from *Fusarium*-infected wheat and maize (Berthiller, Dall'Asta et al., 2005).

In addition, a gene of *A. thaliana* encoding glucosyltransferase was cloned in yeast; the recombinant enzyme (deoxynivalenol-glucosyl transferase (DOGT1) was found to detoxify DON (**56**) and 15-ADON (**58**) to their corresponding β-D-glucosyl derivatives (Fig. 1-12). Transgenic *A. thaliana* plants overexpressing DOGT1 are more resistant to the effect of DON (Poppenberger, Berthiller et al., 2003). This gene can be applied for producing transgenic wheat more resistant to FHB. The gene encoding glucosyltransferases responsible for detoxification of DON (**56**) in wheat was not reported. However a gene encoding glucosyltransferase (*TAUGT2*) was isolated from wheat, *TAUGT2* is expected to be included in resistance to FHB as the expression of the gene is induced by infection by *F. graminearum* (Lin, Lu et al., 2008).

Acetylation of trichothecene to the corresponding 3-acetyl derivatives is another detoxification strategy that was detected in *Fusarium*-producing trichothecene to protect themselves from the effect of these toxins. *Tri101*gene from *F. graminearum* encoding a trichothecene-3-*O*-acetyltransferase (Tri101) was cloned in *Schizosaccharomyces pombe* and *E. coli*. Tri101 was purified from *E. coli* and found to convert DON (**56**) to the corresponding 3-*O*-acetyl derivatives **57** (Fig. 1-12). The enzyme was not specific to DON (**56**), as T-2 toxin (**53**) and 4,15-diacetoxyscirpenol were reported as substrates for Tri101. In addition, transformants of *S. pombe* with *Tri101* gene are resistant to the effect of these toxins (Kimura, Kaneko et al., 1998). The expression of *Tri101* in tobacco (Muhitch, McCormick et al., 2000), wheat (Muhitch,

McCormick et al., 2000) and rice (Ohsato, Ochiai-Fukuda et al., 2007) reduced their FHB infection and DON (**56**) accumulation.

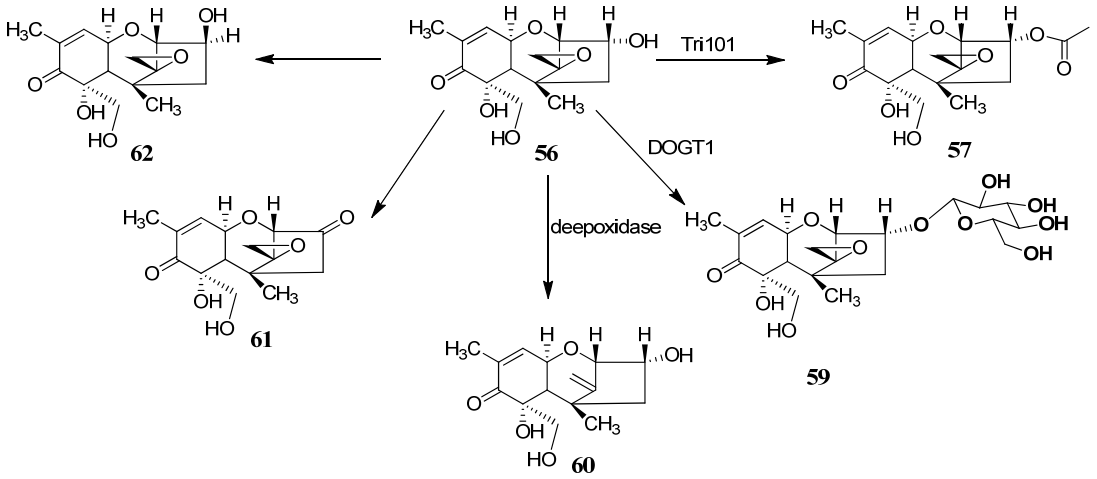

Figure 1-12: Detoxification of deoxynivalenol (DON, **56**) (Awad, Ghareeb et al., 2010; Fuchs, Binder et al., 2002; Ikunaga, Sato et al., 201; Kimura, Kaneko et al., 1998; Poppenberger, Berthiller et al., 2003; Shima, Takase et al., 1997; Völkl, Vogler et al., 2004).

Several bacteria have been screened for their ability to detoxify DON (**56**) in order to be used in crops and food contaminated with DON (**56**). Three detoxification reactions were detected in bacteria (Fig. 1-12). The first metabolic reaction is deepoxidation of DON (**56**) forming 3-epideoxynivalenol (**60**). This reaction was catalyzed by *Eubacterium sp* DSM 11798 isolated from bovine ruminal fluid. This reaction requires anaerobic condition (Awad, Ghareeb et al., 2010; Fuchs, Binder et al., 2002). The second reaction is oxidation of DON to 3-oxodeoxynivalenol (**61**) by soil Gram-negative bacteria strain E3-39 (Shima, Takase et al., 1997; Völkl, Vogler et al., 2004). In addition *Nocardioides* sp. strain WSN05-2, isolated from a wheat fields, degrades deoxynivalenol (**56**) to 3-epi-deoxynivalenol (**62**) (Ikunaga, Sato et al., 2011). Enzymes involved in these biotransformations remain to be identified. The identification of these bacterial enzymes catalyzing oxidation, epimerization and de-epoxidation can be used in the future for engineering resistant plants.

Zearalenones

Zearalenones are among the most widely distributed *Fusarium* mycotoxins, produced by different *Fusarium* species as for example: *F. graminearum*, *F. culmorum*, *F. equiseti* and *F.*

poae. Together with trichothecene and other *Fusarium* toxins zearalenones were detected in cereal crops infected by *Fusarium* and in different processed cereal foodstuffs (Zinedine, Soriano et al., 2007). The ecological roles of zearalenones in pathogenesis of *Fusarium* species and their effects on plants have not been reported. However, they were reported for their negative impact on human and animal health. They showed high binding affinity to oestrogen receptors resulting in reproductive disorders, abortion, infertility and depressed milk production to farm animals. In humans it caused hyperestrogenic syndrome (Zinedine, Soriano et al., 2007). Several members belonging to this family of compounds were isolated and characterized. They are classified to three classes: *trans*-zearalenone derivatives **63-70**, zearalanone derivatives **71-73** and *cis*-zearalenone derivatives **74-76** (Fig. 1-13). Among these compounds zearalenone (F-2 toxin, ZEA, **63**) is the most widely distributed *Fusarium* zearalenone derivatives (Richardson, Hagler et al., 1985).

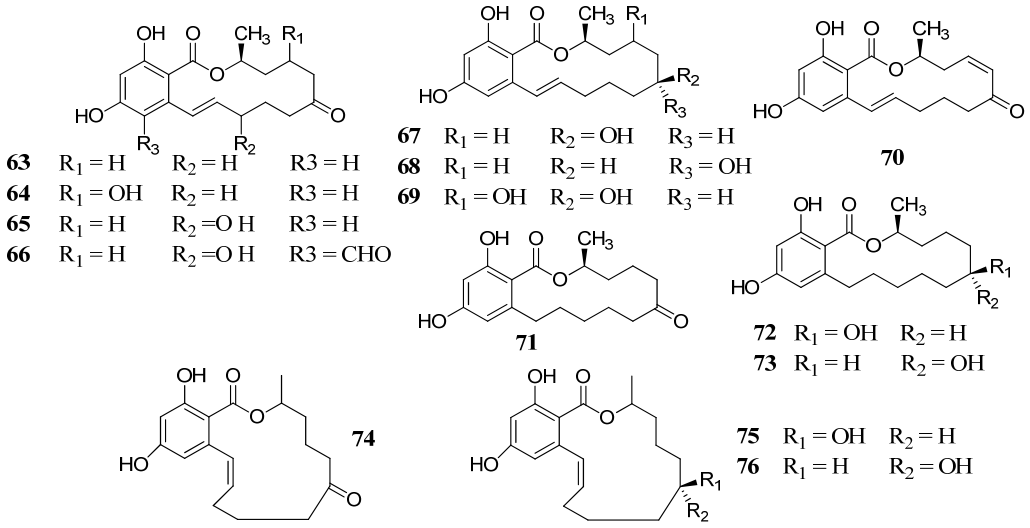

Figure 1-13: Chemical structures of zearalenones from *Fusarium* species: zearalenone (ZEA, **63**), 8'-hydroxyzearalenone (8'-hydroxyZEA, **64**), 3'-hydroxyzearalenone (3-hydroxyZEA, **65**), 5-formylzearalenone (5-formylZEA, **66**), α-zearalenol (α-ZOL, **67**), β-zearalenol (β-ZOL, **68**), 6', 8'-dihydroxyzearalenone (dihydroxyZEA, **69**), 7'-dehydrozearalenone (dehydroZEA, **70**), zearalanone (ZAA, **71**), α-zearalanol (α-ZAOL, **72**), β-zearalenol (β-ZAOL, **73**), *cis*- zearalenone (*cis*-ZEA, **74**), *cis*-α-zearalenol (*cis*-α-ZOL, **75**), *cis*-β-zearalenol (*cis*-β-ZOL, **76**) (Richardson, Hagler et al., 1985).

The metabolism of ZEA (**63**) was studied in bacteria, fungi and plants. Several metabolic pathways of ZEA (**63**) were detected including: conjugation, reduction, oxidation, methylation

and hydrolysis. The metabolism of ZEA (**63**) by conjugation includes either glucosylation or sulfation (Fig. 1-14). For example, ZEA (**63**) was metabolized to ZEA-4-β-D-glucopyranoside (**77**) by maize cell suspension cultures (Engelhardt, Zill et al., 1988) and by the following fungi *Rhizopus* sp. (Kamimura, 1986), *Thamnidium elegans* and *Muco bainieri* (El-Sharkawy and Abul-Hajj, 1987). Additionally *T. elegans* NRRL 1613 metabolized ZEA (**63**) to a mixture of zearalenone 4-*O*-β-D-glucoside (**77**) and zearalenone 2,4-*O*-β-D-diglucoside (**78**) (El-Sharkawy, 1989). The metabolism of ZEA (**63**) to ZEA-4-sulfate (**79**) was reported for *R. arrhizus* (IFO-6155) (El-Sharkawy, Selim et al., 1991), *F. graminearum*, *F. equiseti*, *F. sambucinum*, and *F. roseum* (Plasencia and Mirocha, 1991).

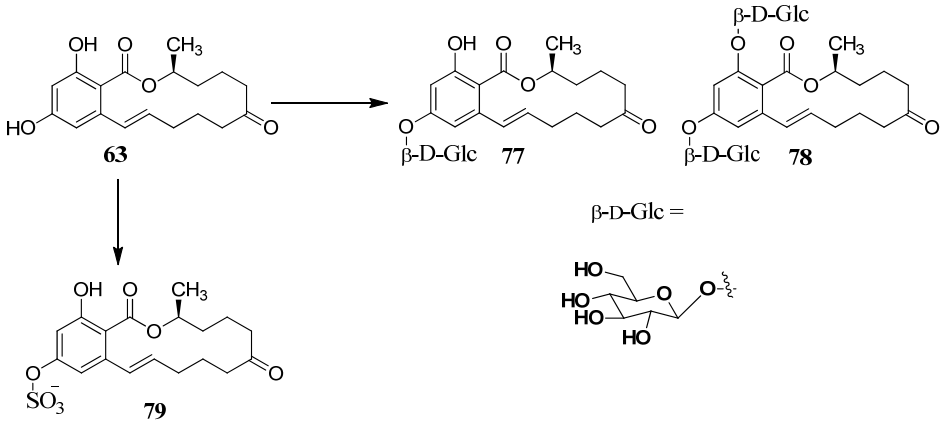

Figure 1-14: Metabolism of zearalenone (**63**) by different microorganisms (El-Sharkawy, 1989; El-Sharkawy, Selim et al.,1991; Engelhardt, Zill et al., 1988; Kamimura, 1986; Plasencia and Mirocha, 1991).

ZEA (**63**) was metabolized to α-zearalenol (α-ZOL, **67**) and β-zearalenol (β-ZOL, **68**) by maize cell suspension cultures (Engelhardt, Zill et al., 1988), *Rhizopus* sp (Kamimura, 1986), *S. griseus* (ATCC 13273), *S. rutgersensis* (NRRL-B 1256), and *A. niger* (ATCC 111394), (El-Sharkawy and Abul-Hajj, 1988b; El-Sharkawy, Selim et al., 1991). *A. niger* (X-170) and *A. ochraceus* metabolized ZEA (**63**) to α-zearalanol (α-ZAOL, **72**) and β-zearalanol (β-ZAOL, **73**). *Saccharomyces cerevisiae* (NRRL Y2034) metabolized ZEA (**63**) to zearalanone (ZAA, **71**), while *S. rimosus* (NRRL 2234) converted ZEA into 8'-(*S*)-hydroxyzearalanone (**80**). *Cunninghamella bainieri* (ATCC 9244B) metabolized ZEA (**63**) to 2, 4-dimethoxyzearalenone (**81**) and 2-methoxyzearalenone (**82**) (Fig. 1-15) (El-Sharkawy and Abul-Hajj, 1988b). The

transformation of ZEA (**63**) to α- and β-zearalenols (**67**, **68**), zearalanone (**71**), α-zearalanol (α-ZAOL, **72**), β-zearalanol (β-ZAOL, **73**) and 2-methoxyzearalenone (**82**) cannot be considered as detoxification as they showed more or similar estrogenic effect as zearalenone (**63**) in bioassays using rat uterine estrogenic receptors (El-Sharkawy and Abul-Hajj, 1988b). However, the phytotoxicity of these metabolites, as well as, the parent compound ZEA (**63**) were not tested on plants.

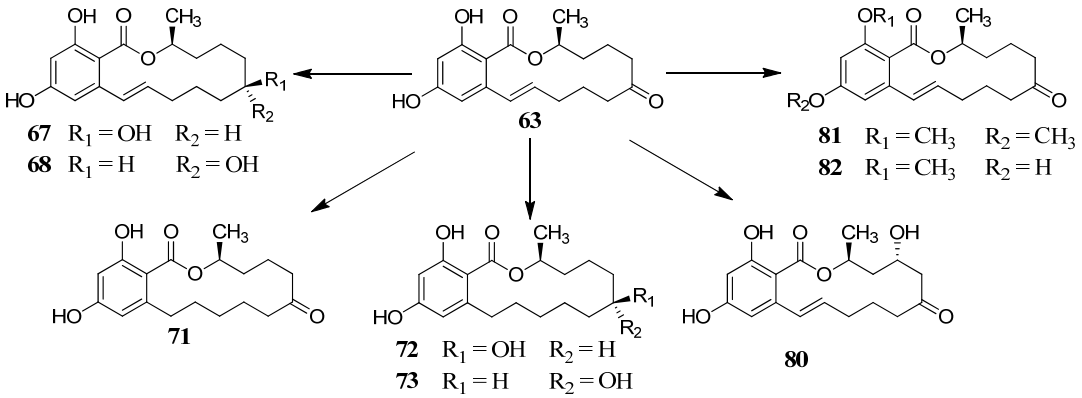

Figure 1-15: Metabolism of zearalenone (**63**) through reduction, hydroxylation and methylation by microorganisms (El-Sharkawy and Abul-Hajj, 1988b; El-Sharkawy, Selim et al., 1991).

The metabolism of ZEA (**63**) was studied in *A. thaliana* seedlings. *A. thaliana* is susceptible to cereal plant ear blight fungal pathogens (Urban, Daniels et al., 2002). Several metabolic pathways of ZEA (**63**) were detected including: glycosylation, sulfation and reduction. The metabolites (17 compounds) were detected and identified by LC-MS/MS analysis: ZEA-4-glucoside (**77**), ZEA-4-sulfate (**79**), α-zearalenol (α-ZAOL, **67**), β-zearalenol (β-ZAOL, **68**), α-4-zearalenol-glucoside (α-ZOL, **83**), β-4-zearaleno-glucoside (β-ZOL, **90**), ZEA-4-malonylglucoside (**87**), α-zearalenol-4-malonylglucoside (**84**) and β-zearalenol-4-malonylglucoside (**91**). In addition di- and tri- substituted saccharide derivatives of ZEA (**88** and **89**), and ZOL (**87**, **92** and **93**) were detected and predicted to diglucoside, triglucosides or glucosyl-xylosyl derivatives; however the exact configuration was not clear (Fig.1-16) (Berthiller, Lemmens et al., 2007; Berthiller, Werner et al., 2006). The glucosylation of ZEA (**63**) to ZEA-4-glucoside (**77**) in *A. thaliana* was catalyzed by UDP-glucosyltransferase UGT7363. The encoding gene was cloned and expressed in *S. cerevisiae* (Berthiller, Hametner et al., 2009; Poppenberger, Berthiller et al., 2006). Similarly, *S. cerevisiae* expressing

sulfotransferase gene for conversion of ZEA (**63**) to ZEA-4-sulfate (**79**) was formed (Schweiger, Berthilleret al., 2008). However, the use of yeast expressing either sulfotransferase gene or *Arabidopsis* UDP-glucosyltransferases is not recommended to decontaminate food rich in ZEA (**63**). Although ZEA-4-glucoside (**77**) and ZEA-4-sulfate (**79**) did not show oestrogenic effect, these metabolites can restore their oestrogenic activity in the gut of swine and rat, respectively by hydrolysis to ZEA (**63**) (Gareis, Bauer et al., 1990; Plasencia and Mirocha, 1991). On the other hand, the effect of ZEA (**63**) and its metabolites on plants were not studied. However, the phytotoxicity of ZEA (**63**) and its metabolites on plants is not reported so far.

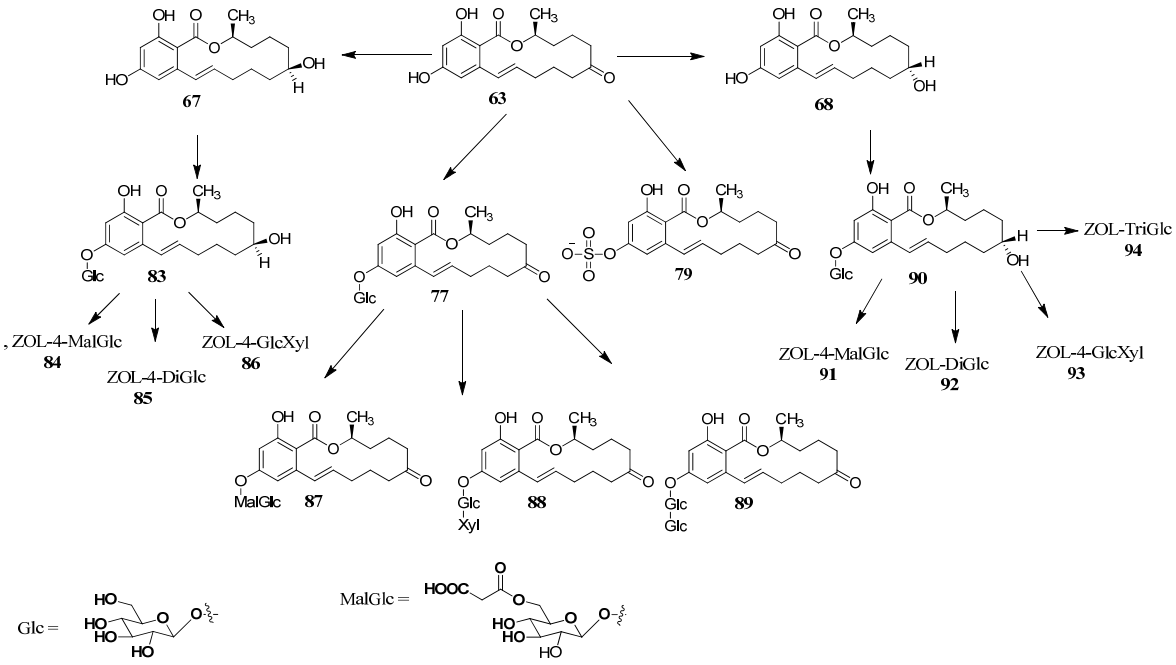

Figure1-16: Metabolism of zearalenone (**63**) by *Arabidopsis thaliana* seedling. (Berthiller, Lemmens et al., 2007; Berthiller, Werner et al., 2006).

In addition to the previous metabolic pathways reported for ZEA (**63**) metabolism by plants and microbes, ZEA (**63**) was detoxified through the hydrolysis of its lactone ring. Among 150 microorganisms screened for their ability to detoxify ZEA (**63**), liquid culture of *Gliocladium roseum* NRRL 1859 metabolized ZEA (**63**) to a mixture of **96** and **97** (Fig. 1-17) (El-Sharkawy and Abul-Hajj, 1988a). Later, Kakeya et al. (Kakeya, Takahashi-Ando et al., 2002) reported a similar metabolic pathway by the fungus *Clonostachy rosea* IFO 7063 that transformed ZEA (**63**) to the less toxic (less estrogenic) metabolite **96**. The reaction involved the

hydrolysis of the lactone ring of ZEA (**63**) forming the intermediate **95**, followed by its decarboxylation to **96** (Fig. 1-17) (Kakeya, Takahashi-Ando et al., 2002). The enzyme catalyzing the biotransformation of ZEA (**63**) to **96** (lactonohydrolase, ZHD101) was purified to homogeneity from *C. rosea* IFO 7063. The gene *ZHD101* was cloned and expressed in *E. coli* and *Schizosaccharomyces pombe* where lactonohydrolase was detected (Takahashi-Ando, Kimura et al., 2002; Takahashi-Ando, Ohsato et al., 2004; Takahashi-Ando, Tokai et al., 2005). In addition, transgenic rice plants were able to detoxify ZEA to **96** (Higa-Nishiyama, Takahashi-Ando et al., 2005; Higa, Kimura et al., 2003).

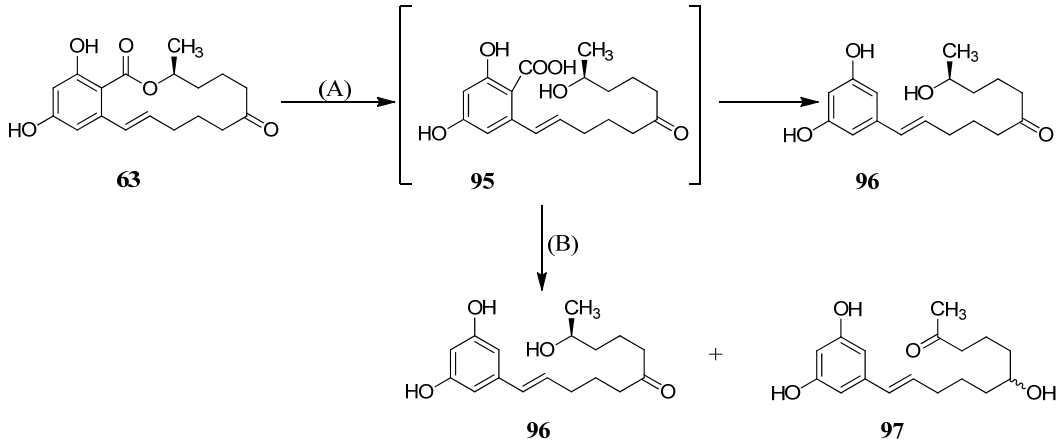

Figure 1-17: Detoxification of the mycotoxin zearalenone (ZEN, **63**): (A) by zearalenone lactonohydrolase (ZHD101) from *Clonostachy rosea* IFO 7063 (Ando et al., 2002; Kakeya, Takahashi- Takahashi-Ando, Kimura et al., 2002); (B) by *Gliocladium roseum* NRRL. 1859 liquid culture (El-Sharkawy and Abul-Hajj, 1988a).

1.3.2 Production of phytoalexins and phytoanticipins

1.3.2.1 Phytoalexins

The term phytoalexins was coined by Műller and Bőrger in 1940 (Műller and Bőrger, 1940) to indicate chemical compounds that are produced by plant cells because of invasion by a parasite. Their studies showed that the protection of susceptible cultivars of potato (*Solanurn tuberosum*) against infection with a virulent race of *Phytophthora infestans* (potato late blight) can be afforded by pre-inoculation of tuber tissue with a race of *P. infestans* to which the potato cultivars are resistant. The resistance to fungal infection was attributed to the production of

antimicrobial compounds that inhibited the growth of the fungus. The production of these antimicrobial compounds (phytoalexins) was found to occur only in infected tubers (inducible) but not in healthy ones. However, the structure of these metabolites was not determined (Müller and Borger, 1940). Later, in 1960 the structure of the first phytoalexin pisatin (**98**) isolated from the pods of the garden pea *Pisum sativum* inoculated with the spores of the fungus *Sclerotinia fructicola* was determined (Cruickshank and Perrin, 1960; Perrin and Bottomley, 1962). The production of phytoalexins is not only restricted to pathogenic attack but was also observed after different abiotic stress, e.g. UV irradiation and heavy metals. Consequently, phytoalexins are defined as "antimicrobial inducible secondary metabolites produced *de novo* by plants in response to biotic and abiotic stresses". Phytoalexins have antimicrobial effect against fungi and bacteria and are important components of plant defenses against pathogenic attack (Mansfield and Bailey, 1982).

Transgenic plants that express genes for the biosynthesis of phytoalexins were found to show increased resistance against plant pathogens. For example, the introduction of the gene responsible for the biosynthesis of the phytoalexin resveratrol (resveratrol synthase) either from peanut or grapevine to alfalfa, tobacco, tomato, rice and barley enhanced the disease resistance of these plants against *Phoma medicanginis* (fungal pathogen for alfalfa) (Hipskind and Paiva, 2000), *Botrytis cinerea* (general plant pathogen) (Hain, Reif et al., 1993), *Pyricularia oryzae* (fungal pathogen to rice) (Stark-Lorenzen, Nelke et al., 1997) and *P. infestans* (fungal pathogen to tomato) (Thomzik, Stenzel et al., 1997). The ability of some plant pathogens to detoxify phytoalexins by producing detoxifying enzymes that can convert phytoalexins to non- or less toxic compounds can impart virulence for these pathogens (Pedras and Ahiahonu, 2005; VanEtten, Sandrock et al., 1995). In several cases, a positive correlation was observed between the presence of the phytoalexin detoxifying enzymes and the pathogenicity and/or virulence of the pathogen to plants (VanEtten, Straney et al., 2001). For example, isolates of *Nectria haematococca* virulent on *P. sativum* have the ability to degrade the pea phytoalexin pisatin (**98**) to non-toxic metabolite **99** using pisatin demethylase (Pda) (Fig. 1-18). Most of the isolates that are highly virulent on the garden pea (*Pisum sativum* L.) were able to degrade the pea phytoalexins pisatin (**98**) (Van Etten, Pueppke et al., 1975; VanEtten, Matthews et al., 1989). Mutants of *N. haematococca* deficient in *Pda* were less virulent on pea in comparison to wild type (Wasmann and VanEtten, 1996). Furthermore, the transformation of the maize pathogen

Cochliobolus heterostrophus with *N. haematococca* MPVI pisatin-detoxifying gene resulted in transformants that were more virulent on pea than the original isolates (Schäfer, Straney et al., 1989).

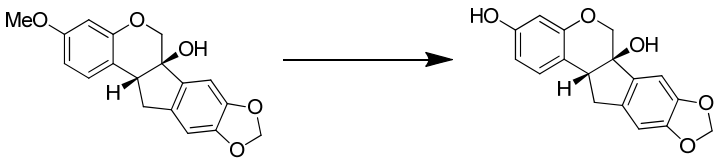

98 **99**

Figure 1-18: Detoxification of the pea phytoalexin (+)-pisatin (**98**) to desmethylpisatin (**99**) by the fungal pathogen: *Nectria haematococca* (Van Etten, Pueppke et al., 1975).

Numerous phytoalexins with various chemical structures were isolated from different plants as a result of different kinds of stresses. However, phytoalexins produced by the same plant family members share similar structures (Mansfield and Bailey, 1982, Grayer and Harborne, 1994). For example, phytoalexins belonging to the family Fabaceae are isoflavones, stilbenoids or pterocarpan; Solanaceae produces phytoalexins with bicyclic sesquiterpene skeleton (Grayer and Harborne, 1994) and crucifer plants produce indole containing phytoalexins (Pedras, Yaya et al., 2011). Cruciferous phytoalexins are derived from the amino acid *S*-tryptophan. So far, 45 phytoalexins were isolated from cruciferous plants. They were isolated from different cultivated plants as *Brassica* species and wild plants as *E. gallicum*, *T. salsuginea* and *A. thaliana*. Recently Pedras et al. published a comprehensive review of cruciferous phytoalexins (Pedras, Yaya et al., 2011). For this reason only work relevant to this thesis will be reviewed. Examples of phytoalexins produced by crucifers and pertinent to this thesis are listed in Table 1.1.

Table 1-1: Phytoalexins of some crucifers: *Sinapis alba* (white mustard), *Arabidopsis thaliana* (thale cress), *Thellungiella salsuginea* (salt cress), *Erucasrum gallicum* (dog mustard), *Brassica rapa* (turnip) and *B. napus* (rutabaga).

plant	Phytoalexins	References for first isolation
Sinapis alba L. (white mustard)	Sinalbin A (**100**), sinalbin B (**101**) and sinalexin (**103**).	(Pedras and Smith, 1997; Pedras and Zaharia, 2000).
Arabidopsis thaliana L. (thale cress)	Camalexin (**105**), rapalexin A (**106**).	(Pedras and Adio, 2008; Tsuji, Jackson et al., 1992).
Thellungiella salsuginea Pallas. (salt cress)	Rapalexin A (**106**), wasalexin A (**107**), wasalexin B (**108**), 1-methoxybrassenin B (**109**), biswasalexin A1 (**110**), biswasalexin A2 (**111**).	(Pedras and Adio, 2008; Pedras, Zheng et al., 2009).
Erucastrum gallicum O.E. Schulz. (dog mustard)	Erucalexin (**112**), 1-methoxyspirobrassinin (**113**), indolyl-3-acetonitrile (**115**), arvelexin (**116**).	(Pedras and Ahiahonu, 2004; Pedras, Suchy et al., 2006).
Brassica rapa L. (turnip)	Cyclobrassinin (102), brassilexin (**104**), spirobrassinin (**114**), brassinin (**117**), 4-methoxybrassinin (**118**), 1-methoxybrassinin (**119**), 4-methoxydehdrocyclobrassinin (**120**).	(Monde and Takasugi, 1991).
Brassica napus L. (rutabaga)	Brassilexin (**104**), spirobrassinin (**114**), brassinin (**117**), 1-methoxybrassinin (**119**), rutalexin (**121**), brassicanal A (**122**), brassicanate A (**123**), isalexin (**124**).	(Pedras, Montaut et al., 2004).

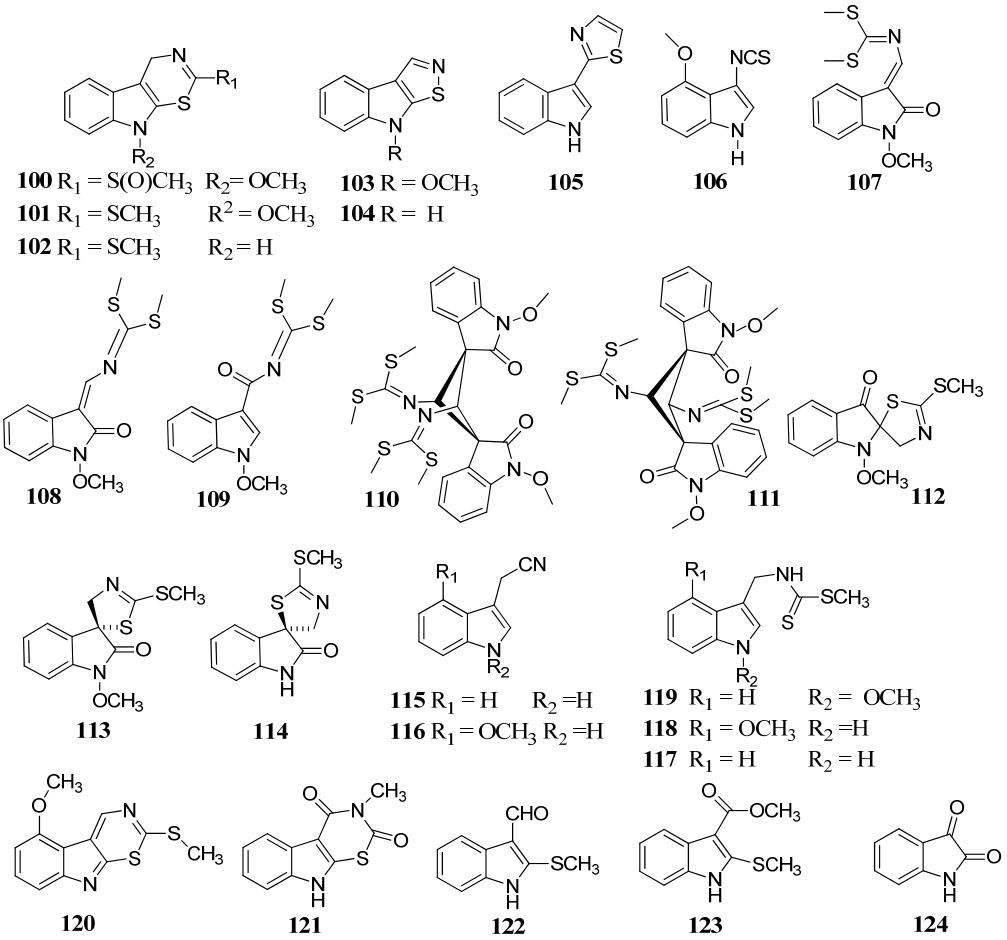

Figure 1-19: Structure of phytoalexins listed in Table 1-1: sinalbin A (**100**); sinalbin B (**101**); sinalexin (**103**); camalexin (**105**); rapalexin A (**106**); wasalexin A (**107**); wasalexin B (**108**); 1-methoxybrassenin B (**109**); biswasalexin A1 (**110**), biswasalexin A2 (**111**); 1-methoxybrassinin (**117**); erucalexin (**112**); 1-methoxyspirobrassinin (**113**); indolyl-3-acetonitrile (**115**); arvelexin (**116**); 4-methoxydehydrocyclobrassinin (**120**); 4-methoxybrassinin (**118**); brassilexin (**104**); cyclobrassinin (**102**); spirobrassinin (**114**); brassinin (**117**); brassicanal A (**122**); brassicanate A (**123**); rutalexin (**121**); isalexin (**124**) (Pedras, Yaya et al., 2011).

1.3.2.2 Phytoanticipins

The term phytoanticipins was coined by Mansfield to indicate a group of plant antimicrobial secondary metabolites which, in contrast to phytoalexins, exist in the healthy plants or produced solely from pre-existing constituents, i.e. constitutive not inducible. The phytoanticipins concentrations might increase during the time of infection (VanEtten, Mansfield et al., 1994). Phytoanticipins includes a wide diversity of plant secondary metabolites as saponins, flavonoids, alkaloids, glucosinolates, cyanogentic glucosides and toxic non-protein amino acids

(Grayer and Harborne, 1994; Morant, Jørgensen et al., 2008; Osbourn, 1996). Phytoanticipins are present in plant cells either in their conjugated or non-conjugated/hydrolyzed form. Examples of phytoanticipins that exist in their non-conjugated forms are flavonoids (e.g. naringenin and xanthohumol), phenolic compounds (as chlorogenic acids, ferulic acid and sinapic acid) and saponins as avenacins and aescin (Grayer and Harborne, 1994). On the other hand, glucosinolates, cyanogentic glucosides, benzoxazinoid glucosides and avenacosides as avenocosides are examples of phytoanticipins that exists in their conjugated form that are activated by the effect of β-glucosidases (Morant, Jørgensen et al., 2008). Phytoanticipins are reported to have a role in plant defense mechanisms against phytopathogens. For example, the triterpenoidal saponin avenacins were detected in oat roots and reported to protect the plant from "take-all" disease caused by the fungal pathogen *Gaeumannomyces graminis* var. *tritici*. Cereals not producing avenacin, e.g. *T. aestivum*, *Avena longiglumis* are susceptible to infection by *G. graminis* var. *tritici* (Osbourn, Clarke et al., 1994). However, fungal isolates producing saponin-detoxifying enzyme avenacinase that detoxify avenacin A-1 (**125**) to less toxic metabolites (**126-128**) as *G. graminis* var. *avenae* are virulent on oat plants (Fig. 1-20) (Crombie, Crombie et al., 1986). Furthermore, mutants of *G. graminis* var. *avenae* lacking avenacinase are not virulent on oats (Bowyer, Clarke et al., 1995).

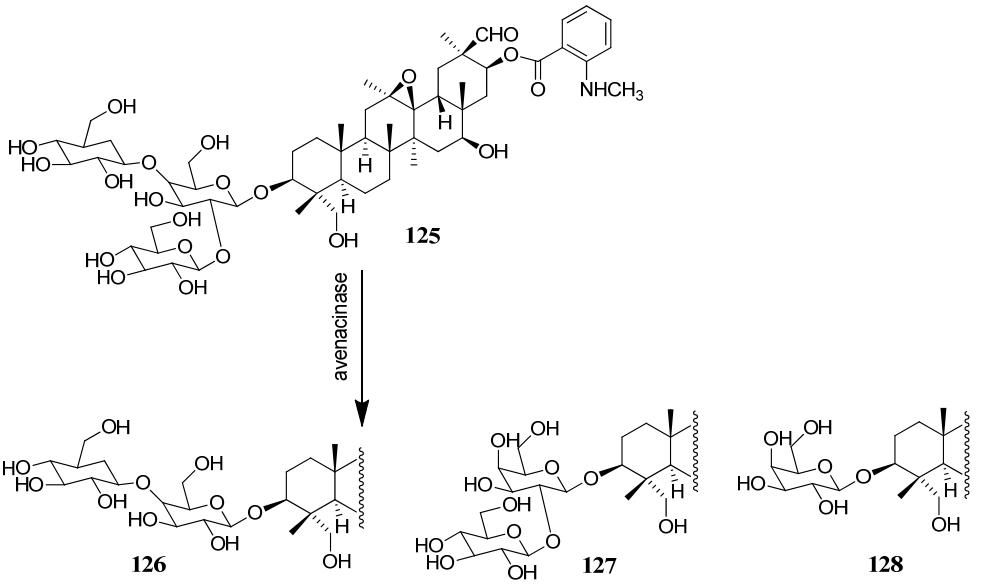

Figure 1-20: Detoxification of the triterpenoidal saponin avenacin A-1 (**125**) by the saponin-detoxifying enzyme (avenacinase) (Crombie, Crombie et al., 1986).

Glucosinolates (**129**) are the major phytoanticipins produced by crucifers (Fahey, Zalcmann et al., 2001). Glucosinolates are divided to three classes; aliphatic glucosinolates, aromatic glucosinolates and indolyl glucosinolates based on their amino acid precursors. Glucosinolates are stored in plant cells separately from glucosinolates degrading enzyme (myrosinases). The damage of plant cells by insects resulted in the release of myrosinases that become in contact with glucosinolates. Myrosinases can hydrolyze glucosinolates to glucose (**131**) and thiohydroximate-*O*-sulfonate (**130**) that undergoes spontaneous rearrangement to give different products (**132**-**134**), of which nitriles (**133**) and isothiocyanates (**132**) are the most toxic to plant pathogens (Fig. 1-21), as they showed antifungal, antibacterial and insect deterrent effect against different plant pathogens (Agerbirk, De Vos et al., 2009; Bones and Rossiter, 2006; Halkier and Gershenzon, 2006; Vig, Rampal et al., 2009). In addition to the role of glucosinolates as phytoanticipins, glucosinolates are biosynthetic precursors for the biosynthesis of most cruciferous phytoalexins. Glucobrassicin (**155**) is a precursor of the phytoalexins wasalexin A (**107**) and B (**108**) (Pedras, Yaya et al., 2010) and many others (Pedras and Yaya, 2013). In addition to glucosinolates, other indolyl derivatives were reported as phytoanticipins from crucifers e.g. ascorbigen (**135**), dihydroascorbigen (**136**), dihydroneoascorbigen (**137**), 3-methylsulfonylmethylindole (**138**) and 1-methoxy-3-methoxymethylindole (**139**) (Pedras, Zheng et al., 2008) (Fig. 1-22).

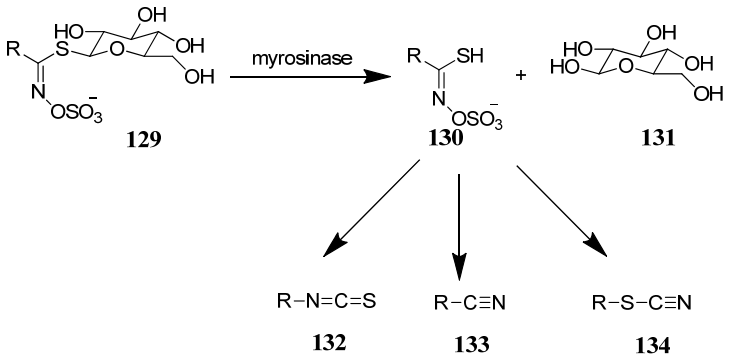

Figure 1-21: Hydrolysis of glucosinolates (**129**) (Fahey, Zalcmann et al., 2001).

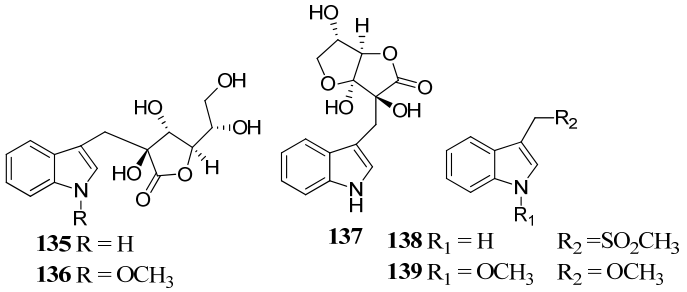

135 R = H
136 R = OCH_3

137

138 R_1 = H R_2 = SO_2CH_3
139 R_1 = OCH_3 R_2 = OCH_3

Figure 1-22: Chemical structures of cruciferous phytoanticipins: Ascorbigen (**135**), dihydroascorbigen (**136**), dihydroneoascorbigen (**137**), 3-methylsulfonylmethylindole (**138**) and 1-methoxy-3-methoxymethylindole (**139**) (Pedras, Zheng et al., 2008).

1.4 Analytical methods to detect products of phytotoxin metabolism in plant tissues

As discussed in the previous section, some plants have the ability to detoxify fungal phytotoxins during fungal attack. Investigation of the metabolism of phytotoxins by susceptible and resistant plant species has important applications in developing disease resistant plants (Karlovsky, 1999). The detection of products of phytotoxin transformation as well as their accurate quantification in plant tissues poses difficulties. Plant tissues are rich in secondary metabolites that can interfere with the detection of phytotoxins and their products. Phytotoxin metabolites are usually produced in low concentrations and in some cases more than one metabolite is produced, e.g. destruxin B (**1**) (presented in section 1.3.1.4) (Pedras, Montaut et al., 2003; 1999; Pedras, Zaharia et al., 2001). Several approaches and techniques can be used for the analysis of phytotoxin metabolism in plants (e.g. the use of radioisotope compounds, mass spectrometry and NMR) which will depend on the particular case as described below.

Radioisotope detection is a widely used strategy to trace, identify and quantify phytotoxin products in plant tissues. In general, radiotracing is a very efficient method for studying metabolism because of high sensitivity and simple quantification. However, the time and cost for synthesizing and purifying radiolabeled compounds, as well as concerns about environmental contamination and human or animal health, restricts its wide application. For example, ^{3}H-HC toxin was used to study the metabolism of HC-toxin in susceptible and resistant maize (Meeley and Walton, 1991). ^{14}C-labelled compounds were used to study the metabolism of phytotoxins

destruxin B (**1**) and homodestruxin B (**2**) by different crucifers (Pedras, Montaut et al., 2003; Pedras, Zaharia et al., 1999; Pedras, Zaharia et al., 2001) and eutypine by grapevine tissue (Colrat, Deswarte et al., 1999).

Mass spectrometry (MS) is another technique that is widely used for studying xenobiotic metabolism in plant tissues. In this technique, the detection of metabolites of interest requires comparison of MS chromatograms of extracts of plants treated with phytotoxin or xenobiotic with MS chromatograms of controls (extracts plants not treated with phytotoxin). Phytotoxin and their products, if present, are only detected in chromatograms of extracts of treated plants not in control. To enhance mass spectrometers capability they are usually used in combination with different chromatographic techniques e.g. gas chromatography (GC-MS) and liquid chromatography (LC-MS) that resolve the complex metabolite profiles and allow the detection of the metabolites in small concentrations without the need of having a purified sample.

Liquid chromatography (LC) combined with mass spectrometry (MS) is a powerful tool for qualitative and quantitative analyses of organic molecules from various matrices, and the use of this technique is very common in bioanalytical studies of plant extracts, blood and urine samples (Scalbert, Brennan et al., 2009). Electrospray ionization (ESI) and matrix-assisted laser desorption (MALDI) spectrometers in combination with quadrepole time-of-flight (QTOF) or ion trap mass analyzers are widely used for the detection of phytotoxin and xenobiotic products in plant tissues. These techniques allow the detection of the molecular ion(s) that corresponds to the products. In addition MS instruments with high-resolution mass measurement provide a tool for the accurate mass measurements that lead to a potential molecular formula, and thus to candidate chemical structures for the detected products. For example, HPLC-ESI-MS analysis was applied for the qualitative and quantitative determination of the metabolism of phytotoxin eutypine (**29**) by different tissues of grapevine into eutypinol (**30**) (Afifi, Monje et al., 2004). The metabolism of the phytotoxin eutypine (**29**) to eutypinol (**30**) and eutypinic acid (**31**) by different fungi was studied using HPLC-ESI-MS (Christen, Tharin et al., 2005).

Tandem mass LC-MS/MS analysis and multistage LC/ $(MS)^n$ analysis is another strategy widely used for the structure determination of products of phytotoxins transformation. HR-tandem mass spectrometry has the advantage of measuring the exact mass and obtains candidate molecular formula for the fragment ions generated from the parent molecules. In many cases, the fragmentation patterns of reference compounds are used as the base for the identification of the

unknown compounds that can be either different plant metabolites with similar skeletons to the reference compounds or the metabolites of the parent compound. The characteristic fragmentation patterns of different plant metabolites allow their unambiguous identification. MS/MS and multistage tandem mass (MS^n) analysis has the advantage of distinguishing between different isomers as they give different fragmentation patterns. For example, HPLC-ESI-MS/MS analysis of the crude extract of *Linum usitatissimum* allowed the identification of eighteen lignans by comparison of their fragmentation patterns with some reference lignans (Schmidt, Alfermann et al., 2008). ESI-MS combined with $(MS)^n$ was applied for the identification of the new alkaloid dehydrocoydaline from *Rhizoma coptidis* (Wang, Liu et al., 2004) and identification of isomeric triterpenoidal saponins from extracts of *Aralia elata* leaves (Guo, Zhang et al., 2009).

In addition to radiotracing and mass spectrometry, nuclear magnetic resonance (NMR) spectroscopy is a powerful technique for the identification and quantitative analysis of plant metabolites. In contrast to mass spectrometry, NMR is a non-destructive technique; however, it is much less sensitive than mass spectrometry (MS) (Pan and Raftery, 2007). The commonly used NMR nuclei for the detection of plant metabolites are ^{1}H, ^{19}F, ^{31}P and ^{13}C. In routine work ^{1}H NMR, ^{13}C NMR as well as 2D NMR techniques are widely used for the elucidation of the purified compounds. However, this approach is time-consuming and requires a lot of effort for the chromatographic isolation of the pure metabolites in sufficient amounts for NMR analysis. To detect phytotoxin products the use of NMR is so far restricted to identification of pure metabolites as these metabolites are produced in very small amounts and are difficult to detect in plant extracts. In addition to the use of ^{1}H and ^{13}C nucleus for the detection of xenobiotics and their degradation products by plants, ^{19}F NMR and ^{31}P NMR are used for studying the metabolism of fluorinated pesticides (Tront and Saunders, 2007) and organophosphorous insecticides (Lu, Sun et al., 2007) by plant extracts, respectively.

1.5 Conclusion

In conclusion, plant-pathogen interactions are complex, usually initiated by the pathogen attack to colonize plant cells. Secondary metabolites from both sides, pathogens and plants, play a crucial role in determining the outcome of the interaction (Dixon, 2001; Schäfer, 1994). Plant

pathogenic fungi can produce phytotoxins that facilitate their invasion and colonization of plant tissues and in response to pathogen attack plants can produce antifungal metabolites (phytoanticipins and phytoalexins) as well as phytotoxin detoxifying enzymes. The ability of some plants to detoxify phytotoxins can impart resistance to these plants against their pathogenic fungi. Studying the interaction of phytotoxins with resistant and susceptible plants gives the opportunity to analyze the metabolic transformations of phytotoxins (if present) and characterize enzymes and genes involved in phytotoxin transformations. This knowledge can be applied in breeding plants resistant to pathogens producing toxins and in engineering disease resistant plants. The detection of phytotoxin detoxification pathways is not restricted to plants. Several microorganisms were reported to convert phytotoxins to less toxic metabolites. These microorganisms are of value as biocontrol agents or for biotechnological production of resistant crops. It is noteworthy that, in addition to the role of phytotoxins in plant diseases, some are reported as food contaminant (i.e. mycotoxins) resulting in diseases for humans and animals. Although hundreds of phytotoxins were isolated and characterized from pathogenic fungi, few were studied for their metabolism.

Cruciferous plants are subjected to attack by several pathogenic fungi that cause severe economical losses in their yield. *L. maculans* and *A. brassiceae*, the causative agents of crucifers blackleg and blackspot, are phytotoxins producing pathogens. Several phytotoxins were isolated from these pathogens and suggested to be involved in pathogenesis of both fungi as destruxin B (**1**) and sirodesmin PL (**13**). Studying the metabolism of these phytotoxins is an important strategy in detecting plant defense mechanisms related with detoxification.

1.6 Aldoxime dehydratases

Aldoxime dehydratases (aldoxime hydro-lyases) are enzymes that catalyze the dehydration of aldoxime to their corresponding nitrile (Fig. 1-23). This group of enzymes is widely distributed in bacteria, fungi, plants and mammals.

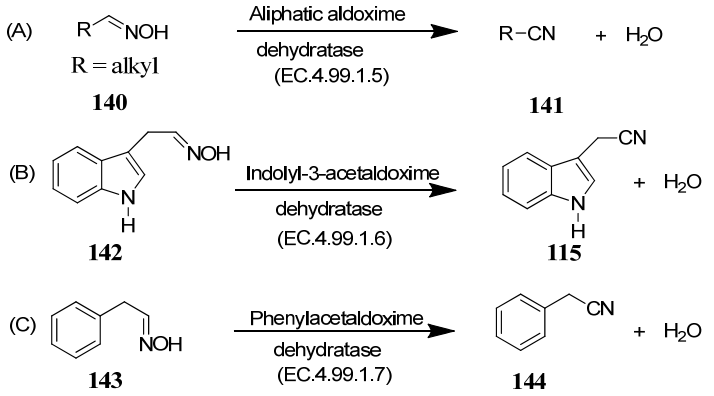

Figure 1-23: Classes of aldoxime dehydratases: (A) aliphatic aldoxime dehydratase; (B) indolyl-3-acetaldoxime dehydratase; (C) phenylacetaldoxime dehydratase.

Aldoxime dehydratases belong to dehydratase-heme superfamily (EC.4.99.1.X). According to their substrate specificity, they are classified into three classes: aliphatic aldoxime dehydratase (EC.4.99.1.5), indolyl-3-acetaldoxime dehydratase (EC.4.99.1.6) and phenyacetaldoxime dehydratase (EC.4.99.1.7). To date four aliphatic aldoxime dehydratases have been purified and identified in microorganisms: OxdRG from *Rhodococcus globerulus* A-4 (Xie, Kato et al., 2003), OxdA from *Pseudomonas chlororaphis* B23 (Oinuma, Hashimoto et al., 2003), OxdRE from *Rhodococcus* sp N-771(Kato, Yoshida et al., 2004) and OxdK from *Pseudomonas* sp. K-9 (Kato and Asano, 2006). Aliphatic aldoxime dehydratases displayed strong preference for aliphatic aldoximes (**140**) as *E/Z*-cyclohexanecarboxaldehyde oximes, *E/Z-n*-butanal oximes (**199**), *E/Z*-isobutanal oximes (**200**) and *E/Z-n*-hexanal oximes (*E/Z-n*-capronaldoximes) over aromatic aldoximes. Indolyl-3-acetaldoxime dehydratases catalyze the conversion of indolyl-3-acetaldoxime (**142**, IAOx) to indolyl-3-acetonitrile (**115**, IAN). Indolyl-3-acetaldoxime dehydratase (IADGf) was partially purified and characterized from the fungus *Gibberella fujikuroi* (Shukla and Mahadevan, 1968; Shukla and Mahadevan, 1970). Recently, indolyl-3-

acetaldoxime dehydratase (IADSs) was purified from the plant pathogenic fungus *S. sclerotiorum*. It is the only representative of IADs that has been purified and identified so far (Pedras, Minic et al., 2010). Phenylacetaldoxime dehydratases showed higher substrate specificities towards phenylacetaldoxime (**143**) than aliphatic and indolyl oximes. So far, two examples of this group were reported: OxdB from *Bacillus* sp strain Oxd-1 (Kato, Nakamura et. al, 2000) and OxdFG from *Fusarium graminearum* (Kato and Asano, 2005).

In addition, cytochrome P450 dependant aldoxime dehydratases belonging to CYPX superfamily (EC.1.14.13.X) were detected in plants and mammals. To date three aldoxime dehydratases belonging to CYP450 were studied: indolyl-3-acetaldoxime dehydratase from *A. thaliana* (CYP71A13) that was expressed in *E. coli* (Nafisi, Goregaoker et al., 2007); 4-hydroxyphenylacetaldoxime monooxygenase from *Sorghum bicolor* L. Moench (EC.1.14.13.68) (Bak, Kahn et al., 1998; Kahn, Bak et al., 1997) and the CYP3A4 NF25 from human liver that was expressed in *S. cerevisiae* (EC.1.14.13.X) (Boucher, Delaforge et al., 1994).

In the following sections aldoxime dehydratases will be discussed based on their origin, aldoxime dehydratases from microorganisms and cytochrome P450 dependant aldoxime dehydratases from plants and mammals.

1.6.1 Aldoxime dehydratases from microorganisms

1.6.1.1 Distribution and physiological roles

Aldoxime dehydratases are widely distributed in microorganisms, including bacteria, and fungi. Kato and colleagues (Kato, Ooi et al., 2000) screened aldoxime dehydratases in 975 microorganisms including: 55 genera of bacteria, 22 genera of yeasts, and 37 genera of fungi using phenylacetaldoxime (**144**, PAOx) and pyridine-3-carboxaldehyde oxime (PyOx) as substrates. Among the tested microorganisms, aldoxime dehydratases were detected in 37 genera of bacteria, 31 genera of fungi and 2 genera of yeast (Kato, Ooi et al., 2000).

Aldoxime dehydratases together with nitrile-hydrolyzing enzymes were proposed to be encoded by aldoxime metabolizing genes that catalyze the metabolism of aldoximes to the corresponding carboxylic acids (aldoxime-nitrile metabolic pathway) via two pathways (Fig. 1-24) (Kato, Ooi et al., 2000). The first pathway includes nitrilases (Nit, EC 3.5.5.1) that hydrolyse

nitriles to the corresponding carboxylic acids. The second pathway includes nitrile hydratases (NHase, EC 4.2.1.84) together with amidases (Ami, EC 3.5.1.4). Nitrile hydratases hydrate nitriles into amides that are further hydrolyzed to the corresponding acid with the release of ammonia by the action of amidases (Fig. 1-24).

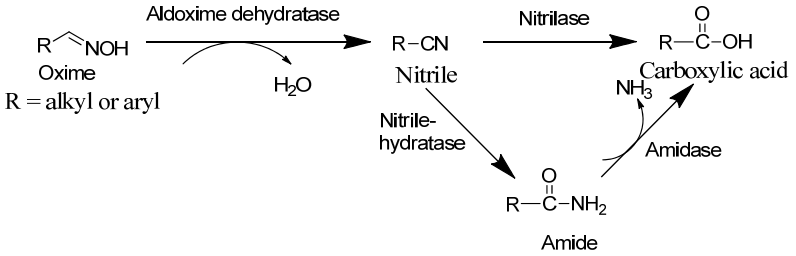

Figure 1-24: Aldoxime-nitrile metabolic pathway in microorganisms (Kato, Ooi et al., 2000).

Despite of the wide distribution of aldoxime dehydratases in microorganisms, their physiological roles are not clear. *S. sclerotiorum* metabolized IAOx (**142**) to IAA (**146**) via IAN (**115**) (Fig. 1-25). IAOx (**142**) showed antifungal activity against *S. sclerotiorum*, while IAN (**115**) and IAA (**146**) had no effect on the fungal growth suggesting that indolyl-3-acetaldoxime dehydratase from *S. sclerotiorum* (IADSs) is a general xenobiotic detoxifying enzyme (Pedras, Minic et al., 2010). Similarly the metabolism of IAOx (**142**) by the cruciferous pathogenic fungi *L. maculans* isolate BJ 125 (virulent on canola) and *Rhizoctonia solani* Kuhn was proposed to be a detoxification process as IAA (**146**) showed no antifungal effect against either species, in contrast to IAOx (**142**) and IAN (**115**) (Pedras and Montaut, 2003).

The metabolism of IAOx (**142**) by the plant pathogenic fungi *L. maculans* isolate BJ 125 (virulent on canola), *L. maculans* isolate Laird 2 (virulent on brown mustard), the general plant pathogens *S. sclerotiorum* and *R. solani* to IAA (**146**) via IAN (**115**) was found to be similar to the metabolism of IAOx by crucifers. On the other hand, the insect pathogenic fungus *Beauveria bassiana* metabolized IAOx (**142**) via a different metabolic pathway that includes the formation of **146** via tryptophol (**145**) (Fig. 1-25) (Pedras and Montaut, 2003). In crucifers IAOx (**142**) is an intermediate involved in the biosynthesis of different cruciferous defense metabolites e.g. phytoalexins and phytoanticipins (Glawischnig, Hansen et al., 2004; Pedras, Montaut et al., 2001; Pedras and Yaya, 2013;) as well as the plant hormone IAA (**146**) (Sugawara, Hishiyama et al., 2009). The similarity between plant pathogenic fungi and crucifers in metabolizing IAOx (**142**)

via similar intermediates is interesting. The isolation and identification of aldoxime dehydratases from pathogenic fungi provide the opportunity to compare these enzymes with plant aldoxime dehydratases to obtain an insight into their co-evolution.

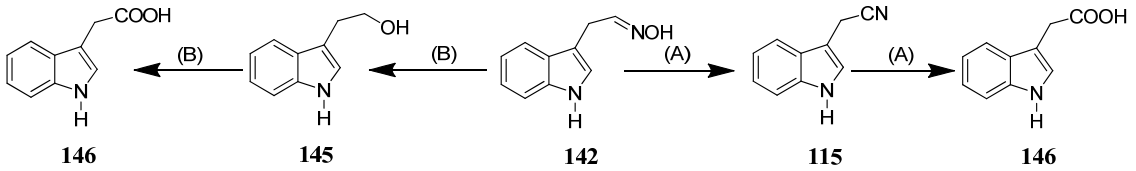

Figure 1-25: Metabolism of *E/Z*-indolyl-3-acetaldoximes (IAOx, **142**) by: (A) the plant pathogenic fungi *Sclerotinia sclerotiorum*, *Leptosphaeria maculans* and *Rhizoctonia solani*; (B) the insect pathogenic fungus *Beauveria bassiana* (Pedras and Montaut, 2003).

1.6.1.2 Purification and characterization

The first attempt to purify an aldoxime dehydratase (indolyl-3-acetaldoxime dehydratase) from the phytopathogenic fungi *Gibberella fujikuroi* (IADGf) was reported by Shukla and Mahadevan (Shukla and Mahadevan, 1968; Shukla and Mahadevan, 1970). The enzyme was partially purified using either ammonium sulfate precipitation or anion-exchange chromatography (Shukla and Mahadevan, 1970; Shukla and Mahadevan, 1968). Further purification of the enzyme was not successful due to the loss of activity during storage and dialysis. The enzyme was activated by pyridoxal-5'-phosphate (PLP), dehydroascobic acid and ferrous ions and showed high substrate specificity towards IAOx (**142**) with K_m value of 0.17 mM (Shukla and Mahadevan, 1968; Shukla and Mahadevan, 1970). Since those times until the end of 1990s, no work on aldoxime dehydratases was reported. Later, in 2000, Asano and colleagues (Kato, Nakamura et al., 2000) reported the purification of the first aldoxime dehydratase (OxdB) from CFE of *Bacillus* sp. strain OxB-1. The gene encoding OxdB was cloned and expressed in *E. coli* for further studies. OxdB was active towards several aryl- and alkyl-aldoximes such as *Z*-PAOx (**143**), *Z*-3-phenylpropanal oxime (**149**), *E/Z*-4-phenylbutanal oximes, *E/Z*-*n*-butanal oximes (**199**), *E/Z*-propanal oximes and *E/Z*-isovaleraldehyde oximes. OxdB showed substrate preference towards *Z*-PAOx (**143**), and hence it was classified as phenylacetaldoxime dehydratase (Kato, Nakamura et al., 2000). After this work, several aldoxime dehydratases were cloned and purified from different bacteria and fungi. For example, the aliphatic aldoxime dehydratases OxdA, OxdK,

OxdRG and OxdRE, were purified from *Pseudomonas chlororaphis* B23 (Oinuma, Hashimoto et al., 2003), *Pseudomonas* sp. K-9 (Kato and Asano, 2006), *Rhodococcus globerulus* A-4 (Xie, Kato et al., 2003) and *Rhodococcus* sp. N-771 (Kato, Yoshida et al., 2004), respectively. OxdRG (Xie, Kato et al., 2003) and OxdRE (Kato, Yoshida et al., 2004) showed highest activity towards *E/Z*-cyclohexanecarboxaldehyde oximes, while OxdK (Kato and Asano, 2006) and OxdA (Oinuma, Hashimoto et al., 2003) showed highest activity towards *E/Z*-isobutanal oximes (**200**) and *E/Z*-butanal oximes (**199**), respectively. In addition two fungal aldoxime dehydratases OxdFG and IADSs were purified from CFE of *F. graminearum* (Kato and Asano, 2005) and *S. sclerotiorum* (Pedras, Minic et al., 2010), respectively. OxdFG showed a wide range of substrate specificities including several aryl and alkylaldoxime e.g.: *Z*-PAOx (**143**), *Z*-3-phenylpropanal oxime (**149**), *E/Z*-IAOx (**142**), *E/Z-n*-butanal oximes (**199**), *E/Z*-valeraldehyde oximes and *E/Z*-isovaleraldehyde oximes and the enzyme was classified as phenylacetaldoxime dehydratase (Kato and Asano, 2005). On the other hand, IADSs from *S. sclerotiorum* displayed the highest activity towards IAOx and it was classified as indolyl-3-acetaldoxime dehydratase (Pedras, Minic et al., 2010). In addition it displayed lower activities against *E/Z*-3-(3-indolyl)propanal oximes (**193**), *E/Z*-4-(3-indolyl) butanal oximes (**194**), *E/Z-p*-hydroxyphenylacetaldoximes and *E/Z*-4-methoxyphenylacetaldoximes, while no activity was detected with *E/Z*-PAOx (**143**) and aliphatic oximes. A list of aldoxime dehydratases from microorganisms, their best substrates and kinetic parameters is presented in Table 1-2.

Aldoxime dehydratases from microorganisms are either inducible or constitutive enzymes. Inducible aldoxime dehydratases require growing the microorganisms in the presence of either aldoximes or nitriles that induce not only aldoxime dehydratases but also the nitrile-hydrolyzing enzymes (Kato, Ooi et al., 2000). For example aldoxime dehydratase OxdRE is induced by the substrate *E*-PyOx, various substrate analogues or nitriles e.g. 3-cyanopyridine, *n*-butyronitrile and isovaleronitrile (**173**) (Kato, Ooi et al., 1998). The purification of OxdB from *Bacillus* sp. strain OxB-1and OxdRG from *R. globerulus* A-4 required growing the bacterial cultures in the presence of 0.05% *Z*-PAOx (**143**) and 0.05% PyOx, respectively (Oinuma, Hashimoto et al., 2003; Xie, Kato et al., 2003). On the other hand, indolyl-3-acetaldoxime dehydratase (IADSs) from *S. sclerotiorum* was constitutively produced by the fungal cultures (Pedras, Minic et al., 2010).

Different protocols were reported for the purification of wild and/or recombinant microbial aldoxime dehydratases. In all cases aldoxime dehydratase activities were reported to

decrease during purification, resulting in low purification yield (2-6%) for OxdRG (Xie, Kato et al., 2003), OxdA (Oinuma, Hashimoto et al., 2003), OxdRE (Kato, Yoshida et al., 2004) and IADSs (Pedras, Minic et al., 2010) and 25% for OxdB (Kato, Nakamura et al., 2000). The loss of activity during purification was attributed to either the loss of the cofactors (e.g. Fe^{2+}, PLP, FMN or protoheme IX) (Oinuma, Hashimoto et al., 2003; Shukla and Mahadevan, 1970) or change of oxidation state of iron-heme protein since the protein is active only when iron-heme is in its ferrous state.

Aldoxime dehydratases from microorganisms are either monomeric proteins as OxdB (42 kDa), OxdFG (34 kDa) and IADSs (44 kDa) or dimeric proteins as OxdRG (76 kDa), OxdA (76 kDa), OxdRE (80 kDa), OxdK (85 kDa). Aldoxime dehydratases showed optimal activities in the pH range 5-8 and temperature optima of 30 °C for OxdB, OxdRG and OxdRE, 20 °C for OxdK, 25 °C for IADSs and 45 °C for OxdA. A comparison between aldoxime dehydratases from microorganisms including prosthetic groups, cofactors, optimal temperature and pH and the molecular weight and number of subunits for each enzyme are summarized in (Table 1-2).

The effect of different compounds as activators or inhibitors of aldoxime dehydratases were reported. A list of aldoxime dehydratases activators and inhibitors are listed in (Table 1-3). In general aldoxime dehydratases were inhibited by -SH reagents (e.g. NEM, PHMB, PTC, iodoacetate and DTNB), electron donors (e.g. hydroquinone, tetramethylphenylamine, pyrogallol and tetramethylphenylamine), carbonyl reagents (e.g. phyenylhydrazine and hydroxylamine) and metal chelating agents (e.g. EDTA, tiron, EGTA, penicillamine and hydroxyquinoline). On the other hand, aldoxime dehydratase activities are enhanced by reducing agents as glutathione, ascorbic acid, and dehydroascorbic acid and anaerobic condition and electron acceptors e.g. flavins, vitamin K_3 and duraquinone (Table 1-3). However, thiol reagents displayed different effects against aldoxime dehydratases. For example, IADGf, OxdB were inhibited by thiol compounds e.g. 2-mercaptoethanol and DTT (Kato, Nakamura et al., 2000; Shukla and Mahadevan, 1968), while OxdRG, OxdFG and OxdK activities were enhanced by 2-mercaptoethanol, DTT, thioglycerol and L-cysteine (Kato and Asano, 2005; Kato and Asano, 2006; Xie, Kato et al., 2003). Metal ions displayed various effects on aldoxime dehydratases. Generally, aldoxime dehydratases are activated by Fe^{2+} and inhibited by Cu^{+}, Cu^{2+}, Co^{2+}, Zn^{2+}, Cd^{2+}, Hg^{2+}, Sn^{2+}, Pb^{2+}, Ag^{+}, Al^{3+} and As^{3+}. However, the divalent ions Zn^{2+}, Sn^{2+}, Co^{2+} activated

OxdRE while OxdB activated by Sn^{2+}. The effect of different compounds on aldoxime dehydratases activities are summarized in Table 1-3.

T**able 1-2:** Sources, best substrates, kinetic parameters (V_{max} and K_m), prosethetic groups and cofactors, pH and temperature optima , molecular weights and number of subunits of aldoxime dehydratases: IADGf from *Gibberellins fujikuroi*, OxdB from *Bacillus* sp. strain Oxd-1, OxdRG from *Rhodococcus globerulus* A-4, OxdA from *Pseudomonas chlororaphis* B23, OxdRE from *Rhodococcus* sp N-771, OxdFG from *Fusarium graminearum*, OxdK from *Pseudomonas* sp. K-9 and IADSs from *Sclerotinia sclerotiorum*.

Enzyme	Source	Substrate	V_{max} (units/mg)[c]	K_m (mM)	Prosthetic group/ cofactor(s)	PH optima / temp optima	Subunits/ Molecular weigh (kDa) (native / Sequence)
IADGf [b]	*Gibberellins Fujikuroi* [d]	Indolyl-3-acetal-doxime		0.17	NS / PLP	pH 7/ 30 °C	Monomer (42/40)
OxdB [a]	*Bacillus* sp strain OxB-1[e]	*Z*-Phenyl-acetaldoxime	19.5	0.87	Protoheme IX / FMN	pH 7/ 30 °C	dimmer (76.2/39.8)
OxdRG [a]	*Rhodococcus globerulus* A-4 [f]	*E/Z*-Cyclohexane-carboxaldehyde oximes	0.38	1.13	Protoheme IX	pH 8/ 30 °C	dimmer (76.2/ 40.1)
OxdA [a]	*Pseudomonas chlororaphis* B23 [g]	*E/Z-n*-Butanal oximes		0.25	Protoheme IX	pH 5.5 / 45 °C	dimmer (80/44.7)
OxdRE [a]	*Rhodococcus* sp N-771 [h]	*E/Z*-Cyclohexane-carboxaldehyde oximes	4.76	0.99	Protoheme IX	pH 8 / 30 °C	monomer (34/44)

Enzyme	Source	Substrate	V_{max} (units/mg) [c]	K_m (mM)	Prosthetic group/ cofactor(s)	PH optima / temp optima	Subunits/ Molecular weigh (kDa) (native / Sequence)
OxdFG [a]	*Fusarium graminearum* [i]	*Z*-Phenyl-acetaldoxime	1.46	19.3	Protoheme IX	pH 5.5 / 25 ^{o}C	dimmer (85/ 44.5)
OxdK [a]	*Pseudomonas* sp. K-9 [j]	*E/Z*-Isobutanal oximes	0.53	5.87	Protoheme IX	pH 7 / 20 ^{o}C	monomer 44 (native)
IADSs [b]	*Sclerotinia sclerotiorum* [k]	*E/Z*-Indolyl-3-acetaldoximes	0.22	0.29	NS	pH 7.2 - 7.5 / 25 ^{o}C	monomer 44 (native)

[a] As His6-tagged form, [b] Wild-type protein, [c] One unit (U) of the enzyme activity is defined as the amount of enzyme that catalyzes the conversion of the substrate to the product at a rate of 1µmol/min. [d] (Shukla and Mahadevan,1968; Shukla and Mahadevan, 1970), [e] (Kato and Nakamura et al, 2000), [f] (Xie, Kato et al., 2003), [g] (Oinuma, Hashimoto et al., 2003), [h] (Kato, Yoshida et al., 2004), [i] Kato and Asano, 2005), [j] (Kato and Asano, 2006), [k] (Pedras, Minic et al., 2010). NS: not studied.

Table 1-3: Effect of various compounds on the activity of aldoxime dehydratases: IADGf from *Gibberellins fujikuroi*, OxdB from *Bacillus* sp. strain Oxd-1, OxdRG from *Rhodococcus globerulus* A-4, OxdA from *Pseudomonas chlororaphis* B23, OxdRE from *Rhodococcus* sp N-771, OxdFG from *Fusarium graminearum*, OxdK from *Pseudomonas* sp. K-9 and IADSs from *Sclerotinia sclerotiorum.*

Enzyme	Inhibitors	Activators
IADGf [a]	SH reagents (NEM, PHMB, PTC), Metal chelating reagents, THFA, cysteine, 2-mercaptoethanol, phenylacetaldoxime and KCN	Glutathione, ascorbic acid, dehydroascorbic, dihydrofolic acid PLP, Fe^{+2}.
OxdB [b]	Metal chelating reagents (EDTA, EGTA, Tiron, 8-hydroxyquinoline), carbonyl reagents (phenylhydrazine, hydroxylamine), electron donors (hydroquinone, tetramethylphenylamine) and ferri- and ferrocyanides, DTT, 2-mercaptoethanol, SH reagents (NEM, PHMB, DTNB)	Anaerobic condition, reducing agents (Na_2S, $Na_2S_2O_4$), Fe^{+2}, Sn^{+2}, SO_3^{-2}, NaN_3, FMN
OxdRG [c]	Cu^{1+}, Cu^{2+}, Co^{2+}, Zn^{2+}, Cd^{2+} , Hg^{2+}, Sn^{2+}, Pb^{2+} , Ag^{+}, Al^{3+} (for all metals at 1 mM), phenylhydrazine, SH reagents (iodoacetate, DTNB, PHMB), metal chelating reagents (8-hydroxyquinoline, penicillamine), electron donors (pyrogallol, tetramethylphenylamine, …)	Anaerobic conditions reducing agents (Na_2S,$Na_2S_2O_4$, Na_2SO_3, $Na_2S_2O_5$, 2-mercaptoethanol, thioglycerol, cystamine, cysteine), flavins (FMN, FAD, riboflavin) Fe^{+2}, Fe^{+3}, $K_3[Fe(CN)_6]$, electron acceptors (vit K_3, and duroquinone) , 0.1 mM of the following metals (Cu^{1+}, Cu^{2+}, Co^{2+}, Zn^{2+}, Cd^{2+}),
OxdA [d]	$CuCl_2$, $HgCl_2$, $AgNO_3$, hydroxylamine, phenylhydrazine,NaN_3, KCN, metal chelating agents (diethyldithiocarbamate , EDTA)	Anaerobic conditions reducing agents ($Na_2S_2O_4$)

Enzyme	inhibitors	Activators
OxdRE [e]	[EDTA, Tiron, (absence of Na_2S)] phenylhydrazine, *E*-benzaldehyde oxime, phenylacetone, acetophenone, electron donors (pyrogallol,…), Cu^{1+}, Cu^{2+}, As^{3+}, Hg^{2+}, Cd^{2+}	reducing agents (Na_2S,Na_2S2O_4, Na_2SO_3, $Na_2S_2O_5$, 2-mercaptoethanol, thioglycerol, cystamine, cysteine), PLP, ascorbic acid, Fe^{+2}, Fe^{+3}, Zn^{2+}, Sn^{2+}, Co^{2+}, $K_3[Fe(CN)_6]$, electron acceptors (vit K_3, and duroquinone, FMN, FAD, riboflavin), [EDTA, Tiron, D-cycloserine-(presence of Na_2S)]
OxdFG [f]	Hydroxylamine, phenylhydrazine, Fe^{+3}, Cu^{+}, Ag^{+}, electron donors (trimethylhydroquinone, *p*-phenylenediamine, and dimethoxybenzidine)	reducing agents ($Na_2S_2O_4$),thiol compounds (2-mercaptoethanol, thioglycerol, L-cysteine, $FeSO_4$, $K_4[Fe(CN)_6]$
OxdK [g]	Hydroxylamine, phenylhydrazine, KCN, Fe^{3+}, Cu^{+}, Ag^{+}, Cr^{3+}, Co^{2+}, Pb^{2+}	Electron acceptors (FMN), reducing agents (DTT, Na_2S)
IADSs [h]		Anaerobic conditions, reducing agents ($Na_2S_2O_4$), Fe^{+2}

[a] (Shukla and Mahadevan,1968; Shukla and Mahadevan, 1970), [b] (Kato and Nakamura et al, 2000), [c] (Xie, Kato et al., 2003), [d] (Oinuma, Hashimoto et al., 2003), [e] (Kato, Yoshida et al., 2004), [f] (Kato and Asano, 2005), [g] (Kato and Asano, 2006), [h] (Pedras, Minic et al., 2010), DTNB: dithiobis (2-nitrobenzoic acid); NEM: *N*-ethylmaleimide; PHMB: *p*-hydroxymercuribenzoate; PLP: pyridoxal-5'-phosphate; PTC: phenylthiocyanate; THFA: tetrahydrofolic acid.

1.6.1.3 Aldoxime dehydratase active sites

Based on spectroscopic analysis, sequence alignment and site directed mutagenesis, the active site of aldoxime dehydratases was proposed to include the prosthetic group protoheme IX in addition to two histidine residues, proximal and distal histidine (Kato and Asano, 2003; Kato, Nakamura et al., 2000) (Fig. 1-26). The oxidation state of the protoheme iron is crucial for

aldoxime dehydratase activity. Thus, aldoxime dehydratases exist in two forms: active form and resting form. In the active form, iron is in its reduced state (Fe^{2+}), while in the resting form iron is in its oxidized state (Fe^{3+}). Aldoxime dehydratases displayed activities only in their active forms but not in the resting forms. The active form of the enzyme can be converted (oxidized) to the resting form during purification and storage processes resulting in the loss of the activity. However, the oxidation reaction is reversible and activity can be restored by reducing agents (Kobayashi, Yoshioka et al., 2005; Oinuma, Hashimoto et al., 2003).

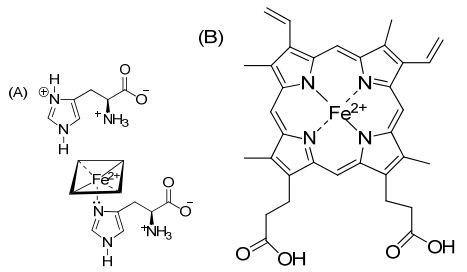

Figure 1-26: Active site of aldoxime dehydratases showing: (A) the prosthetic group protoporphyrin IX with iron in its ferrous state as well as distal and proximal histidine residues; (B) chemical structure of protoheme IX (Sawai, Sugimoto et al., 2009).

Amino acid sequence comparisons of aldoxime dehydratases revealed the presence of conserved histidine residues suggesting their role in catalysis. Spectroscopic analysis and site-directed mutagenesis studies of OxdA and OxdB indicated the involvement of two histidine residues in catalysis, proximal and distal histidine. Proximal histidine binds directly to the heme while the distal histidine is the catalytic residue. For OxdB, His-306 and His-282 were assigned as the distal and proximal histidine residues, respectively (Kobayashi, Yoshioka et al., 2005). In case of OxdA, both His-320 and His-299 were proposed as the distal and proximal histidine residues, respectively (Oinuma, Ohta et al., 2004). Both H320A and H299A mutants exhibited no activity in comparison to the wild-type OxdA (Konishi, Ishida et al., 2004, Oinuma, Kumita et al., 2005). The heme content of H320A and wild-type OxdA were identical (1.06 mol heme/mol subunit) however, the heme content for H299A mutant was zero, indicating the role of His-299 in holding the heme (Oinuma, Ohta et al., 2004). Mutation of catalytic histidine residues H306A mutant for OxdB (Kobayashi, Yoshioka et al., 2005) and H320A mutant for (OxdA) (Oinuma, Kumita et al., 2005) resulted in the accumulation of the substrate-coordinated mutants in the reaction mixture

that showed similar absorption spectra to the wild enzyme-substrate intermediate confirming the role of the distal histidine residues in catalysis.

The crystal structure of substrate-free OxdRE and the *n*-butanal oxime and *n*-propanal oxime bound OxdRE confirmed the proposed structure of the aldoxime dehydratase active site. The crystal structure of OxdRE revealed the presence of a protoheme IX and proximal histidine, which was in agreement with data obtained from spectroscopy, and site directed mutagenesis. The active site was hydrophobic in nature and a histidine residue in the distal pocket of heme was detected and assigned as the distal histidine residue, which was important for catalysis and consistent with previous mutagenic studies (Sawai, Sugimoto et al., 2009).

1.6.1.4 Catalytic mechanism

Aldoxime dehydratases are examples of heme proteins that do not catalyze a redox reaction hence; their mechanism of action was of great interest. In addition, they are the only example of heme proteins that have hydro-lyase catalytic activity. The mechanism of catalysis of aldoxime dehydratases was proposed based on studies using various aldoxime dehydratases: OxdB using phenylacetaldoxime as substrate, OxdA using *n*-butanal oxime as substrate and OxdRE using *n*-butanal oxime and *n*-propanal oxime as substrates. Different approaches as well as several techniques were involved in these studies including: sequence alignments of different aldoxime dehydratases, site-directed mutagenesis, spectroscopic analysis, X-ray crystallography and quantum mechanics coupled with molecular mechanics (QQ/MM) calculations. Based on these studies the mechanism for alkylaldoxime dehydratases was proposed to be via three major steps: Binding of aldoxime to the enzyme forming Michaelis-complex (intermediate I, OS-1 complex), dehydration step that involved the elimination of the aldoxime hydroxyl group with the formation of intermediate II and finally the deprotonation step with the release of nitrile. These steps are described in detail in the following sections.

Binding of aldoxime to the enzyme

The reaction mechanism of aldoxime dehydratase starts with binding of the oxime via its nitrogen atom (*N*-coordination) to the iron heme (Fe^{+2}) forming the enzyme-substrate complex (Intermediate I, Michaeils complex, OS-I) (Fig. 1-27). Stopped-flow UV rapid scan analysis of

wild-type ferrous OxdB in the presence of phenylacetaldoxime (Kobayashi, Yoshioka et al., 2005), as well as OxdA (Oinuma, Kumita et al., 2005) and OxdRE (Kobayashi, Pal et al., 2006) in the presence of butanal oxime showed that these enzymes rapidly transformed their substrates (~ 3 - 64 ms) into species with blue-shifted electronic absorption maxima (Soret peaks) at λ_{max} = 415-416 nm. The absorbances of these enzyme-bound species are typical for *N*-coordinate Fe (II) heme. The substrate-binding intermediates were trapped using enzymes mutated at their catalytic histidine residues. The reaction of ferrous H306A mutant of OxdB with phenylacetaldoxime (Konishi, Ishida et al., 2004; Oinuma, Kumita et al., 2005) and ferrous H320A mutant of OxdA with butanal oximes (Konishi, Ishida et al., 2004; Oinuma, Kumita et al., 2005) resulted in the accumulation of substrate-coordinated mutants in the reaction mixture that was detected on standard UV-visible spectrometer and showed similar absorption spectra to the wild enzyme-substrate intermediate (Kobayashi, Yoshioka et al., 2005; Konishi, Ishida et al., 2004; Oinuma, Kumita et al., 2005; Oinuma, Ohta et al., 2004). In contrast to the ferrous form of aldoxime dehydratase, aldoxime dehydratases in their ferric states binded to their substrates via oxime oxygen atom (*O*-coordination) forming dead-end complexes that are inactive for catalysis (Fig. 1-27). The electronic absorption spectra of ferric OxdA (Oinuma, Kumita et al., 2005), OxdB (Kobayashi, Yoshioka et al., 2005;) and OxdRE (Kobayashi, Pal et al., 2006) using phenylacetaldoxime and butanal oxime as substrates resulted in stable red-shifted Soret peaks that corresponded to *O*-coordination between ferric heme and oxime. Furthermore, the crystal structure of the substrate bound OxdRG using *n*-butanal oximes and *n*-propanal oxime as substrates confirmed the *N*- and *O*- coordination of OxdRE with heme iron in its reduced and oxidized forms, respectively (Sawai, Sugimoto et al., 2009).

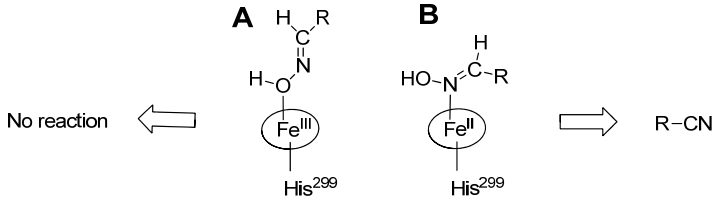

Figure 1-27: Structures of the aldoxime-heme complex: (A) ferric forms (dead-end complex, inactive form); (B) ferrous form (Michaelis complex, active form).

Dehydration and detection of intermediate OS-II

For aliphatic aldoxime dehydratases OxdA and OxdRE, the substrate-complex intermediate (Fe (II)-N-(OH)=CH-R, OS1) using *n*-butanal oxime as substrate was proposed to be converted to the nitrile by the distal histidine residue (Oinuma, Kumita et al., 2005). Based on resonance Raman spectroscopy (RR spectroscopy) of the ferrous and CO-bound forms of wild-type OxdA and its His320A mutants as well as the pH profile of wild-type OxdA, the distal histidine residue His-320 was proposed to protonate the OH group of the substrate butanal oxime bound to the heme iron. This protonation drives the loss of water from the aldoxime, which is followed by abstraction of the β-proton of the aldoxime with the formation of triple bond and release of the product (Fig. 1-28) (Konishi, Ishida et al., 2004; Oinuma, Ohta et al., 2004; Oinuma, Kumita et al., 2005).

The abstraction of OH group from aldoxime by His-320 resulted in the formation of intermediate II (OS-II). This intermediate was detected by UV-vis spectrum after reaction of ferrous OxdA in low concentration (5 μM) with high concentration of butanal oxime (200 mM) (Konishi, Ohta et al., 2006). However, OS-II was not detected in reactions using lower concentrations of butanal oximes (≤ 50 mM). Based on UV-vis spectrum and RR spectroscopic analysis OS-II was suggested as ferryl-oxo heme intermediate that showed a direct binding of the substrate nitrogen atom to the heme iron of the OxdA (Fig. 1-28) (Konishi, Ohta et al., 2006). However, QM/MM calculations based on X-ray crystal structure of the aliphatic aldoxime dehydratase (OxdRE) excluded the ferryl heme nature of OS-II and indicated the formation of ferric heme iron intermediate (Fig. 1-28) (Liao and Thiel, 2012; Pan, Cui et al., 2012).

The abstraction of OH group by the catalytic histidine residue to form water is controlled by the proper orientation of the heme-bound substrate. Crystal structure of substrate-free and *n*-butanal oxime and *n*-propanal oxime bound to OxdRE showed that the proper orientation of the heme-bound substrate is controlled by the hydrogen bonding between the OH group of the aldoxime and the side chains of Ser-219 and His-320 as well as the hydrogen bonding between Glu-143, Arg-178 and His-320. Site directed mutagenesis of any of these amino acids resulted in 70-90 % loss in activity in comparison to wild-type activity (Sawai, Sugimoto et al., 2009).

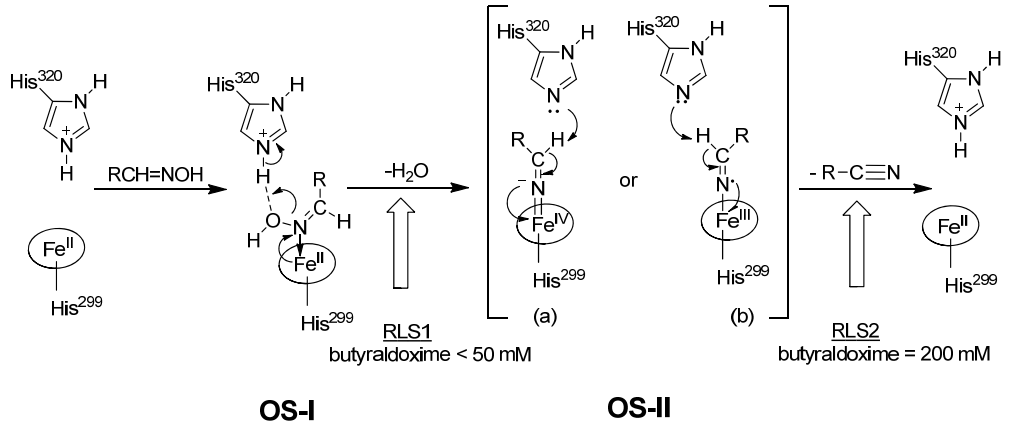

Figure 1-28: Proposed catalytic mechanisms of aldoxime dehydratase showing the intermediates OS-I and proposed structures of OS-II: (a) highly oxidized ferryl-oxo heme OS-II intermediates (Konishi, Ohta et al., 2006); (b) ferric heme iron OS-II intermediates (Pan, Cui et al., 2012). In addition it shows the change in the rate liming-step (RLS1 & RLS2) in the presence of low and high concentration of the substrate *n*-butanal oxime (Konishi, Ohta et al., 2006; Liao and Thiel, 2012; Pan, Cui et al., 2012)

Deprotonation step and release of the product

How is the intermediate OS-II converted to nitrile? As shown in Fig. 1-28, the elimination of the β-proton from OS-II intermediate resulted in the formation of the triple bond and the release of nitrile. The abstraction of the β-proton of the intermediate OS-II was proposed to be assisted by weak base in the enzyme active site (Konishi, Ishida et al., 2004). However, the crystal structure of the OxdRE ruled out this hypothesis (Sawai, Sugimoto et al., 2009). On the other hand QQ/MM calculations of the Michaelis complex (OS-I) of OxdRE with *n*- butanal oxime showed that His-320 acts as a general base that abstracts the β-proton of the substrate with the formation of the intermediate OS-II (Fe^{III}por-N=CH-R). The rotation of the substrate about Fe-N bond for 180°, allows the ε nitrogen atom of His-320 to abstract the β-hydrogen of the intermediate OS-II with the formation of the nitrile (Pan, Cui et al., 2012).

The release of the nitrile is achieved via a channel that connects the active site to the surface of the protein. The crystal structure of substrate-free OxdRE showed two conformations for the enzyme, open and closed conformations, which are in equilibrium in solution. The residue Phe-306 monitors the conformational change. In the open conformation, the substrate-binding cavity is connected to the protein surface through a channel that allows the access of the substrate into the binding site and the release of the product to the surface of the protein. The binding of the

substrate to the enzyme active site favoured the closed conformation where the entrance of the channel in the protein surface is closed because of sliding Phe-306 3 Å vertically to the heme plane (Sawai, Sugimoto et al., 2009).

At low oxime concentration, the rate-limiting step of the reaction is the conversion of the intermediate OS-I into OS-II. However, at high oxime concentration the rate-limiting step is the deprotonation of OS-II intermediate (Fig. 1-28). Ferrous OxdA in presence of ~ 50 mM butanal oxime resulted in the accumulation of OS-I intermediate in the reaction mixture (Oinuma, Kumita et al., 2005), whereas the addition of 200 mM butanal oxime to ferrous OxdA resulted in increasing the life time of OS-II (Konishi, Ohta et al., 2006). Based on QQ calculations this change in the rate-limiting step in the presence of high concentration of aldoxime resulted from the release of large amount of water that accumulated in the active site that blocked the deprotonation of OS-II to His-320 (Konishi, Ohta et al., 2006; Pan, Cui al., 2012). The change in the rate limiting step was also observed in the presence of low concentration of butanal oxime (50 mM), and high concentration of butyronitrile (150 mM) suggesting that the change in the rate-limiting step can be a suppression mechanism of the nitrile synthesis as nitrile at high concentration is toxic for *P. chlororaphis* B23 (Konishi, Ohta et al., 2006).

Overall, the mechanism of aldoxime dehydratases is an acid-base mechanism where the catalytic histidine residue acts as a general acid and a general base. First, histidine in its protonated form (general acid) dehydrates the substrate-bound complex (OS-I) with the formation of the intermediate OS-II. Later, the generated deprotonated histidine residue acts as a base and deprotonates OS-II with the formation of the nitrile. However, this mechanism represents aliphatic aldoxime dehydratases (OxdA and OXdRG).

Similarly, the phenylacetaldoxime dehydratase OxdB was proposed to act via acid-base mechanism. The general acid that assists in the dehydration of OS-1 was not assigned while the catalytic histidine residue (His-306) was proposed to abstract the β-proton with the formation of the nitrile (Kobayashi, Yoshioka et al., 2005). OxdB showed five conserved histidine residues with respect to OxdA and it is most likely that histidine is the general acid in this reaction however, this has to be proven. On the other hand and in contrast to aliphatic aldoxime dehydratases FMN was reported as cofactor for phenylacetaldoxime dehydratase OxdB that is essential for the enzyme activity indicating a difference in its mechanism from aliphatic aldoxime dehydratases. In addition, OxdB is a monomeric protein in contrast to known aliphatic aldoxime

dehydratases (OxdA, OxdRG, OxdK and OxdRE) which are dimeric and it showed relatively low sequence similarity (31-33%) with them. The role of FMN in catalysis is not clear. However, FAD was reported as cofactor for 4-hydroxybutyrl-CoA dehydratase from *Clostridium aminobutyricum* that catalyzed the elimination of water via a ketyl radical anion formation (Buckel, Martins et al., 2005). Further studies have to be done to figure out the mechanism.

To date there is no report about the mechanism of indolyl-3-acetaldoxime dehydratases. However, PLP was reported as cofactor for indolyl-3-acetaldoxime dehydratases IADGf from *G. fujikuroi* (Kumar and Mahadevan, 1963) and was proposed to have a structural function as the enzyme activity was not significantly affected by reduction with $NaBH_4$ (Shukla and Mahadevan, 1968; Shukla and Mahadevan, 1970). PLP was reported as cofactors for other dehydratases e.g. L-threonine dehydratases and L-serine dehydratases. It forms a Schiff base with the amino group and assisted in the elimination of α-proton (Hofmeister, Grabowski et al., 1993). PLP did not show any effect on indolyl-3-acetaldoxime dehydratase (IADSs) from *S. sclerotiorum* (Pedras, Minic et al., 2010).

1.6.1.5 Biotechnological applications

Aldoxime dehydratases from microorganisms have been paid much attention as biocatalysts for the synthesis of different nitriles. Nitriles are important starting materials for the synthesis of several pharmaceuticals and organic chemicals. The enzymatic synthesis of nitriles has several advantages in comparison to chemical synthesis. Enzymatic synthesis of nitriles is carried out under mild conditions of moderate temperature and pH, with high efficiency and wide substrate specificity that can be applied for the synthesis of different nitriles. Several examples were reported for the efficient large-scale synthesis of nitriles using aldoxime dehydratases. Phenylacetaldoxime dehydratase (OxdB) from *Bacillus* sp. Strain OxB-1 was expressed in *E. coli* JM 109 and used for the efficient synthesis of several aryl and alkyl nitriles at pH 8.0 and temperature of 30 °C. For example, 3-phenylpropionitrile (3-PPN, **150**) was synthesized in 70% yield from 3-phenylpropionaldehyde (3-PPAH, **147**) and hydroxylamine (**148**) in a water-*n*-butylacetate biphasic system using *E. coli* JM 109/Pox D-90F (Fig. 1-29). The use of the purified phenylpropanal oxime (**149**) in high concentration (0.75 M) increased the yield to 100 % (98 g/L). Additionally 3-phenylacetonitrile as well as several aliphatic nitriles: acetonitrile, propanonitrile,

n-butanonitrile, *n*-valeronitrile, isovaleronitrile and *n*-capronitrile were prepared in 100% yield from the corresponding *E/Z* aldoximes (Xie, Kato et al., 2001).

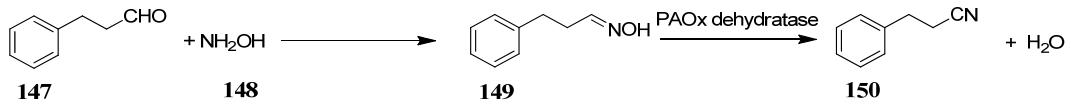

Figure 1-29: Synthesis of 3-phenylpropionitrile (3-PPN, **150**) in *Escherichia coli* JM 109/Pox D-90F cells from 3-phenylpropanal (3-PPAH, **147**) and hydroxylamine (**148**) (Xie, Kato et al., 2001).

Heat-treated cells of *Rhodococcus* sp. strain YH3-3 3 in 0.1 M potassium phosphate buffer containing 1 mM DTT and 5 mM 2-mercaptoethanol at pH 7.0 at 30 °C were used for large scale production of 3-cyanopyridine from *E*- PyOx in 100% yield. In addition the culture can convert the following aryl aldoximes to the corresponding nitriles in a moderate yield: *E*-furan-2-carboxaldehyde oxime (62%), *O*-acetyl-*E*-pyridine-3-carboxaldehyde oxime (73%), *E*/*Z*-*n*-butanal oximes (**199**, 45%), *E*-pyridine-2-carboxaldehyde oxime (30%), *E*-pyrazinecarboxaldehyde oxime (22%), *p*-methylbenzaldehyde oxime (tolualdoxime) (24%) and *Z*- PyOx (20%). (Kato, Ooi et al., 1999).

The use of aldoxime dehydratases as biocatalysts is promising for the synthesis of optically active nitriles. OxdRG (Xie, Kato et al., 2003), OxdRE (Kato, Yoshida et al., 2004) and OxdFG (Kato and Asano, 2005) can convert *E/Z* mandelaldehyde oximes (**151**) to the corresponding nitriles **152**. OxdRG (Xie, Kato et al., 2003), OxdRE (Kato, Yoshida et al., 2004), OxdK (Kato and Asano, 2006) and OxdFG (Kato and Asano, 2005) showed catalytic activity against *E*/*Z*-2-phenylpropanal oximes (**153**) (Fig. 1-30).

Figure 1-30: Catalytic conversion of *E/Z*-mandelaldehyde oximes (**151**) and 2-phenylpropanal oximes (**153**), by different aldoxime dehydratases to corresponding nitriles. The catalytic efficiency (V_{max}/K_m) of each enzyme is presented in brackets (Kato and Asano, 2005; Kato and Asano, 2006; Kato, Yoshida et al., 2004; Xie, Kato et al., 2003).

1.6.2 Cytochrome P450s dependant aldoxime dehydratases

Cytochrome P450s are heme proteins that catalyze redox reactions. However, cytochrome P450s dependant aldoxime dehydratases are examples of cytochrome P450s catalyzing non-redox reactions. So far, all cytochrome P450s dependant aldoxime dehydratases were reported from either plants or animals. In the following sections cytochrome P450 dependent aldoxime dehydratases will be discussed.

1.6.2.1 Aldoxime dehydratases from plants

Plant aldoximes: Detection, physiological roles and metabolism

In plants, aldoximes have important physiological roles. They are biosynthesized from amino acids by cytochrome P450 belonging to CYP79 family. For example IAOx (**142**) derived from tryptophan (**157**) (Mikkelsen, Hansen et al., 2000) is involved in the biosynthesis of the main plant hormone IAA (**146**) through the formation of the intermediates indolyl-3-acetonitrile (**115**) and indolyl-3-acetamide (**156**) (Fig. 1-31) (Sugawara, Hishiyama et al., 2009). IAOx (**142**) is also a precursor of crucifer defense metabolites e.g. biosynthesis of phytoalexins brassinin (**117**) (Pedras, Montaut et al., 2001; Pedras and Yaya, 2013) and camalexin (**105**) (Glawischnig, Hansen et al., 2004) (Fig. 1-31). Other examples of plant metabolites derived from aldoximes are glucosinolates and cyanogenic glycosides. Glucosinolates as glucobrassicin (**155**), benzylglucosinolate (**163**) and 4-methylthiobutylglucosinolate (**164**) are derived from the amino acids tryptophan (**157**) (Mikkelsen, Hansen et al., 2000), phenylalanine (**158**) (Wittstock and Halkier, 2000) and dihomomethionine (**160**) (Hansen, Wittstock et al., 2001) via the formation of the corresponding aldoximes; IAOx (**142**), phenylacetaldoxime (**143**) and 5-methylthiopentanal oxime (**162**), respectively (Fig. 1-32) (Hansen, Wittstock et al., 2001; Mikkelsen, Hansen et al., 2000; Wittstock and Halkier, 2000). Cyanogentic glycosides are derived from aldoximes through the formation of nitriles, e.g. dhurin (**166**) from *Sorghum bicolor* (L.) is derived from tyrosine (**159**) via the formation of *p*-hydroxyphenylacetaldoxime (**162**) and *p*-hydroxyphenylacetonitrile (**165**) (Fig. 1-32) (Bak, Kahn et al., 1998).

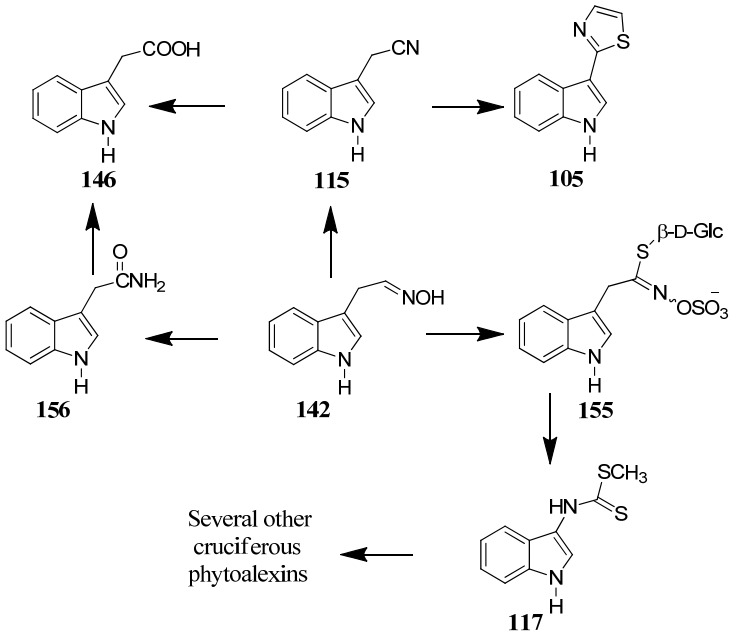

Figure 1-31: *E/Z*-Indolyl-3-acetaldoxime (**142**) is a biosynthetic precursor of cruciferous phytoalexins and the phytoanticipin glucobrassicin (**155**) (Glawischnig, Hansen et al., 2004; Pedras and Yaya, 2013; Sugawara, Hishiyama et al., 2009).

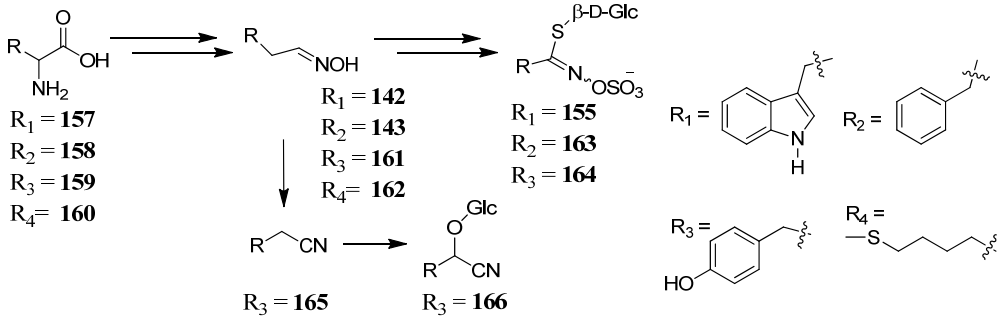

Figure 1-32: Biosynthesis of glucosinolates (Bak, Kahn et al., 1998; Hansen, Wittstock et al., 2001; Mikkelsen, Hansen et al., 2000; Wittstock and Halkier, 2000).

The biosynthesis of plant aldoximes from amino acids as well as their role as precursors of plant metabolites was determined by feeding experiments using labelled amino acids and oximes, isolation and cloning of enzymes included in these steps and mutagenic studies. However, the endogenous detection of aldoximes in plant tissues was reported in few cases and in low conc. For example, IAOx (**142**) was detected by LC-ESI-MS/MS in the fractionated acetone extract of Chinese cabbage seedlings (121 pmol/ gram fresh leaves) and in *Arabidopsis* leaves (1.7 ng/gram fresh leaves) (Bak, Tax et al., 2001; Ludwig-Müller and Hilgenberg, 1988; Sugawara, Hishiyama et al., 2009). The low production of IAOx (**142**) was attributed to its role

as a branching point for the biosynthesis of several metabolites and hence IAOx (**142**) did not accumulate in plant cells. In addition IAOx (**142**) showed low K_m (three μM) and K_s (dissociation constant, 0.2 μM) values with respect to CYPB83B1 (Bak, Tax et al., 2001; Ludwig-Müller and Hilgenberg, 1988; Sugawara, Hishiyama et al., 2009). IAOx (**142**) was biotransformed by different plant tissues (24 plant tissues representing 17 plant families) to either indolyl-3-acetic acid (**146**) or tryptophol (**145**) via formation of several intermediates indolyl-3-acetonitrile (**115**), indolyl-3-acetamide (**156**) or indolyl-3-acetaldehyde (**167**) (Fig.1-33) (Rajagopa and Larsen, 1972). In addition, *B. rapa* roots were reported to metabolize IAOx (**142**) into its oxoindole derivative (**168**) and tryptophol (**145**) (Fig.1-33) (Pedras, Nycholat et al., 2002).

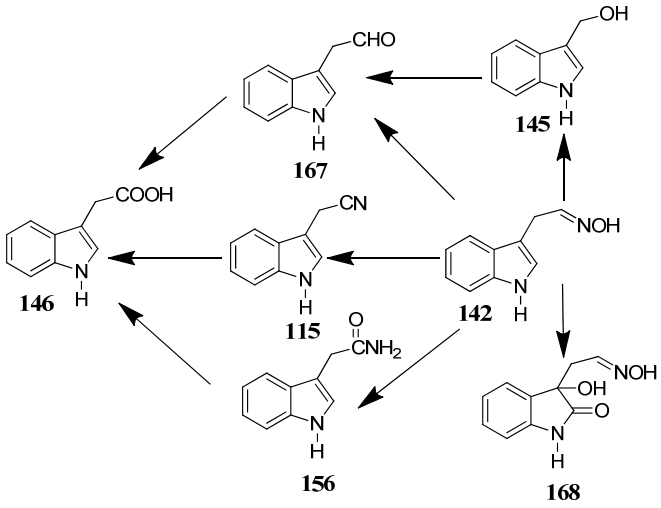

Figure 1-33: Metabolism of indolyl-3-acetaldoxime (**142**) by plants (Pedras, Nycholat et al., 2002; Rajagopa and Larsen, 1972; Sugawara, Hishiyama et al., 2009).

In addition to the role of aldoximes as intermediates in the biosynthesis of different plant metabolites; oximes were isolated and identified from plants (Fig. 1-34). For example, citaldoxime (**169**) was isolated as constitutive metabolite from roots of *C. sinensis* (Dubery and Schabort, 1987) and from pitted regions of γ-irradiation-induced-citrus fruits (*C. sinensis* and *C. lemon*) (Dubery, Holzapfel et al., 1988). Citaldoxime (**169**) showed antifungal activity against *Cladosporium cucumerinum* and was proposed to have a protective role in the oxidative stress in plants (Dubery, Holzapfel et al., 1988). Several aliphatic oximes and nitriles were detected in plant volatiles induced by herbivore attack (i.e. herbivore-induced volatiles). For example, 2-

methylbutanal-*O*-methyloxime (**170**), 3-methylbutanal-*O*-methyloxime (**171**), 2-methylpropanenitrile (isobutyronitrile, **174**), 2-methylbutanonitrile (**172**) and 3-methylbutanonitrile (isovaleronitrile, **173**) were detected in the induced volatiles of cucumber leaves infested with the herbivore spider mite *Tetranychus urticae* (Takabayashi, Dicke et al., 1994). In apple leaves infested with *T. urticae* 3-methylbutanal-*O*-methyloxime (**171**), 2-methylbutanonitrile (**172**), 3-methylbutanonitrile (**173**) and phenylacetonitrile (**144**) were detected as herbivore induced volatiles (Takabayashi, Dicke, et. al, 1991) (Fig. 1-34).

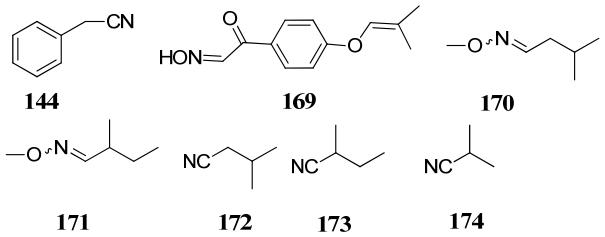

Figure 1-34: Chemical structures of naturally occurring plant oximes and nitriles: citaldoxime (**169**), 2-methylbutanal-*O*-methyloxime (**170**), 3-methylbutanal-*O*-methyloxime (**171**), 2-methylpropanenitrile (**174**), 3-methylbutanalenitrile (**173**), 2-methylbutanalenitrile (**172**) and phenylacetonitrile (**144**) (Dubery, Holzapfel et al., 1988; Takabayashi, Dicke et al, 1991; Takabayashi, Dicke et al., 1994).

Furthermore, the plant toxin L-canaline (**175**), the hydrolytic product of the non-protein amino acid canavanine, was detoxified by *Canavalia ensiformis* via the formation of substituted oxime (**177**) with glycoxylic acid (**176**) (Fig. 1-35) (Rosenthal, Berge et al., 1989).

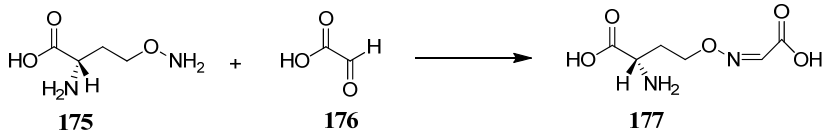

Figure 1-35: Detoxification of L-canaline (**175**) via formation of L-canaline glyoxylate (**177**) (Rosenthal, Berge et al., 1989).

Aldoxime dehydratases

Although aldoxime dehydratases seem to be important in the biosynthesis of different plant metabolites, very little about plant aldoxime dehydratases has been reported. In 1963, Mahadevan reported a soluble indolyl-3-acetaldoxime dehydratase in banana leaves (Mahadevan,

1963). Later, in Chinese cabbage, a membrane bound indolyl-3-acetaldoxime dehydratase was reported using [^{14}C]-IAOx as substrate (Helmlinger, Rausch et al., 1985; Ludwig-Müller and Hilgenberg, 1990). The enzyme was activated by reducing agents e.g. ascorbic acid, DTT and glutathione. The enzyme showed a K_m value of 6.3 μM and pH optima at 6.0 (Helmlinger, Rausch et al., 1985; Ludwig-Müller and Hilgenberg, 1990).

In *A. thaliana* a cytochrome P450 (CYP71A13) was reported to convert IAOx (**142**) to IAN (**115**), an enzymatic step in the biosynthesis of camalexin (**105**). CYP71A13 was expressed in *E. coli*. The recombinant enzyme metabolizes IAOx (**142**) into IAN (**115**) and it seems to be specific to IAOx (**142**) as no metabolism for phenylacetaldoxime (**143**) was reported although its binding to the active site was detected (Nafisi, Goregaoker et al., 2007).

Another cytochrome P450 with aldoxime dehydratase activity (CYP71E) was purified from the microsomes of the etiolated seedlings of *S. bicolour* Moench. The enzyme involved in the biosynthesis of cyanogentic glucoside dhurrin (**166**). A multifunctional enzyme catalyzed the dehydration of *Z*-phenylacetaldoxime to *p*-hydroxyphenylacetonitrile (**165**) as well as the subsequent C-hydroxylation of the resulting nitrile into *p*-hydroxymandelonitrile. The enzyme required NADPH as cofactor (Kahn, Bak et al., 1997). The enzyme was expressed in *E. coli* (Bak, Kahn et al., 1998) and it was specific for tyrosine-derived oximes (Kahn, Fahrendorf et al., 1999).

1.6.2.2 Animal aldoxime dehydratases

Cytochrome P450-dependant dehydration of aldoximes was not restricted to plants but also detected in animals. So far, two animal cytochrome P450s with aldoxime dehydratase activity were reported: the phenobarbital-induced rat liver microsomes (Boucher, Delaforge et al., 1994) and the human liver CYP3A4 NF25 (DeMaster, Shirota et al., 1992). The rat liver microsomes displayed a wide range of substrate specificities against several aryl- and alkyl-aldoximes e.g. benzaldehyde oxime, 4-chlorobenzaldehyde oxime, 4-(hexyloxy)benzaldoxime, phenylacetaldoxime (**143**), *n*-heptanal oxime and *n*-butanal oxime (**199**). The human liver CYP3A4 NF25 was expressed in yeast and it catalyzed the dehydration of *Z*-benzaldehyde oxime into the corresponding nitrile (Boucher, Delaforge et al., 1994).

The physiological role of animal oxime-metabolizing cytoP450s is not clear. However, it was proposed as xenobiotic metabolizing enzyme as it is involved in the metabolism of aldoxime into thiocyanate and their subsequent excretion in the urine (Mathews, Black et al., 1998)

1.6.2.3 Catalytic mechanism

Cytochrome P450s are heme proteins known to catalyze redox reactions. The active site of cytochrome P450s has an iron protoporphyrin IX center coordinating to a cysteine thiolate (Fig. 1-36) (Groves, 2005). However, oxime-metabolizing P450s are an example of non-redox P450s reaction that requires the presence of iron (II) porphyrin for their activity.

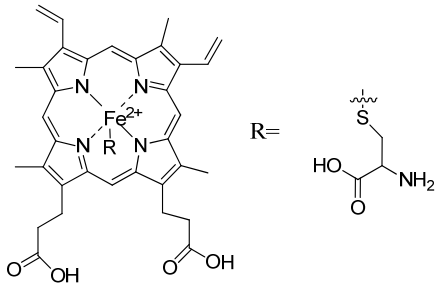

Figure 1-36: Active site of cytochrome P450 showing the prosthetic group protoporphyrin IX with iron in its ferrous state coordinating to cysteine residue (R).

The detailed mechanism of the oxime-metabolizing P450 is not known. No crystal structures of these enzymes are available and the intermediates involved in these reactions were not characterized. In addition, the structure of the heme environment including the proximal legend is not determined. However, the mechanism for the oxime-metabolizing P450s was proposed based on spectroscopic analysis of rat liver microsomes and the recombinant human liver CYP3A4 NF25 in presence of various substrates as well as by developing various iron porphyrin model systems that mimic cytochrome P450-catalyzed dehydration of oximes (Boucher, Delaforge et al., 1994; DeMaster, Shirota et al., 1992; Hart-Davis, Battioni et al., 1998).

Similar to aldoxime dehydratases from microorganisms, the iron porphyrin ring and the oxidation state of the iron is crucial for cytochrome P450s dependant aldoxime dehydratases. The replacement of Fe(II)-porphyrin catalyst by Co(II)-porphyrin, Zn(II)-porphyrin or Mn (II)-porphyrin and/or the removal of the reducing agents from various iron porphyrin model systems resulted in the total loss of the activity for the developed porphyrin systems (Hart-Davis, Battioni et al., 1998). Moreover, the reducing agents NADPH or sodium dithionite and/or anaerobic conditions were essential for plant and animal oxime-metabolizing P450s activities (Boucher,

Delaforge et al., 1994; DeMaster, Shirota et al., 1992; Kahn, Bak et al., 1997; Nafisi, Goregaoker et al., 2007).

The first step in the reaction of oxime-metabolizing P450s is the binding of aldoximes to the enzyme iron. Spectroscopic analysis of rat liver microsomes and the recombinant human liver CYP3A4 NF25 in their ferrous and ferric forms and in the presence of different oximes indicated the binding of the oximes to the iron in the reduced (Fe^{2+}) and oxidized forms (Fe^{3+}), respectively. Similar to aldoxime dehydratases from microorganisms, oxime-metabolizing P450s in their ferric states bind to their substrates via oxime oxygen atom forming dead-end complexes while in their ferrous states they bind to their substrates via oxime nitrogen atom giving enzyme-complex intermediate (ES complex) that can further give products (Boucher, Delaforge et al., 1994). The binding of the aldoxime to the iron via their nitrogen atoms was confirmed by ^1H NMR analysis of the complex [$Fe(TDCPCl_8P)(CH_3CHNOH)_2$] resulting from the reaction of the iron porphyrin $Fe(II)(TDCPCl_8P)$ with acetaldoximes (Hart-Davis, Battioni et al., 1998).

The conversion of the intermediate ES complex formed between cyto iron(II) and aldoxime into the nitrile was proposed to occur via two different mechanisms. In the first mechanism (mechanism A, Fig. 1-37) the OH group of the ES complex is eliminated in the form of water by the assistance of acidic amino acid residue followed by the elimination of the β-proton of the aldoxime and the release of the nitrile, whereas in the second mechanism (mechanism B, Fig. 1-37) the β-proton of the ES complex is abstracted by a basic amino acid residue that is followed by the elimination of the hydroxyl group with the formation of the nitrile (Boucher, Delaforge et al., 1994). The intermediate resulting from the abstraction of either hydroxyl group (mechanism A) or the β-proton (mechanism B) was not characterized for any of the oxime-metabolizing P450s.

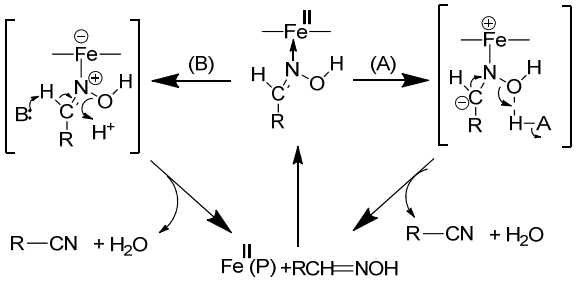

Figure 1-37: Proposed mechanisms A and B of oxime-metabolizing P450s (Hart-Davis, Battioni et al., 1998).

The first mechanism is more likely. In the developed aldoxime dehydration porphyrin systems electron-donating, substituents on porphyrin rings increased the activity of the developed systems. This supports the hypothesis of the charge transfer from the Fe(II) to the aldoxime C=N-OH moiety in the transition state of the reaction that facilitated the removal of OH with the formation of highly oxidized heme cyto P450 Fe(IV)-N=CHR (Fig.1-38) (Hart-Davis, Battioni et al., 1998). This is in accordance with the general mechanism of cytochrome P450 that includes the formation of highly oxidized oxoiron (IV) intermediate. The formation of this intermediate increased the acidity of the β-proton and facilitated its abstraction by a weak base (Fig.1-38).

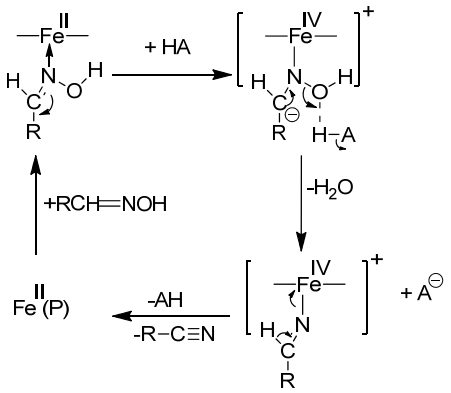

Figure 1-38: Proposed catalytic mechanism of cytochrome P450-dependant aldoxime dehydratase using iron (II) porphyrin systems (Hart-Davis, Battioni et al., 1998).

Both rat liver microsomes and CYP3A4 NF25 dehydrated their substrates in *anti*-manner. They catalyzed the dehydration of only *Z*-isomers. The lack of activity with *E*-isomers resulted from their inability to bind the enzyme in its ferrous state. This was explained by the steric hindrance effect of the aryl- or alkyl-substituent in position *trans* to the OH group of oximes that prevent their approach to the porphyrin ring. This hypothesis was supported by the lack of activity with ketoximes (Boucher, Delaforge et al., 1994). On the other hand, aldoxime dehydratases from microorganisms are catalyzing both *anti*- and *syn*-dehydration reactions. For example, OxdB was proposed to be active against *Z*-PAOx (**143**) but not the *E*-isomer (Kato, Nakamura et al., 2000) whereas, OxdRE showed activity against several *E*-aldoximes e.g. *E*-thiophene-2-acetaldoxime, *E*-thiophene-2-carboxaldehyde oxime, *E*-benzaldehyde oxime, *E*-*p*-chlorobenzaldehyde oxime, *E*-furan-2-carboxaldehyde, *E*-*p*-methylbenzaldehyde oxime and *E*-pyridine-3-carboxaldehyde oxime

(Kato, Yoshida et al. 2004). Also pyridine-3-carboxaldehyde oxime dehydratase from *Rhodococcus* sp. strain YH3-3 showed lower activity against *Z*-pyridine-3-carboxaldehyde oxime (18%) in comparison to *E*-PyOx (Kato, Ooi, et. al, 1999).

1.7 Conclusions

In conclusion, two groups of aldoxime dehydratases are found in nature; aldoxime dehydratase superfamily (Kato and Asano, 2006; Kato, Yoshida et al., 2004; Oinuma, Hashimoto et al., 2003 Xie, Kato et al., 2003) and cytochrome P450 dependant aldoxime dehydratases (Bak, Kahn et al., 1998; Boucher, Delaforge et al., 1994; Kahn, Bak et al., 1997; Nafisi, Goregaoker et al., 2007). Although the two groups catalyze the same reactions, amino acid sequence comparisons of the members of the two groups revealed no sequence similarities between them. Additionally, they showed different distribution in nature. Members of aldoxime dehydratase superfamily exist in microorganisms (Kato and Asano, 2006; Kato, Yoshida et al., 2004; Oinuma, Hashimoto et al., 2003 Xie, Kato et al., 2003), while oxime-metabolizing P450 are detected only in plants (Bak, Kahn et al., 1998; Kahn, Bak et al., 1997; Nafisi, Goregaoker et al., 2007) and animals (Boucher, Delaforge et al., 1994). The physiological role of microbial aldoxime dehydratases is not clear although they are widely spread in microorganisms. Several aldoxime dehydratases from microorganisms were identified and have biotechnological application in nitrile synthesis (Kato, Ooi et al., 1999; Xie, Kato et al., 2001). On the other hand, plant cytochrome P450 dependant aldoxime dehydratases are involved in the biosynthesis of several plant metabolites. In crucifers, IAOx (**142**) is a precursor for the biosynthesis of several defense metabolites as phytoalexins and phytoanticipins (Glawischnig, Hansen et al., 2004; Pedras and Yaya, 2013). It is interesting that both plant pathogenic fungi and crucifers metabolise IAOx (**142**) to IAN (**115**) (Pedras and Montaut, 2003). This poses the question about the correlation between plant aldoxime dehydratases and their fungal pathogen aldoxime dehydratases and the role of these enzymes in plant-pathogen interaction. Indolyl-3-acetaldoxime dehydratase was partially purified from the fungal culture of *G. fujikuroi* (Shukla and Mahadevan, 1968; Shukla and Mahadevan, 1970). However, indolyl-3-acetaldoxime dehydratase (IADSs) purified from the plant pathogenic fungus *S. sclerotiorum* (Pedras, Minic et al., 2010) is

the only representative of purified and identified indolyl-3-acetaldoxime dehydratases so far. In this work, aldoxime dehydratase will be screened in cruciferous pathogenic fungi and the fungus with highest specific activity will be subjected for further studies.

2. Chapter 2: Results and Discussion

2.1 Metabolism of destruxin B (1) and sirodesmin PL (13) by crucifers and cereals

Crucifers are subjected to attack by pathogenic fungi that cause severe economical losses. *A. brassicae*, the causative agent of blackspot disease, and *L. maculans*, the causative agent of blackleg disease, are two major fungal pathogens of crucifers causing severe economical losses of rapeseed (*B. napus*, *B. rapa* and *B. juncea*) and canola (*B. napus*, *B. rapa* and *B. juncea*). Both fungal species produce phytotoxins. Destruxin B (**1**) is the major phytotoxin (HST) produced by *A. brassicae* (Ayer and Pena-Rodriguez, 1987a; Buchwaldt and Jensen, 1991), while sirodesmin PL (**13**) is the major phytotoxin (non-HST) produced by *L. maculans* (Pedras and Yu, 2009). Destruxin B (**1**) was detected in *B. napus* and *S. alba* leaves infected by *A. brassicae* (Buchwaldt and Jensen, 1991; Pedras and Smith, 1997) and sirodesmin PL (**13**) was detected in *B. napus* leaves infected with *L. maculans* (Elliott, Gardiner et al., 2007). In response to pathogenic fungi, plants defend themselves by producing antimicrobial secondary metabolites as phytoanticipins and phytoalexins in addition to detoxifying enzymes that can transform fungal phytotoxins into non-toxic metabolites. Destruxin B (**1**) is metabolized to hydroxydestruxin B (**32**) and β-D-glucosylhydroxydestruxin B (**34**) at faster rates in resistant plants (*S. alba*, *C. sativa*, *C. bursa-pastoris*, and *E. sativa*) than susceptible plants (*B. napus* and *B. juncea*) (Pedras, Montaut et al., 2003; Pedras, Zaharia et al., 2001). In addition, destruxin B (**1**) elicited the production of phytoalexins sinalexin (**103**) and sinalbin A (**100**) in *S. alba* leaves (resistant to blackleg) (Pedras and Smith, 1997). On the other hand sirodesmin PL (**13**) elicited the production of the phytoalexins brassilexin (**104**), cyclobrassinin (**102**), rutalexin (**121**), and spirobrassinin (**114**) in *B. juncea* (resistant to blackleg) (Pedras and Yu, 2008a), however, its metabolism was not studied in crucifers.

To understand the interaction of the fungal pathogens *A. brassicae* and *L. maculans* with their host and non-host plants, the molecular interaction of sirodesmin PL (**13**) and destruxin B (**1**) with different crucifers and non-crucifers was studied. The objective of this study was to

investigate the ability of different plant tissues to metabolize these phytotoxins and their ability to elicit the production of phytoalexins. Several crucifers were used in this study: roots of turnip (*B. rapa*), roots of rutabaga (*B. napus*), leaves of thale cress (*A. thaliana*), leaves of dog mustard (*E. gallicum*) and leaves of salt cress (*T. salsuginea*). In addition, leaves of oats (*A. sativa*) and wheat (*T. aestivum*) were used as examples of non-crucifers. In the following sections a detailed description of HPLC analysis and HPLC-ESI-MS^n analysis of the different plant extracts treated with destruxin B (**1**) and sirodesmin PL (**13**) is described followed by brief description of the isolation and structural elucidation of destruxin B (**1**) metabolites from oat leaves.

2.1.1 Isolation of destruxins and sirodesmin PL

To study the interaction of destruxin B (**1**) and sirodesmin PL (**13**) with different plants, these toxins were isolated and purified from their fungal cultures. Destruxin B (**1**) and desmethyldestruxin B (**3**) were isolated from *A. brassicae* as previously reported (Pedras and Smith, 1997), while sirodesmin PL (**13**) and deacetylsirodesmin PL (**14**) were isolated from fractions obtained from *L. maculans* IBCN 57 isolate (BJ 125) (Pedras and Yu, 2008a; Pedras, Séguin-Swartz et al., 1990). The isolation and purification of these toxins are described in detail in the experimental. The authenticity and purity of each compound were confirmed by HPLC, ^{1}H NMR, HREI-MS and comparison with authentic synthetic samples.

2.1.2 LC-ESI-MS^n analysis of destruxins and sirodesmins

LC-ESI-MS^n analysis is a useful technique for the identification of cyclic (depsi)peptides. In comparison to NMR, LC-ESI-MS^n allows the sequencing of nanograms of (depsi)peptides (Ngoka and Gross, 1999). ESI-MS fragmentation of cyclic (depsi)peptide results in the cleavage of peptidic bonds after protonation of the amide nitrogen(s) with the formation of ring-opened isomers (depsi)peptides. The position at which the ring cleaves depends mainly on the basicity of the amide nitrogen of the different amino acids composing the (depsi)peptides under investigation. The fragmentation site(s) is usually located between the most basic protonated amide nitrogen and the adjacent carbonyl carbons (Butt, Ben El Hadj et al., 2009; Morais, Lira et al., 2010; Seger, Sturm et al., 2004). The linear peptides resulting from the cyclic molecules can

further fragment by sequential loss of carbonyl and amino/hydroxy acid residues to yield characteristic fragment ions. Thus, the amino/hydroxyacid sequence information is readily obtained by MS analysis.

Destruxins are hexadepsipeptides composed of five amino acids and one α-hydroxy acid (Pedras, Zaharia et al., 2002). HPLC-ESI-MS/MS analysis was widely used for the identification and quantification of destruxins. For example, nano-scale HPLC-ESI-MS analysis coupled with collision-induced dissociation (CID)-MS^n fragmentation of the fungal culture extracts of *Lecanicillium longisporum* was useful in the identification of destruxins: destruxin B (**1**), destruxin E, destruxin B diol, destruxin E diol and desmethyldestruxin B (**3**) (Butt, Ben El-Hadjj et al., 2009). In addition, HPLC-ESI-MS analysis of the fungal extract from *Metarhizium anisopliae* allowed the qualitative and quantitative identification of destruxins in sub-ppm range (Seger, Sturm et al., 2004). In the following sections the HPLC-ESI-MS analysis coupled with MS^n fragmentation of authentic destruxin B (**1**), hydroxydestruxin B (**32**) and desmethyldestruxin B (**3**) were analysed. These compounds were used as standards for the detection and identification of destruxin B (**1**) and derived metabolites.

2.1.2.1 HPLC-ESI-MS^n analysis of destruxin B (1)

Destruxin B (**1**) is a cyclic hexadepsipeptide composed of: α-hydroxy-4-methylpentanoic acid (isoleucinic acid, LeA), *N*-methylvaline (*N*-Me-Val), isoleucine (Ile), *S*-proline (Pro), β-alanine (Ala) and *N*-methyl-*S*-alanine (*N*-Me-Ala). HPLC-ESI-MS analysis of destruxin B (**1**) showed a pseudo-molecular ion $[M+H]^+$ at *m/z* 594. The CID-MS^2 analysis of the molecular ion at *m/z* 594 generated a fragment ion at *m/z* 566, and a base peak at *m/z* 481. The fragment ion at *m/z* 566 resulted from the ring opening with the loss of the carbonyl group (loss of 28 Da). The base peak at *m/z* 481 (loss of 113 Da) resulted mainly from the cleavage of the peptidic bond between *N*-Me-Val and *N*-Me-Ala with the loss of either *N*-Me-Ala or *N*-Me-Val residues (Fig. 2-1). Further fragmentation of the base peak at *m/z* 481 (MS^3) showed a molecular ion at *m/z* 453 (loss of 28 Da, CO), that was further fragmented (MS^4) producing a major peak at *m/z* 368 (loss of 85 Da, Ile), *m/z* 175 (loss of 85 Da, CO, pro and LeA), *m/z* 158 (loss of 17 Da) and a base peak at *m/z* 194 due to the fragment $[pro - LeA + H]^+$ (Fig. 2-1).

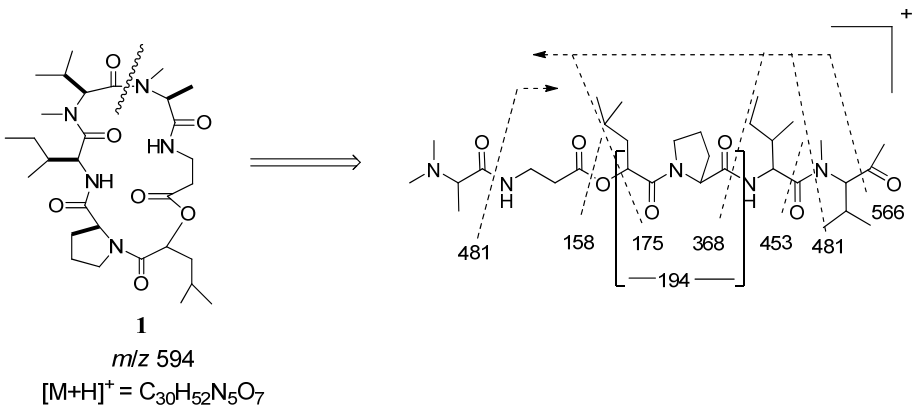

Figure 2-1: Fragmentation pattern of destruxin B (**1**, $C_{30}H_{51}N_5O_7$) using HPLC–ESI-MS^n (Pedras and Khallaf, 2012).

2.1.2.2 LC-ESI-MS^n analysis of hydroxydestruxin B (32)

HPLC-ESI-MS analysis of hydroxydestruxin B (**32**) showed a pseudo-molecular ion $[M+H]^+$ at *m/z* 610 mass unit. The MS^2 of the fragment ion at *m/z* 610 resulted in a base peak at *m/z* 592 $[M-H_2O+H]^+$ indicating the dehydration at the α-hydroxy acid residue. The MS^3 of the fragment ion *m/z* 592 resulted in two major peaks at *m/z* 479 and *m/z* 418 (Fig. 2-2). The fragment ion at *m/z* 479 resulted from the ring opening at the peptidic bonds between *N*-Me-Ala and *N*-Me-Val residues followed by the loss of *N*-Me-Val residue. Further fragmentation of the base peak at *m/z* 479 (MS^4) showed a molecular ion at *m/z* 451 (loss of 28 Da, CO), which was further fragmented (MS^5) producing a major peak at *m/z* 366 (loss of 85 Da, Ile) and a base peak at *m/z* 192 due to the fragment $[pro\text{-}LeA + H]^+$. These fragment ions (*m/z* 479, *m/z* 451, *m/z* 366 and *m/z* 192) are two mass units less than the fragments observed in case of destruxin B (**1**). On the other hand, the fragment ion at *m/z* 418 is due to the cleavage of the peptidic bond between *N*-Me-Ala and *N*-Me-Val, and the loss of *N*-Me-Ala, β-Ala residues (Fig. 2-2). The fragment ion at *m/z* 418 was further fragmented (MS^4) producing fragment ions at *m/z* 305 (loss of 85 Da, *N*-Me-Val), *m/z* 277 (loss of 28 Da, CO), and at *m/z* 192 due to the fragment $[pro\text{-}LeA + H]^+$ (Fig. 2-2).

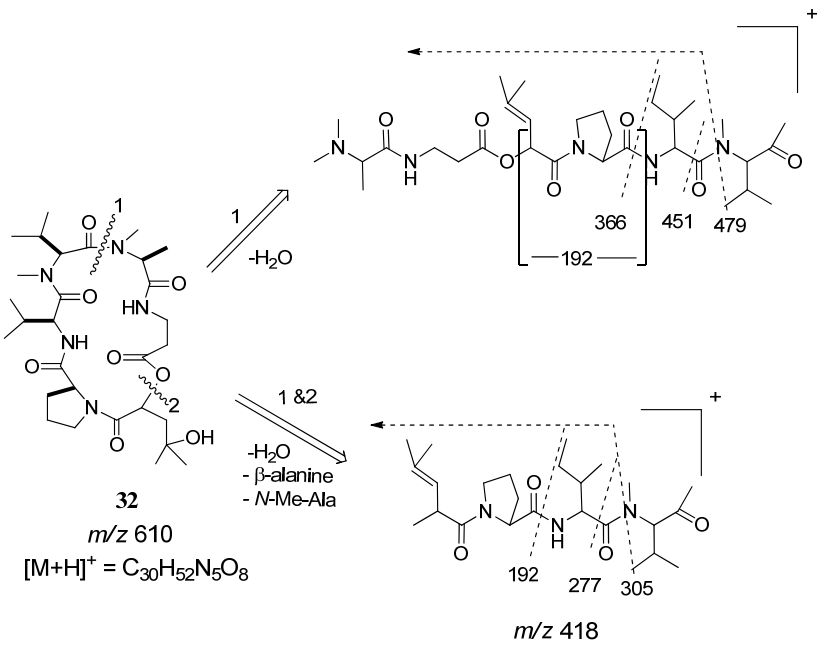

Figure 2-2: Fragmentation pattern of hydroxydestruxin B (**32**, $C_{30}H_{51}N_5O_8$) using HPLC–ESI-MS^n (Pedras and Khallaf, 2012).

2.1.2.3 LC-ESI-MS^n analysis of desmethyldestruxin B (3)

Desmethyldestruxin B (**3**) is a natural phytotoxin isolated from the plant pathogenic fungus *A. brassicae* lacking the *N*-methyl at the valine residue. Similar to destruxin B (**1**), desmethyldestruxin B (**3**) is fragmented via ring opening of the peptidic bond between *N*-Me-Ala and *N*-Me-Val residues followed by the loss of carbonyl group (CO, loss of 28 Da), giving a molecular ion at *m/z* 552. The MS^2 analysis of the molecular ion at *m/z* 552 generated a base peak at *m/z* 481resulting from the loss of valine residue (loss of 71 Da). The base peak at *m/z* 481 is further fragmented giving the following molecular ions at *m/z* 453 (loss of 28 Da, CO), *m/z* 368 (loss of 85 Da, Ile residue), *m/z* 175 (loss of 193 Da, pro and LeA residues,) and *m/z* 194 due to the fragment $[pro – LeA + H]^+$ (Fig. 2-3) (Pedras and Khallaf, 2012).

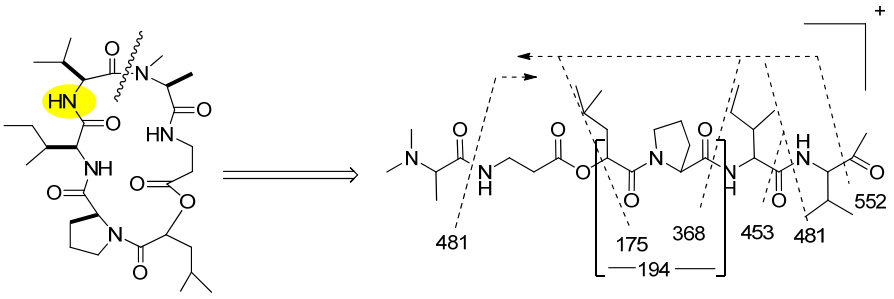

3

m/z 580

$[M+H]^+ = C_{29}H_{50}N_5O_7$

Figure 2-3: Fragmentation pattern of desmethyldestruxin B (**3**, $C_{29}H_{49}N_5O_7$) using HPLC-ESI-MS^n (Pedras and Khallaf, 2012).

2.1.2.4 LC-ESI-MS^n analysis of sirodesmin PL (13) and deacetylsirodesmin PL (14)

The HPLC–ESI-MS^n spectra positive mode analysis of sirodesmin PL (**13**) did not show a pseudo-molecular ion $[M+H]^+$. It showed a base peak at *m/z* 423 which corresponds to sirodesmin PL lacking the two sulphur atoms $[M-S_2 + H]^+$. The ESI-MS^2 analysis of the peak *m/z* 423 resulted in major peaks at *m/z* 469 that corresponds to the formic acid adduct of sirodesmin PL lacking two sulphur atoms $[M-S_2 + CO_2H_2]^+$ and a peak at *m/z* 327 and *m/z* 229.

Similarly, the HPLC-ESI-MS^n spectra of deacetylsirodesmin PL (**14**) in positive mode showed a base peak at *m/z* 381 corresponding to the loss of two sulfur atoms $[M-S_2+H]^+$, without a pseudo-molecular ion $[M+H]^+$ peak; further fragmentation yielded peaks at *m/z* 363 and *m/z* 229.

2.1.3 Metabolism of destruxin B (1) and metabolite elicitation in crucifers

The metabolism of destruxin B (**1**) to hydroxydestruxin B (**32**) and hydroxydestruxin B β-D–glucopyranoside (**34**) was reported both in the blackspot resistant plants (*S. alba*, *C. sativa* and *C. bursa-pastoris*) and in blackspot susceptible plants (*B. napus* and *B. juncea*). While the hydroxylation process was the rate-determining step in case of susceptible plants, the glucosylation was the rate-determining step in case of resistant plants (Pedras, Montaut et al., 2003; Pedras, Zaharia et al., 2001). To find out if the metabolism of destruxin B (**1**) into hydroxydestruxin B (**32**) is restricted to the studied crucifers or it is a conserved metabolic

pathway across crucifers, destruxin B (**1**) metabolism was studied in the following tissues: *A. thaliana* leaves, *T. salsuginea* leaves, *E. gallicum* leaves, *B. rapa* roots and *B. napus* roots. In case of *A. thaliana* leaves, *T. salsuginea* leaves and *E. gallicum* leaves, time-course studies were carried out using 7-8 week old plant leaves. Leaf uptake experiments with the appropriate concentration of destruxin B, followed by incubation for one, three and five days and extraction with dichloromethane (non-polar extract) and methanol (polar extract) were carried out. The extracts were analyzed by HPLC-DAD, as well as LC-ESI-MS and compared to control leaves to detect potential destruxin B metabolites and phytoalexin elicitation. Two concentrations of destruxin B (**1**) were used in this study (4×10^{-5} M and 4×10^{-4} M) depending on the ability of different plant tissues to tolerate toxin solution. *A. thaliana* leaves were fed with the lower concentration (4×10^{-5} M), *T. salsuginea* leaves were treated with the higher concentration (4×10^{-4} M) while *E. gallicum* leaves were treated with both concentrations (4×10^{-5} M, 4×10^{-4} M). It is noteworthy that all leaves used in this study (*A. thaliana*, *T. salsuginea* and *E. gallicum*) showed higher stress symptoms (desiccation and wilting) than control leaves.

In case of *B. rapa* and *B. napus* roots destruxin B solutions were added to wells of freshly cut turnip and rutabaga slices (2×10^{-5} M, 960 nmol per slice). After incubation for 4 days, the aqueous solutions in the wells were collected and extracted with EtOAc and tissues surrounding the wells were extracted with methanol and analyzed by HPLC as described in the experimental. HPLC chromatograms obtained from various extracts were compared with those chromatograms of control and UV elicited roots (positive controls). Control roots were treated in a similar way but without application of toxin. UV elicited roots were prepared by exposing the freshly cut tubers to UV light and incubation with carrier solution (used as positive control to detect the ability of the tissues to produce phytoalexins).

2.1.3.1 Arabidopsis thaliana L. (thale cress)

The model plant *A. thaliana* is a wild crucifer that produces the phytoalexins camalexin (**105**) (Tsuji, Jackson et al., 1992) and rapalexin A (**106**) (Pedras and Adio, 2008) under abiotic stress. The HPLC-DAD and HPLC-ESI-MS analyses of non-polar extracts of *A. thaliana* leaves treated with destruxin B solution (4×10^{-5} M, 20 μmoles) displayed two peaks not detected in control leaves. The first peak at t_R = 8.5 min corresponded to hydroxydestruxin B (**32**) and the second peak at t_R = 18.3 min corresponded to destruxin B (**1**). The metabolism of destruxin B (**1**)

in thale cress leaves was much slower than *S. alba* leaves as destruxin B (**1**) was detected after five days of incubation of leaves with the toxin solution (Fig. 2-5), while destruxin B was totally metabolized in *S. alba* leaves within 24 hours (Pedras, Montaut et al., 2003; Pedras, Zaharia et al., 2001). In addition, a peak with t_R = 14.5 min was detected in the non-polar extracts of all treated leaves but not in control leaves. Based on its UV spectrum and t_R, it was identified as camalexin (**105**) after comparison with authentic phytoalexins available in our library. Production of the phytoalexin camalexin (**105**) was associated with a substantial decrease in the production of indolyl-3-acetonitrile (**115**) (Fig. 2-5) (Pedras and Khallaf, 2012). Indolyl-3-acetonitrile (**115**) is a plant phytoanticipin detected in the extracts of control leaves in much higher amounts than in treated leaves and is a biosynthetic precursor of camalexin (Nafisi, Goregaoker et al., 2007; Pedras, Yaya et al., 2011). It is noteworthy that in previous work, destruxin B (**1**) was transformed by three species that also produced the phytoalexin camalexin (**105**) (*C. sativa*, *E. sativa*, and *C. bursa-pastoris*), but camalexin (**105**) was not detected in any of those species treated with destruxin B (**1**) (Pedras, Montaut et al., 2003; Pedras, Zaharia et al., 2001).

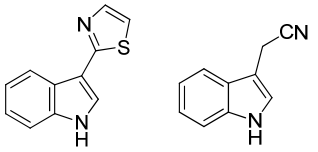

105 **115**

Figure 2-4: Structures of the phytoalexin and phytoanticipin detected in *Arabidopsis thaliana* leaves treated with destruxin B (**1**): camalexin (**105**) and indolyl-3-acetonitrile (**115**) (Pedras and Khallaf, 2012).

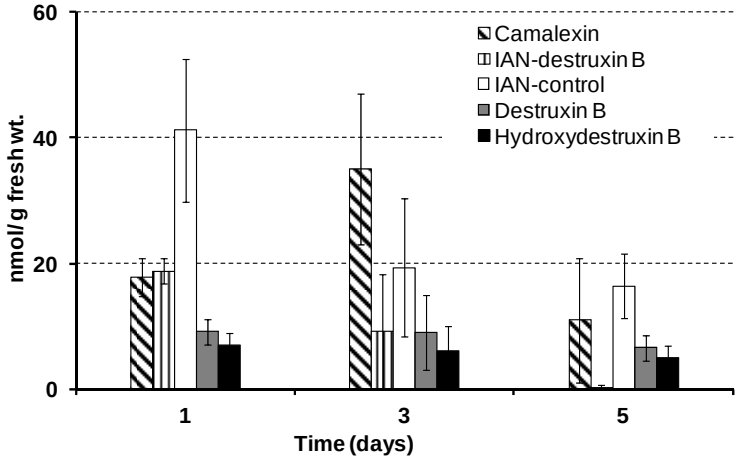

Figure 2-5: Metabolites in the leaves of *Arabidopsis thaliana* treated with destruxin B (**1**) (22 ± 5 nmol/g fresh leaf) after one, three and five days of incubation: Camalexin (**105**), indolyl-3-acetonitrile (**115**, IAN in control and treated leaves), destruxin B (**1**) and hydroxydestruxin B (**32**). Error bars represent standard deviations of two experiments conducted in triplicate (Pedras and Khallaf, 2012).

2.1.3.2 Thellungiella salsuginea Pallas (salt cress)

T. salsuginea is a cruciferous extremophile that shows resistance to stress caused by salinity, cold and draught (Inan, Zhang et al., 2004). Several phytoalexins were reported in salt cress upon elicitation with different biotic and abiotic stress. *T. salsuginea* leaves stressed abiotically with $CuCl_2$ or biotically with the crucifer pathogen: *A. candida* races 2V and 7V and *L. maculans* isolates Laird 2 and BJ 125 resulted in the production of the phytoalexins wasalexins A (**107**), wasalexin B (**108**), 1-methoxybrassenin B (**109**) and rapalexin A (**106**) (Pedras and Adio, 2008). In addition, UV elicitation of the leaves resulted in the production of wasalexins A (**107**) and B (**108**), as well as the biswasalexins A1 (**110**) and A2 (**111**) (Pedras, Zheng et al., 2009).

Feeding destruxin B (**1**, 185 ± 29 nmol/g fresh weight) to salt cress leaves resulted in the elicitation of the phytoalexins wasalexin A (**107**) wasalexin B (**108**) and 1-methoxybrassenin B (**109**) (Fig. 2-6) (traces were detected in controls). Compounds detected in each extract were identified by direct comparison with authentic samples available in Dr. Pedras metabolite libraries (HPLC-DAD and HPLC–ESI-MS). Only wasalexin A (**107**) was produced in quantity sufficient for quantification (263 ± 40 nmol/g of fresh tissue). In addition, salt cress metabolized destruxin

B (**1**) to hydroxydestruxin B (**32**) that was detected by UV and LC-MS-MS analysis (Pedras and Khallaf, 2012).

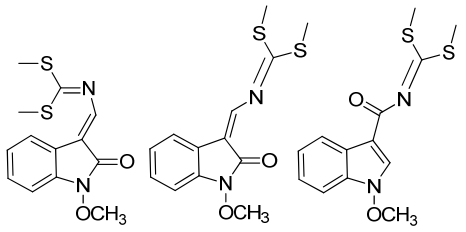

107 **108** **109**

Figure 2-6: Structures of the phytoalexins detected in the leaves of *Thellungiella salsuginea* treated with destruxin B (**1**): wasalexin A (**107**), wasalexin B (**108**), 1-methoxybrassenin B (**109**) (Pedras and Khallaf, 2012).

2.1.3.3 Erucastrum gallicum O.E. Schulz (dog mustard)

Dog mustard (*E. gallicum*) is a wild crucifer resistant to *S. sclerotiorum*, a fungal plant pathogen causing stem rot disease in crucifers and other plant families. The elicitation of dog mustard leaves with *S. sclerotiorum* or $CuCl_2$ resulted in the detection of the phytoalexins erucalexin (**112**), indolyl-3-acetonitrile (**115**), 1-methoxyindolyl-3-acetonitrile (arvelexin) (**116**) and 1-methoxyspirobrassinin (**113**) (Fig. 2-7) (Pedras and Ahiahonu, 2004; Pedras, Suchy et al., 2006). In this study the effect of destruxin B (**1**, 4×10^{-5} M and 4×10^{-4} M) on dog mustard leaves was examined. The HPLC chromatograms analysis of the non-polar extracts of the elicited leaves displayed several peaks that were not detected in control leaves. Leaves treated either with the higher or lower concentration displayed a peak at t_R = 8.5 min corresponded to hydroxydestruxin B (**32**) and another peak at t_R = 18.3 min that corresponding to the remaining destruxin B (**1**). Destruxin B (**1**) at 4×10^{-4} M elicited the phytoalexins: erucalexin (**112**), spirobrassinin (**114**, ca. 1 nmol/g fresh weight) and 1-methoxyspirobrassinin (**117**, ca. 5 nmol/g fresh weight) (Fig. 2-7). However, destruxin B (**1**) at 4×10^{-5} M elicited only erucalexin (**112**), and 1-methoxyspirobrassinin (**113**). The elicited phytoalexins showed a maximum production profile after three days of incubation (Fig. 2-8). However, no change in the metabolic profile of methanolic extracts of control and elicited leaves was observed (Pedras and Khallaf, 2012).

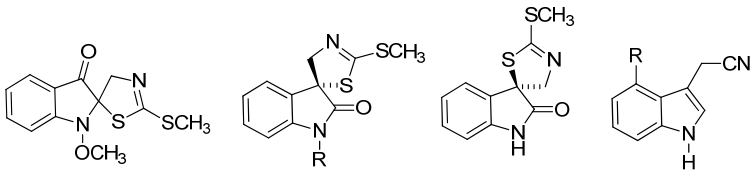

112 **113** **114** **115** R=H **116** R=OCH3

Figure 2-7: Structures of the phytoalexins detected in *Erucastrum gallicum* leaves treated with destruxin B (**1**): Erucalexin (**112**), 1-methoxyspirobrassinin (**113**), spirobrassinin (**114**), indolyl-3-acetonitrile (**115**) and arvelexin (**116**), (Pedras and Khallaf, 2012).

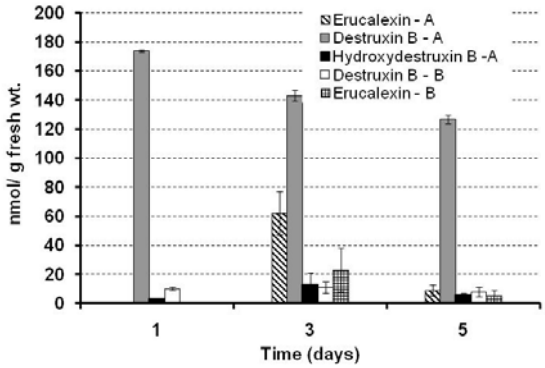

Figure 2-8: Metabolites detected in leaves of *Erucastrum gallicum* incubated with destruxin B (**1**) after one, three and five days of incubation (A, 207 ± 67 nmol/ g fresh weight; B, 16 ± 3 nmol/g fresh weight): erucalexin (**112**) and hydroxydestruxin B (**32**). Error bars represent standard deviations of two experiments conducted in triplicate (Pedras and Khallaf, 2012).

2.1.3.4 Brassica rapa L. (turnip) and B. napus L. (rutabaga).

The HPLC-DAD and HPLC-MS analyses of the chromatograms of EtOAc extracts of both *B. rapa* and *B. napus* roots treaded with destruxin B (**1**) indicated the metabolism of destruxin B (**1**) by both tissues into hydroxydestruxin B (**32**) (Fig. 2-9). After four days of incubation of destruxin B (2×10^{-5} M, 960 nmol per slice) with freshly cut slices of either tissues two peaks with t_R = 8.5 min (corresponds to hydroxydestruxin B) and t_R = 18.3 min. (corresponds to destruxin B) were detected in the treated slices but not in control ones. However, no phytoalexins were detected in any of extracts of turnip or rutabaga roots treated with destruxin B (**1**). Phytoalexins were only detected in UV irradiated slices (Pedras and Khallaf, 2012).

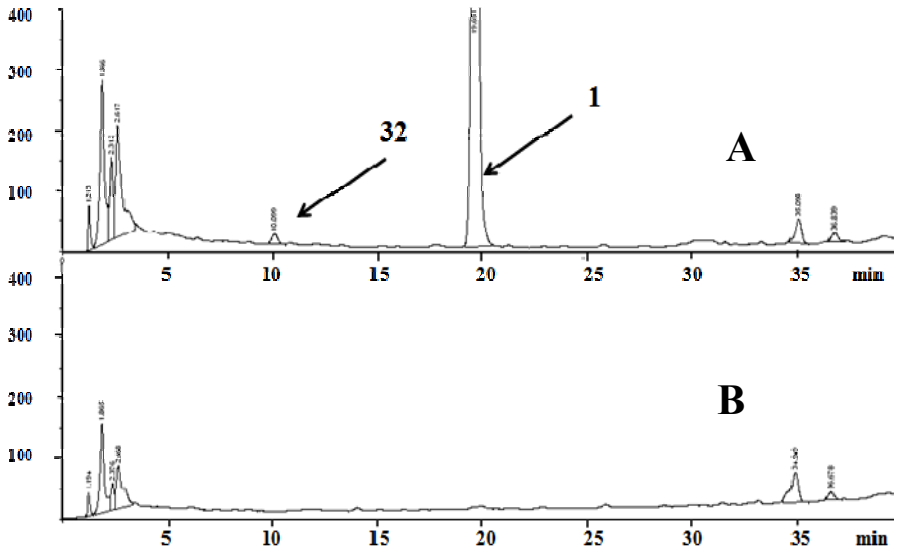

Figure 2-9: HPLC profile of EtOAc extract of *Brassica rapa* slices A) treated with destruxin B (**1**); B: control; showing destruxin B (**1**) and hydroxydestruxin B (**32**).

2.1.4 Metabolism of destruxin B (1) in cereals

To investigate whether destruxin B (**1**) metabolism is restricted to crucifers or not, its metabolism was studied in monocot plants. Two concentrations of destruxin B (**1**): 4 x 10^{-5} M (20 µmole / leaf) and 4 x 10^{-4} M (200 µmole / leaf) were applied to 21-days old oat and wheat leaves. Treated leaves were incubated for one and three days, extracted with dichloromethane and methanol to give non-polar and polar extracts, respectively. The extracts were analyzed by HPLC-DAD as well as LC-ESI-MS and compared to control leaves to detect any destruxin B metabolites and phytoalexin elicitation. No signs of desiccation or wilting were observed in oat leaves treated with both concentrations.

2.1.4.1 Avena sativa L. (oat)

Oat leaves treated with the lower concentration of destruxin B (4 x 10^{-5} M, 20 µmole), neither destruxin B (**1**) nor destruxin B metabolites were detected in the non-polar extracts after three days of incubation. However, HPLC-DAD and HPLC-ESI-MS analysis of the non-polar extracts of oat leaves incubated with the higher concentration of destruxin B (4 x 10^{-4} M, 200 µmole) showed five peaks not detected in extracts of controls (Fig. 2-10). HPLC-ESI-MS

(positive mode) analysis of these peaks showed molecular ions at *m/z* 594 that corresponded to destruxin B (**1**), *m/z* 610 that corresponded to hydroxydestruxin B, *m/z* 592 (**178**, t_R = 16.5 min), *m/z* 592 (**179**, t_R = 16.5 min), and *m/z* 580 (**180**, t_R = 17.5 min). Metabolites **178** and **179** had two hydrogen atoms less than destruxin B (**1**) indicating the presence of isobaric dehydrodestruxin B, while compound **180** was proposed as demethylated derivative of destruxin B from its molecular ion *m/z* 580 (14 unit less than destruxin B) and its HRMS analysis. To localize the position of the double bond in case of dehydrodestruxins B (**178 & 179**) and demethylation position in case of desmethyldestruxin B (**180**), a scaling up experiment was carried out. 55-Oat leaves were fed with destruxin B (**1**, 4 x 10^{-4} M), incubated for three days, extracted with dichloromethane followed by fractionation as described in experimental. The fractionation process was monitored by HPLC and HPLC-ESI-MS. Fractions rich in dehydrodestruxins B (**178 & 179**) and desmethyldestruxin B (**180**) were further analyzed by HPLC-ESI-MS^n and ^{1}H NMR and compared with data obtained from destruxin B (**1**), hydroxydestruxin B (**32**) and the natural phytotoxin desmethyldestruxin B (**3**).

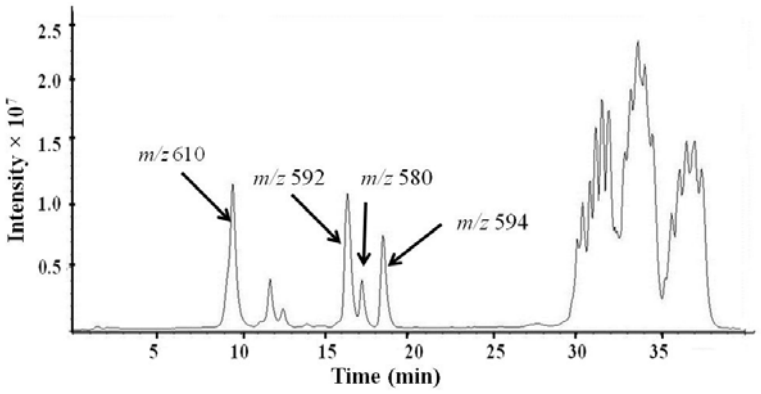

Figure 2-10: TIC chromatogram obtained by HPLC–ESI-MS (positive ion mode) analysis of a non-polar extract of oat leaves incubated with destruxin B (**1**) (peak at *m/z* 594) for 3 days: peak at *m/z* 610 (hydroxydestruxin B, **32**), *m/z* 592 (compounds **178** &**179**), *m/z* 580 (**180**).

Hydroxydestruxin B was identified by comparison of its UV spectrum, ^{1}H NMR data and LC-MS/MS analysis with authentic samples. However, the structure of the metabolites: dehydrodestruxin B (**178**, *m/z* 592), dehydrodestruxin B (**179**, *m/z* 592) and desmethyldestruxin B (**180,** *m/z* 580) were proposed based on their LC-MS^n analysis and comparison of their fragment ions with fragment ions of the reference compounds: destruxin B (**1**), hydroxydestruxin B (**32**)

and the phytotoxin desmethyldestruxin B (**3**). Due to the extremely small amounts of the separated compounds (≤ 50 µg), ^{1}H NMR was used to detect the presence of the methyl groups.

*Identification of dehydrodestruxin B (**178**)*

The HPLC–ESI-MS^{n} analysis of dehydrodestruxin B (**178**) showed the fragment ions: *m/z* 564 (loss of 28 Da, CO), *m/z* 479 (loss of 85 Da, *N*- Me-Val), *m/z* 451 (loss of 28 Da, CO), *m/z* 366 (loss of 85 Da, Ile), *m/z* 338 (loss 28 Da, CO), *m/z* 269 (loss of 69 Da, Pro), *m/z* 158 (loss of 111 Da, IleA) and *m/z* 192 due to the fragment ion [pro – LeA + H]$^{+}$ (Fig. 2-11). These fragments indicated a fragmentation pattern similar to destruxin B (**1**) that results from the cleavage of the peptidic bond between *N*-Me-Ala and *N*-Me-Val residues followed by the sequential loss of carbonyl groups and amino acid residues. The fragments at *m/z* 564, *m/z* 479, *m/z* 451, *m/z* 366, *m/z* 338 and *m/z* 269 are two units less than the fragment ions detected in case of destruxin B, which excludes the presence of the double bond in *N*-Me-Val, Ile and pro residues. However, the fragment ion at *m/z* 192 (due to the fragment [pro –LeA + H]$^{+}$) indicates the presence of the double bond in IleA residues. Based on the ^{1}H NMR for dehydrodestruxin B (**178**), the double bond locates between C-2 and C-3 of LeA residue as the methyl group can be detected by ^{1}H NMR (Pedras and Khallaf, 2012).

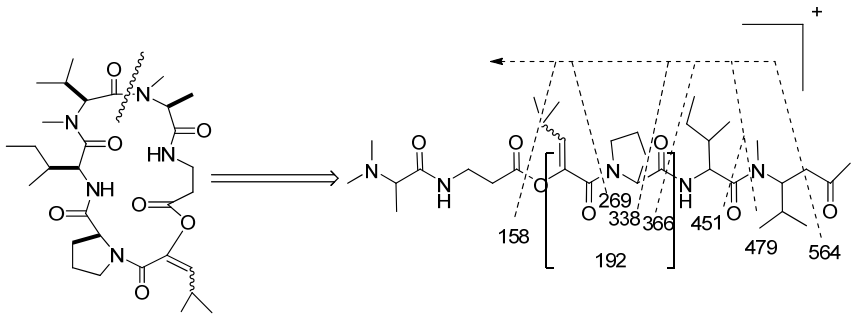

178

m/z 592

$[M+H]^{+} = C_{30}H_{50}N_5O_7$

Figure 2-11: Fragmentation pattern of dehydrodestruxin B (**178**, $C_{30}H_{49}N_5O_7$) using HPLC-ESI-MS^{n} (Pedras and Khallaf, 2012).

*Identification of dehydrodestruxin B (**179**)*

The HPLC–ESI-MS^n analysis of dehydrodestruxin B (**179**) showed fragment ions resulting from the cleavage of the peptidic bond between *N*-Me-Ala and *N*-Me-Val residues followed by the sequential loss of carbonyl groups and amino acid residues with the formation of the following fragment ions: *m/z* 564 (loss of 28 Da, CO), *m/z* 479 (loss of 85 Da, *N*-Me-Val), *m/z* 451(loss of 28 Da, CO), *m/z* 366 (loss of 85 Da, Ile), *m/z* 338 (loss 28 Da, CO), *m/z* 269 (loss of 69 Da, Pro), and *m/z* 194 due to the fragment ion $[pro–LeA + H]^+$ (Fig. 2-12). This fragmentation of dehydrodestruxin B (**179**) suggests the presence of the double bond either in the β-Ala or *N*-Me-Ala residues. ^1H NMR spectrum of the isomer (**179)** displayed a clear quartet at δ 5.2 (*J* = 7 Hz) (proton of *N*-methyl alanine residue coupling with the methyl group) and a doublet at δ 1.3 (3H, d, *J* = 7 Hz) (representing the methyl group of *N*-Me-Ala residue). These data exclude the presence of the double bond in *N*-Me-Ala residue and suggested the presence of the double bond in β-Ala residue (Fig. 2-12). Due to the small amount of this sample, ^1H NMR expected changes in the β-alanine residue were not detectable because the protons of β-alanine appear in a congested area of the spectrum. Similarly, it was not possible to assign the configuration of the double bond (Pedras and Khallaf, 2012).

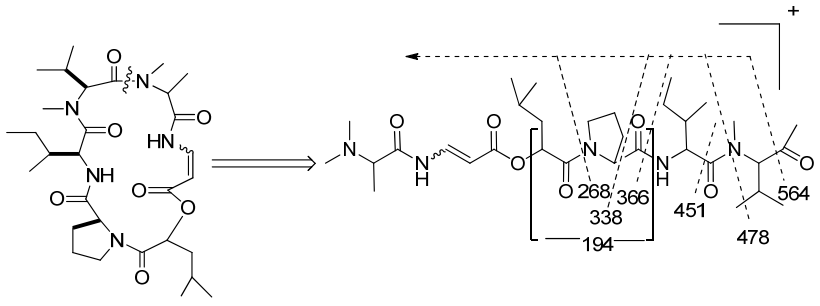

179

m/z 592

$[M+H]^+ = C_{30}H_{50}N_5O_7$

Figure 2-12: Fragmentation pattern of dehydrodestruxin B (**179**, $C_{30}H_{49}N_5O_7$) using HPLC–ESI-MS^n (Pedras and Khallaf, 2012).

*Identification of desmethyldestruxin B (**180**)*

The HRMS analysis of compound (**180**) ($C_{29}H_{49}N_5O_7$) indicated that it is a desmethyldestruxin B derivative. However, the HPLC–ESI-MS^n analysis showed a different fragmentation pathway from the phytotoxin desmethyldestruxin B (**3**). The HPLC-ESI-MS^n analysis of the metabolite desmethyldestruxin B (**180**) showed the following fragment ions at *m/z* 552 (loss of 28 Da, CO), *m/z* 467 (loss of 85 Da, LeA), *m/z* 439 (loss of 28 Da, CO), *m/z* 396 (loss of 43 Da, β-Ala), *m/z* 368 (loss 28 Da, CO), *m/z* 325 (loss of 43 Da, Ala), *m/z* 212 (loss of 85 Da, Me-N-Val) and *m/z* 184 (loss of 28 Da, CO). This fragmentation pattern indicated that the ring cleavage occurred at the peptidic bond between *N*-Pro and the carbonyl of LeA (Fig. 2-13) suggesting that the *N*-methyl group of Ala was absent in this compound. This was confirmed by comparing the ^{1}H NMR spectrum of this metabolite (**180**) with the ^{1}H NMR spectrum of desmethyldestruxin B (**3**). ^{1}H NMR spectrum of the metabolite desmethyldestruxin B (**180**) showed only one singlet at δ 3.23 that corresponds to the methyl group of *N*-methylvaline, while no singlet at δ 2.73 was observed. In addition a doublet at δ 6.8 (J = 8.3 Hz) represents NH of *N*-methylalanine was detected. On the other hand, the ^{1}H NMR spectra the naturally occurring desmethyldestruxin B (**3**) showed only one singlet at δ 2.73 that corresponds to the methyl group of *N*-methylalanine while, no singlet at δ 3.23 was observed (Pedras and Khallaf, 2012).

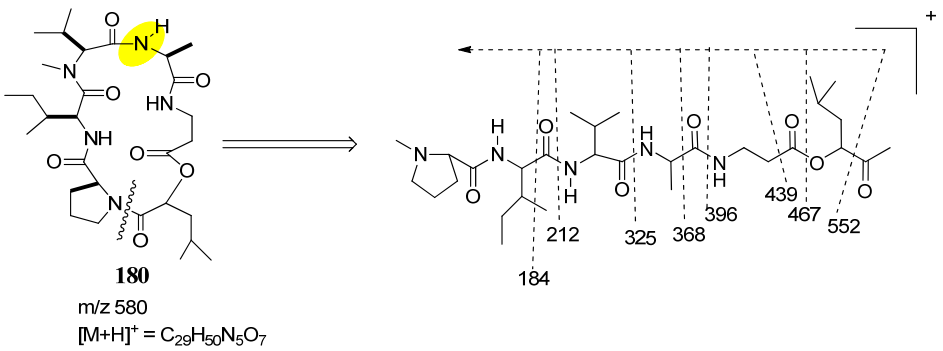

Figure 2-13: Fragmentation pattern of desmethyldestruxin B (**180**, $C_{29}H_{49}N_5O_7$) using HPLC–ESI-MS^n (Pedras and Khallaf, 2012).

2.1.4.2 Triticum aestivum L. (wheat)

The metabolic pathway of destruxin B (**1**) in wheat leaves was similar to oat leaves. HPLC-DAD and HPLC-ESI-MS analysis of the non-polar extracts of wheat leaves incubated with destruxin B (4 x 10^{-4} M, 200 µmole) showed destruxin B (**1**), hydroxydestruxin B (**32**), dehydrodestruxins B (**178**, **179**) and desmethyldestruxin B (**180**) that were not detected in control leaves. However, the transformation rate of destruxin B (**1**) was much faster in wheat leaves than in oat leaves; destruxin B (**1**) was totally metabolized in wheat leaves within 24 h of incubation whereas destruxin B (**1**) was detected in oat leaves extracts after 72 h of incubation (Fig. 2-14). In addition, destruxin B (**1**) and its metabolites hydroxydestruxin B (**32**), dehydrodestruxins B (**178**, **179**) and desmethyldestruxin B (**180**) were detected in the extracts of wheat leaves treated with destruxin B. However, these metabolites were detected in much lower concentration than in oat leaves which can be due to the high conversion rate of destruxin B metabolism that does not give time for destruxin B metabolites to accumulate (detected only by LC-MS) (Pedras and Khallaf, 2012).

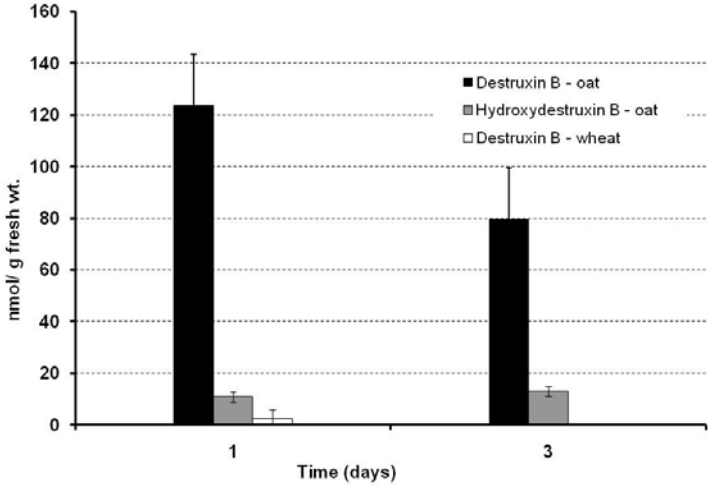

Figure 2-14: Metabolites in leaves of *Avena sativa* and *Triticum aestivum* treated with destruxin B (**1**) (187 ± 38 nmol/g fresh weight) after one and three days of incubation: hydroxydestruxin B (**32**). Error bars represent standard deviations of one experiment conducted in triplicate (Pedras and Khallaf, 2012).

2.1.5 Metabolism of sirodesmin PL (13) and metabolite elicitation in crucifers and cereals

In this section, the metabolism of sirodesmin PL (**13**) was studied in the following crucifers: *A. thaliana* leaves, *T. salsuginea* leaves, *E. gallicum* leaves, *B. rapa* roots and *B. napus* roots, as well as in *A. sativa* and *T. aestivum* leaves as examples of cereals. Sirodesmin PL (**13**) was applied to plant tissues as described for destruxin B (**1**). Two concentrations of sirodesmin PL (**13**) were used in this study (4×10^{-5} M and 4×10^{-4} M) depending on the ability of different plant tissues to tolerate toxin solution. *A. thaliana* leaves were fed with the lower concentration (4×10^{-5} M), *T. salsuginea* leaves were treated with the higher concentration (4×10^{-4} M) while *E. gallicum* leaves were treated with both concentrations. In case of *A. thaliana*, *T. salsuginea* and *E. gallicum* leaves higher stress symptoms (desiccation and wilting) were observed in leaves treated with sirodesmin PL (**13**) in comparison to control leaves. However, no signs of desiccation or wilting were observed in oat and wheat leaves treated with both concentrations.

2.1.5.1 Arabidopsis thaliana L. (thale cress)

The interaction of sirodesmin PL (**13**) with *A. thaliana* leaves were studied in a similar way as in case of destruxin B (**1**). Although the concentration of sirodesmin PL (**13**) decreases, no metabolites were detected. Hence, it cannot be concluded whether sirodesmin PL (**13**) was metabolized or not. As in case of destruxin B (**1**), sirodesmin PL (**13**) elicited the phytoalexin camalexin (**105**) that was associated with the substantial decrease in the production of indolyl-3-acetonitrile (**115**) (Fig. 2-15) (Pedras and Khallaf, 2012).

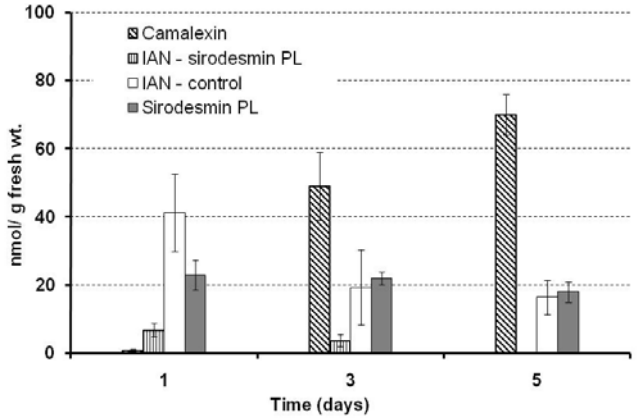

Figure 2-15: Metabolites in leaves of *Arabidopsis thaliana* incubated with sirodesmin PL (**13**) (21 ± 3 nmol/g fresh weight) after one, three and five days of incubation: camalexin (**105**) and IAN (indolyl-3-acetonitrile, **115**). Error bars represent standard deviations of six experiments conducted in triplicate (Pedras and Khallaf, 2012).

2.1.5.2 Thellungiella salsuginea Pallas. (salt cress)

Feeding sirodesmin PL (**13**) to salt cress leaves (4×10^{-4} M, 170 ± 34 nmol/g fresh weight) resulted in elicitation of the phytoalexins wasalexins A (**107**) and B (**108**) and 1-methoxybrassenin B (**117**). Compounds detected in each extract were identified by direct comparison with authentic samples available in Dr. Pedras metabolite libraries (HPLC-DAD and HPLC-ESI-MS). Only wasalexin A (**107**) was produced in quantity sufficient for quantification (203 ± 30 nmol/g of fresh tissue). No metabolites for sirodesmin PL (**13**) were detected. In addition, no change in the methanolic profile was detected upon elicitation with sirodesmin PL (**13**) (Pedras and Khallaf, 2012).

2.1.5.3 Erucastrum gallicum O.E. Schulz. (dog mustard)

To study the interaction of sirodesmin PL (**13**) with *E. gallicum* leaves, eight weeks old leaves were fed with sirodesmin PL (**13**). Two concentrations (4×10^{-5} M and 4×10^{-4} M) were used in this study. Several phytoalexins were detected in the dichloromethane extract of leaves elicited with 4×10^{-4} M (172 ± 55 nmol/g fresh weight) and detected by their UV and LC-MS; spirobrassinin (**114**, ca. 1 nmol/g fresh weight**)** and 1-methoxyspirobrassinin (**113**, ca. 5 nmol/g fresh weight) and erucalexin (**112**). However, only erucalexin (**112**) and 1-methoxyspirobrassinin (**113**) were detected when sirodesmin PL (**13**) was used at 4×10^{-5} M (14 ± 6 nmol/g fresh weight).

The elicited phytoalexins showed a maximum production after three days of incubation. However, no change in the metabolic profile of methanolic extracts of control and elicited leaves was observed (Fig. 2-16). No metabolites of sirodesmin PL (**13**) were detected (Pedras and Khallaf, 2012).

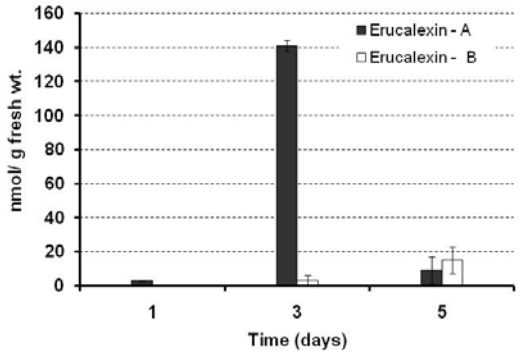

Figure 2-16: Metabolites detected in leaves of *Erucastrum gallicum* incubated with sirodesmin PL (**13**) after one, three and five days incubation (A, 172 ± 55 nmol/ g fresh weight; B, 14 ± 3 nmol/g fresh weight): erucalexin (**112**). Error bars represent standard deviations of two experiments conducted in triplicate (Pedras and Khallaf, 2012).

2.1.5.4 Brassica rapa L. (turnip) and B. napus L. (rutabaga)

The interaction of sirodesmin PL (**13**) with turnip and rutabaga roots was studied as in case of destruxin B (**1**). Sirodesmin PL solution (**13**, 2×10^{-5} M, 960 nmol/slice) was applied to turnip and rutabaga tissues and incubated for four days. In contrast to destruxin B (**1**), sirodesmin PL (**13**) was found to be a strong elicitor of phytoalexins. It elicited several compounds that were detected in the EtOAc extract. These compounds were identified by the comparison of their t_R, UV spectra and LC-MS-MS data with the available compounds in Dr. Pedras library. Sirodesmin PL (**13**) elicited the following phytoalexins in turnip roots: brassicanal A (**122**), spirobrassinin (**114**), brassilexin (**104**), indolyl-3-acetonitrile (**115**), arvelexin (**116**), brassicanate A (**123**), rutalexin (**121**) and cyclobrassinin (**102**) (Fig. 2-17). Only spirobrassinin (**114**), cyclobrassinin (**102**) and brassilexin (**104**) were produced in amounts sufficient for quantification (Fig. 2-18). No elicited compounds or change in the metabolite profiles were detected in the polar extracts of turnip roots. In addition, no metabolites of sirodesmin PL (**13**) were detected in both polar and non-polar extracts. In case of rutabaga sirodesmin PL (**13**) elicited the following phytoalexins:

spirobrassinin (**114**), brassicanal A (**122**), indolyl-3-acetonitrile (**115**), arvelexin (**116**), brassicanate A (**123**), rutalexin (**121**), rapalexin A (**106**) and cyclobrassinin (**102**) (Fig. 2-17). The ability of sirodesmin PL (**13**) as an elicitor was compared with UV elicited roots. Sirodesmin PL (**13**) was found as a strong elicitor as UV. Only spirobrassinin (**114**), cyclobrassinin (**102**), brassicanal A (**122**) and rapalexin A (**106**) were produced in quantity sufficient for quantification (Fig. 2-18). No elicited compounds or change in the metabolic profiles were detected in the polar extracts of rutabaga roots (Pedras and Khallaf, 2012).

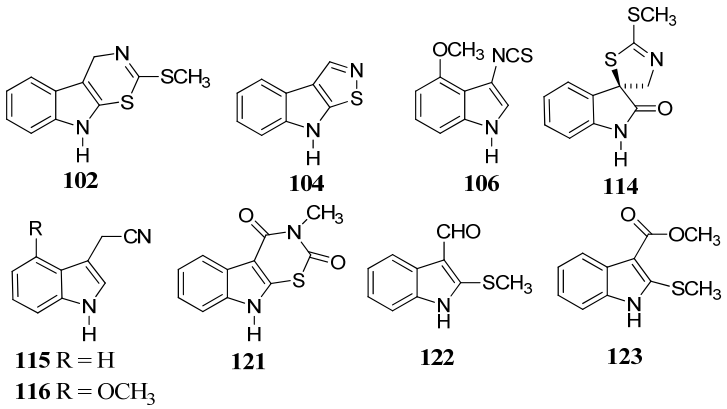

Figure 2-17: List of the phytoalexins induced by sirodesmin PL (**13**) in turnip and rutabaga roots: cyclobrassinin (**102**), brassilexin (**104**), rapalexin A (**106**), spirobrassinin (**114**), indolyl-3-acetonitrile (**115**), arvelexin (**116**), rutalexin (**121**), brassicanal A (**122**) and brassicanate A (**123**) (Pedras and Khallaf, 2012).

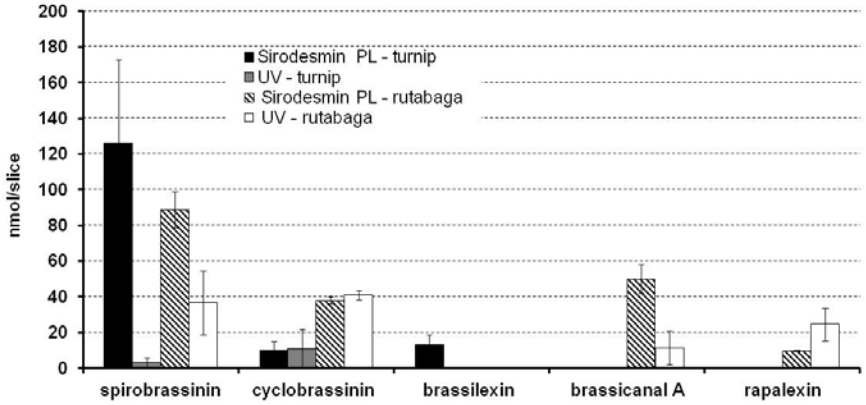

Figure 2-18: Metabolites in roots of *Brassica rapa* (turnip) and *B. napus* (rutabaga) treated with UV and sirodesmin PL (**13**, 2.4×10^{-4} M, 960 nmol/slice) after four days of incubation: spirobrassinin (**114**), cyclobrassinin (**102**), brassilexin (**104**), brassicanal A (**122**) and rapalexin (**106**). Error bars represent standard deviations of two experiments conducted in triplicate (Pedras and Khallaf, 2012).

2.1.5.5 Metabolism of sirodesmin PL (13) in cereals

The interaction between the phytotoxin sirodesmin PL (**13**) and oat and wheat leaves was examined. Leaf uptake experiments of the phytotoxin solution (4 x 10^{-4} M) followed by the extraction of the leaves with dichloromethane and methanol at different time intervals were carried out. Comparison of the HPLC chromatograms of the various polar and non-polar extracts with controls showed no elicited components or metabolites were detected. The metabolism of the sirodesmin PL (**13**) was monitored via the quantification of its quantity in dichloromethane extracts (non-polar extracts). Although a significant decrease in the concentrations of the toxin was observed, no potential metabolites were detected except a peak at that corresponds to deacetylsirodesmin PL (**14**) (Fig. 2-19). However, it was not clear if **14** was a product of simple chemical hydrolysis of sirodesmin PL (**13**) or whether it resulted from an enzymatic reaction (Pedras and Khallaf, 2012).

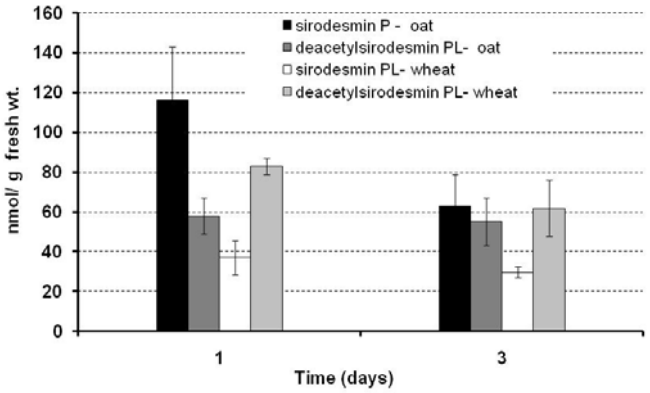

Figure 2-19: Metabolites in leaves of *Avena sativa* and *Triticum aestivum* treated with sirodesmin PL (**13**) (218 ± 30 nmol/g fresh weight) after one and three days of incubation: sirodesmin PL (**13**) and deacetylsirodesmin PL (**14**). Error bars represent standard deviations of two experiments each conducted in triplicate (Pedras and Khallaf, 2012).

2.1.6 Destruxin B hydroxylase in white mustard leaves

The detoxification of destruxin B (**1**) to hydroxydestruxin B (**32**) by crucifers is an important transformation that appears to impart resistance to white mustard against blackspot

disease. Thus, the isolation, purification and identification of destruxin B hydroxylase (DBH) are important.

To investigate the enzymatic activity of DBH several factors were taken into consideration: tissues to test for activity, inducers (it is not known if DBH is a constitutive or inducible enzyme) and the conditions of protein extractions and assays. White mustard leaves were selected to be tested for DBH, as they showed the highest rate of transformation of destruxin B (**1**) into hydroxydestruxin B (**32**) (Pedras and Khallaf, 2012; Pedras, Montaut et al., 2003; Pedras, Zaharia et al., 2001). To induce DBH, homodestruxin B (**2**) was used. Homodestruxin B (**2**) is a phytotoxin produced by *A. brassicae*, and was shown to be metabolized by white mustard leaves via a similar pathway as destruxin B (**1**) (Pedras, Zaharia et al., 1999).

Hydroxylation reactions of saturated carbons in plants are catalyzed by specific enzymes including: dioxygenases (De Carolis and De Luca, 1994), monooxygenases (peroxygenases and P450 dependent monooxygenases) (Bolwell, Bozak et al., 1994) and flavin containing monooxygenases (Schlaich, 2007). Thus, the following cofactors were examined in assays to detect DBH activity in white mustard leaves: α-ketoglutaric acid + ascorbate + Fe^{2+} as cofactors for dioxygenases, NADPH, NADH, FAD, FMN used as potential cofactors for cytochrome P450 dependent monooxygenases and flavin-containing monooxygenases as well as H_2O_2 for the detection of peroxygenases. Three extraction buffers were applied: 250 mM sodium acetate buffer pH 5.0 (Buffer A), Tris-HCl buffer pH 7.2 (Buffer B) and 250 mM Tricine buffer pH 8.0 (Buffer C); each buffer containing 250 mM sucrose, 2 mM EDTA, 2 mM DTT, 100 mM ascorbic acid, 50 mM $NaHSO_3$, 1 mM PMSF and 5 mg of BSA/mL. Enzymatic assays were conducted as described in experimental and hydroxydestruxin B (**32**), the expected product of the enzymatic assays, was monitored by HPLC-DAD and HPLC-LC-MS analysis.

The detection of DBH activity in white mustard CFE was not consistent. Although hydroxydestruxin B (**32**) was consistently detected by LC-MS analysis (showing a $[M+H]^+$peak at *m/z* 610), it was not consistently detected by HPLC-DAD. In addition, highest activity was detected using NADPH (2 mM) as a cofactor suggesting that the enzyme is a monooxygenase. This inconsistency in detecting DBH activity could be attributed to, for example, the very small amounts of the induced enzyme, enzyme stability and the presence of inhibitory compound(s). In order to increase the concentration of the enzyme, *S. alba* CFE was fractionated into microsomal and soluble fractions and the DBH activity was tested in both fractions. No activity was detected

in microsomal fractions and soluble fractions. In addition, enzymatic activities for marker enzymes: phenylalanine ammonia lyase (PAL) and cinnamic acid-4-hydroxylase (C4H) were tested in soluble and microsomal fractions, respectively to insure proper extraction procedures.

PAL and C4H are two widely distributed enzymes in the plant kingdom as they are involved in the biosynthesis of lignin. PAL is a soluble enzyme that converts phenylalanine (**158**) into cinnamic acid (**181**) (Young, Towers et al., 1966), while C4H is a membrane enzyme that transforms cinnamic acid (**181**) into *p*-hydroxycinnamic acid (coumaric acid, **182**) (Ehlting, Hamberger et al., 2006) (Fig. 2-20).

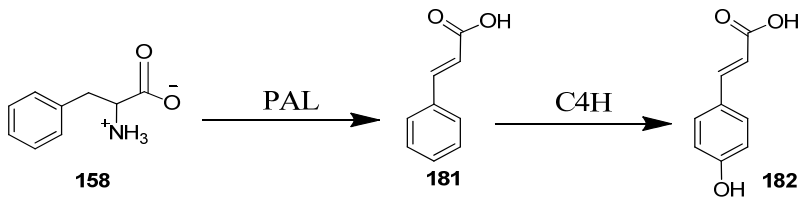

Figure 2-20: Conversion of phenylalanine (**158**) into cinnamic acid (**181**) and *p*-hydroxycinnamic acid (**182**) in plant tissue by phenylalanine ammonia-lyase (PAL) and cinnamic acid-4-hydroxylase (C4H).

PAL was detected in CFE and soluble fractions of white mustard leaves while C4H was inconsistently detected in the microsomal fractions of white mustard leaves (Table 2-1). However, no DBH activity was detected in either microsomal or soluble fractions.

Table 2-1: Detection of phenylalanine ammonia-lyase (PAL) and cinnamic acid-4-hydroxylase (C4H) activity in soluble and microsomal fractions of *Sinapis alba* (white mustard) leaves.

Enzyme tested	Protein (mg mL^{-1})	Total activity (nmol min^{-1}) [c]	Specific activity (nmol min^{-1} mg^{-1})
PAL (soluble fraction) [a]	8.7	9 ± 2 [d]	0.13 ± 0.04
C4H (microsomal fraction) [b]	5.6	6 ± 0.14 [e]	0.24 ± 0.005

[a] Extraction buffer: 250 mM Tricine buffer pH 8.0 containing 250 mM sucrose, 100 mM ascorbic acid, 50 mM sodium metabisulfite, 2 mM DTT, 2 mM EDTA, 5 mg. mL^{-1} BSA and 1 mM PMSF. [b] Microsomes were resuspended in 100 mM Tricine buffer pH 8.0, containing 250 mM sucrose, 50 mM sodium chloride, 2 mM DTT and 15% glycerol. [c] Total activity from 7.0 g of *Sinapis alba* leaves elicited with homodestruxin B (**2**). [d] Two experiments conducted in triplicate. [e] One experiment conducted in triplicate.

2.1.6.1 4-Hydroxybenzylisothiocyanate

White mustard (*S. alba*) leaves are rich in sinalbin (**183**), an aromatic glucosinolate that undergoes hydrolysis during extraction by myrosinases to 4-hydroxybenzylisothiocyanate (**184**) (Fig. 2-21) (Kawakishi and Muramatsu, 1966; Kawakishi, Namiki et al., 1967). Isothiocyanates were reported to inhibit enzyme activities by reacting with their –SH group forming dithiocarbamate derivative (Lykkesfeldt and Møller, 1993; Tang, 1974) (Fig. 2-22). In order to minimize the formation of isothiocyanates during homogenization, ascorbic acid (100 mM) was added to the extraction buffer. Ascorbic acid at high concentration was reported to inactivate myrosinases and consequently minimize the formation of isothiocyanates (Du, Lykkesfeldt et al., 1995). In addition, ascorbic acid can complex with the isothiocyanates degradation product of glucosinolates after conversion into carbinol derivatives (ascorbigens) and prevent their inhibitory activity (Bones and Rossiter, 2006).

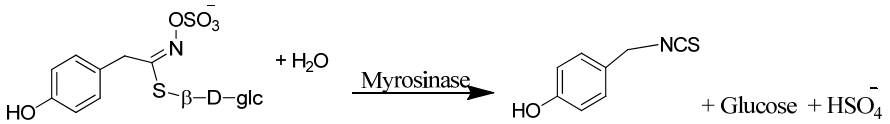

183 **184**

Figure 2-21: Hydrolysis of glucosinolate sinalbin (**183**) to the corresponding isothiocyanate (**184**) by plant myrosinases.

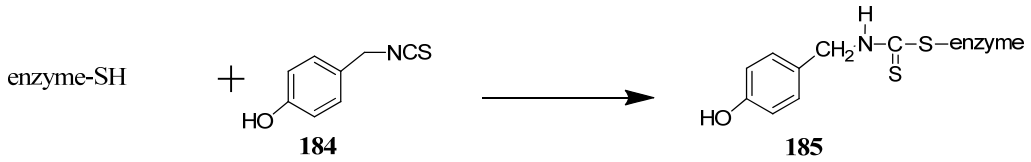

184 **185**

Figure 2-22: Reaction of 4-hydroxybenzylisothiocyanate (**184**) with -SH group of enzyme.

HPLC analysis of EtOAc extracts of the CFE of leaves of *S. alba* (control assays) homogenized with (buffer A) showed two peaks with t_R = 6.5 min and t_R = 12 min. The two peaks showed UV spectrum similar to *p*-hydroxybenzyldithiocarbamate. However, these compounds were not stable in the extraction buffer (buffer A); only 10 % were detected after incubation of CFE for one hour. To identify if these compounds were enzymatic products of 4-hydroxybenzylisothiocyanate or degradation products of 4-hydroxybenzylisothiocyanate, the

stability of 4-hydroxybenzylisothiocyanate (**184**) was studied in sodium acetate buffer pH 5.0 containing the same components (buffer A). Analysis of the EtOAc extract of sodium acetate buffer (buffer A) in the presence of 1 mM 4-hydroxybenzylisothiocyanate (**184**) showed the same peaks detected in EtOAc extract of *S. alba* CFE with same t_R at 6.5 min and 12 min).

p-Hydroxyphenylisothiocyanate (**184**) was added to buffer A, stirred for 10 min and extracted as described in the experimental. The peak with t_R = 6.5 (**187**) was isolated as major product. The HRMS spectrum of the compound with t_R = 6.5 min (**187**) showed a molecular ion at *m/z* = 318.0297 that indicated the molecular formula of $C_{12}H_{16}NO_3S_3$. In addition, mass analysis of the compound (**187)** showed fragments at *m/z* 153 that corresponds to dithiothreitol (DTT, **186**). Consequently, structure of **187** was suggested as the coupling product of reaction of 4-hydroxybenzylisothiocyanate (**184**) with DTT (**186**). The ^{1}H NMR spectrum of this compound showed two aromatic signals at δ_H 7.12 (d, *J* = 8.4, 2H) and δ_H 6.76 (d, *J* = 8.4, 2H) and a methylene group at δ_H 4.75 (d, *J* = 5.4, 2H) assigned to a para-disubstituted benzyl group. In addition, signals for methylene groups at δ 2.63 (m, 2H), 2.63 (m, 2H), and CH groups at δ 3.80 (m, 1H), 3.52 (m, 1H), 3.42 (m, 1H) and 3.36 (m, 1H) were assigned to protons from DTT (**186**).

ESI-MS analysis of compound with t_R = 12 min (**188**) showed a molecular ion peak at 426 indicating the coupling of *p*-hydroxyisothiocyanate (**184**) with two molecules of DTT (Fig 2-23). This was confirmed by analyzing the EtOAc extracts of CFE of *S. alba* leaves homogenized with extraction buffer A in absence of DTT (**186**) and by analyzing EtOAc extract of buffer A that did not contain DTT (**186**) in presence of 1 mM *p*-hydroxybenztlisothiocyanate (**184**). In both cases, the two compounds **187** and **188** were not detected.

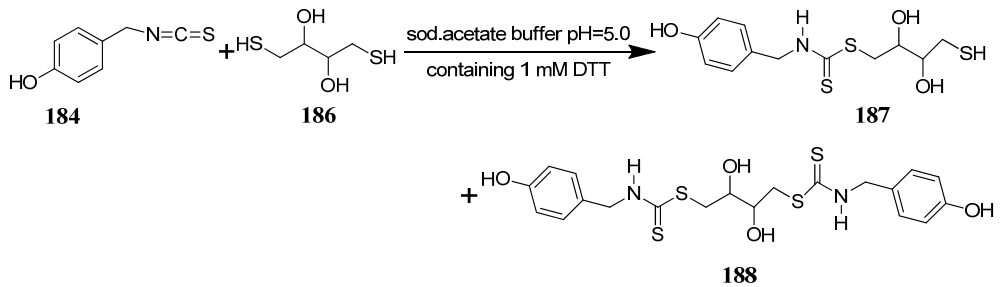

Figure 2-23: Interaction between *p*-hydoxybezylisothiocyanate (**184**) and dithiothreitol (**186**) in 250 mM sodium acetate buffer.

2.1.7 Metabolites from *Erucastrum gallicum* O.E. Schulz. (dog mustard) leaves

Several phytoalexins were detected in dog mustard (*E. gallicum*) under different biotic and abiotic stress. The elicitation of dog mustard leaves with *S. sclerotiorum* or $CuCl_2$ resulted in the detection of the phytoalexins erucalexin (**112)**, indolyl-3-acetonitrile (**115**), 4-methoxyindole-3-acetonitrile (arvelexin, **116**) and 1-methoxyspirobrassinin (**113**) (Pedras and Ahiahonu, 2004; Pedras, Suchy et al., 2006). As discussed in the previous section, administration of the HST destruxin B (**1**) and non-HST sirodesmin PL (**13**) to the leaves of dog mustard induced the production of the phytoalexins: erucalexin (**112**), 1-methoxyspirobrassinin (**113**) and spirobrassinin (**114**) (Pedras and Khallaf, 2012). In addition, a metabolite with t_R = 14.1 min was detected in dichloromethane extracts of leaves elicited with sirodesmin PL (**13**) but not in control leaves. A search in our HPLC database showed that the UV spectrum of this metabolite with t_R = 14.5 min (**190**) did not match with any of the phytoalexins in our library. This compound **190** was suggested to represent a putative phytoalexin as it is produced in *E. gallicum* leaves only in response to stress. However, the isolation of this metabolite was not feasible as it was produced in very small amount. To find out conditions under which this metabolite might be produced in higher quantity, the abiotic elicitation of dog mustard leaves with UV followed by HPLC-DAD analysis was investigated.

2.1.7.1 Time-course analysis

In preliminary experiments, time course analyses were conducted by eliciting eight-week-old plants with UV for one hour. After incubation for 24 hours, leaves were excised, extracted with dichloromethane (non-polar extract) and methanol (polar extract) and subjected to HPLC-DAD analyses. Additional leaves were harvested every 24 hours up to 120 h; control leaves were not subjected to UV elicitation, were extracted and analyzed similarly as elicited leaves. Comparison of the metabolite profiles of elicited and control leaf extracts displayed peaks in the chromatograms of elicited extracts absent in the chromatogram of control extracts. These peaks were identified by comparing their retention time and UV spectra with those of authentic samples: indolyl-3-acetonitrile (**115**, t_R = 6.5 min), arvelexin (**116**, t_R = 8.5 min), caulilexin C (**189**, t_R = 10.3 min), spirobrassinin (**114**, t_R = 12.3 min), 1-methoxyspirobrassinin (**113**,t_R = 12.9 min),

erucalexin (**112**, t_R = 15.5 min) (Fig. 2-24) and the unknown metabolite (**190**, t_R =14.1 min). The highest amount of arvelexin (**116**) and caulilexin C (**189**) was detected in leaf extracts obtained after 72 h incubation period. However, the largest amounts of erucalexin were detected after 24 to 48 hours of elicitation and the new metabolites (**190**) showed highest production after 48 hours of elicitation (Fig. 2-25).

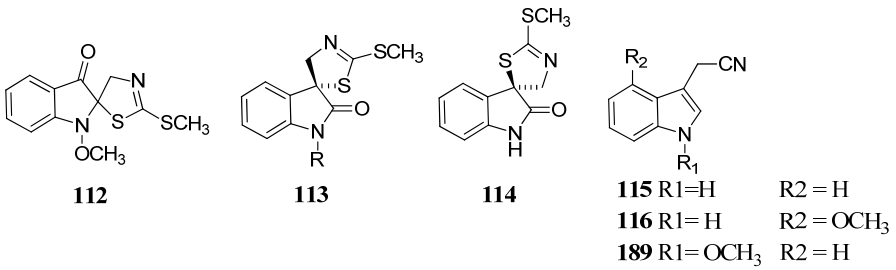

Figure 2-24: Structures of the phytoalexins detected in *Erucastrum gallicum* leaves elicited with UV: erucalexin (**112**), 1-methoxyspirobrassinin (**113**), spirobrassinin (**114**) indolyl-3-acetonitrile (**115**), arvelexin (**116**) and caulilexin (**189**).

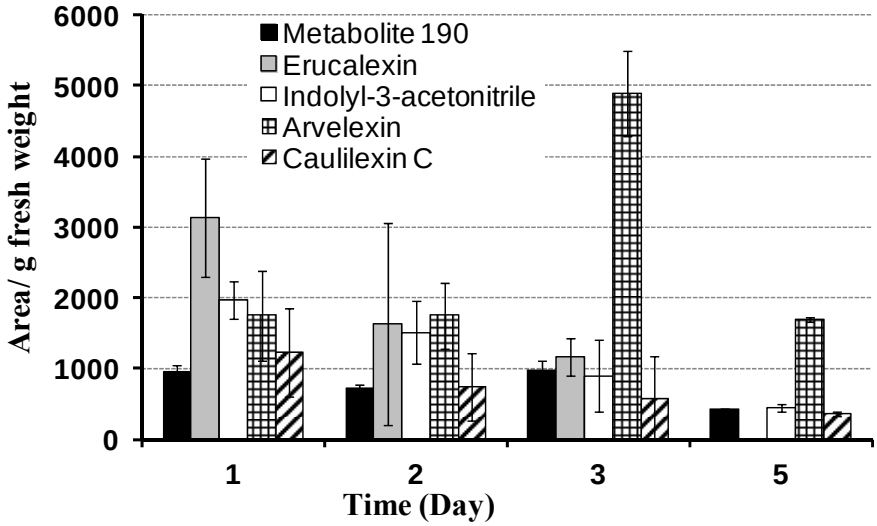

Figure 2-25: Metabolites in leaves of *Erucasrum gallicum* treated with UV for one hour after one, two, three, four and five days of incubation: indolyl-3-acetonitrile (**115**) arvilexin (**116**), erucalexin (**112**), caulilexin (**189**) and metabolite **190**.

For the identification of this metabolite **190**, a large-scale experiment was carried out. *E. gallicum* plants (60 plants) were exposed to UV for one h and incubated for two days, extracted

with dichloromethane followed by fractionation as described in the experimental. Fractions were analyzed by HPLC and LC-MS to detect the compound of interest **190**.

HREI-MS of metabolite **190** showed a likely molecular ion at *m/z* 234.0467 corresponding to molecular formula of $C_{11}H_{10}N_2O_2S$, thus an unsaturation number of 8. In addition, the ^{1}H NMR spectrum of compound **190** showed four signals in the aromatic region: a broad singlet at δ 7.82 (s, 1H), three doublets at δ 7.10 (d, *J* = 3 Hz, 1H), δ 6.98 (d, *J* = 8.5 Hz, 1H) and δ 6.94 (d, *J* = 9 Hz, 1H). The singlet at δ 7.82 was assigned to NH of the indole, while the doublet at δ 7.10 could be assigned to the hydrogen at H-2 of the indole ring and the two doublets at δ 6.98 and δ 6.94 represent two aromatic protons with *ortho*- coupling. In addition, a methoxy group at δ 4.01 (s, 3H) and methyl group at δ 3.88 (s, 3H) were detected (Fig. 2-27). At this point, a trisubstituted indole ring containing a methoxy group can be deduced based on the ^{1}H NMR and HRMS data. The following structures (**190a**, **190b**, **190c** &**190d**) are proposed (Fig. 2-26). However, structures **190c** and **190d** are more likely based on the biosynthetic origin of crucifers phytoalexins (Pedras and Yaya, 2013).

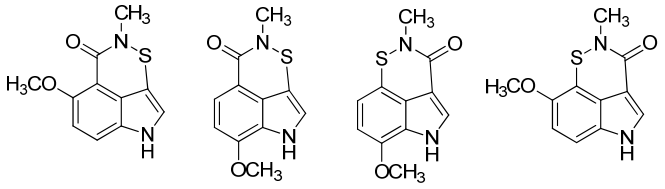

190a **190b** **190c** **190d**

Figure 2-26: Possible structures of metabolite **190**.

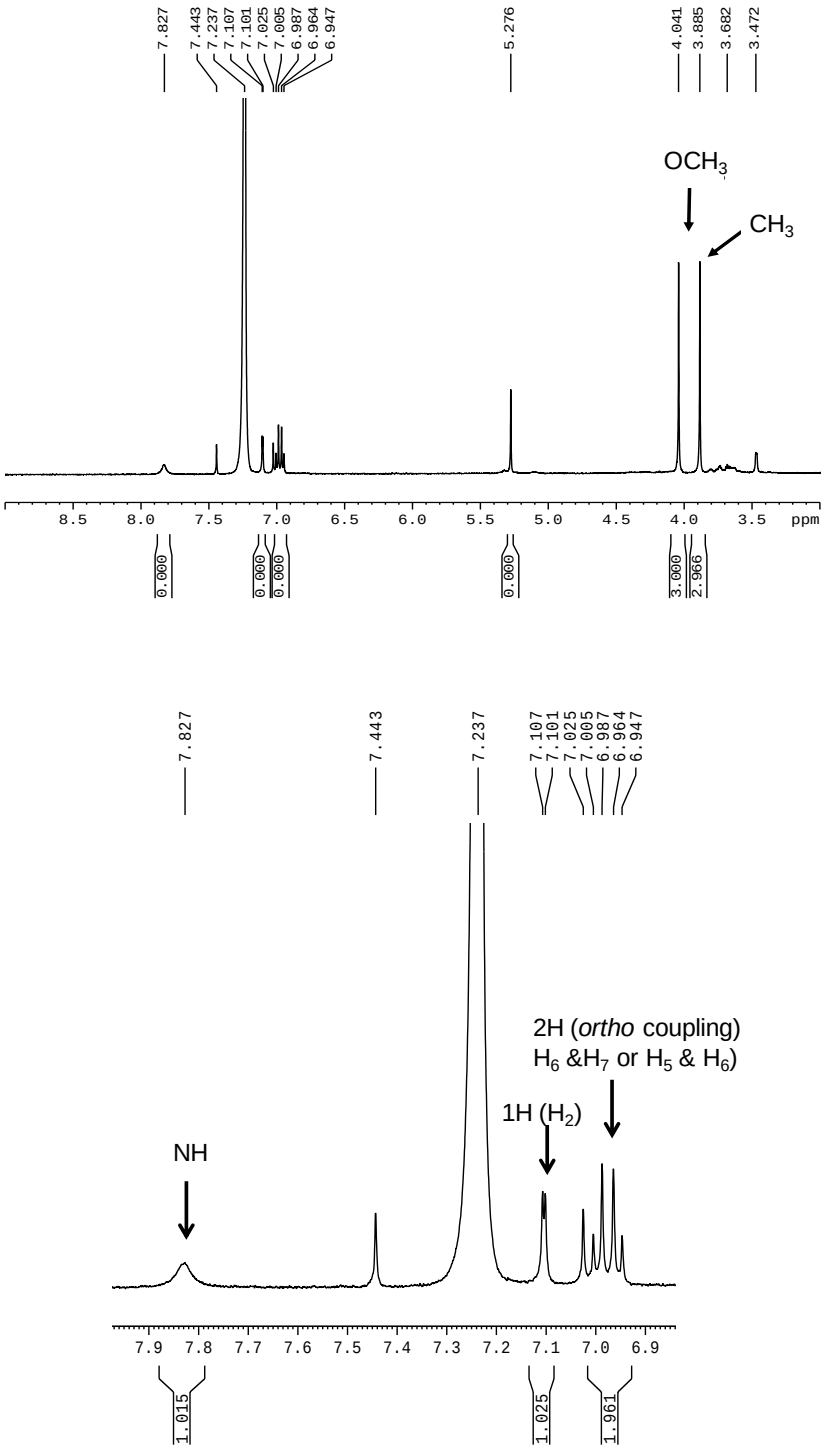

Figure 2-27: ^{1}H NMR spectrum of metabolite **190**.

The confirmation of the exact structure of the metabolite **190** requires further experiments (^{13}C NMR and 2D NMR). However, it was not feasible to further characterize the compound due to the small amount isolated. To find out better conditions for obtaining this compound at higher concentration, the amount of **190** was monitored after different UV elicitation times. Eight-week-old plants were elicited with UV for different time intervals; 0.5, 1.0, 2.0 and 3.0 hours. After two days of incubation, leaves were extracted, with dichloromethane and methanol and the extracts were subjected to HPLC-DAD analyses. Control leaves (not subjected to UV elicitation), were extracted and analyzed similarly. The highest amounts of indolyl-3-acetonitrile (**115**), arvelexin (**116**) and caulilexin C (**189**) were detected in leaf extracts obtained after two hours of UV elicitation, while the maximum production of erucalexin (**112**) and the new metabolites (**190**) were detected in extracts of leaves exposed for three hours to UV elicitation (Fig. 2-28).

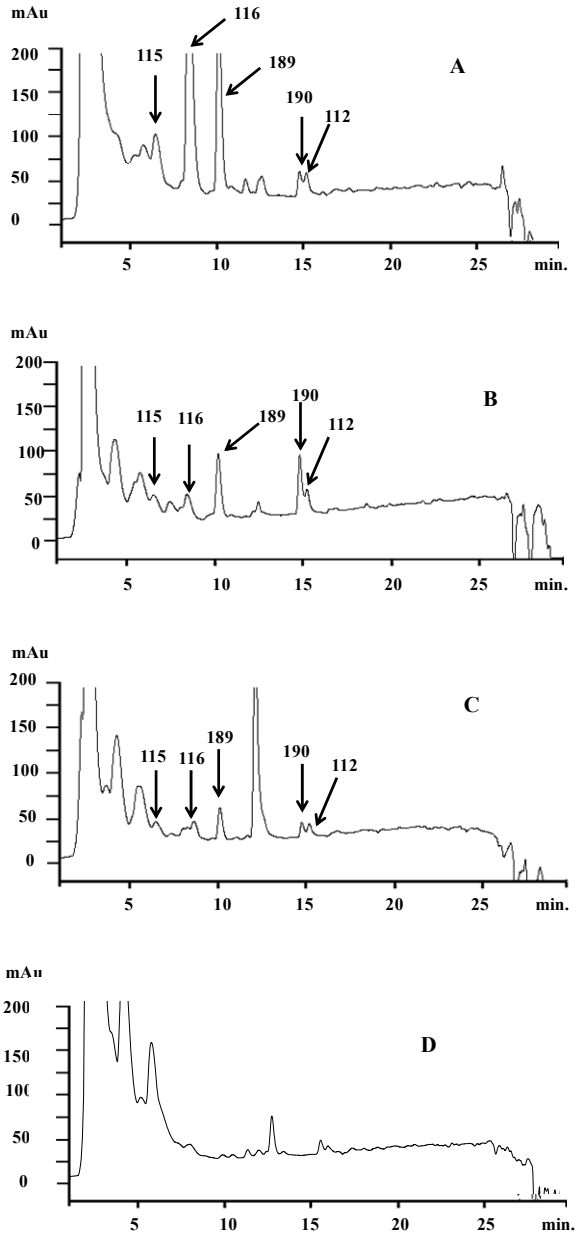

Figure 2-28: HPLC-DAD chromatograms of dichloromethane extracts of *Erucastrum gallicum* leaves two days after UV elicitation for: (A) one hour, (B) two hours, (C) three hours, (D) and non-elicited plants (control). Chromatograms show the following peaks: indolyl-3-acetonitrile (**115**), arvelexin (**116**), caulilexin C (**189**), metabolite (**190**) and erucalexin (**112**).

Additionally, sinalexin (**103**) was detected from dichloromethane extracts of leaves elicited by UV. The structure of the compound was confirmed by comparison of its t_R, mass and UV spectrum with an authentic sample. Sinalexin (**103**) is a crucifer phytoalexin isolated from *S.*

alba leaves stressed either biotically (*A. brassicae*) or abiotically (UV elicitation) (Pedras and Smith, 1997). Also it was elicited in *S. alba* leaves (resistant to *A. brassicae*) by hydroxydestruxin B (**32**) (detoxification product of destruxin B, **1**), but not in *B. juncea* or *B. napus*, (susceptible to *A. brassicae*) (Pedras, Zaharia et al., 2001). This is the first time sinalexin (**103**) is detected in *E. gallicum* leaves.

2.2 Indolyl-3-acetaldoxime dehydratase from pathogenic fungi

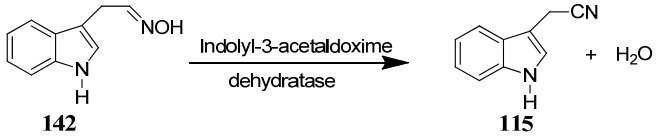

142 **115**

Figure 2-29: Conversion of indolyl-3-acetaldoxime (**142**) into indolyl-3-acetonitrile (**115**) by indolyl-3-acetaldoxime dehydratase

In crucifers aldoxime dehydratases are involved in the biosynthesis of defense metabolites such as the phytoalexins camalexin (**105**) (Glawischnig, Hansen et al., 2004), brassinin (**117**) and the phytoanticipin glucobrassicin (**155**) (Pedras and Yaya, 2013) in addition to the plant hormone indolyl-3-acetic acid (**146**) (Sugawara, Hishiyama et al., 2009). However, the function of these enzymes in plant pathogenic fungi is not clear. Studying aldoxime dehydratases from fungi will allow the comparison of fungal aldoxime dehydratases with plant aldoxime dehydratases and to understand the role of these enzymes in the interaction of plants with their fungal pathogens. So far, indolyl-3-acetaldoxime dehydratase from *S. sclerotiorum* was isolated and characterized (Pedras, Minic et al., 2010). *S. sclerotiorum* is a general plant pathogen that infects a wide range of hosts; however, no indolyl-3-acetaldoxime dehydratase has been isolated from specific cruciferous fungal pathogens. Previous study showed that indolyl-3-acetaldoxime (**142**) was metabolized into indolyl-3-acetonitrile (**115**) by cruciferous pathogenic fungi: *L. maculans* isolates Laird 2 and Mayfair 2 (virulent on brown mustard) and *L. maculans* isolate BJ 125 (virulent on canola) as well as the general pathogen *R. solani* (Pedras and Montaut, 2003). Consequently, these pathogenic fungi (*L. maculans* isolate BJ 125, *L. maculans* isolate Laird 2, *S. sclerotiorum*, *R. solani* as well as *A. brassicicola*) were screened for indolyl-3-acetaldoxime dehydratases as described in the following sections.

2.2.1 Screening indolyl-3-acetaldoxime dehydratases in pathogenic fungi

Indolyl-3-acetaldoxime dehydratase (IAD) activity was evaluated in the cruciferous pathogenic fungi: *L. maculans* isolate BJ 125 (causative agent of blackleg disease, virulent on canola), *L. maculans* isolate Laird 2 (causative agent of blackleg disease, virulent on brown mustard) and *A. brassicicola* (causative agent of blackspot of canola and brown mustard), in addition to the general pathogens *S. sclerotiorum* and *R. solani*. IAD activity was detected in *L. maculans* Laird 2, *L. maculans* BJ 125, and *S. sclerotiorum. L. maculans* isolate Laird 2 CFE showed the highest specific activity among the tested fungi. The specific activity in Laird 2 CFE was in the range of (110-170 nmol min^{-1} mg^{-1}) which is 50-100 higher than IAD detected in *L. maculans* isolate BJ 125 (1.3-2.1 nmol min^{-1} mg^{-1}) and *S. sclerotiorum* (1.5-3.5 nmol min^{-1} mg^{-1}) (Table 2.2). Consequently, *L. maculans* isolate Laird 2 was chosen for the purification and characterization of indolyl-3-acetaldoxime dehydratase. No IAD activity was detected in *A. brassicicola* CFE. IAD activity should have been detected in *A. brassicicola*, as indolyl-3-acetaldoxime (**142**) was biotransformed into indolyl-3-acetonitrile (**115**) by *A. brassicicola* liquid culture (data not shown). In addition, no IAD activity was detected in *R. solani* (3 and 5 days old cultures) CFE. This can be attributed to the small amount of the enzyme as the biotransformation of IAOx (**142**) by *R. solani* liquid culture was slow in comparison to the biotransformation of IAOx (**142**) by *L. maculans* isolate BJ 125 and *S. sclerotiorum* (Pedras and Montaut, 2003).

Table 2-2: Indolyl-3-acetaldoxime dehydratase in pathogenic fungi: *Leptosphaeria maculans* isolate BJ 125; *Leptosphaeria maculans* isolate Laird 2, *Sclerotinia sclerotiorum*, *Rhizoctonia solani* and *Alternaria brassicicola*.

Fungus (incubation time)	Mycelia weight (g) [a]	Total protein (mg)	Specific activity (nmol min^{-1} mg^{-1})	Total activity (nmol min^{-1})
L. maculans isolate Laird 2 (3 d)	2 ± 0.3	7.5 ± 1	140 ± 30	1819 ± 530
L. maculans isolate BJ 125 (3 d)	0.6 ± 0.2	5.3 ± 0.2	1.7 ± 0.4	8.8 ± 3.5
S. sclerotiorum (5 d)	1.4 ± 0.5	8.3 ± 1	2.5 ± 1	21± 3
R. solani (3 d)	0.8 ± 0.2	12 ± 1	ND	ND
A. brassicicola (3d)	0.8 ± 0.3	2.0 ± 0.3	ND	ND

ND. Not detected, [a] mycelia obtained from 100 mL culture of the tested fungus.

2.2.2 Indolyl-3-acetaldoxime dehydratase in *Leptosphaeria maculans* isolate Laird 2

Three days old mycelia of *L. maculans* Laird 2 were used in this study. Mycelia were prepared by inoculating *L. maculans* isolate Laird 2 spores (5×10^8 / 100 mL) in liquid culture. After three days, mycelia were filtered, washed with cold water and extracted with extraction buffer (10 mM Tris-HCl pH 7.4) as described in experimental. The homogenate was centrifuged at 10,000 *g* and the supernatant (CFE) was tested for IAD activity using standard assay. The stability of IAD from *L. maculans* was tested using either CFE or partially purified enzyme. Partially purified enzyme was prepared by loading CFE to DEAE-Sephacel anion exchange chromatography. Active fractions were used either for studying stability, effect of different additives or for further purification.

Testing stability and the effect of different additives on IAD activity in *L. maculans* CFE was crucial, more than 50% of IAD activity was lost after 24 hours of storage of CFE in the extraction buffer either at + 4 ^{o}C or -20 ^{o}C. Trials for purification of IAD from freshly prepared CFE using DEAE-Sephacel chromatography resulted in a recovery less than 1%. Consequently, different conditions for stabilizing and detecting IAD both in CFE and partially purified enzyme obtained after DEAE-Sephacel chromatography were tested. The tested parameters included; storage temperature, the use of different additives, reducing agents and cofactors as described in the following sections.

2.2.2.1 Effect of temperature

To study the effect of storage temperature on IAD activity in *L. maculans* CFE, IAD activity was tested in CFE at the time of extraction (zero time). In addition CFE aliquots were stored in the extraction buffer (10 mM Tris-HCl pH 7.4) at + 4 ^{o}C and -20 ^{o}C and tested for IAD activity after one, three and five days of storage. Activity and total protein were compared to those measured at the time of extraction (zero time). The enzyme activity is attenuated by storing the CFE either at + 4 ^{o}C or -20 ^{o}C. 70% of enzyme activity detected at zero time was lost after 24 h of storing CFE either at + 4 ^{o}C or -20 ^{o}C. However, the enzyme was more stable at -20 ^{o}C than at + 4 ^{o}C. While activity was not detected in CFE after three days of storage at + 4 ^{o}C, about 25% of the enzyme activity can be detected up to five days of storage for aliquots stored at -20 ^{o}C (Table 2-3).

Table 2-3: Indolyl-3-acetaldoxime dehydratase in cell-free extracts of *Leptosphaeria maculans* Laird 2 at the time of extraction (zero time) and after one, three and five days of storage at + 4 ^{o}C and - 20 ^{o}C [a].

Time (Days) - storage temperature (^{o}C)	Protein (mg mL) [b]	Specific activity (nmol min^{-1} mg^{-1}) [b]	Total activity (nmol min^{-1})	Relative activity (%)
Zero time	2.4	26 ± 2	251 ± 4	100 ± 2
1 - (+ 4 ^{o}C)	1.9	11 ± 1	82 ± 5	33 ± 2
1- (- 20 ^{o}C)	2.3	11 ± 1	85 ± 3	34 ± 2
3- (+ 4 ^{o}C)	0.7	ND	ND	ND
3 - (- 20 ^{o}C)	1.9	6 ± 1	58 ± 1	23 ± 2
5- (+ 4 ^{o}C)	0.7	ND	ND	ND
5 - (- 20 ^{o}C)	1.8	9 ± 0	66 ± 2	26 ± 2

[a] Extraction buffer: 10 mM Tris-HCl pH 7.4. [b] Mycelia obtained from 100 mL culture of *Leptosphaeria maculans* (Laird 2); ND, not detected.

2.2.2.2 Effect of reducing agents

The effects of reducing agents and air on IAD activity from *L. maculans* CFE or partially purified enzyme after DEAE-Sephacel chromatography were determined.

CFE was prepared by extracting the mycelia with 10 mM Tris-HCl pH 7.4 and activity was tested in the presence of 2.5 mM $Na_2S_2O_4$ in the assay solution at the time of extraction (zero time) as well as after storing the crude extracts at + 4 ^{o}C and - 20 ^{o}C for one, three and five days. The addition of $Na_2S_2O_4$ to the assay solution resulted in the partial restoring of the activity. While no activity was detected for samples stored for three days at + 4 ^{o}C in case of excluding $Na_2S_2O_4$ from the assay mixture (Table 2-3), the presence of $Na_2S_2O_4$ in the assays mixture resulted in 40%, 23% and 19% detection of the original activity after storage for one, three and five days, respectively. However, for samples stored at - 20 ^{o}C the decrease in activity was observed only after third day of storage (Table 2-4).

Table 2-4: Indolyl-3-acetaldoxime dehydratase in cell-free extract of *Leptoshaeria maculans* Laird 2 at the time of extraction (zero time) and after one, three and five days of storage at + 4 ^{o}C and - 20 ^{o}C. Assays were done in the presence of 2.5 mM $Na_2S_2O_4$ in the assay solution [a].

Time (Days) - storage temperature (^{o}C)	Protein (mg mL^{-1})[b]	Specific activity (nmol min^{-1} mg^{-1})	Total activity (nmol min^{-1})	Relative activity (%)
Zero time	2.4	316 ± 12	3083 ± 114	100 ± 2
1 - (+ 4 ^{o}C)	1.9	104 ± 11	1230 ± 68	40 ± 2
1- (- 20 ^{o}C)	2.3	338 ± 3	3122 ± 29	101 ± 2
3- (+ 4 ^{o}C)	0.7	419 ± 7	715 ± 25	23 ± 2
3 - (- 20 ^{o}C)	1.9	307 ± 27	2953 ± 1	96 ± 4
5- (+ 4 ^{o}C)	0.7	197 ± 3	596 ± 38	19 ± 1
5 - (- 20 ^{o}C)	1.8	411 ± 8	2343 ± 60	76 ± 2

[a] Extraction buffer: 10 mM Tris-HCl pH 7.4. [b] Mycelia obtained from 100 mL culture of *Leptosphaeria maculans* isolate Laird 2.

For partially purified IAD (DEAE-Sephacel chromatography) the addition of $Na_2S_2O_4$ in the assay solution enhanced the activity 20- to 25-fold (Table 2-5). To find the proper concentration of $Na_2S_2O_4$ required for detecting IAD activity, enzyme assays were done in the presence of different concentrations of $Na_2S_2O_4$ (0.5, 1.0, 2.5, 5.0, 7.5 and 10.0 mM). The addition of 2.5 to 5.0 mM $Na_2S_2O_4$ to the assay solution is the optimal concentration for detecting IAD activity (Table 2-5). In addition, IAD activity was enhanced 3-fold under anaerobic condition in the presence of 2.5 mM $Na_2S_2O_4$ in comparison to the activity measured aerobically (Table 2-6). These results indicated that the detection of IAD activity requires reducing environment, which is in accordance with other aldoxime dehydratases. Several aldoxime dehydratase activities are reported to be enhanced by reducing agents under anaerobic condition. For example, indolyl-3-acetaldoxime dehydratase activity from *S. sclerotiorum* is 2- and 23-fold enhanced when assays are done in the presence of 1 mM $Na_2S_2O_4$ aerobically and anaerobically, respectively (Pedras, Minic et al., 2010). The addition of 5.0 mM $Na_2S_2O_4$ to the assay solution of aldoxime dehydratase from *P. chlororaphis* B23 (Oinuma, Hashimoto et al., 2003) and phenylacetaldoxime dehydratase from *Bacillus* sp Strain OXB-1(Kobayashi, Yoshioka et al., 2005) resulted in 1150- and 250- fold increase in the activity in comparison to the control done in absence of $Na_2S_2O_4$ from the assay mixture. Aldoxime dehydratases are heme proteins that are active only when the iron heme is in its reduced form.

Table 2-5: Effect of different concentration of $Na_2S_2O_4$ on the activity of IAD obtained from mycelia of *Leptosphaeria maculans*

$Na_2S_2O_4$ (mM)	Relative activity (%) [a]
0	100 ± 9
0.5	569 ± 10
1.0	854 ± 50
2.5	2332 ± 219
5.0	2650 ± 37
7.5	1159 ± 64
10	632 ± 7

[a] Activities are expressed as percentage of the activity of IAD obtained in the absence of $Na_2S_2O_4$; results are the means ± SD of three independent experiments. The enzyme activities were measured using protein extracts obtained from DEAE-Sephacel chromatography (elution buffer: 10 mM Tris-HCl buffer pH 7.4 containing 3% glycerol, 0.015% Triton-X100 and 0.1 mM 2-mercaptoethanol). The relative specific activity of IAD for 100% is equivalent to 100 nmol min^{-1} mg^{-1}.

Table 2-6: Effect aerobic and anaerobic conditions on IAD activity obtained from mycelia of *Leptosphaeria maculans*.

Conditions	Relative activity (%) [a]
Aerobic	100 ± 4
Anaerobic	327 ± 20

[a] Activities are expressed as percentage of the activity of IAD obtained in the presence of 2.5 mM $Na_2S_2O_4$ in the presence of the air; results are the means ± SD of three independent experiments. The enzyme activities were measured using protein extracts obtained from DEAE-Sephacel chromatography using 10 mM Tris-HCl buffer pH 7.4 containing 3% glycerol, 0.015% Triton-X100 and 0.1 mM 2-mercaptoethanol. The relative specific activity of IAD for 100% is equivalent to133 nmol min^{-1} mg^{-1}.

The effect of sulfhydryl compounds dithiothreitol (DTT) and 2-mercaptoethanol on IAD activity was tested. The enzyme activity was 75% inhibited by DTT and slightly activated by 2-mercaptoethanol at 1 mM concentration. The effect of different concentrations of DTT and 2-mercaptoethanol on IAD was tested at the time of extraction and after three and seven days of incubation at -20 ^oC for three and seven days. While DTT was inhibiting IAD activity, the effect of 2-mercaptoethanol on IAD activity was found to be concentration dependant. High concentration of 2-mercaptoethanol (10 mM and 5 mM) caused 30 % to 20% inhibition of IAD activity, while lower concentration (1 mM and 0.1 mM) caused 20 % to 40% enhancement of the enzyme activity. It also enhances the activity during storage at -20 ^oC (Fig. 2-30). The

enhancement of the enzyme activity by lower concentration of 2-mercaptoethanol can be attributed to its antioxidant effect that can protect the oxidation of the enzyme.

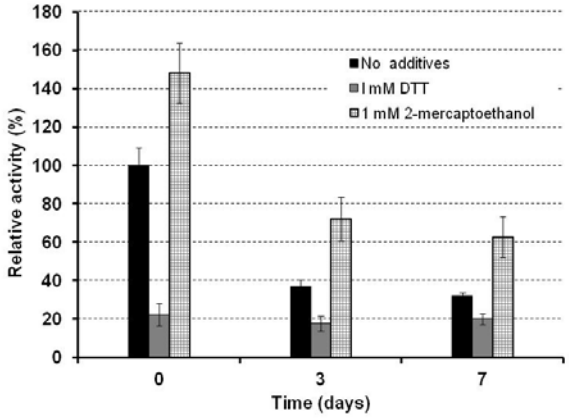

Figure 2-30: Effect of DTT and 2-mercaptoethanol on IAD activity from *Leptosphaeria maculans* at zero time and after three and seven days of storage at – 20 °C. Relative activities are expressed as percentage of activity measured at zero time in the absence of additives. 100% of activity is equivalent to 245 nmol min^{-1} mg^{-1}. The enzyme activities were measured using protein extracts obtained from DEAE-Sephacel chromatography using 10 mM Tris-HCl buffer pH 7.4 containing 3 % glycerol, 0.015% Triton-X100 and 0.1 mM 2-mercaptoethanol.

2.2.2.3 Effect of glycerol

The effect of different concentrations of glycerol (0, 1, 2, 3 & 5%) on the activity of partially purified IAD (after DEAE-Sephacel chromatography) was tested at the time of elution (zero time) and after three and seven days of storage at - 20 °C. Total loss of activity was observed in control (no glycerol) and aliquot stored with 1% glycerol after 3 days of storage at -20 °C. However, IAD activity was enhanced in the presence of 3% and 5% glycerol. 20- 30% of the initial activity was detected after seven days of storage at -20 °C in presence of 3% and 5% of glycerol respectively (Fig. 2-32).

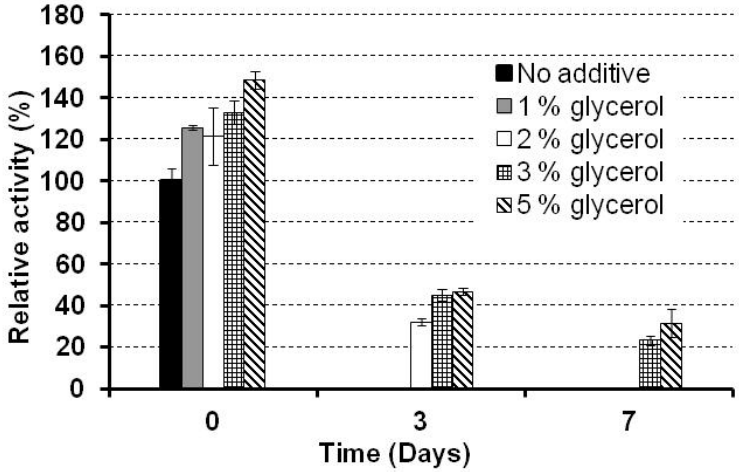

Figure 2-31: Effect of different concentrations of glycerol on IAD activity from *Leptosphaeria maculans* after three and seven days of storage at -20 °C. Relative activities are expressed as percentage of activity measured at zero time in the absence of additives. The enzyme activities were measured using protein extracts obtained from DEAE-Sephacel chromatography using 10 mM Tris-HCl buffer pH 7.4. The relative specific activity of IAD for 100% is equivalent to 115 nmol min^{-1} mg^{-1}.

2.2.2.4 Effect of detergents

The effect of detergents: Triton X-100, Tween 20, Tween 80, CHAPS and CHAPSO on partially purified IAD activity as well as the effect of these detergents on the enzyme activity after storage at -20 ^{o}C for three and seven days was tested in the presence of 3% glycerol. The enzyme activity was enhanced 3.3-, 1.6-, 1.7-, 3.6- and 3.2- fold in the presence of Triton X-100, Tween 20, Tween 80, CHAPS and CHAPSO, respectively. Samples stored with Triton X-100 and CHAPSO show higher activities in comparison to samples stored without detergents. Samples stored without detergents showed 70 % and 17% of the original activity after three and seven days of storage, respectively. However, in case of using Triton X-100 the activities detected are 178% (three days) and 78% (seven days) of the original activity. In case of using CHAPSO, the activities detected are 328% (three days) and 209% (seven days) of the original activity. These data showed that although the enzyme appears to be losing activities by storage in all the cases, the loss of activity is attenuated by the addition of Triton X-100 and CHAPSO. The ability of these detergents to stabilize the enzyme can be attributed to inhibiting the dissociation of the essential cofactor from the active site or by inhibiting the enzyme aggregation (Table 2-7, Fig. 2-32).

Table 2-7: Effect of different detergents on IAD activity from *Leptosphaeria maculans* after three and seven days of storage at – 20 °C.

Additives	Conc. (mM)	Relative activity (%) [a]	Relative activity (%) [b]	Relative activity (%) [c]
Control	0	100 ± 4	70 ± 9	17 ± 2
Triton X-100	0.25	328 ± 10	178 ± 10	78 ± 3
Tween 20	0.05	163 ± 10	63 ± 5	34 ± 3
Tween 80	0.01	168 ± 3	62 ± 5	15 ± 2
CHAPS	6.5	357 ± 9	71 ± 5	59 ± 5
CHAPSO	6.3	332 ± 26	328 ± 17	209± 33

[a] Activities are expressed as percentage of activity relative to the activity obtained with control (no detergents) (100% of activity for IAD is equivalent to 96 nmol min^{-1} mg^{-1}; [a]ctivities measured after three days of storage at – 20 °C. [c]aptivities measured after seven days of storage at - 20 °C.

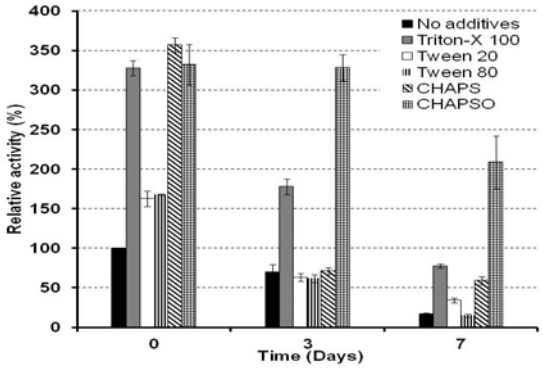

Figure 2-32: Effect of different detergents on IAD activity from *Leptosphaeria maculans*. The enzyme activities were measured using protein extracts obtained from DEAE-Sephacel chromatography using 10 mM Tris-HCl buffer pH 7.4, 3 % glycerol was added to all fractions. The relative specific activity of IAD for 100% is equivalent to 96 nmol min^{-1} mg^{-1}.

2.2.2.5 Effect of cofactors on IAD activity

Some aldoxime dehydratases require cofactors for their activity. For example, FMN was reported as a cofactor for phenylacetaldoxime dehydratase from *Bacillus sp* strain OxB-1 (Kato, Nakamura et al., 2000). Aldoxime dehydratase from rat liver microsomes was activated by the addition of either NADPH (1 mM) or $Na_2S_2O_4$ (10 mM) to the assay mixture (Boucher, Delaforge et al., 1994). In addition, indolyl-3-acetaldoxime dehydratase from *G. fujikuroi* was reported to be activated by PLP (Kumar and Mahadevan, 1963; Shukla and Mahadevan, 1968; Shukla and Mahadevan, 1970). The effect of the following cofactors was tested on partially purified IAD: NADPH, FMN, PLP and $Na_2S_2O_4$. One mM of each of the indicated cofactors was incubated with

assay mixture for 5 minutes and activity was tested and compared to control (activity measured in the absence of cofactors from the assay mixture). IAD activity was enhanced 6.7- and 2.3- fold in the presence of 1 mM of $Na_2S_2O_4$ and NADPH, respectively. PLP showed no effect on IAD activity while FMN inhibited 50% of the enzyme activity (Table 2-8). These results indicated that PLP and FMN are not a cofactor for IAD from *L. maculans* isolate Laird 2.

Table 2-8: Effect of various cofactors at 1.0 mM on the activity of IAD obtained from mycelia of *Leptosphaeria maculans* Laird 2.

Additives (1 mM)	Relative activity (%) [a]
No additives	100 ± 5
$Na_2S_2O_4$	676 ± 64
NADPH	233 ± 4
PLP	92 ± 11
FMN	49 ± 2

[a] Activities are expressed as percentage of the activity of IAD obtained in the absence of $Na_2S_2O_4$; results are the means ± SD of three independent experiments. The enzyme activities were measured using protein obtained from DEAE-Sephacel chromatography, using 10 mM Tris-HCl buffer pH 7.4 containing 3% glycerol and 0.015% Triton-X100. The relative specific activity of IAD for 100% is equivalent to 32 nmol min^{-1} mg^{-1}.

2.2.2.6 Effect of metals

Several aldoxime dehydratases are reported to have iron heme as cofactor. The enzymes are active when iron is in the reduced form while the oxidized forms of these enzymes are not active (Kato, Nakamura et al., 2000; Kato, Yoshida et al., 2004; Oinuma, Hashimoto et al., 2003). In addition, Ca^{2+} was detected in alkylaldoxime dehydratase (OxdA) from *P. chlororaphis* B23 (Oinuma, Hashimoto et al., 2003a). In this section, the effect of various metal ions and EDTA at 1.0 mM on partially purified IAD activity from *L. maculans* was tested in the presence of $Na_2S_2O_4$ in the assay solution. No significant effect was detected in the presence of Ca^{2+} and Ni^{2+} suggesting the absence of these metals from the active site of the enzyme. The enzyme activity was increased 1.8- fold by the addition of 1 mM Fe^{2+} suggesting the involvement of Fe^{2+} in the active site of the enzyme. However, the metal ions Mn^{2+}, Fe^{3+}, Zn^{2+}, Cu^{2+} and Co^{2+} inhibited 27%, 63%, 94%, 97% and 98% of the enzyme activity, respectively. In addition, no effect of EDTA on enzyme activity was detected (Table 2-9).

Table 2-9: Effect of various metals and EDTA at 1.0 mM conc. on the activity of IAD obtained from *Leptosphaeria maculans* Laird 2.

Additives [a]	Relative activity [b]	Additives [a]	Relative activity (%) [b]
No	100 ± 9	Ni^{2+}	120 ± 5
Ca^{2+}	95 ± 10	Co^{2+}	6 ± 2
Zn^{2+}	3 ± 1	Fe^{2+}	180 ± 9
Mn^{2+}	73 ± 6	Fe^{3+}	37 ± 3
Cu^{2+}	2 ± 1	EDTA	110 ± 7

[a] All metals used as chloride salts. [b] Activities are expressed as percentage of the activity of IAD activity obtained in the presence of 2.5 mM $Na_2S_2O_4$; results are the means ± SD of three independent experiments. The enzyme activities were measured using protein extracts obtained from DEAE-Sephacel chromatography using 10 mM Tris-HCl buffer pH 7.4 containing 3 % glycerol and 0.015% Triton X-100. The relative specific activity of IAD for 100% is equivalent to 30 nmol min^{-1} mg^{-1}.

2.2.2.6 Effect of protease inhibitors

The effect of protease inhibitor cocktail (P-8215; Sigma, Mississauga, Canada) (1:200 v/v) was tested on IAD from *L. maculans* after DEAE-Sephacel chromatography at the time of extraction (zero time) and after storage for three and seven days at -20 ^{o}C. Protease inhibitor inhibited 25%, 80% and 90% of enzyme activity at zero time and after storage for three and seven days at -20 ^{o}C respectively (Table 2-10).

Table 2-10: Effect of protease inhibitor cocktail (1:200 v/v) on IAD activity obtained from mycelia of *Leptosphaeria maculans.*

Time (day)	Additive	Relative activity(%) [a]
0	No additive	100 ± 9
0	Protease inhibitor	75 ± 17
3	No additive	37 ± 3
3	Protease inhibitor	16 ± 4
7	No additive	32 ± 2
7	Protease inhibitor	7 ± 2

[a] Activities are expressed as percentage of the activity of IAD obtained in the absence of additives at zero time; results are the means ± SD of three independent experiments. The enzyme activities were measured using protein extracts obtained from DEAE-Sephacel chromatography using 10 mM Tris-HCl buffer pH 7.4 containing 3% glycerol and 0.015% Triton-X-100. The relative specific activity of IAD for 100% is equivalent to 135 nmol min^{-1} mg^{-1}.

2.2.3 Purification & characterization of indolyl-3-acetaldoxime dehydratase (IAD) from *Leptosphaeria maculans* isolate Laird 2

2.2.3.1 Chromatographic purification

The purification of IAD from the CFE of *L. maculans* was difficult due to the loss of enzyme activity during purification. From the stability studies discussed in the previous sections, it was found that glycerol, detergents and 2-mercaptoethanol could stabilize the enzyme. Consequently, glycerol (2-3%), 0.015% Triton X-100 and 0.1 mM 2-mercaptoethanol were added to all purification buffers. Trials to purify the enzyme in the absence of glycerol and Triton X-100 from the purification buffers resulted in low recoveries. In addition, storage of the purified active fractions (in particular after the second step purification) at -20 ^{o}C resulted in significant decreases in enzyme activity. Therefore, after each purification step, the enzyme fractions were stored up to a maximum of 24 h at -20 ^{o}C. Taking these precautions, IAD was purified from CFE of *L. maculans* isolate Laird 2 using three steps in 1-3% yield. Aldoxime dehydratase activity was monitored using a mixture of unseparable *E/Z* indolyl-3-acetaldoximes (**142**) as substrate. The enzymatic assays were done in presence of 2.5 mM $Na_2S_2O_4$ and enzymatic assays were started by the addition of indolyl-3-acetaldoxime. After incubation for 15 minutes, assays were stopped and extracted by EtOAc. The EtOAc extracts were concentrated and samples were analyzed by HPLC-DAD. The product (indolyl-3-acetonitrile, **115**) was quantified using calibration curve built with authentic sample as described in experimental. Two purification protocols were developed.

In protocol 1 the following chromatographic purification steps were used: (1) anion exchange chromatography using DEAE-Sephacel (Fig. 2-33), (2) chromatofocusing with PBE 94 resin (Fig. 2-34), (3) gel filtration chromatography on Superdex 75 (Fig. 2-35).

In the first step, CFE equivalent to 18 mg proteins was loaded to a DEAE-Sephacel column. Proteins were eluted using NaCl gradient (0-0.3 M) with flow rate 0.5 mL.min^{-1} as described in experimental. IAD activity was detected in the range of 0.15 to 0.17 M NaCl (Fig. 2-33).

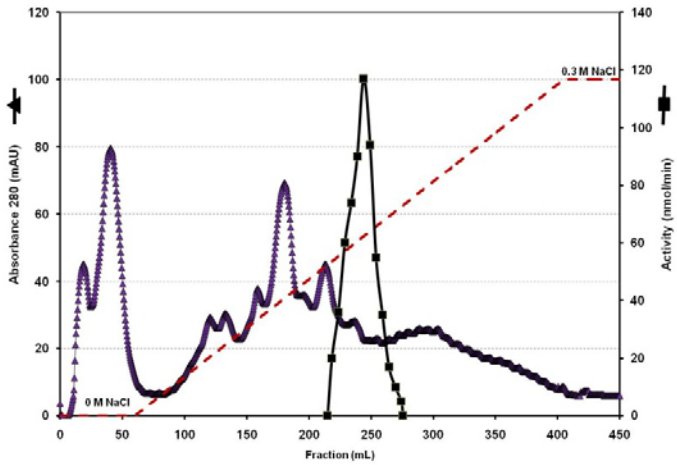

Figure 2-33: Elution profile of DEAE-Sephacel chromatography of *L. maculans* cell-free extract. Elution buffer 10 mM Tris-HCl pH 7.4 containing 0.015% Triton X-100, 3% glycerol and 0.1 mM 2-mercaptoethanol using NaCl gradient (0-0.3 M); flow rate 0.5 mL min^{-1}.

Fractions showing highest activity from first step were pooled together, dialyzed against histidine buffer pH 6.2 containing 2% glycerol, 0.015% Triton X-100 and 0.1 mM 2-mercaptoethanol and applied for chromatofocusing with PBE 94 resin as described in experimental. The pH gradient (6.2-4.0) was generated using polybuffer 74 with flow rate 0.6 mL min^{-1}. IAD was eluted in fractions corresponds to pH range of 5.0 to 4.8. The p*I* of the enzyme was predicted to be 4.9 as highest activity was detected in fractions corresponds to pH 4.9 (Fig. 2-34).

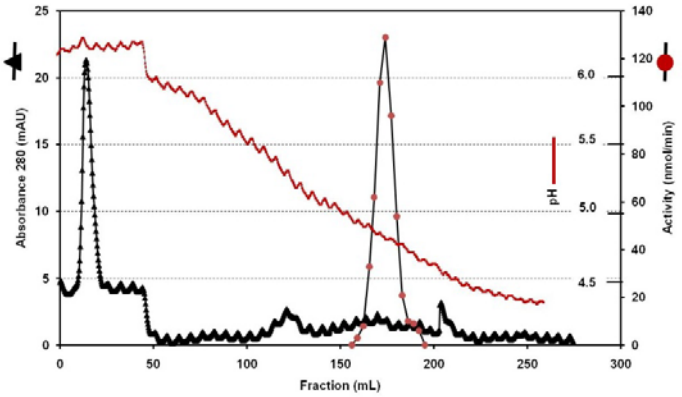

Figure 2-34: Elution profile of chromatofocusing column with PBE 94 resin using polybuffer 74. Starting buffer: histidine buffer pH 6.2 containing 0.015% Triton X-100, 2% glycerol and 0.1 mM 2-mercaptoethanol and titrated against polybuffer 74 pH 4.0 containing 0.015% Triton X-100, 2% glycerol and 0.1 mM 2-mercaptoethanol; flow rate 0.6 mL min^{-1}.

Fractions with highest IAD activity obtained from second step were pooled together and applied to gel-filtration chromatography on Superdex 75 that was pre-calibrated with the marker proteins of known molecular mass as described in experimental. The enzyme was eluted at a position corresponding to a molecular mass of 40-45 kDa (Fig. 2-35).

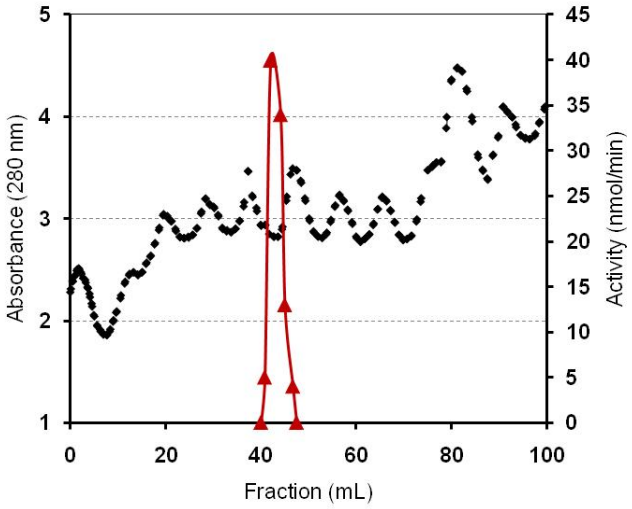

Figure 2-35: Elution profile of Superdex 75 column chromatography. Elution buffer 25 mM phosphate buffer pH 6.8 containing 0.015 % Triton X-100, 3% glycerol, 0.1 mM 2-mercaptoethanol and 50 mM NaCl; flow rate 0.6 mL min^{-1}.

The purity of the protein isolated after Superdex 75 chromatography was examined by SDS-PAGE, which upon staining with Coomassie brilliant blue R-250, revealed a major band having the apparent molecular mass of 40 kDa (Fig. 2-36). In addition, Superdex 75 chromatography of the purified protein suggested that it was a native monomer because it was eluted at a position corresponding to a molecular mass similar to that determined by SDS-PAGE. Table 2-11 indicates the degree of purification and yield obtained for each step.

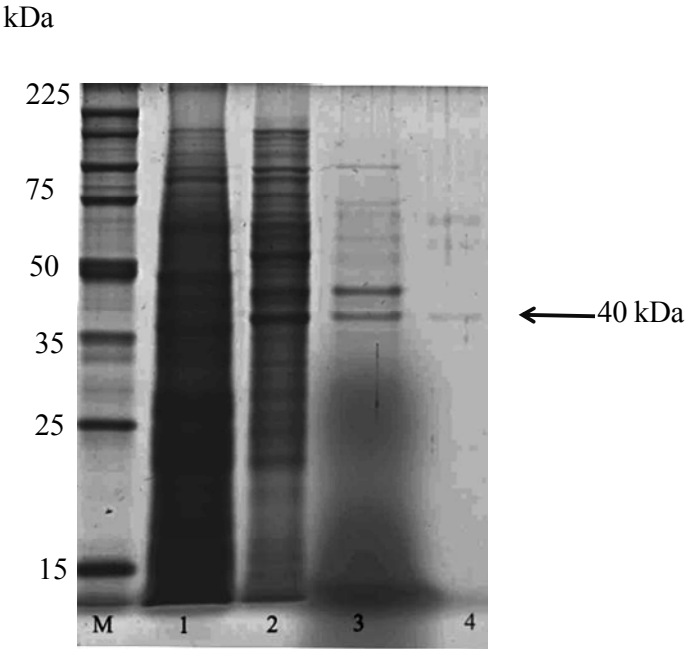

Figure 2-36: SDS-PAGE of protein fractions from purification of IAD using protocol 1: Lane M, marker proteins (molecular masses are indicated); lane 1, crude homogenate (50 µg); lane 2, pooled fractions of DEAE-Sephacel chromatography (30 µg); lane 3, pooled fractions of chromatofocusing chromatography (8 µg); lane 4, pooled fractions after Superdex 75(2 µg).

Table 2-11: Enzyme yields and purification factors of indolyl-3-acetaldoxime dehydratase from *Leptosphaeria maculans* isolate Laird 2 using protocol 1.

Purification step	Protein (mg)	Activity (nmol $min^{-1)}$	Specific activity (nmol min^{-1} $mg^{-1)}$	Recovery (%) [a]	Purification factor (fold) [a]
Crude extract [b]	18.0	5552	307	100	1
DEAE-Sephacel	0.4	2365	5817	43	19
Chromatofocusing	0.09	561	6211	10	20
Superdex 75	0.01	161	14505	3	47

[a] Recoveries are expressed as a percentage of initial activity and purification factors are calculated on the basis of specific activity Mycelia from 300 mL liquid culture.

In protocol 2, IAD was purified from *L. maculans* CFE using the following chromatographic techniques: (1) hydroxyapatite chromatography, (2) chromatofocusing with PBE resin, (3) gel filtration chromatography on Superdex 75. CFE (39.0 mg in two steps) was dialyzed against phosphate buffer pH 6.8 containing 0.015% Triton X-100, 2% glycerol and 0.1 mM 2-mercaptoethanol and loaded to hydroxyapatite column. Proteins were eluted using gradient of phosphate buffer (5.0- 300 mM) at 0.5 mL min^{-1}. The enzyme was eluted at 100-123 mM

phosphate buffer. Fractions with highest activity were loaded to second and third step chromatography as described in protocol 1. The enzyme was purified in 1% recovery with 59-fold purification (Table 2-12).

Table 2-12: Enzyme yields and purification factors of purification of indolyl-3-acetaldoxime dehydratase from *Leptosphaeria maculans* isolate Laird 2 using protocol 2.

Purification step	Protein (mg) [b]	Activity (nmol $min^{-1)}$	Specific activity (nmol min^{-1} $mg^{-1)}$	Recovery (%) [a]	Purification factor (fold) [a]
Crude extract [b]	39.0	9361	240	100	1
Hydroxyapatite	0.4	1738	4345	19	18
Chromatofocusing	0.09	678	7533	7	31
Superdex 75	0.007	71	10142	1	59

[a] Recoveries are expressed as a percentage of initial activity and purification factors are calculated on the basis of specific activity. [b] Mycelia from 800 mL liquid culture.

The SDS-PAGE of the purified fraction showed a major band that corresponds to 40 kDa (Fig. 2-37) which is consistent with results obtained from protocol 1. However, the enzyme was purified in lower recovery (1%) (Table 2-12).

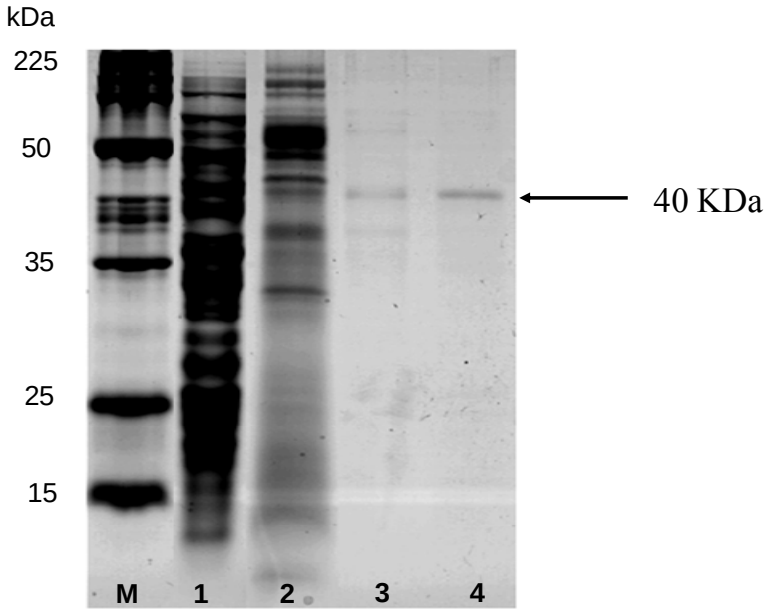

Figure 2-37: SDS-PAGE of protein fractions from purification of IAD using protocol 2: Lane M, marker proteins (molecular masses are indicated); lane 1, crude homogenate (40 µg); lane 2,

Hydroxyapatite pooled fractions (20 µg); lane 3, pooled fractions of chromatofocusing PBE resin chromatography (4 µg); lane 4, purified IAD after Superdex 75 (1 µg).

2.2.3.2 Characterization of indolyl-3-acetaldoxime dehydratase

Characterization of IAD from *L. maculans* was done using active fractions either after first step purification (DEAE-Sephacel chromatography) or active fractions after Superdex 75 using protocol 1. Characterization of IAD includes determination of kinetic parameters (k_m and V_{max}), pH and temperature optima and substrate specificity as described below.

Kinetic properties

The kinetic parameters of IAD were determined on active fractions after Superdex 75 using *E/Z*-IAOx (**142**) as substrate. The substrate saturation curve of IAD was determined in the presence of increasing concentration of IAOx (**142**) (0-1.4 mM). The plot of enzyme velocity (nmol min^{-1}) against substrate concentration (µM) fits to Michaelis-Menten equation (Fig. 2-38 A). In addition, it fits with Linerweaver-Burk plot as plotting of 1/[v] versus 1/[s] gives a straight line (Fig. 2-38 B). From Michaelis-Menten equation and Linerweaver-Burk plot K_m and V_{max} were found to be 0.29 ± 0.05 mM, 2.3 ± 0.11 µmol min^{-1}, respectively. The apparent and k_{cat} was found to be 1317 s^{-1} (Table 2-13).

A comparison of the kinetic parameters for IAD from *L. maculans* and IADSs from *S. sclerotiorum* showed that both enzymes have similar K_m value. However, k_{cat} for IAD enzyme is 132-fold higher than IADSs, which can explain the higher activity detected in *L. maculans* isolate Laird 2.

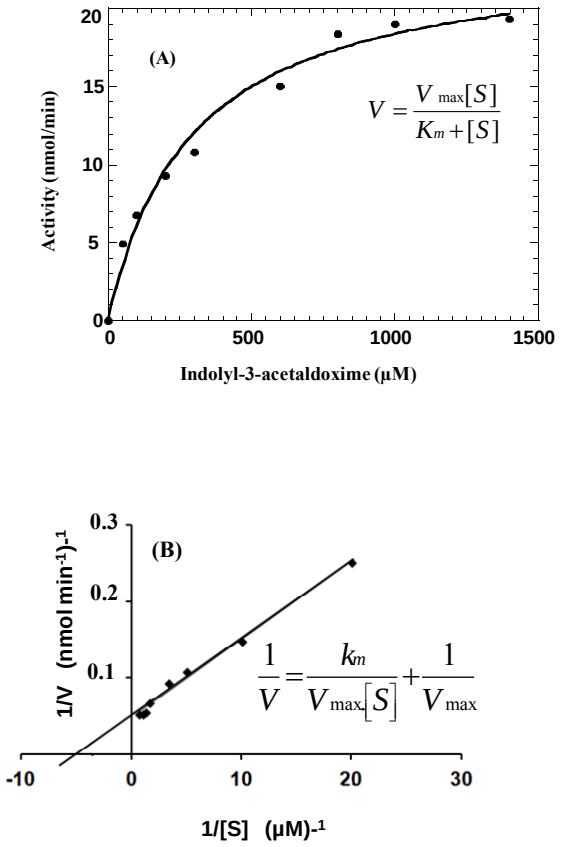

Figure 2-38: Substrate saturation curves of indolyl-3-acetaldoxime dehydratase from *Leptosphaeria maculans* isolate Laird 2. The mixture was incubated at 23 °C for 15 min in the presence of increasing concentrations of *E/Z*-indolyl-3-acetaldoximes (0-1.4 mM). (A) Michaelis-Menten plot using KaleidaGraph. (B) Lineweaver-Burk plots using KaleidaGraph. Purified enzyme obtained from Superdex 75 chromatography using protocol 1.

Determination of pH optima

The temperature and pH optima were determined using active fractions from DEAE-Sephacel chromatography. The influence of pH on IAD activity was investigated in pH range 5.0–10.0 using the following buffer 50 mM diethanolamine, 50 mM *N*-ethylmorpholine, and 100 mM morpholine-ethanesulfonic acid. The assays were carried out for 15 minutes at 23 °C as described in experimental. The enzyme was not active in the basic pH values. The pH optimum for the enzyme activity was found to occur in the pH range of 6.0–7.0 with maximum activity at pH 6.8 (Fig. 2-39). This pH dependence is similar to the pH dependence of the alkylaldoxime dehydratase (OxdA) from *P. chlororaphis* (optimal pH 6.0) (Konishi, Ishida, et al., 2004).

The temperature dependence of IAD activity was tested in the range 10-60 ^{o}C. The enzyme was incubated for 15 min at various temperatures in 25 Mm Tris-HCl pH 7.4 as described in the experimental. The apparent optimum temperatures of IAD were 25-28 ^{o}C (Fig. 2-40). An Arrhenius plot of the enzyme rates at different temperatures (10, 16, 22 and 25 ^{o}C) showed that the enzyme activation energy is 43 kJ mol^{-1}. This value is much lower than the activation energy calculated for phenylacetaldoxime dehydratase from *Bacillus* sp (118 kJ mol^{-1}) (Kato, Nakamura et. al, 2000).

A list of the kinetic parameters of IAD from *L. maculans* Laird 2 is summarized in Table 2-13.

Table 2-13: Kinetic parameters, pH and temperature optima of indolyl-3-acetaldoxime dehydratase (IAD) from *Leptosphaeria maculans* isolate laird 2 (kinetic parameters were obtained from the saturation curves presented in Fig. 2-38 and fitted to Michaelis-Menten equation).

Enzyme	V_{max} (nmol min^{-1})	K_m (mM)	k_{cat} (s^{-1})	pH optimum	Temp. optimum (^{o}C)
IAD	2.3 ± 0.11	0.29 ± 0.05	1317	6.0-7.0	22-25

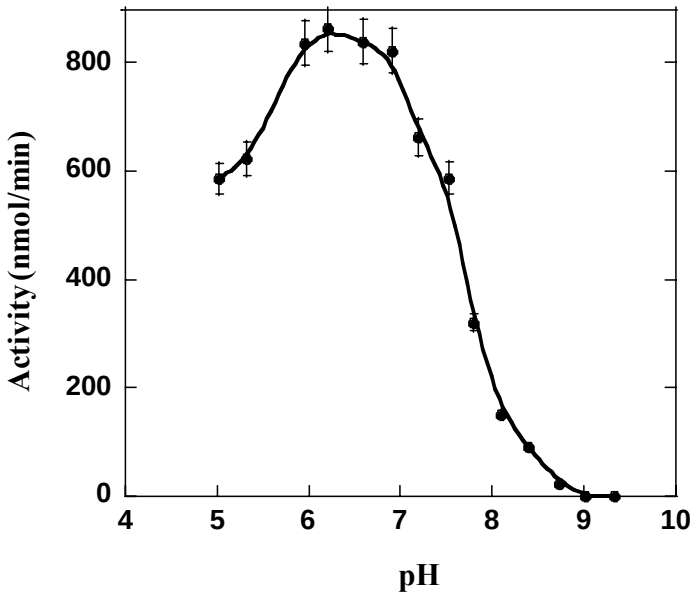

Figure 2-39: pH dependence of IAD activity from *Leptosphaeria maculans* isolate Laird 2. The enzyme activities were measured using protein extracts obtained after DEAE-Sephacel chromatography. The plot was drawn using KaleidaGraph.

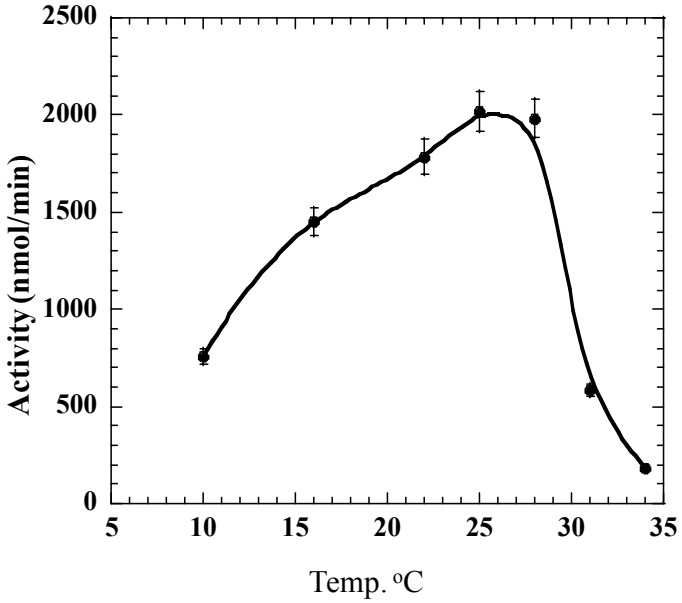

Figure 2-40: Temperature dependence of IAD activity from *Leptosphaeria maculans* isolate Laird 2. The enzyme activities were measured using protein extracts obtained after DEAE-Sephacel chromatography. The plot was drawn using KaleidaGraph.

Substrate specificity

The substrate specificity for IAD was screened using various synthetic indolyl, naphthyl, phenyl and alkyl oximes as summarized in (Table 2-14). The enzyme was incubated with each substrate at 1.5 mM in the presence of 2.5 mM $Na_2S_2O_4$ at 23 ^oC. After 15 min of incubation, the enzyme reaction mixtures were stopped and extracted as described in experimental. Samples were analyzed by DAD-HPLC and products (if present) were determined from calibration curves built with authentic samples. At the beginning, all substrates were tested for IAD activity using active fractions from first step purification (DEAE-Sephacel chromatography). IAD showed activity towards the following indolyl, and naphthyl derivatives: indolyl-3-acetaldoxime (**142**), 3-(3-indolyl) propanal oxime (**193**), 4-(3-indolyl) butanal oxime (**194**), 1-methylindole-3-acetaldoxime (**191**), and naphthyl-2-acetaldehyde oxime (**198**). However, no activity was detected towards the tested aliphatic oximes; butanal oxime (**199**), 3-methylbutanal oxime (**200**) and cyclopentanecarboxaldehyde oxime (**201**). In addition, no activity was detected with indolyl-3-carboxaldehyde oxime (**192**), naphthalene-1-carboxaldehyde oxime (**195**), naphthalene-1-acetaldehyde oxime (**197**), naphthalene -2-carboxaldehyde oxime (**196**) and phenylacetaldoxime (**143**). Highest activity was detected with indolyl-3-acetaldoxime (**142**). However, the methylation

of the indole nitrogen and changing the length of the side chain of the indolyl oximes resulted in a significant decrease in the activity. 3-(3-Indolyl) propanal oxime (**193**) and 4-(3-indolyl) butanal oxime (**194**) showed 5% and 6% activity relative to activity detected with indolyl-3-acetaldoxime (**142**). *N*-methylindolyl-3-acetaldoxime (**191**) showed 3% activity relative to activity detected with indolyl-3-acetaldoxime (**142**). The replacement of the indolyl group by phenyl or naphthyl groups also displayed lower activity towards the enzyme in comparison with indolyl-3-acetaldoxime (**142**). naphthalene-2-acetaldehyde oxime (**198**) showed 18% activity in comparison with indolyl-3-acetaldoxime (**142**).

Substrates that showed activities: indolyl-3-acetaldoxime (**142**), 1-methylindole-3-acetaldoxime (**191**), 3-(3-indolyl) propanal oxime (**193**), 4-(3-indolyl) butanal oxime (**194**) and naphthalene-2-acetaldehyde oxime (**198**), were further tested for IAD activity using fractions from Superdex 75 (protocol 1). Oximes that did not show activity with the enzyme after DEAE-Sephacel chromatography was not tested anymore. Similar results were obtained with IAD after DEAE-Sephacel chromatography. Highest activity was detected with indolyl-3-acetaldoxime (**142**). naphthalene-2-acetaldehyde oxime (**198**) showed 24 % of the activity detected with indolyl-3-acetaldoxime (Table 2-14). These results suggested that IAD from *L. maculans* isolate Laird 2 is an indolyl-3-acetaldoxime dehydratase as no activity was detected with the tested aliphatic oximes and lower activities were detected with the naphthyl derivatives. Also, it seems that the presence of unsubstituted heteroatom is essential for the enzyme activity. In case of indolyl substrates, the 1-methylindole-3-acetaldoxime (**191**) showed 3% activity relative to the non-methylated derivative indolyl-3-acetaldoxime (**142**).

Table 2-14: Relative activity of aldoxime dehydratase from *Leptosphaeria maculans* isolate Laird 2 using different aldoximes as potential substrates.

Compound	Chemical structures	Relative activity (%) [a]	Relative activity (%) [d]
E/Z-Indolyl-3-ethanal oximes) (*E/Z*-Indolyl-3-acetaldoximes) (**142**) [b]	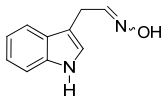	100 ± 8	100 ± 3
E/Z-1-methylindole-3-acetaldoximes (**191**) [b]	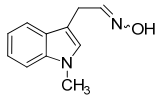	2 ± 1	4 ± 2
E/Z-Indolyl-3-carboxaldehyde oximes (**192**) [b]	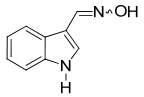	ND	---
E/Z-3-(3-Indolyl)propanal oximes (**193**) [b]	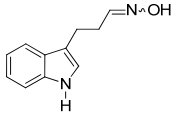	5 ± 3	6 ± 2
E/Z-4-(3-Indolyl)butanal oximes (**194**) [b]	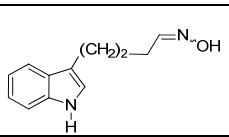	6 ± 2	9 ± 3
E/Z-Naphthalene-1-carboxaldehyde oximes (**195**) [b]	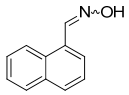	ND	---
E/Z- Naphthalene -2-carboxaldehyde oximes (**196**) [b]	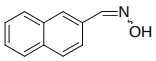	ND	---
E/Z-Naphthalene-1-acetaldehyde oximes (**197**) [b]	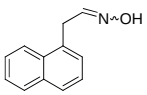	ND	---
E/Z-Naphthalene-2-acetaldehyde oximes (**198**) [b]	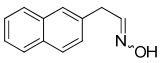	18 ± 2	24 ± 2
E/Z-Phenylethanal oximes (*E/Z*-Phenylacetaldoximes) (**143**) [b]		ND	---
E/Z-Butanal oximes (**199**) [c]	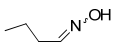	ND	---

Compound	Chemical structures	Relative activity (%) [a]	Relative activity (%) [d]
E/Z-3-Methylbutanal oximes (**200**) [c]	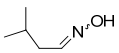	ND	---
E/Z-Cyclopentanecarboxaldehyde oximes (**201**) [c]		ND	---

[a] Activities are expressed as percentage of activity relative to the activity obtained with indolyl-3-acetaldoxime (1.5 mM) after first step of purification (DEAE-Sephacel chromatography). Assays were done for 15 min in 25 mM Tris-HCl pH 7.4 using 50 µl of active fractions; results are expressed as means and standard deviations of four independent experiments (100% of activity for IAD is equivalent to 101 nmol min^{-1} mg^{-1}); ND = not detected. [b] The nitriles (reaction products) were detected and quantified by HPLC-DAD using calibration curves built with authentic samples, as described in experimental part. [c] The aldoximes and their potential products were detected by GC-MS, as described in experimental part. [d] Relative activities measured after third step of purification (Superdex 75 chromatography). Assays were done for 60 min in 25 mM Tris-HCl pH 7.4 using 300 µl of active fractions (100% of activity for IAD is equivalent to 1637 nmol min^{-1} mg^{-1}).

2.2.3.3 Chemical modification reagents

Different protein modifying reagents were used to get information about the nature of the amino acid residues occurring in the IAD active site. The enzyme was incubated with the following reagents: 2,3-butanedione (Butt, **202**, Arg), ethyl acetimidate (EAM, **203**, for Lys), *N*-acetylimidazole (NAI, **204**, for Tyr), diethyl pyrocarbonate (DPEC, **205**, for His), 1-ethyl-3-(3-dimethylaminopropyl)carbodiimide (EDC, **206**, for Asp, Glu), iodoacetamide (IACA, **207**, Cys) and phenylmethanesulfonyl fluoride (PMSF, **208**, for Ser) (Fig. 2-41, Table 2-15).

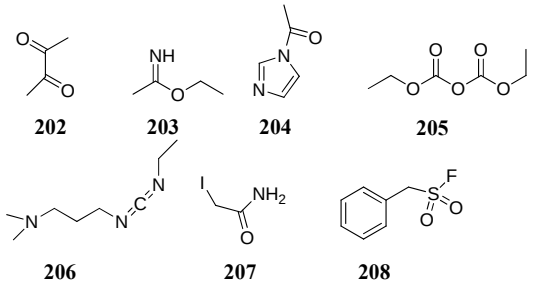

Figure 2-41: Chemical structures of protein modifying reagents: 2,3-butanedione (Butt, **202**), ethyl acetimidate (EAM, **203**), *N*-acetylimidazole (NAI, **204**), diethyl pyrocarbonate (DPEC,

205), 1-ethyl-3-(3-dimethylaminopropyl)carbodiimide (EDC, **206**), iodoacetamide (IACA, **207**) and phenylmethanesulfonyl fluoride (PMSF, **208**).

No significant inactivation of IAD was observed with EAM (**203**, specific for Lys), NAI (**204**, specific for Tyr), PMSF (**208**, specific for Ser) or with EDC (**206**, specific for Asp and Glu). On the other hand 40%, 35% and 23% inactivation of IAD activity was observed with Butt (**202**, specific for Arg), DEPC (**205**, specific for His) and IACA (**207**, specific for Cys), respectively. These results suggest that Arg, His and Cys are involved in the catalytic activity of IAD. The involvement of histidine in the catalytic activity of the enzyme is reported for aldoxime dehydratases OxdA, OxdB and OxdRE. Two histidine residues are involved in the catalysis: proximal histidine residue that binds directly to the heme, while the distal histidine residue that interacts with the substrate (Kobayashi, Yoshioka et al., 2005; Konishi, Ishida et al., 2004). However, the inhibition observed with IACA (**207**) is either due to the involvement of -SH group in IAD activity or due to the lack of the reagent specificity as IACA (**207**) is reported to alkylate histidine as well (Fruchter and Crestfield, 1967). The role of arginine in enzyme activity is not clear at this stage. However, the crystal structure of the aliphatic aldoxime dehydratase OxdRE from *Rhodococcus* sp showed that Arg-178 is involved in hydrogen network with His-320 and Glu-143, which is essential for the proper orientation of His^{320} towards the heme-bound substrate. Site-directed mutagenesis R178Q resulted in 60% loss in activity (Sawai, Sugimoto et al., 2009).

Table 2-15: Effects of protein modifying reagents on indolyl-3-acetaldoxime dehydratase activity.

Reagent for chemical modification	Possible amino acid residues modified	Reaction buffer	Relative activity (%) [c]
But (**202**,10 mM)	Arg	A [a]	60 ± 7
EAM (**203**, 2.5 mM)	Lys	A	97 ± 10
NAI (**204**, 2.5 mM)	Tyr	A	90 ± 3
DEPC (**205**, 2.5 mM)	His	A	65 ± 3
EDC (**206**, 50 mM)	Asp, Glu	B [b]	151 ± 24
IACA (**207,** 2.5 mM)	Cys	B	77 ± 4
PMSF (**208**, 2.5 mM)	Ser	B	113 ± 15

[a] 100 mM phosphate buffer pH 7.5 ,[b] 100 mM MES buffer pH 6.0,[c] Results represent one experiment conducted in triplicate

2.2.4 Antifungal activity

To determine if the biotransformation of indolyl-3-acetaldoxime (**142**) by *L. maculans* is a detoxification process, the antifungal activities of the metabolites indolyl-3-acetonitrile (**115**) and indolyl-3-acetic acid (**146**) as well as the antifungal activity of indolyl-3-acetaldoxime (**142**) against *L. maculans* isolate Laird 2 were determined using the mycelia radial growth bioassay as reported in the experimental part.

The antifungal activities of indolyl-3-acetaldoxime (**142**) and indolyl-3-acetonitrile (**115**) at 0.5 mM showed 30% and 26% inhibition while indolyl-3-acetic acid (**146**) (0.5 mM) showed 9% inhibition (Table 2-16). These results suggested that the biotransformation of indolyl-3-acetaldoxime to indolyl-3-acetic acid by *L. maculans* Laird 2 is a detoxification process.

Table 2-16: Percentage of growth inhibition of *Leptosphaeria maculans* Laird 2 after three days of incubation with indolyl-3-acetaldoxime (**142**), indolyl-3-acetonitrile (**115**) and indolyl-3-acetic acid (**146**).

Compound	Inhibition ± SD (%) [a]		
	0.50 mM	0.20 mM	0.10 mM
Indolyl-3-acetaldoxime (**142**)	30 ± 4	11 ± 1	2 ± 0
Indolyl-3-acetonitrile (**115**)	26 ± 2	13 ± 1	2 ± 0
Indolyl-3-acetic acid (**146**)	9 ± 1	1 ± 0	2 ± 1

[a] The % of inhibition was calculated using the formula: 100-[(growth on treated/growth in control)×100] + standard deviation; results are the mean of at least two independent experiment conducted in triplicates.

2.2.5 Synthesis of aldoxime substrates

The following oximes I used in my research project: *E/Z*-naphthalene-2-acetaldehyde oximes (**198**), *E/Z*- naphthalene-1-acetaldehyde oximes (**197**), *E/Z*-butanal oximes (**199**), were available in Prof. Pedras laboratory. Other oximes were synthesized according to published procedures. The synthesis of *E/Z*-naphthalene-1-carboxaldehyde oximes (**195**), *E/Z*-naphthalene-2-carboxaldehyde oximes (**196**), 1-cyclopentanecarboxaldehyde oxime (**201**) and 3-methylbutanal oxime (**200**) were obtained by direct oximation of the corresponding commercially available

aldehydes using hydroxylamine hydrochloride and sodium acetate in ethanol solution (Pedras, Minic et al., 2010). In addition, the synthesis of *E/Z*-1-methylindole-3-acetaldoximes (**191**) (Pedras, Okinyo-Owiti et al., 2009) and *E/Z*-3-(3-indolyl) propanal oximes (**193**) (Pedras, Minic et al., 2010) were carried out as shown in the experimental part. Indolyl-3-acetaldoxime (**142**) was synthesized by a modification of the previously reported synthetic procedure (Pedras, Minic et al., 2010). Indolyl-3-acetalaldehyde was prepared by the reduction of indolyl-3-acetonitrile using DIBAL-H, the reaction mixture was quenched with HCl and the crude indolyl-3-acetaldehyde (**167**) was treated with hydroxylamine hydrochloride and sodium acetate to yield indolyl-3-acetaldoxime (**142**) as a mixture of *E/Z* isomers as previously reported (Pedras, Minic et al., 2010). However, in this procedure the reaction mixture was quenched by methanol instead of HCl. The use of methanol for quenching resulted in increasing the reaction yield to 75% instead of 30%. Similarly, *E/Z*-4-(3-indolyl) butanal oximes (**194**) were prepared from 4-(3-indolyl) butanoic acid (**209**) by modifying the previously reported synthetic procedure (Pedras, Minic et al., 2010). First, the ethyl ester of 4-(3-indolyl) butanoic acid (**210**) was prepared by treating the acid with EtOH and catalytic amount of H_2SO_4 (10 mol%) at reflux temperature. Next, the ester was reduced with DIBAL-H (1.5 M in toluene) to afford the aldehyde. The reaction mixture was quenched by methanol. Treatment of the aldehyde with hydroxylamine hydrochloride and sodium acetate in EtOH afforded the corresponding oxime as a mixture of *E/Z*- isomers in 70 % yield. When HCl was used for quenching, the reaction was messy and afforded the oxime in 20% yield.

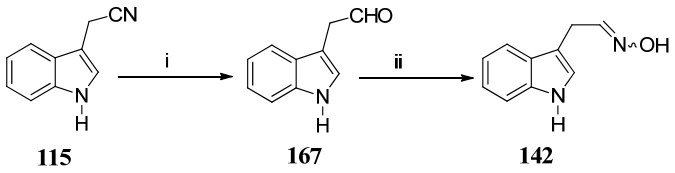

Scheme 2-1: Synthesis of indolyl-3-acetaldoxime (**142**). Reagents and conditions: (i) DIBAL-H, (1.5 M in toluene), CH_2Cl_2, -78 ^oC, 20 min; (ii) NH_2OH-HCl, AcONa, 95% EtOH, 0 ^oC - r.t., 3 h.

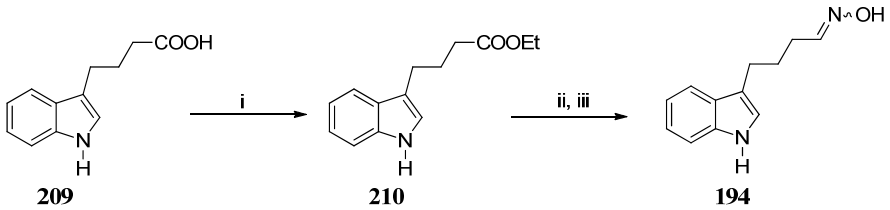

209 **210** **194**

Scheme 2-2: Synthesis of 4-(3-indolyl) butanal oximes (**194**). Reagents and conditions: (i) H_2SO_4 (10 mol%), 95% EtOH, reflux, 2 h; (ii) DIBAL-H, (1.5 M in toluene), CH_2Cl_2, -78 ^oC, 20 min; (iii) NH_2OH-HCl, AcONa, 95% EtOH, 0 ^oC - r.t.

3. Chapter 3: Conclusions and Future Work

3.1 Part 1: Metabolism of destruxin B (1) and sirodesmin PL (13) by crucifers and cereals

In this study, the metabolism of the phytotoxins destruxin B (**1**) and sirodesmin PL (**13**) was investigated in five crucifers: *A. thaliana*, *T. salsuginea*, *E. gallicum*, *B. rapa*, *B. napus* roots; as well as the leaves of the cereals *A. sativa* and *T. aestivum*. In all of the studied crucifers destruxin B (**1**) was metabolized to hydroxydestruxin B (**32**). This metabolic pathway of destruxin B (**1**) to hydroxydestruxin B (**32**) was previously reported in other crucifers: *S. alba*, *C. sativa* and *C. bursa-pastoris* (all blackspot resistant), *B. napus* and *B. juncea* (both blackspot susceptible). The rate of transformation was faster in resistant plants than in susceptible plants (Pedras, Montaut et al., 2003; Pedras, Zaharia et al., 2001). These results indicate that the transformation of destruxin B (**1**) to hydroxydestruxin B (**32**) is conserved among crucifers. All studied crucifers seem to produce a destruxin B hydroxylase that converts destruxin B (**1**) into hydroxydestruxin B (**32**). However, the rate of biotransformation of destruxin B (and likely the amount destruxin B hydroxylase) in all of the plants used in this work was lower as compared with *S. alba* leaves. *S. alba* leaves show the fastest rate of detoxification of destruxin B and the highest degree of resistance to *A. brassicae*. Consequently, *S. alba* was chosen for detection of destruxin B hydroxylase. However, experiments to detect the DBH in CFE were not successful.

In addition, destruxin B (**1**) elicited phytoalexins in some of the studied crucifers: camalexin (**105**) in *A. thaliana*, wasalexins A (**107**) & B (**108**) and 1-methoxybrassenin B (**109**) in *T. salsuginea* leaves and erucalexin (**112**), 1-methoxyspirobrassinin (**113**) and spirobrassinin (**114**) in *E. gallicum*.

Interestingly, destruxin B metabolism was not restricted to crucifers, destruxin B (**1**) was biotransformed by cereals *A. sativa* and *T. aestivum* into several metabolites: hydroxydestruxin B (**32**), dehydrodestruxins B (**178**, **179**) and desmethyldestruxin B (**180**), indicating the presence of multiple enzymes. These metabolites were identified using HPLC–ESI-MS^n (Pedras and Khallaf, 2012) (Fig 3-1).

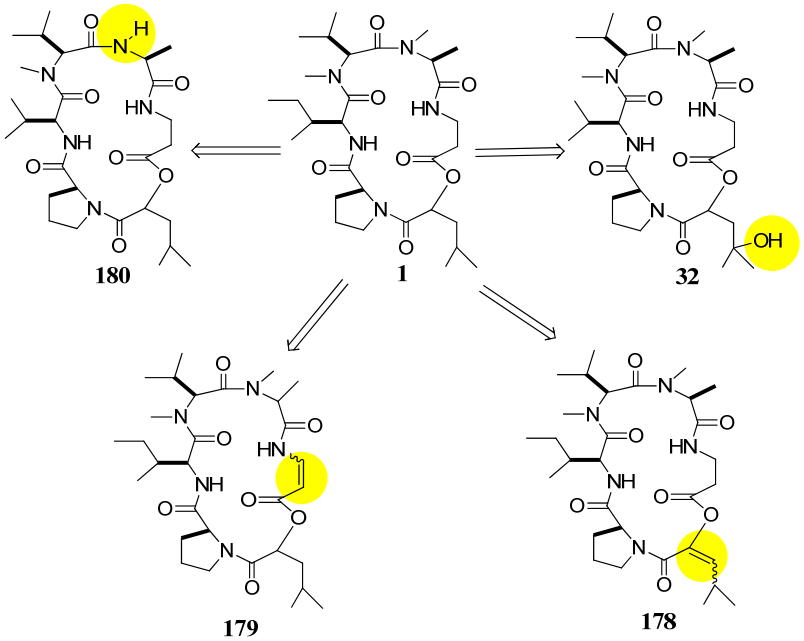

Figure 3-1: Metabolism of destruxin B (**1**) in cereals: *Avena sativa* and *Triticum aestivum* into hydroxydestruxin B (**32**), dehydrodestruxins (**178**, **179**) and desmethyldestruxin B (**180**) (Pedras and Khallaf, 2012).

On the other hand, sirodesmin PL (**13**) was found to be a stronger elicitor than destruxin B (**1**). Sirodesmin PL (**13**) elicited phytoalexin production in *A. thaliana*, *E. gallicum*, *T. salsuginea*, *B. rapa* and *B. napus*. No metabolites of sirodesmin PL (**13**) were detected in any of the studied crucifers. However, in cereals deacetylsirodesmin PL (**14**) was detected, a potential reaction catalyzed by non-specific hydrolases. In addition, no phytoalexins were detected in *A. sativa* or *T. aestivum* after treatment with either destruxin B (**1**) or sirodesmin PL (**13**).

3.2 Part 2: Indolyl-3-acetaldoxime dehydratase from pathogenic fungi

Aldoxime dehydratase activity was screened in pathogenic fungi: *L. maculans* isolate Laird 2, *L. maculans* isolate BJ 125, *R. solani*, *A. brassicicola* and *S. sclerotiorum*. *L. maculans* isolate Laird 2 showed higher specific activity than other tested pathogenic fungi and for this reason, it was chosen for the isolation and characterization of aldoxime dehydratase. However, the enzyme was unstable and loss of activity from CFE or during purification rendered this process difficult. The enzyme was partially stabilized by detergents and glycerol. Also enzymatic

activity was enhanced by reducing agents. The addition of sodium dithionite to enzymatic assays partially restored activity. The activity was also enhanced under anaerobic conditions and in the presence of 2-mercaptoethanol. The effect of different metals on the enzyme activity was tested in the presence of sodium dithionite in the assay mixtures. Enzyme activity was enhanced by Fe^{2+}. These results suggested the presence of iron centre in the active site of IAD similar to other aldoxime dehydratase. The enzyme was partially purified in 1 to 3% recovery. Based on SDS-PAGE analysis and size exclusion chromatography (Superdex 75) the enzyme is monomeric with approximately 40 kDa. However, the identification of the enzyme sequence was not possible due to the extremely small amounts. Screening substrate specificity of the enzyme using indolyl, naphthyl, phenyl and aliphatic aldoximes showed highest activity with IAOx (**142**) (100%) These results suggested that aldoxime dehydratase from *L. maculans* isolate Laird 2 is an indolyl-3-acetaldoxime dehydratase as the highest activity was detected with IAOx (**142**). So far one indolyl-3-acetaldoxime dehydratase from plant pathogenic fungi *S. sclerotiorum* (IADSs) is registered in IUBMB enzyme nomenclature database (Pedras, Minic et al., 2010). In addition, an aldoxime dehydratase designated as indolyl-3-acetaldoxime dehydratase was partially purified from pathogenic fungi *G. fujikuroi* (Shukla and Mahadevan, 1970). Similar to IADSs from *S. sclerotiorum* IAD from *L. maculans* isolate Laird 2 showed K_m value 0.3 mM. However, IAD from Laird 2 showed higher V_{max} value (10 fold more, 2.3 μmol min^{-1}) and higher apparent k_{cat} value (100 fold more 1317 s^{-1}) than IADSs that can explain the higher specific activity in Laird 2.

4. Chapter 4: Experimental

4.1 General experimental procedures

All reagents and chemicals were purchased from Sigma-Aldrich. All solvents were HPLC grade and were used as such. The solvents used in the syntheses were dried and freshly distilled before use according to established procedures (pyridine and DMF with 3 Å molecular sieves, THF over sodium and DCM, CH_3CN and toluene over CaH_2). Organic extracts were dried over Na_2SO_4 and solvents were removed under reduced pressure in a rotary evaporator.

Analytical thin layer chromatography (TLC) was carried out on alumina sheets pre-coated with silica gel, Merk, Kieselgel 60 F_{254} 60 F_{254} (5 × 2 cm × 0.2 mm). Compounds developed on the TLC plates were visualized under UV light (254/366 nm) and/or by dipping in a solution of 5% (w/v) aqueous phosphomolybdic acid containing 1% (w/v) ceric sulphate and 4% (v/v) H_2SO_4, followed by charring on hot plate at 200 ºC.

Flash column chromatography (FCC) was carried out using silica gel grade 60, mesh size 230-400 Å. Preparative thin layer chromatography (prep TLC) was carried out on silica gel plates, Kieselgel 60 F_{254} (20 × 20 cm × 0.25 mm).

NMR spectra were obtained on Bruker Avance 500 spectrometers. For ^1H NMR (500 MHz), the chemical shift values (δ) are reported in parts per million (ppm) relative to tetramethylsilane. The δ values were referred to $CDCl_3$ ($CHCl_3$ at 7.27 ppm) and CD_3CN (CHD_2CN at 1.94 ppm). First-order behaviour was assumed in analysis of ^1H NMR spectra and multiplicities are indicated by the following notations; s = singlet, d = doublet, t = triplicate, q = quartet, m = multiplet and br = broad.

HPLC analysis was carried out with Agilent high performance liquid chromatography instruments equipped with quaternary pump, automatic injector, and diode array detector (DAD, wavelength range 190-600 nm), degasser, a column having an in-line filter. Several methods were used: Method A: (for non-polar fractions in case of turnip, rutabaga, thale cress, oat and wheat): a hypersil octadecylsilane (ODS) column (5 μm particle size silica, 4.6 i.d. × 200 mm), mobile phase H_2O-CH_3CN (75:25, v/v) to (25:75, v/v), in 35.0 min, to (0:100, v/v) for 5.0 min, linear

gradient, and a flow rate of 1.0 mL min^{-1}; Method B (for polar fractions in case of turnip, rutabaga roots, thale cress, oat and wheat leaves): hypersil octadecylsilane (ODS) column (5 µm particle size silica, 4.6 i.d × 200 mm), mobile phase H_2O-CH_3CN (90:10, v/v) to (50:50, v/v), in 35.0 min, linear gradient at a flow rate of 1.0 mL min^{-1}; Method C: (non-polar fractions in case of dog mustard and salt cress leaves): Zorbax Eclipse XDB-C18 column (5 µm particle size silica, 4.6 i.d. × 150 mm), mobile phase H_2O-CH_3OH (50:50, v/v) to (0:100, v/v) , for 25.0 min, linear gradient, flow rate of 0.75 mL min^{-1}; Method D (polar fractions in case of dog mustard and salt cress leaves, both solvents contain 0.1% TFA): Zorbax SB-C18 column (3.5 µm particle size silica, 3.0 i.d. × 100 mm), mobile phase of H_2O-CH_3OH (85 : 15, v/v) to (70:30, v/v), for 25.0 min, to (50:50, v/v), for 5.0 min., to (40:60, v/v) in 5.0 min., linear gradient, flow rate of 0.40 mL min^{-1}. Method E: (for indolyl-3-acetaldoxime dehydratases enzymatic assays): Zorbax Eclipse XDB-C18 column (5 µm particle size, 4.6 i.d. × 150 mm), mobile phase H_2O-CH_3CN (75:25, v/v), to (51:49, v/v), in 15.0 min, to (70:30, v/v) in 5.0 min., linear gradient, flow rate of 0.75 mL min^{-1}.

Samples were dissolved in CH_3CN for method A and C and E and dissolved in CH_3CN-H_2O (1:1) for method B and D.

GC–MS analysis was carried out using a Fisons GC 8060 coupled to a VG-70SE magnetic sector mass spectrometer operated at a mass resolution of 1000, using electron-impact ionization performed at electron energy of 70 eV. Chromatographic separation was achieved in a GS-HP-20M (Carbowax 20 M) capillary column (20 m × 0.32 mm). The column temperature program was started at 40 ^oC for 5.0 min, increased to 200 ^oC (10 ^oC/min) and then kept at 200 ^oC for 5.0 min; the injection volume was 1.0 µl, using He as carrier, head pressure of 4 psi, and flow rate 1 $mL.min^{-1}$. The samples were introduced using the direct injection mode, utilizing on column injector. The injection port temperature was 25 ^oC and a scan range at 25-250 amu was used at a scan speed of 0.5 s.

The HPLC-MS-ESI analysis was carried out with an Agilent 1100 series HPLC system equipped with an autosampler, binary pump, degasser and DAD connected directly to a mass detector (Agilent G2440A MSD-Trap-XCT ion trap mass spectrometer) with an ESI source. Chromatographic separations were carried out at room temperature using an Eclipse XSB C-18 column (5µm particle size silica, 4.6 i.d. × 150 mm), both solvents of mobile phase contains 0.2% formic acid, H_2O-CH_3CN (75:25, v/v) to (25:75, v/v) in 35.0 min, to (0:100 v/v) in 5 min, linear

gradient, flow rate of 1.0 mL min^{-1}. The interface and MS parameters were as follows: nebulizer pressure, 70.0 psi (N_2); dry gas, N_2 (12.0 L min^{-1}); dry gas temperature, 350 °C; spray capillary voltage 3500 V; skimmer voltage, 40.0V; ion transfer capillary exit, 100 V; scan range, *m*/*z* 100-500. Ultrahigh pure He was used as the collision gas. MS^2 analyses were carried out using the data dependent acquisition capabilities of the LC/MSD. Data were acquired in positive and negative modes in a single LC run, using the continuous polarity switching ability of the mass spectrometer. The MS^2 spectra were acquired automatically in a data dependent mode that used criteria from the previous MS scan to select the target precursor peak. All data acquired were processed by Agilent Chemstation software. Samples were dissolved in acetonitrile. From these MS/MS spectra, the most abundant product ion was automatically isolated and further fragmented generating data-dependent MS^n spectra.

HPLC-HRMS-ESI was performed on an Agilent HPLC 1100 series directly connected to a QSTAR XL Systems Mass Spectrometer (Hybrid Quadrupole-TOF LC-MS/MS) with turbo spray ESI source. Chromatographic separation was carried out at room temperature using a Hypersil ODS C-18 column (5 μm particle size silica, 2.1 i.d. × 200 mm) or a Hypersil ODS C-18 column (5 μm particle size silica, 2.1 i.d. × 100 mm), both solvents of mobile phase contains 0.2% formic acid, H_2O-CH_3CN (75:25 v/v) to (25 : 75 v/v) in 35.0 min, to (0:100 v/v) in 5.0 min, linear gradient, flow rate of 0.25 mL min^{-1}. Data acquisition was carried out in either positive or negative polarity mode per LC runs. Data processing was carried out by Analyst QS Software. Samples were dissolved in acetonitrile.

HREI-MS were obtained on a VG 70 SE mass spectrometer employing a solid probe.

Minimal medium (MM) contains the following chemicals:

Solution 1: KNO_3 (3.12 g/L, 30.82 mM), K_2HPO_4 (0.75 g/L, 4.31 mM), KH_2PO_4 (0.75 g/L, 5.51 mM), NaCl (0.10 g/L, 1.71 mM), asparagine (0.28 g/L, 2.12 mM);

Solution 2: $CaCl_2.2H_2O$ (0.10 g/L, 0.68 mM), $MgSO_4.7H_2O$ (0.50 g/L, 2.03 mM);

Solution 3: $ZnSO_4.7H_2O$ (0.39 mg/L, 1.37 μM), $CuSO_4.5H_2O$ (0.079 mg/L, 0.32 μM, $MnSO_4.4H_2O$ (0.041 mg/L, 0.18 μM), MoO_3 (85%, 0.05 mg/L, 0.12 μM), ferric citrate (0.54 mg/L, 2.16 μM), $Na_2B_4O_7.10H_2O$ (0.038 mg/L, 0.10 μM);

Solution 4: thiamine (0.1 mg/L, 0.38 μM);

Glucose (15 g/L, 83.31 mM)

Solutions 1 and 3 were mixed and the pH of the mixed solution was adjusted to 6.55 and autoclaved. The autoclaved solution was combined with solutions 2 and 4 (solution 2 and 4 were sterilized separately by autoclaving and sterile filtration, respectively).

Potato dextrose broth (PDB) was prepared by suspending PDB in water (24 g/L) and autoclaving.

Potato dextrose Agar (PDA) was prepared by suspending PDA in water (39 g/L) and autoclaving.

4.2 Fungal cultures

Fungal spores from *L. maculans* isolate Laird 2, *L. maculans* isolate BJ 125, *S. sclerotiorum*, *R. solani* and *A. brassicicola* were employed in this study. In case of *L. maculans* isolate Laird 2 and *L. maculans* isolate BJ 125, the fungal isolates were grown on V8 agar plates [20% (v/v) V8 juice, 0.75 g/L $CaCO_3$, 100 mg/L streptomycin sulfate, 40 mg/L Rose Bengal, 15 g/L agar] at 23 ± 2 ^oC, under continuous light for 14 days. *A. brassicicola* isolate ATCC 96866 was subcultured in PDA plates under constant light at 23 ± 2 ^oC for 10 days. Spore suspensions of each isolate were prepared by overlaying the V8 agar plates or PDA plates with 10 mL of sterile distilled water, and the plate surfaces were rubbed with a flamed glass rod to dislodge the pycnidiospores. The suspension was filtered and transferred to centrifuge tubes and the spores were separated by centrifugation at 3000*g* for 10 min. After one washing with sterile distilled water, the spores were counted and stored at -20 °C.

R. solani, virulent isolate AG2-1, obtained from the AAFC collection (Saskatoon, SK) was grown on potato dextrose agar (PDA) plates at 23 ± 2 ^oC, under constant light for five days. *S. sclerotiorum* clone #33 was grown on PDA plates (one sclerotium per plate) at 23 ± 2 ^oC, under constant darkness and sclerotia were collected after 15 days of incubation up to 21 days.

Liquid cultures of each pathogen were grown in 250 mL Erlenmeyer flasks containing 100 mL of minimal medium inoculated fungal spores for a final concentration of 5×10^8 per 100 mL for *L. maculans* isolate Laird 2, *L. maculans* isolate BJ 125, 5×10^6 per 100 mL for *A. brassicicola*, or six mycelial plugs (6 mm diameter) per 100 mL PDB for *R. solani* and five sclerotia in 100 mL of PDB *S. sclerotiorum*. Cultures were incubated on a shaker at 120 rpm at

23 ± 2 ^{o}C for 3 days for *L. maculans* isolate Laird 2, and *A. brassicicola*; three and five days for *L. maculans* isolate BJ 125 and *R. solani* and five days for *S. sclerotiorum*. After incubation the mycelia were filtered off and used for the preparation of crude protein extracts as described in section 4.9.1.

4.3 Isolation of destruxins and sirodesmin PL

A. brassicae isolate UAMH 4936, obtained from the University of Alberta Microfungus Collection and Herbarium (Devonian Botanic Garden, University of Alberta, AB, Canada) was grown on V8 agar plates (20 % V8 juice, 0.75 g/L $CaCO_3$, 100 mg/L streptomycin sulfate, 4 mg/L rose Bengal; 15 g/L agar), under constant light at room temperature for 15 days. Liquid cultures were initiated by inoculating Fernbach flasks containing sterile PDA medium (1.68 g, 70 mL) with agar plugs (7 mm diameter plugs, 7 plugs per flask containing 70 mL of PDA, 14 flasks). After incubation for 20 days in the dark, the contents of each flask were diluted with H_2O (100 mL/flask) and homogenized in a blender. The homogenate was centrifuged (3,000 *g* for 20 min) and the supernatant was filtered through eight layers of cheesecloth. The precipitate was discarded and the filtrate was extracted three times with equal volumes of EtOAc, the combined organic layers were dried over Na_2SO_4 and concentrated under reduced pressure. The residue (307 mg) was fractionated by FCC (CH_2Cl_2-CH_3OH, 95:5). The fractions containing destruxin B (**1**) were combined and further fractionated using (hexane-acetone, 70:30 v/v). Finally, fractions containing destruxin B (**1**) were combined and fractionated by C18 silica gel (H_2O-CH_3CN), (60:40 v/v) to yield purified destruxin B (**1**) as white crystals (19 mg) and desmethyldestruxin B (**3**) as a white powder (1 mg).

Sirodesmin PL (**13**) and deacetylsirodesmin PL (**14**) were isolated from fractions obtained from cultures of Canadian virulent isolate of *L. maculans* IBCN 57 (BJ 125) as previously reported (Pedras and Yu, 2008a; Pedras, Séguin-Swartz et al., 1990).

Destruxin B (1)

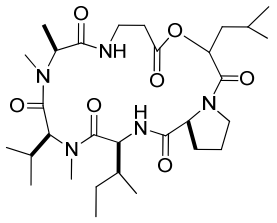

1

HPLC-DAD Method A, t_R = 18.3 min; Method C, t_R = 17.2 min

^{1}H NMR ($CDCl_3$, 500.3 MHz) δ: 8.20 (1H, d, *J* = 9.0 Hz, HN), 7.15 (1H, d, *J* = 9.0 Hz, HN), 5.22 (1H, q, *J* = 7.0 Hz), 4.95 (1H, d, *J* = 11 Hz), 4.91 (1H, dd, *J* = 11.2, 3.1 Hz), 4.86 (1H, dd, *J* = 9.1, 7.0 Hz), 4.65 (1H, d, *J* = 7.0 Hz), 4.11 (1H, m), 3.92 (1H, dd, *J* = 8.0, 8.5 Hz), 3.44 (1H, ddd, *J* = 8, 7 Hz), 3.23 (3H, s), 3.01 (1H, dd, *J* = 12.0, 13.0 Hz), 2.73 (3H, s), 2.68 (1H, ddd, *J* = 18.0, 10.0, 2.0 Hz), 2.52-2.65 (2H, m), 2.32 (1H, dsept, *J* = 11, 6.5 Hz), 2.07 (1H, m), 1.92-2.0 (4H, m), 1.85 (1H, m), 1.40-.45 (1H, m), 1.37 (1H, ddd, *J* = 14.0, 9.0, 3.0 Hz), 1.24-1.32 (1H, m), 1.32 (3H, d, *J* = 7.0 Hz), 0.99 (3H, d, *J* = 6.6 Hz), 0.94 (3H, d, *J* = 6.6 Hz), 0.93 (3H, d, *J* = 6.5 Hz), 0.89 (3H, d, *J* = 6.5 Hz), 0.86 (3H, d, *J* = 5.5 Hz), 0.85 (3H, t, *J* = 7.0 Hz).

HR-EIMS *m/z* measured 593.3771 (593.3775 calc. for $C_{30}H_{51}N_5O_7$).

EIMS *m/z* (% relative int.) 593 $[M]^+$ (100), 536 (51), 508 (38), 451 (39), 423 (26), 340 (30), 177 (46), 86 (100).

Sirodesmin PL (13)

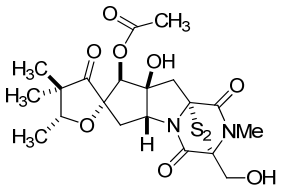

13

HPLC-DAD Method A, t_R = 15.6 min; Method C, t_R = 15.1 min

^{1}H NMR ($CDCl_3$, 500.3 MHz) δ: 5.56 (1H, s), 4.35 (1H, m), 4.34 (1H, m), 4.31 (1H, m), 4.20 (1H, s, OH), 3.95 (1H, q, *J* = 6.2 Hz), 3.39 (1H, dd, *J* = 9.0, 6.4 Hz, OH), 3.27 (2H, br ABq,

J = 17.1), 3.15 (3H, s), 2.77 (1H, dd, *J* = 14.2, 8.2 Hz), 2.11 (3H, s), 1.75 (1H, dd, *J* = 14.2, 8.2 Hz), 1.27 (3H, d, *J* = 6.3 Hz),1.04 (3H, s), 1.12 (3H, s).

HR-EIMS *m/z* measured 422.1689 (calc. for $C_{20}H_{26}N_2O_8$).

EIMS *m/z* (% relative int.) 422 $[M\text{-}S_2]^+$ (100), 344 (10), 246 (47), 205 (22), 140 (21).

ESIMS *m/z* (% relative int.) $[M\text{-}S_2 + H]^+$, 423 (100).

4.4 Plant materials: growth conditions and administration of toxin solution

Seeds of *A. thaliana* (Columbia ecotype) were purchased from the Arabidopsis Information Resource (TAIR). Seeds were grown in small pots and placed in the dark at 4 ºC for 6 days. The pots were transferred to a growth cabinet under white fluorescent lamps (75-100 $\mu Em^{-2}\ s^{-1}$, at 22 ºC/16 h light and 16 ºC/8 h dark cycles). Seedlings were transplanted into larger pots at ca. 14 days and were watered regularly up to eight weeks. *T. salsuginea* (Shandong ecotype) was obtained from TAIR. Seeds were sown in a perlite and nutrient free LG-3 soil (Sun Gro Horticulture Canada) in a Petri dish and incubated at 4 ^oC. After 10 days, the Petri dishes containing seeds were transferred to a growth chamber at 16 h of light/8 h of dark, 23 ^oC day/16 ^oC night, light intensity of 150 $\mu Em^{-2}\ s^{-1}$, and with ambient humidity. After seven days, the seedlings were transferred into soil in small pots, and kept under the same conditions. Seeds of *E. gallicum* were obtained from Plant Gene Resources, Agriculture and Agri-Food Canada (AAFC), Saskatoon, SK. Seeds were sown in a commercial potting soil mixture, and plants were grown in a growth chamber under controlled environmental conditions (20/18 ^oC with 16/8 day/night cycle). Turnip and rutabaga roots were purchased from local stores in Saskatoon. Leaves (eight-week old plants of *A. thaliana, T. salsuginea* and *E. gallicum*) were cut at the base of the petiole and immediately placed in tubes containing destruxin B (**1**) or sirodesmin PL (**13**), as follows. Leaves *A. thaliana* and *T. salsuginea* were immersed in solutions of phytotoxins (0.5 mL solution 4×10^{-5} M in 2% acetonitrile in water per seven leaves). After the solution was taken up, leaves were transferred to an incubator with fluorescent lighting (16 h light/8 hours dark cycle, temperature 20 ± 0.5 ºC) and incubated for one, three and five days, while keeping the base of the petiole in water. A similar procedure was used for leaves of *E. gallicum,* but since the leaves were larger, solutions of each toxin at 4×10^{-4} M, 0.5 mL per leaf were used. After incubation, leaves were frozen in liquid N_2, crushed with glass rod and extracted first with dichloromethane (twice

for ca. 60 min) followed by methanol (twice for 60 min.), and extracts were concentrated to dryness. Control leaves, incubated with 2% acetonitrile in water instead of toxin solution, were treated similarly. Dichloromethane extracts were dissolved in acetonitrile while methanolic extracts were dissolved in methanol-water (50:50) and analyzed by HPLC using method A or C for dichloromethane extracts and method B or D for methanolic extracts. Turnip and rutabaga roots were sliced horizontally (15 mm thick) and cylindrical wells were made on one surface with a cork-borer (16 mm in diameter, 8 wells per slice). Phytotoxin solutions of either destruxin B or sirodesmin PL (2×10^{-5} M) dissolved in 2% acetonitrile in water was applied to each well (0.5 mL/well). The slices were incubated for four days (both for turnip and rutabaga roots) in the dark at 20 ± 0.5 ºC. The aqueous solutions were harvested and extracted with EtOAc, the extracts were dried over Na_2SO_4, concentrated and analyzed by HPLC (Method A). For each slice, the tissue around the wells was cut, homogenized and extracted with methanol. Methanolic extracts were filtered, concentrated to dryness and analyzed by HPLC (Method B). Control samples were treated similarly but using 2% acetonitrile in water. For UV elicited samples, slices were irradiated with UV for 20 min, followed by addition of 2% acetonitrile in water (0.5 mL/well) and incubated and extracted similarly. Seeds of oat (*A. sativa*) and wheat (*T. aestivum*) were obtained from Dr. R. Chibbar, University of Saskatchewan, Department of Plant Sciences, Saskatoon, SK. Seeds were sown in individual pots and incubated at 22 ºC/16 h, light and 16 ºC/ 8 h dark. Wheat and oat leaves were cut at their base and immediately immersed in tubes containing solutions of each phytotoxin (0.5 mL solution 4×10^{-4} M in 2% acetonitrile in water per leaf). After the solution was taken up, leaves were transferred to an incubator with fluorescent lighting (16 h light/8 h dark cycle, temperature 20 ± 0.5 ºC) and incubated for one and three days, while keeping the base of the petiole in water. After incubation, the leaves were treated as described above. Control leaves were incubated with 2% acetonitrile in water solution instead of toxin solution and treated similarly.

4.5 Isolation of destruxin B metabolites from oat leaves

Leaves of *A. sativa* (55 plants, three-week-old) were cut at their base and incubated with destruxin B (**1**) as described above. After incubation for three days, leaves were frozen in liquid

N_2, crushed with a glass rod and extracted with dichloromethane and methanol. The dichloromethane extract (0.74 g) was subjected to fractionation as summarized in Fig. 4-1. In brief, the dichloromethane extract was fractionated using FCC (gradient elution, CH_2Cl_2, 100% to CH_2Cl_2-MeOH, 10:90), fractionation was monitored by HPLC and LC-ESIMS. Three fractions F8, F9 and F11 were used for further purification. F11 was fractionated by RP followed by analytical HPLC (method C) to give hydroxydestruxin B (**32**, identified by LC-ESI- MS and ^{1}H NMR). F8 and F9 were fractionated separately by RP-FCC (gradient elution, CH_3CN-H_2O, 65:35, to CH_3CN, 100%) followed by analytical HPLC (gradient elution, CH_3CN-H_2O, 50:50, to CH_3CN, 100% for 25 min) to give four fractions containing dehydrodestruxin B (**178**), dehydrodestruxin B (**179**), desmethyldestruxin B (**180**) and destruxin B (**1**) (Fig. 4-1). The four fractions were analyzed by HPLC-ESI-MS/MS and ^{1}H NMR. Fragment ions obtained by HPLC-ESI-MS (ion trap) with CID-MS^5 analyses of: destruxin B (**1**), desmethyldestruxin B (**3**), hydroxydestruxin B (**32**), dehydrodestruxin B (**178**), dehydrodestruxin B (**179**) and desmethyldestruxin B (**180**) are presented in Table 4-1.

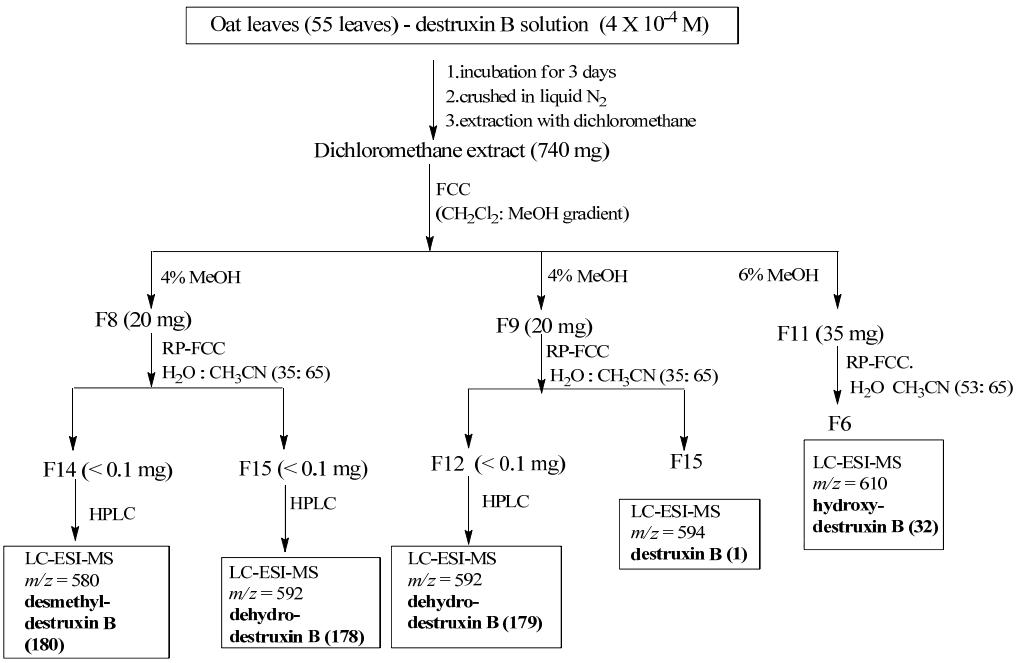

Figure 4-1: Flow chart for fractionation of dichloromethane extracts of *Avena sativa* (oat) leaves incubated with destruxin B (**1**) for three days.

Table 4-1: Fragment ions [a] obtained by HPLC-ESI-MS (ion trap) with CID-MS^5 analyses of: destruxin B (**1**), desmethyldestruxin B (**3**), hydroxydestruxin B (**32**), dehydrodestruxin B (**178**), dehydrodestruxin B (**179**) and desmethyldestruxin B (**180**).

Compound	$[M+H]^+$	MS^2 (%)	MS^3 (%)	MS^4 (%)	MS^5 (%)	MS^5 (%)
Destruxin B (**1**)	**594**	566 (22), **481**(100), 453 (59)	481 ⟶ **453** (100)	453 ⟶ **368** (59), 225(20),194 (100), 175 (15)	368 ⟶ 351 (21), 323(31), 283 (30), **194** (23), 166 (48), 158 (94), 140 (100)	194 ⟶ 166 (100), 152 (92), 138 (36), 114 (83)
Desmethyl-destruxin B (**3**)	**580**	**552**(100),507(15), 481 (78), 453(41)	552 ⟶ 535 (31), 507(55), **481** (100), 453 (99)	481 ⟶ **453** (100)	453 ⟶ 368 (100), 225(33), 194 (96), 175 (34)	
Hydroxydest-ruxin B (**32**)	**610**	**592**(100), 324 (22)	592 ⟶ 503 (63), **479**(86), 451(52),418 (100),305 (20),277(20), 192 (25)	479 ⟶ **451** (100), 390 (15), 366 (20)	451 ⟶ 366 (100), 243 (17), 192 (43), 179 (29), 164 (19) 136 (15)	

Compound	$[M+H]^+$	MS^2 (%)	MS^3 (%)	MS^4 (%)	MS^5 (%)	MS^5 (%)
Dehydrodest-ruxin B (**178**)	**592**	564 (47), **479** (100), 451 (71)	479 ⟶ **451** (100)	451 ⟶ **366** (100), 277(37), 269 (16), 243(15),192 (60), 164 (21)	366 ⟶ 338 (90), 321(37), 277 (62), 192 (74), 175 (35), 164 (100), 158 (50), 140 (20), 136 (32)	
Dehydrodest-ruxin B (**179**)	**592**	**564** (100), 479 (23), 451 (36)	564 ⟶ **451** (100), 368 (76), 366 (17), 268 (21), 194 (60), 169 (18)	451⟶ **366** (100), 338 (78) 325(32), 269(18), 268(57), 213(42) B, 194(35)	**366** ⟶ 194 (100)	
Desmethyldest-ruxin B (**180**)	**580**	**552** (100), 467(15), 439 (17), 396 (12), 368 (23)	552⟶ **439** (100), 368 (63), 194 (23).	439 ⟶ 354 (25), 325 (29), 229 (51), **211** (99), **194** (100).	194 ⟶ 166 (77), 151 (97), 138 (100), 124 (21)	211⟶ 184 (100), 170 (22), 169 (31), 157 (16), 140 (17), 112 (95)

[a] Only fragment ions with relative intensity >10% are shown; ⟶ represents CID step and ions in bold represent those ions subjected to further CID-MS.

4.6 Analysis of elicited metabolites from *Erucastrum gallicum* O.E. Schulz.

4.6.1 Time-course analysis

Time course analysis was carried out to determine the production of UV elicited metabolites by *E. gallicum*. Eight-week old plants were elicited with UV (1 h). Leaves were excised at 24-hour intervals up to 120 hours (each experiment was carried out in triplicate). Fresh leaf weights were measured and the leaves were frozen in liquid N_2, crushed with a glass rod, and then extracted in EtOAc (30 mL) overnight. The EtOAc extract was filtered off and the solvent was removed under reduced pressure. Non-elicited leaves (control experiment) were similarly treated. EtOAc extracts from both elicited and control leaves were analyzed using HPLC-UV profiles (Method C).

4.6.2 Isolation of secondary metabolites from *Erucastrum gallicum*

In order to isolate the elicited compounds, a large-scale experiment was carried out. Elicited *E. gallicum* leaves from 40 pots (358 g of fresh leaf weight) were divided into three Erlenmeyer flasks, then frozen in liquid N_2, crushed with a glass rod, and extracted with dichloromethane (250 mL per flask) overnight. The dichloromethane extract was filtered off and the remaining residue was sequentially extracted with CH_3OH (250 mL per flask). The combined crude extracts were purified by FCC (hexane-CH_2Cl_2, 80:20 to 0 : 100, then CH_2Cl_2-CH_3OH, 95:5 v/v) (Fig. 4-2). The resulting fractions were analyzed by HPLC-DAD (Method C) and TLC. A fraction showing a peak at t_R = 14.1 min on HPLC chromatogram was further purified by FCC (hexane: CH_2Cl_2, 20:80). Fraction rich in the compound of interest was fractionated by analytical HPLC (method C) to give metabolite **190** (> 1mg) and identified by LC-ESI- MS and ^{1}H NMR.

HPLC-DAD Method C, t_R = 14.1 min

^{1}H NMR ($CDCl_3$, 500.3 MHz) δ: 7.82 (s, 1H), 7.10 (d, *J* = 3 Hz, 1H), 6.98 (d, *J* = 8.5 Hz, 1H) and 6.94 (d, *J* = 9 Hz, 1H), 4.04 (3H, s), 3.88 (3H, s).

HR-EIMS *m/z* measured 234.0467 (calc. for $C_{20}H_{26}N_2O_8$).

EIMS *m/z* (% relative int.) 234 $[M]^+$ (100), 219 (28), 176 (18), 149 (20), 133 (42).

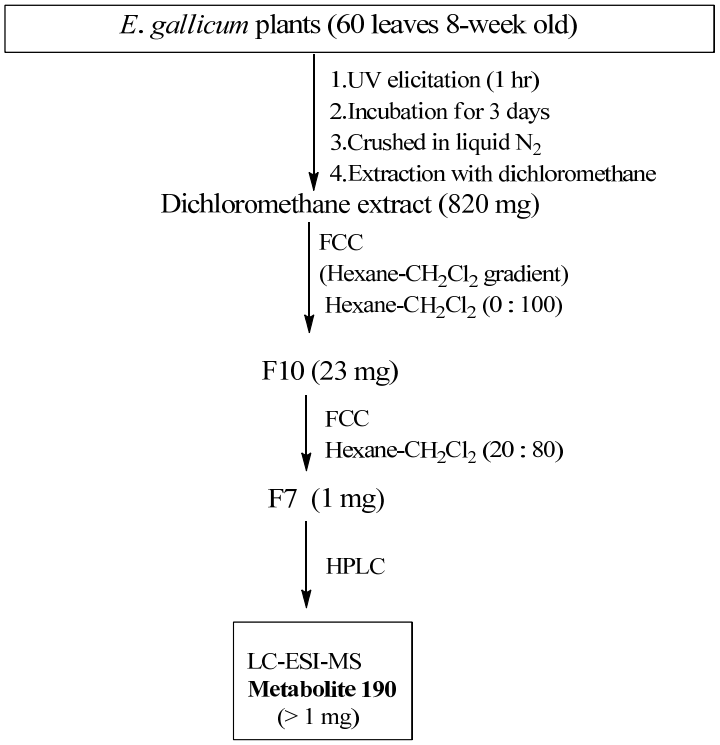

Figure 4-2: Flow chart for fractionation of dichloromethane extracts of *Erucastrum gallicum* (dog mustard) leaves elicited with UV (1 h elicitation, 3 days of incubation).

4.7 Screening for destruxin B hydroxylase (DBH) activity in *Sinapis alba* (white mustard) cell-free extract

Leaves of *S. alba* (22-28 days old) were cut at the base of their petioles and each leaf was immediately placed in tubes containing solutions of homodestruxin B (**2**, 0.5 mL, 5×10^{-5} M in 2 % acetonitrile in water). After the solution was taken up, leaves were immersed in water and transferred to an incubator with fluorescent lighting at temperature 20 ± 0.5 ºC for 12 h. After incubation, plant leaves were homogenized with two volumes (w/v) of extraction buffers (A, B or C) in the presence of equal weight of Ottawa sand in a pre-chilled mortar and pestle. The mycelial homogenate was centrifuged at 3,000 *g* for 10 min to remove sand and uncrushed mycelia and then the supernatant was further subjected to centrifugation at 10,000 *g* at 4 ^{o}C for 10 min. The resulting supernatant was taken as the crude protein extract for enzymatic assays.

The assays to determine DBH activity contained 100 mM Tris-HCl buffer pH 7.5, 0.2 mM destruxin B, 5 µl of the cofactors and 400 µL proteins extract in a total volume of 500 µl. The reaction mixture was incubated at 30 ^{o}C for 60 min under constant shaking. The reaction was stopped by adding EtOAc and extracted two times with EtOAc (2 mL). A control reaction was stopped similarly at time zero. The organic layers were combined and concentrated to dryness under reduced pressure. The extracts were dissolved in CH_3CN (200 µl) and analyzed by HPLC using Method A. The buffers used for extraction are: Buffer A: 250 mM sodium acetate buffer pH 5.0 containing 2 mM EDTA, 2 mM DTT, 50 mM sodium metabisulfite, 250 mM sucrose, 100 mM ascorbic acid and 1mM PMSF, 5 mg/mL BSA and 10 % (w/v) PVPP; Buffer B: 250 mM Tis-HCL buffer pH 7.2 containing 2 mM EDTA, 2 mM DTT, 50 mM sodium metabisulfite, 250 mM sucrose, 100 mM ascorbic acid and 1mM PMSF, 5 mg/mL BSA and 10 % (w/v) PVPP; Buffer C: 250 mM Tricine buffer pH 8.0 containing 2 mM EDTA, 2 mM DTT, 50 mM sodium metabisulfite, 250 mM sucrose, 100 mM ascorbic acid, 1 mM PMSF, 5 mg/mL BSA and 10 % (w/v) PVPP. The following cofactors were used: NADH (2 mM), NADPH (2 mM), NADPH (2 mM) + FMN (25 µM) + FAD (25 µM), NADH (2 mM) + FAD (25µM) + FMN (25 µM), α-ketoglutaric acid (0.5 mM), Fe^{2+} (0.1 mM) and ascorbic acid (4 mM). Soluble and microsomal fractions were prepared as described ain the following section (4.8) and used for detecting DBH activity.

4.8. Detection of phenylalanine ammonia lyase (PAL) and Cinnamic acid-4-hydroxylase (C4H) activities in *Sinapis alba* (white mustard) cell-free extracts

White mustard leaves were elicited with homodestruxin B (**2**) as described in the previous section. The leaves were homogenized with two volumes (w/v) of 250 mM Tricine buffer pH 8.0 containing 250 mM sucrose, 100 mM ascorbic acid, 50 mM sodium metabisulfite, 2 mM DDT, 2 mM EDTA, 5 mg/mL BSA and 1mM PMSF in the presence of equal weight of Ottawa sand in a pre-chilled mortar and pestle. The mycelial homogenate was centrifuged at 10,000 *g* for 10 min. The supernatant (CFE) was further subjected to centrifugation at 200,000 *g* for 60 min to get soluble fraction (supernatant) and pellets (microsomal fraction). Both CFE and the soluble fraction were tested for PAL activity while pellet was subjected to further treatment and used for

testing C4H activity. The pellet was resuspended in 100 mM Tricine buffer pH 8.0 containing 250 mM sucrose, 50 mM NaCl and 2 mM DDT and then pelletized by centrifugation at 200,000 *g* for 30 minutes. The resulting pellets were suspended in 100 mM Tricine buffer pH 8.0, containing 250 mM sucrose, 50 mM sodium chloride, 2 mM DDT and 15% glycerol and used for detecting C4H activity.

The standard assay to determine PAL activity contained 100 mM Tricine buffer pH 8.0, 1 mM phenylalanine and 400 µl of enzyme aliquot (CFE or soluble fractions) in a total volume of 1.0 mL. The reaction mixture was incubated for 60 min at 37 ^{o}C. The reaction was stopped by 200 µl of 1.5 M H_2SO_4, then the reaction products were extracted two times with Et_2O (2 mL). A control reaction was stopped similarly at time zero. The organic layers were combined and concentrated to dryness, dissolved in acetonitrile (200 µl) and analyzed by HPLC using Method A. C4H assays were tested in the microsomes by the incubation of 400 µl of microsomes with 1 mM cinnamic acid in the presence of 2 mM NADPH in a total volume of 1.0 mL of 100 mM Tricine buffer pH 8.0 at 30 ^{o}C for 60 min. The reaction mixture was acidified with 200 µl 1.5 M H_2SO_4 and extracted two times with Et_2O (2 mL). The ether extract was concentrated, dissolved in acetonitrile (200 µl) and analysed by HPLC using Method A.

Protein estimation was performed by Bradford method (Bradford, 1976) using bovine serum albumin as the standard and Bradford reagent from Sigma Aldrich. One unit of activity is defined as the amount of enzyme that produces 1 µmol of cinnamic acid (PAL activity) or 4-hydroxycinnamic acid (C4H activity) per min.

4.9 Indolyl-3-acetaldoxime dehydratase

4.9.1 Protein extraction and activity assays

The extraction buffer consisted of 10 mM Tris-HCl buffer pH 7.4 containing 3% glycerol. Mycelia were homogenized in a chilled mortar with equal weight of Ottawa sand and extracted with two volumes (w/v) of extraction buffer. The mycelial homogenate was centrifuged at 3,000 *g* for 10 min to remove sand and uncrushed mycelia and then the supernatant was further subjected to centrifugation at 10,000 *g* at 4 ^{o}C for 10 min. The resulting supernatant was taken as the crude

protein extract for chromatographic purification of enzyme. Protein concentrations were determined by the Bradford's method using Bradford reagent from Sigma Aldrich and BSA as standard (Bradford, 1976). One unit of activity is defined as the amount of enzyme that produces 1 µmol of indolyl-3-acetonitrile (**115**) per min. The standard assay to determine IAD activity contained 25 mM Tris-HCl buffer pH 7.4, 1.0 mM aldoxime substrate and 100 µL (20 time diluted enzyme aliquot in case of using CFE) in a total volume of 500 µl. The reaction mixture was incubated for 15 min at 23 ^{o}C under constant shaking. The reaction was stopped by adding EtOAc (2 mL), then the reaction products were extracted two times with EtOAc (2 mL). A control reaction was stopped similarly at time zero. The organic layers were combined and concentrated to dryness. The extracts were dissolved in 300 µL CH_3CN and analyzed by HPLC using Method E. The amount of product formed was determined from calibration curves built using a commercial sample of indolyl-3 acetonitrile (**115**) or other nitriles, as applicable. In experiments to determine the aliphatic nitriles, the reaction was stopped with an equal volume of dichloromethane, extracted and the extract analyzed by GC-MS.

4.9.2 Purification and characterization of indolyl-3-acetaldoxime dehydratase from *Leptosphaeria maculans*

Chromatographic techniques

An Äkta FPLC (GE Healthcare, Baie d´Urfé, Canada), equipped with a P-920 pump, UPC-900 UV absorbance monitor and a Frac950 fraction collector was used for all protein separations at 4 ^{o}C.

Protocol 1: Step 1: The CFE obtained from extracting *L. maculans* frozen mycelia (10 mL) was loaded on DEAE-Sephacel (Amersham Biosciences) anion-exchange column (1.6 × 12 cm). protein were eluted first with 10 mM Tris-HCl pH 7.4 containing 0.015% (v/v) Triton X-100, 3% glycerol and 0.1 mM 2-mercaptoethanol (60 mL) and then with 0.0-0.3 M NaCl gradient in the same buffer. Fractions of 5.0 mL were collected at a flow rate of 0.5 mL min^{-1} and 50 µL assayed for indolyl-3-acetaldoxime dehydratase. Fractions (29-31) showing IAD activity were pooled and used in the second step of purification.

Step 2: The protein extract (15 mL) obtained from step 1 was equilibrated by dialysis against 25 mM histidine buffer (pH 6.2) containing 0.015% Triton X-100, 1% glycerol and 0.1 mM 2-mercaptoethanol. The protein extract was concentrated to 2 mL (Amicon Ultra-15, 10 kDa; Millipore, Etobicoke, Canada) and applied to a column (0.9 × 20 cm) of polybuffer exchanger PBE 94 resin (GE Healthcare) equilibrated in the same buffer. Elution was performed with Polybuffer 74, eight-fold diluted with distilled water and adjusted to pH 4.0. Fractions of 3 mL were collected at a flow rate of 0.6 mL min^{-1}. A peak of IAD activity was observed at pH 4.8-5.0. Fractions (51-53) showing IAD activity were pooled and used in the third step of purification. 150 µL of each fraction were assayed for IAD activity.

Step 3: Active fractions obtained from chromatofocusing chromatography were concentrated to 2 mL (Amicon Ultra-15, 10 kDa; Millipore, Etobicoke, Canada) and fractionated by fast protein liquid chromatography (GE Healthcare) on a Superdex 75, pre-calibrated with the following markers of known molecular mass: blue dextran (2000 kDa), BSA (67 kDa), ovalbumin (43 kDa), chymotrypsin (25 kDa) and ribonuclease (13.7 kDa). Equilibration and elution were performed at 4 ^{o}C with 25 mM phosphate buffer (pH 6.8), 2% glycerol and 0.05 M NaCl. Fractions of 1.5 mL were collected at a flow rate of 0.6 mL min^{-1}, and 100 µl of each fraction were assayed for IAD activity.

Protocol 2: Step 1: The CFE obtained from extracting *L. maculans* frozen mycelia (39 mg protein, 10 mL) was dialyzed against 5 mM phosphate buffer 6.8 containing 2% glycerol, 0.015% Triton X-100 and loaded to hydroxyapatite column (1.6 × 6.0 cm) (Bio-Rad). Proteins were eluted first with 5 mM phosphate buffer 6.8 containing 2% glycerol, 0.015% Triton X-100 (60 mL) and then with using a linear gradient of sodium phosphate (5-300 mM) in the same buffer. Fractions of 3.0 mL were collected at a flow rate of 0.5 mL min^{-1} and 100 µl was assayed for IAD activity. Fractions 28-30 were pooled and used in the second step of purification.

Step 2 and Step 3 were conducted as described with protocol 1.

4.9.3 SDS/PAGE

Protein-denaturing SDS-PAGE was carried out using 10% polyacrylamide gels. Standard markers (molecular mass range 10-225 kDa; V8491; Promega, Madison, WI, USA) were used to

determine the approximate molecular mass values of purified proteins in gels stained with Coomassie Brilliant Blue R-250.

4.9.4 Effect of additives and anaerobic condition on IAD activity

The activity of IAD in 25 mM Tris-HCl buffer pH 7.4 was examined in presence of several compounds and cofactors by incubating an appropriate dilution of the partially purified enzyme (after first step; DEAE-Sephacel chromatography) with the additive of interest for 5 min followed by the addition of sodium dithionite (final concentration 2.5 mM). The reaction was started by the addition of indolyl-3-acetaldoxime (1 mM), and the reaction mixtures were then incubated for an additional 15 min at 23 ^{o}C. In addition the effect of some additives (glycerol, detergents, DTT, 2-mercaptoethanol, EDTA and protease inhibitor) on the enzyme stability during storage for one, three and seven days at -20 ^{o}C were tested. The conditions used for testing effect of different additives are summarized in Table 4.2.

The enzyme activity was measured and expressed as the percentage of activity calculated as the ratio of the specific activity of IAD in the presence of additives and a control reaction (aerobic conditions, assay without additives).

For anaerobic conditions, the enzymatic assays were performed under argon; the reaction mixture (2.0 mL), stored in a capped and sealed vial, was first purged with a stream of argon for 5 min and then kept under a steady stream of argon for the duration of the experiment; 0.5 mL of the reaction mixture was collected after 15 min using a needle and syringe. The reaction was stopped by adding EtOAc (2 mL), then the reaction products were extracted two times with EtOAc (2 mL). A control reaction was stopped similarly at time zero. The organic layers were combined and concentrated to dryness. The extracts were dissolved in 300 µl CH_3CN and analyzed by HPLC using Method E. The amount of product formed was determined from calibration curves built using a commercial sample of indolyl-3-acetonitrile (**115**).

Table 4-2: Additives tested for their effects on partially purified indolyl-3-acetaldoxime dehydratase [a].

Additives	Concentration	Elution buffer
Glycerol	1%, 2%, 3% and 5% (v/v)	A [b]
Detergents Triton X-100, Tween 20, Tween 80, CHAPS, CHAPSO	 0.25 mM (0.015% v/v), 0.05 mM, 0.01 mM, 6.5 mM, 6.3 mM.	B [c]
protease inhibitor cocktail (P-8215; Sigma, Mississauga, Canada)	1:200 (v/v)	C [d]
EDTA	1 mM	C
DTT	0.05, 0.1, 0.5, 0.75, 1.0, 5.0, 10.0 (mM)	C
2-mercaptoethanol [b]	0.05, 0.1, 0.5, 0.75, 1.0, 5.0, 10.0 (mM)	C
$Na_2S_2O_4$	0.5. 1.0, 2.5, 5.0, 7.5, 10.0 (mM)	D [e]
NADPH	1 mM	D
FMN	1 mM	D
PLP	1mM	D
Metals: Ca^{2+}, Zn^{2+}, Mn^{2+}, Cu^{2+}, Ni^{2+}, Co^{2+}, Fe^{2+}, Fe^{3+}	1 mM	D

[a] Cell-free extract was loaded to DEAE-Sephacel chromatography (Amersham Biosciences) anion exchange column (1.6 × 12 cm) and proteins were eluted first with buffer (A, B, C or D) and then with 0.0-0.3 M NaCl gradient in the same buffer (A, B, C or D). Fractions of 5 mL were collected at a flow rate of 0.6 mL min^{-1} and 100 µl assayed for IAD; [b] Buffer A: 10 mM Tris-HCl pH 7.4; [c] Buffer B: 10 mM Tris-HCl pH 7.4 and 3% glycerol; [c] Buffer C: 10 mM Tris-HCl pH 7.4 containing 3% glycerol; [d] 10 mM Tris-HCl pH 7.4 containing 0.015% Triton X-100, 3% glycerol. [e] Buffer D: 10 mM Tris-HCl pH 7.4 containing 0.015% Triton X-100, 3% glycerol and 0.1 mM 2-mercaptoethanol.

4.9.5 Chemical modification of IAD

Chemical modifications of IAD were carried out either in 100 mM phosphate buffer (pH 7.5) and 10 µl of one of the following reagents: 2,3-butanedione (But, **202**, 10 mM), ethyl

acetimidate (EAM, **203**, 2.5 mM), *N*-acetylimidazole (NAI, **204**, 2.5 mM), diethyl pyrocarbonate (DEPC, **205**, 2.5 mM) or in 100 mM MES buffer (pH 6.0) in the presence of 10 µl of one of the following reagents iodoacetamide (IACA, **207**, 2.5 mM), *N*-(3-dimethylaminopropyl)-*N*'-ethylcarbodiimide (EDC, **206**, 5 mM) and phenylmethanesulfonyl fluoride (PMSF, **208**, 2.5 mM). The enzyme activity was measured and expressed as percentage of specific activity calculated as the ratio of specific activity of IAD with chemical modification reagents and that without chemical modification reagents.

4.9.6 Characterization and substrate specificity of IAD

The kinetic parameters of IAD were determined using *E/Z*-IAOx (**142**) as substrate. The concentration of the substrate in the assay mixture was varied from 0 to 1.2 mM using standard assay procedure as described in section 4.9.1. The substrate specificity was tested using active fractions after first step purification (DEAE-active fraction, protocol 1) and active fractions after third step purification (Superdex 75, protocol 1) using the *E/Z*-aldoximes. IAD activity was assayed in presence of 1.5 mM of each oxime using standard assay procedure as described in section 4.9.1. Product formation was determined by HPLC using the nitriles corresponding to dehydration of each oxime as standards. Calibration curves were built using synthetic compounds. In case of testing substrate specificity after third step purification, assays were done for 60 min in 25 mM Tris-HCl pH 7.4 using 300 µl of active fractions.

4.9.7 Effect of pH and temperature on the activity of IAD

The effect of pH on the enzyme activity was studied by assaying the partially purified enzyme (after first step purification, DEAE-Sephacel chromatography) in buffers with pHs ranging from 5.0 to 9.5 in 50 mM diethanolamine, 50 mM *N*-ethylmorpholine, and 100 mM morpholine-ethanesulfonic acid buffer. To determine the optimum temperature for IAD activity, assay mixtures were incubated at different temperatures starting from 10 to 60 ^{o}C. In both cases, assays were done in presence of 2.5 mM sodium dithionite and 1.0 mM IAOx (**142**). The reactions were stopped after incubating for 15 min and indolyl-3-acetonitrile (**115**) was estimated as described above.

4.10 Synthesis of compounds

The following substrates were synthesized: indolyl-3-acetaldoxime, 1-methylindole-3-acetaldoxime (**211**), 3-(3-indolyl) propanal oxime (**193**), 4-(3-indolyl) butanal oxime (**194**), naphthaldehyde-1-carboxaldehyde oxime (**195**), naphthyl-2-carboxaldehyde oxime (**196**), 3-methylbutanal oxime (**200**), cyclopentanecarboxaldehyde oxime (**201**).

4.10.1 Indolyl-3-acetaldoxime (142)

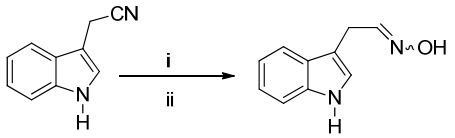

115 **142**

Reagents and conditions: (i) DIBAL-H, (1.5 M in toluene), CH_2Cl_2, -78 ^oC, 20 min; (ii) NH_2OH-HCl, AcONa, 95% EtOH, 0 ^oC - r.t., 3 h.

Compound **142** was prepared by modifying reported procedure (Pedras, Minic et al., 2010). A solution of DIBAL-H (1.6 mL, 340.8 mg, 2.4 mmol) in toluene was added drop wise to a solution of indolyl-3-acetonitrile (**115**, 200 mg, 1.2 mmol) in dry dichloromethane (9 mL). The solution was cooled to -78 ^oC under an atmosphere of argon. The reaction mixture was allowed to stir at -78 ^oC for 10 min. After that the reaction mixture was diluted with ice-cold MeOH (20 mL) and immediately extracted in dichloromethane (20 mL × 5). The combined organic extract was washed with H_2O (20 mL × 2), dried over Na_2SO_4 and the residue (120 mg) was used for the following step without purification. A solution of $HONH_2.HCl$ (209 mg, 1.9 mmol) and CH_3COONa (247 mg, 1.9 mmol) in 1 mL H_2O was added to a cooled solution (1 ^oC) of crude residue in EtOH (8 mL). The reaction mixture was allowed to stir at 1 ^oC for 10 min, and then at r.t. for 3 h. The reaction mixture was concentrated, the residue was taken in H_2O (10 mL), extracted with EtOAc (20 mL × 3), the combined organic extract was dried over Na_2SO_4 and concentrated under reduced pressure. Separation by FCC (CH_2Cl_2-EtOH, 94:6, v/v) yielded indolyl-3-acetaldoxime (146 mg, 70% yield). Integration of ^1H NMR signals indicated the presence of both *syn* and *anti* isomers (1:0.8).^1H NMR data are in agreement with reported data (Pedras, Minic el al., 2010).

Indolyl-3-acetaldoxime: R_f 0.4 (CH_2Cl_2-CH_3OH, 98:2, v/v),

HPLC-DAD t_R = 7.9 min. and 8.6 min (Method E)

^{1}H NMR (500 MHz, CD_3CN): δ 9.15 (br s, D_2O exchangeable, 1.8H, -NH), 8.85 (br s, 1H, D_2O exchangeable, =NOH) and 8.35 (br s, D_2O exchangeable 0.8H, =NOH), 7.56 (m, 1.8H), 7.47 (t, *J* = 6.2, 0.8H), 7.39 (d, *J* = 8.1, 1.8H), 7.14 (dd, *J* = 7.8, 7.4, 1.8H), 7.13 (s, 0.8H), 7.05 (t, *J* = 7.2, 1.8H), 6.82 (t, *J* = 5.3, 1H), 3.75 (d, *J* = 5.3, 2H), 3.55 (d, *J* = 6.1, 2H).

HR-EIMS *m/z* measured 174.0794 (174.0793 calc. for $C_{10}H_{10}N_2O$).

EIMS *m/z* (% relative int.) 174 $[M]^+$ (78), 157 (20), 130 (100).

4.10.2 1-Methylindole-3-acetonitrile (211)

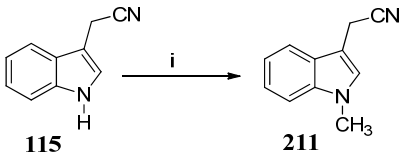

115 **211**

Reagents and conditions: (i) NaH, CH_3I, THF, 0 ^oC, 15 min.

NaH (102.5 mg, 2.6 mmol) and CH_3I (161.0 µl, 2.6 mmol) were added to cooled solution (0 °C) of indolyl-3-acetonitrile (**115**, 200 mg, 1.3 mmol) in dry THF (10 mL) under stirring. After 15 min, the reaction mixture was diluted with ice-cold H_2O (30 mL) and was extracted with CH_2Cl_2 (30 mL × 3). The combined organic extract was dried over Na_2SO_4, was concentrated under reduced pressure and the residue obtained was then subjected to FCC (CH_2Cl_2-hexane, 60:40) to yield 1-methylindole-3-acetonitrile (**211**, 217 mg, 97 % yield).

HPLC-DAD t_R = 17.7 min (Method E)

^{1}H NMR (500.3 MHz, $CDCl_3$) δ: 7.58 (d, *J* = 8 Hz, 1H), 7.35 (d, *J* = 8.2 Hz, 1H), 7.29 (dd, *J* = 6.9, 8.1 Hz, 1H), 7.19 (dd, *J* = 7.4, 7.4 Hz, 1H), 7.10 (s, 1H), 3.84 (s, 2H), 3.80 (s, 3H).

HR-EIMS *m/z* measured 170.0843 (170.0844 calc. for $C_{11}H_{10}N_2$).

EIMS *m/z* (% relative int.) 170 $[M]^+$ (100), 144 (60), 128 (13), 115 (12).

4.10.3 1-Methylindole-3-acetaldoxime (191)

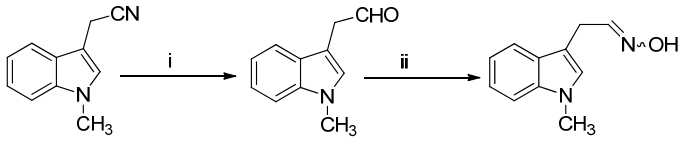

Reagents and conditions: (i) DIBAL-H, (1.5 M in toluene), CH_2Cl_2, -78 ^oC, 20 min; (ii) NH_2OH-HCl, AcONa, 95% EtOH, 0 ^oC - r.t., 3 h (Pedras, Okinyo-Owiti et al., 2009).

Compound **191** was prepared according to a reported procedure (Pedras, Okinyo-Owiti et al., 2009). A solution of DIBAL-H (1.2 mL, 1.18 mmol) in toluene was added drop wise to a solution of 1-methylindolyl-3-acetonitrile (**211**, 150 mg, 0.88 mmol) in dry toluene (12 mL) cooled to -78 °C under argon atmosphere. The reaction mixture was allowed to stir at -78 °C for 10 min, was diluted with ice-cold HCl (10 mL, 2 M) and immediately extracted with EtOAc (30 mL × 2). The combined organic extract was washed with H_2O (20 mL × 2), dried over Na_2SO_4 and concentrated under reduced pressure to yield *N*-methylindolyl-3-acetaldehyde which was used for the next step without purification. A solution of $HONH_2$·HCl (155 mg, 2.25 mmol) and CH_3COONa (184 mg, 2.25 mmol) in H_2O (1 mL) was added to a cooled solution (0 °C) of *N*-methylindolyl-3-acetaldehyde (**212**) in EtOH (13 mL) under stirring. The reaction mixture was treated as reported above for indolyl-3-acetaldoxime (**142**). Separation by FCC (CH_2Cl_2-EtOAc, 98:2, v/v) yielded 1-methylindole-3-acetaldoxime (**191**, 73.3 mg, 66% yield). ^1H NMR data are in agreement with reported data (Pedras, Okinyo-Owiti et al., 2009).

HPLC-DAD t_R = 12.0 and 11.3 min. (Method E)

^1H NMR (500.3 MHz, CD_3CN); *E/Z* isomer ratio (1:0.9) δ: 8.79 (br s, OH), 8.32 (br s, OH), 7.54 (m, 1.9H), 7.47 (t, *J* = 6.2 Hz, 0.9H), 7.35 (d, *J* = 8.1 Hz, 1.9 H), 7.20 (dd, *J* = 7.1, 8.1 Hz, 1.9 H), 7.06 (dd, *J* = 7.8, 7.1 Hz, 1.9 H), 7.03 (s, 1H), 7.01 (s, 0.9H), 6.81 (t, *J* = 5.3 Hz, 1H), 3.74 (m, 7.5H), 3.56 (d, *J* = 6.8 Hz, 2H).

HR-EIMS *m/z* measured 188.0951 (188.0949 calc. for $C_{11}H_{12}N_2O$).

EIMS *m/z* (% relative int.) 188 $[M]^+$ (65), 171 (22), 144 (100), 131 (12).

4.10.4 3-(3-Indolyl)propanal oxime (193)

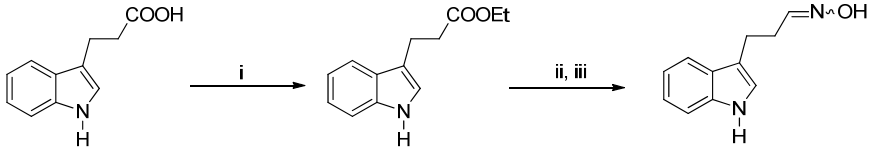

213 **214** **193**

Reagents and conditions: (i) H_2SO_4 (10 mol%), 95% EtOH, reflux, 2 h; (ii) DIBAL-H, (1.5 M in toluene), CH_2Cl_2, -78 ^oC, 20 min; (iii) NH_2OH-HCl, AcONa, 95% EtOH, 0 ^oC - r.t., 3 h.

Compound **193** was prepared according to the reported procedure by Pedras et al. (Pedras, Minic et al., 2010). To a stirred solution of 3-(3-indolyl) propanoic acid (**213**) (150 mg, 0.79 mmol) in 95% EtOH (5 mL), H_2SO_4 (10 mol%) was added dropwise at 0 ^oC. The reaction mixture was allowed to warm to room temperature and heated until reflux began, this being maintained for 2 h. EtOH was removed under reduced pressure, the residue was dissolved in EtOAc (15 mL), and the mixture was washed with saturated $NaHCO_3$ solution and concentrated. The product was purified using FCC (EtOAc–hexane; 15:85, v/v) to afford ethyl 3-(3-indolyl)propanoate (**214**) (165 mg, 98%) as a white solid. To a stirred solution of ethyl 3-(3-indolyl)propanoate (**214**) (100 mg, 0.47 mmol) in anhydrous toluene (6 mL) under argon atmosphere at -78 ^oC, DIBAL-H (1.5 M in toluene; 406 µl, 0.61 mmol) was added slowly and the reaction was stirred for about 30 min at the same temperature. The reaction mixture was quenched with ice-cold 2N HCl and extracted with EtOAc. The combined organic extract was washed with H_2O, dried over Na_2SO_4, and concentrated. The crude residue 3-(3-indolyl) propanal was directly used for the next step without further purification. A solution of $HONH_2$-HCl (48.9 mg, 0.70 mmol) and NaOAc (57.8 mg, 0.70 mmol) in H_2O (1 mL) was added to a cooled solution (0 ^oC) of crude 3-(3-indolyl) propanal in 95% EtOH (4 mL). The reaction mixture was allowed to stir at 0 ^oC for 5 min, and then at room temperature for 3 h. The reaction mixture was concentrated and the residue was dissolved in H_2O (5 mL), was extracted with EtOAc. The combined organic extract was dried over Na_2SO_4 and was concentrated under reduced pressure. Separation by FCC (EtOAc–hexane, 20:80, v/v) yielded 3-(3-indolyl)propanal oxime (**193**) (59 mg, 67% yield, over two steps) as a white solid. Integration of ^1H NMR signals indicated the presence of both *syn* and *anti* isomers (1:0.1).^1H NMR data are in agreement with reported data (Pedras, Minic el al., 2010)

HPLC-DAD t_R = 10.2 and 10.6 min. (Method E)

^{1}H NMR (500.3 MHz, CD_3CN): *E/Z* ratio; (1:0.1) δ: 9.05 (br s, 1H), 8.63 (s, 0.97H, major), 8.28 (s, 0.09H), 7.57 (d, *J* = 8.0 Hz, 1H), 7.56 (overlapping t, 0.09H, CH=NOH), 7.38 (d, *J* = 8.0 Hz, 1H), 7.13 (t, *J* = 7.5 Hz, 1H), 7.07 (s, 1H), 7.05 (t, *J* = 7.5 Hz, 1H), 6.71 (t, *J* = 5.5 Hz, 0.97H, –CH=NOH), 2.91 (t, *J* = 7.5, 2H), 2.68 (m, 1.8H), 2.52 (m, 0.2H).

4.10.5 3-(3-Indolyl)butanal oxime (194)

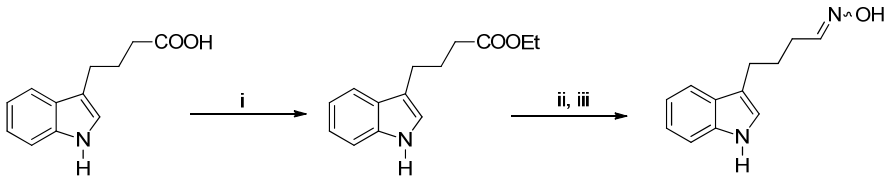

209 **210** **194**

Reagents and conditions: (i) H_2SO_4 (10 mol%), 95% EtOH, reflux, 2 h; (ii) DIBAL-H (1.5 M in toluene), CH_2Cl_2, -78 ^oC, 20 min; (iii) NH_2OH-HCl, AcONa, 95% EtOH, 0 ^oC - r.t., 3 h (Pedras, Minic el al., 2010).

Ethyl 4-(3-indolyl) butanoate (**210**) was prepared from 4-(3-indolyl) butanoic acid (**209**) (100 mg, 0.049 mmol), employing the procedure described for ethyl 3-(3-indolyl) propanoate (**214).** Ethyl 4-(3-indolyl)butanoate (**210**) (107 mg, 95%) was obtained as a white solid and used for preparation of the corresponding oxime **194** as described for indolyl-3-acetaldoxime (**142**). 3-(3-Indolyl)butanal oxime (**194**) was obtained as white solid (17.5 mg, 68% yield). Integration of ^{1}H NMR signals indicated the presence of both *syn* and *anti* isomers (1:0.8).^{1}H NMR data are in agreement with reported data (Pedras, Minic el al., 2010).

^{1}H NMR (500.3 MHz, $CDCl_3$): *E/Z* (5:4) δ: 8.81 (br s, 0.45H), 8.41 (br s, 0.55H), 7.94 (s, 1H), 7.63 (dd, *J* = 7.5, 2.0 Hz, 1H), 7.49 (t, *J* = 6.0 Hz, 0.55H, CH=NHOH), 7.36 (d, *J* = 7.5 Hz, 1H), 7.22 (t, *J* = 7.5 Hz, 1H), 7.15 (dd, *J* = 7.5, 2.0 Hz, 1H), 6.98 (d, *J* = 7.5, 1H), 6.79 (t, *J* = 5.5 Hz, 0.45H, –CH=NHOH), 2.84 (m, 2H), 2.50 (m, 0.9H), 2.30 (m, 1.1H), 1.94 (apparent quintet, 2H).

HPLC-DAD t_R = 12.3 and 12.8 min (Method E)

HR-EIMS *m/z* measured 202.1108 (188.0949 calc. for $C_{11}H_{12}N_2O$).

EIMS *m/z* (% relative int.) 202 $[M]^+$ (34), 168 (18), 143 (75), 130 (100).

4.10.5 Naphthalene-1-carboxaldehyde oxime (195)

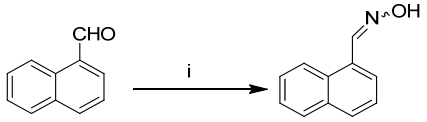

215 **195**

Reagents and conditions: (i) NH_2OH-HCl, AcONa, 95% EtOH, 0 ^oC- r.t, 3 h.

Compound **195** was prepared by direct oximation of commercially available aldehyde **215** (Pedras, Minic et al., 2010). A solution of $HONH_2$-HCl (108 mg, 1.63 mmol) and NaOAc (128 mg, 1.63 mmol) in H_2O (1 mL) was added to a cooled solution (0 ^oC) of crude 1-naphthaldehyde (**216**, 200 mg, 1.32 mmol) in 95% EtOH (5 mL). The reaction mixture was allowed to stir at 0 ^oC for 5 min, and then at r.t. for 3 h. The reaction mixture was concentrated and the residue was taken in H_2O (5 mL), extracted with EtOAc. The combined organic extract was dried over Na_2SO_4 and was concentrated under reduced pressure. Separation by FCC (EtOAc–hexane, 20:80, v/v) yielded naphthalene-1-carboxaldehyde oxime (**195**) (207 mg, 93 % yield, over two steps) as a white solid. ^1H NMR data are in agreement with reported data (Allen, Davulcu, et al., 2010).

^1H NMR, 500.3 MHz, $CDCl_3$) δ: 8.83 (s, 1H), 8.50 (d, *J* = 8.0 Hz, 1H), 7.91 (dd, *J* = 7.0, 6.0 Hz, 2H), 7.78 (d, *J* = 7.0 Hz, 1H), 7.49-7.61 (m, 3H)

HR-EIMS *m/z* measured 171.0686 (171.0684 calc. for $C_{11}H_9NO$).

EIMS *m/z* (% relative int.) 171 $[M]^+$ (100), 154 (68), 127 (64), 115 (20).

4.10.7 Naphthalene-2-carboxaldehyde oxime (196)

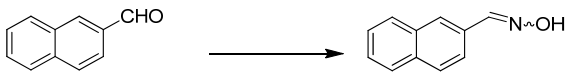

216 **196**

Reagents and conditions: (i) NH_2OH-HCl, AcONa, 95% EtOH, 0 ^oC - r.t., 3 h.

Naphthalene-2-carboxaldehyde oxime (**196**) was prepared in a similar way reported for naphthalene-1-carboxaldehyde oxime (**195**). The compound was yielded as a white solid (210 mg,

94 % yield, over two steps) as a white solid (Pedras, Minic et al., 2010). ^{1}H NMR data are in agreement with reported data (Ramón, Bosson et al., 2010).

^{1}H NMR, $CDCl_3$) δ: 8.3 (s, 1H); 7.89-7.84 (m, 5H), 7.54-7.48 (m, 2H).

HR-EIMS *m/z* measured 171.0680 (171.0684 calc. for $C_{11}H_9NO$).

EIMS *m/z* (% relative int.) 171 $[M]^+$ (100), 144 (38), 127 (53), 115 (23).

4.10.8 1-Cyclopentanecarboxaldehyde oxime (201)

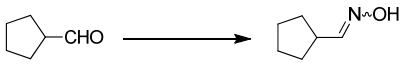

217 **201**

Reagents and conditions: (i) NH_2OH-HCl, AcONa, 95% EtOH, 0 ^oC - r.t., 3 h.

A solution of $HONH_2$.HCl (289 mg, 4.16 mmol) and NaOAc (341 mg, 4.16 mmol) in water (0.5 mL) was added to a solution of cyclopentanecarboxaldehyde (**217**) (50 mg, 0.51 mmol) in 95% EtOH (4 mL). The reaction mixture was stirred at room temperature for 3 h and concentrated (water bath temperature below 10 ^oC). The residue was taken in H_2O (5 mL) and extracted with CH_2Cl_2. The combined organic extract was dried over Na_2SO_4 and concentrated under reduced pressure (water bath temperature below 10 ^oC). Separation by FCC (EtOAc-hexane, 20:80, v/v) yielded 1-cyclopentanecarboxaldehyde oxime (**201**) (50 mg, 88% yield) was obtained as a light yellow liquid. ^{1}H NMR data are in agreement with reported data (Pedras, Minic el al., 2010).

^{1}H NMR (500.3 MHz, $CDCl_3$) : *E/Z* isomers (1:0.5); δ: 9.25 (br s, 1.5H), 7.37 (d, *J* = 7.2 Hz, 1H, –CH=NOH), 6.67 (d, *J* = 7.2 Hz, 0.5H, –CH=NOH), 3.26 (m, 0.5H), 2.62 (m, 1H), 1.92-1.84 (m, 2.9), 1.69–1.57 (m, 6 H), 1.49–1.36 (m, 2.9 H).

HR-EIMS: *m/z* measured 113.0841, (171.0680 calc. for C_4H_9ON).

4.10.9 3-Methylbutanal oxime (200)

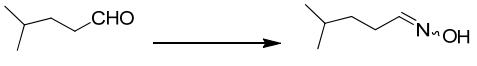

218 **200**

Reagents and conditions: (i) NH_2OH-HCl, AcONa, 95% EtOH, 0 ^oC - r.t., 3 h.

3-Methylbutanal oxime (**200**) was prepared from 3-methylbutanal (**218**), (100 mg, 1.16 mmol) employing the procedure described for 1-cyclopentanecarboxaldehyde oxime (**201**). 3-Methylbutanal oxime (**200**) (103 mg, 88% yield) was obtained as pale yellow liquid. ^{1}H NMR data are in agreement with reported data (Pedras, Minic el al., 2010).

^{1}H NMR (500.3 MHz, $CDCl_3$): *E/Z* isomers, (1:0.9), δ: 7.44 (t, *J* = 6.5 Hz, 1H, –CH=NOH), 6.76 (t, *J* = 5.5 Hz, 0.9H, CH=NOH), 2.29 (m, 1.8H), 2.09 (t, *J* = 6.5 Hz, 2H), 1.84 (m, 1.9H), 0.97 (m, 11.6H).

HR-EIMS: *m/z* measured 115.0997 (115.1735 calc. for C_4H_9ON).

4.10.10 4-Hydroxybenzylisothiocyanate (184)

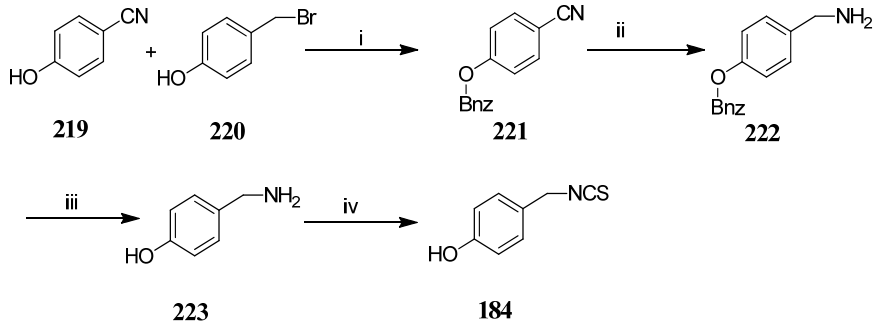

Reagents and conditions: (i) K_2CO_3, KI, DMF, 2h, 25 ^oC; (ii) $LiAlH_4/AlCl_3$, Et_2O, 2h, 25 ^oC; (iii) Pd/C, AcOH, H_2, 2h, 0 ^oC; (iv) $CSCl_2$, Et_3N, 0 ^oC; Bnz, benzyl (Pedras and Smith, 1997).

Compound **184** was prepared according to a reported procedure (Pedras and Smith, 1997). Benzyl bromide (**220**) (420 µl, 3.52 mmol), K_2CO_3 (487 mg, 3.52 mmol) and KI (10 mg, 0.01mmol) were added to a solution of 4-cyanophenol (**219**) (350 mg, 3 mmol) in DMF (5 mL) at 25 ^oC. After 2 hr the reaction mixture was diluted with water (9 mL), extracted with Et_2O (2 × 30 mL) and the combined organic layers were concentrated under reduced pressure. The crude product was crystallized from hexane-Et_2O to give 4-hydroxybenzonbitrile (**221**) (95%, 570 mg, 2.73 mmol) that was dissolved in THF (4 mL) and added dropwise to a solution of $LiAlH_4/AlCl_3$ in THF (10 mL) and kept at 25 ^oC. After 2 h, water was added dropwise to the reaction mixture and the aqueous layer was basified with 1 N NH_4OH and extracted with EtOAc (3 × 20 mL). The combined organic layers were dried over Na_2SO_4 and concentrated under reduced pressure to yield crude amine **222** (500 mg, 86%). A suspension of the crude amine **222** in C_2H_5OH:NH_4OH and 10% Pd/H_2 (125 mg) in EtOH-NH_4OH (10:3 mL) was stirred under H_2 (one atm) for 2 hr at 0

^{o}C. The reaction mixture was filtered, concentrated under reduced pressure and the crude product was purified by FCC (CH_2Cl_2-MeOH-NH_4OH, 90:10:1) to give 4-hydroxybenzylamine (**223**, 220 mg, 1.82 mmol, 74%). A solution of 4-hydroxybenzylamine (**223**) (10 mg, 0.08 mmol) and Et_3N (17 mg, 0.16 mmol) in $CHCl_3$: MeOH (3:1) was added dropwise over 30 min to a solution of thiocarbonylchloride (10.27 mg, 0.089 mmol) in $CHCl_3$ (1 mL) at 0 ^{o}C. After 60 min the reaction mixture was concentrated under reduced pressure and the product was purified by FCC (CH_2Cl_2) to yield 4-hydroxybenzylisothiocyanate (**184**) (7 mg, 53%). ^{1}H NMR data are in agreement with reported data (Pedras and Smith, 1997).

R_f 0.25, CH_2Cl_2-EtOAc, (49:1).

HPLC-DAD t_R = 15.7 min. (Method A)

^{1}H NMR (500.3 MHz, $CDCl_3$) δ: 7.21 (d, *J* = 8.49, 2H), 6.82 (d, *J* = 8.5, 2H), 4.9 (s, 1H, exchangeable with D_2O), 4.6 (s, 2H).

HREIMS *m/z* (% relative abundance) measured: 165.0249 (165.0247 calc. for C_8H_7NOS)

EIMS *m/z* (% relative abundance): 165 [Ml^+ (8), 107 (100) 106 (25), 78 (22), 77 (17), 59 (14) 52 (10)

4.10.11 Preparation of S-(4-sulfanyl-2,3-dihydroxybutyl)-4-hydroxybenzyldithiocarbamate (187)

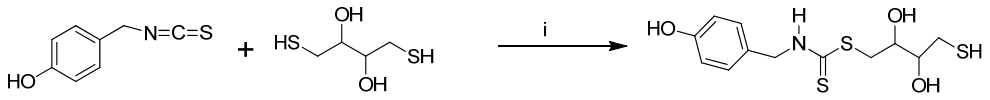

184 **186** **187**

Reagents and conditions: (i) 250 mM sodium acetate buffer pH 5.0 containing 1 mM DTT (**186**), 250 mM sucrose, 2 mM EDTA, 100 mM ascorbic acid and 50 mM sodium metabisulfite; 10 min.

4-Hydroxybenzylisothiocyanate (**184**, 10 mg) was dissolved in 1 mL acetonitrile and added to 15 mL of 250 mM sodium acetate buffer pH 5.0 containing 1 mM DTT, 250 Mm sucrose, 2 mM EDTA, 100 mM ascorbic acid and 50 mM sodium metabisulfite. The solution was stirred for 10 min followed by extraction with EtOAc (20 mL × 3). The extract was concentrated under reduced pressure to give 50 mg residue. The residue was subjected to FCC (CH_2Cl_2-MeOH, 96 : 4) and compound **135** was isolated as white powder (4 mg).

HPLC-DAD t_R = 12.0 min. (Method A)

^{1}H NMR (500.3 MHz, CD_3CN): δ 7.2 (d, *J* = 8.38, 2H), 6.8 (d, *J* = 8.4 ,2H), 4.7(d, *J* = 5.4 Hz, 2H), 3.7 (m,1H), 3.5 (m, 1H), 3.3 (*m*, 1H), 3.5 (m, 1H), 2.6 (m, 2H).

HREIMS *m/z* (% relative abundance) measured: 318.0306 (318.0297 calc. for $C_{12}H_{16}NO_3S_3$).

EIMS *m/z* (% relative int.) 318 $[M]^+$ (100), 212 (13), 153(13).

5. Chapter 5: References

Afifi, M., Monje, M. C., Legrand, V., Roustan, J. P., Nepveu, F., 2004. Metabolisation of eutypine by plant tissues: An HPLC determination. Analytica Chimica Acta 513, 21-27.

Agerbirk, N., De Vos, M., Kim, J. H., Jander, G., 2009. Indole glucosinolate breakdown and its biological effects. Phytochemistry Reviews 8, 101-120.

Ahn, J. H., Cheng, Y. Q., Walton, J. D., 2002. An extended physical map of the *tox2* locus of *Cochliobolus carbonum* required for biosynthesis of HC-toxin. Fungal Genetics and Biology 35, 31-38.

Allen, C. L., Davulcu, S., Williams, J. M. J, 2010. Catalytic acylation of amines with aldehydes or aldoximes. Organic Letters12, 5096-5099

Awad, W. A., Ghareeb, K., Böhm, J., Zentek, J., 2010. Decontamination and detoxification strategies for the *Fusarium* mycotoxin deoxynivalenol in animal feed and the effectiveness of microbial biodegradation. Food Additives and Contaminants Part A Chemistry Analysis Control Exposure and Risk Assessment 27, 510-520.

Ayer, W. A., Pena-Rodriguez, L. M., 1987a. Metabolites produced by *Alternaria brassicae*, the blackspot pathogen of canola .1. The phytotoxic components. Journal of Natural Products 50, 400-407.

Ayer, W. A., Pena-Rodriguez, L. M., 1987b. Metabolites produced by *Alternaria brassicae*, the blackspot pathogen of canola .2. Sesquiterpenoid metabolites. Journal of Natural Products 50, 408-417.

Bains, P. S., Tewari, J. P., 1987. Purification, chemical characterization and host specificity of the toxin produced by *Alternaria brassicae*. Physiological and Molecular Plant Pathology 30, 259-271.

Bains, P. S., Tewari, J. P., Ayer, W. A., 1993. A note on phytotoxicity of homodestruxin B, a compound produced by *Alternaria brassicae*. Phytoprotection 74, 157–160.

Bak, S., Kahn, R. A., Nielsen, H. L., Møller, B. L., Halkier, B. A., 1998. Cloning of three A-type cytochromes P450, CYP71E1, CYP98, and CYP99 from *Sorghum bicolor* (L.) Moench by a PCR approach and identification by expression in *Escherichia coli* of CYP71E1 as a multifunctional cytochrome p450 in the biosynthesis of the cyanogenic glucoside dhurrin. Plant Molecular Biology 36, 393-405.

Bak, S., Tax, F. E., Feldmann, K. A., Galbraith, D. W., Feyereisen, R., 2001. CYP83B1, a cytochrome P450 at the metabolic branch paint in auxin and indole glucosinolate biosynthesis in *Arabidopsis*. Plant Cell 13, 101-111.

Ballio, A., 1991. Non-host-selective fungal phytotoxins - biochemical aspects of their mode of action. Experientia 47, 783-790.

Basnayake, W. V. S., Birch, R. G., 1995. A gene from *Alcaligenes denitrificans* that confers albicidin resistance by reversible antibiotic binding. Microbiology 141, 551-560.

Berthiller, F., Dall'Asta, C., Schuhmacher, R., Lemmens, M., Adam, G., Krska, R., 2005. Masked mycotoxins: Determination of a deoxynivalenol glucoside in artificially and naturally contaminated wheat by liquid chromatography-tandem mass spectrometry. Journal of Agriculture and Food Chemistry 53, 3421-3425.

Berthiller, F., Hametner, C., Krenn, P., Schweiger, W., Ludwig, R., Adam, G., Krska, R., Schuhmacher, R., 2009. Preparation and characterization of the conjugated *Fusarium* mycotoxins zearalenone-4-*O*-β-D-glucopyranoside, α-zearalenol-4-*O*-β-d-glucopyranoside and β-zearalenol-4-*O*-β-D-glucopyranoside by MS/MS and two-dimensional NMR. Food additives and contaminants Part A 26, 207-213.

Berthiller, F., Lemmens, M., Werner, U., Krska, R., Hauser, M.-T., Adam , G., Schuhmacher, R., 2007. Short review: Metabolism of the *Fusarium* mycotoxins deoxynivalenol and zearalenone in plants. Mycotoxin Research 23, 68-72.

Berthiller, F., Werner, U., Sulyok, M., Krska, R., Hauser, M. T., Schuhmacher, R., 2006. Liquid chromatography coupled to tandem mass spectrometry (LC-MS/MS) determination of phase II metabolites of the mycotoxin zearalenone in the model plant *Arabidopsis thaliana*. Food Additives and Contaminants 23, 1194-1200.

Birch, R. G., 1987. Correlation between albicidin production and chlorosis induction by *Xanthomonas albilineans*, the sugarcane leaf scald pathogen. Physiological and Molecular Plant Pathology 30, 199-206.

Birch, R. G., Patil, S. S., 1985a. Antibiotic and process for the production thereof. USA patent 4525354.

Birch, R. G., Patil, S. S., 1985b. Preliminary characterization of an antibiotic produced by *Xanthomonas albilineans* which inhibits DNA-synthesis in *Escherichia coli*. Journal of General Microbiology 131, 1069-1075.

Birch, R. G., Patil, S. S., 1987. Evidence that an albicidin-like phytotoxin induces chlorosis in sugarcane leaf scald disease by blocking plastid DNA-replication. Physiological and Molecular Plant Pathology 30, 207-214.

Bischoff, V., Cookson, S. J., Wu, S., Scheible, W. R., 2009. Thaxtomin A affects CESA-complex density, expression of cell wall genes, cell wall composition, and causes ectopic lignification in *Arabidopsis thaliana* seedlings. Journal of Experimental Botany 60, 955-965.

Bolwell, G. P., Bozak, K., Zimmerlin, A., 1994. Plant cytochrome P450. Phytochemistry 37, 1491-1506.

Bones, A. M., Rossiter, J. T., 2006. The enzymic and chemically induced decomposition of glucosinolates. Phytochemistry 67, 1053-1067.

Boucher, J. L., Delaforge, M., Mansuy, D., 1994. Dehydration of alkyl- and arylaldoximes as a new cytochrome P450-catalyzed reaction: Mechanism and stereochemical characteristics. Biochemistry 33, 7811-7818.

Bowyer, P., Clarke, B. R., Lunness, P., Daniels, M. J., Osbourn, A. E., 1995. Host-range of a plant-pathogenic fungus determined by a saponin detoxifying enzyme. Science 267, 371-374.

Bradford, M. M., 1976. A rapid and sensitive method for the quantification of microgram quantities of protein utilizing the principle of protein dye-binding. Analytic Biochemistry 72, 248–254.

Bruins, M. B. M., Karsaï, I., Schepers, J., Snijders, C. H. A., 1993. Phytotoxicity of deoxynivalenol to wheat tissue with regard to in vitro selection for Fusarium head blight resistance. Plant Science 94, 195-206.

Buchwaldt, L., Green, H., 1992. Phytotoxicity of destruxin B and its possible role in the pathogenesis of *Alternaria brassicae*. Plant Pathology. 41, 55–63.

Buchwaldt, L., Jensen, J. S., 1991. HPLC purification of destruxins produced by *Alternaria brassicae* in culture and leaves of *Brassica napus*. Phytochemistry 30, 2311-2316.

Buckel, W., Martins, B. M., Messerschmidt, A., Golding, B. T., 2005. Radical-mediated dehydration reactions in anaerobic bacteria. Biological Chemistry 386, 951-959.

Butt, T. M., Ben El Hadj, N., Skrobek, A., Ravensberg, W. J., Wang, C. S., Lange, C. M., Vey, A., Shah, U. K., Dudley, E., 2009. Mass spectrometry as a tool for the selective profiling of destruxins; their first identification in *Lecanicillium longisporum*. Rapid Communications in Mass Spectrometry 23, 1426-1434.

Christen, D., Tharin, M., Perrin-Cherioux, S., Abou-Mansour, E., Tabacchi, R., Défago, G., 2005. Transformation of Eutypa dieback and esca disease pathogen toxins by antagonistic fungal strains reveals a second detoxification pathway not present in *Vitis vinifera*. Journal of Agriculture and Food Chemistry53, 7043-7051.

Colrat, S., Deswarte, C., Latché, A., Klaebe, A., Bouzayen, M., Fallot, J., Roustan, J. P., 1999. Enzymatic detoxification of eutypine, a toxin from *Eutypa lata*, by *Vitis vinifera* cells: Partial purification of an NADPH dependent aldehyde reductase. Planta 207, 544-550.

Colrat, S., Latché, A., Guis, M., Pech, J. C., Bouzayen, M., Fallot, J., Roustan, J. P., 1999. Purification and characterization of a NADPH-dependent aldehyde reductase from mung bean that detoxifies eutypine, a toxin from *Eutypa lata*. Plant Physiology 119, 621-626.

Comstock, J. C., Scheffer, R. P., 1973. Role of host-selective toxin in colonization of corn leaves by *Helminthosporium carbonum*. Phytopathology 63, 24-29.

Crombie, W. M. L., Crombie, L., Green, J. B., Lucas, J. A., 1986. Pathogenicity of take-all fungus to oats - its relationship to the concentration and detoxification of the 4 avenacins. Phytochemistry 25, 2075-2083.

Cruickshank, I. A. M., Perrin, D. R., 1960. Isolation of a phytoalexin from *Pisum sativum* L. Nature 187, 799-800.

Dahiya, J. S., Tewari, J. P. and Woods, D. L., 1991. Abscisic acid from *Alternaria brassicae*. Phytochemistry 27, 2 983-2 984.

Dahiya, J. S., Tewari, J. P., 1991. Plant growth factors produced by the fungus *Alternaria brassicae*. Phytochemistry 3 0, 2 825-2 828.

De Carolis, E., De Luca, V., 1994. 2-oxoglutarate dependent dioxygenase and related enzymes - biochemical-characterization. Phytochemistry 36, 1093-1107.

DeMaster, E. G., Shirota, F. N., Nagasawa, H. T., 1992. A Beckmann-type dehydration of *n*-butyraldoxime catalyzed by cytochrome P-450. Journal of Organic Chemistry 57, 5074-5075.

Desjardins, A. E., Proctor, R. H., 2007. Molecular biology of *Fusarium* mycotoxins. International Journal of Food Microbiology 119, 47-50.

Dixon, R. A., 2001. Natural products and plant disease resistance. Nature 411, 843-847.

Du, L. C., Lykkesfeldt, J., Olsen, C. E., Halkier, B. A., 1995. Involvement of cytochrome P450 in oxime production in glucosinolate biosynthesis as demonstrated by an in vitro microsomal enzyme system isolated from jasmonic acid-induced seedlings of *Sinapis alba* L. Proceedings of the National Academy of Sciences of the United States of America 92, 12505-12509.

Dubery, I. A., Holzapfel, C. W., Kruger, G. J., Schabort, J. C., Van Dyk, M., 1988. Characterization of a gamma-radiation-induced antifungal stress metabolite in citrus peel. Phytochemistry 27, 2769-2772.

Dubery, I. A., Schabort, J. C., 1987. 6,7-dimethoxycoumarin - a stress metabolite with antifungal activity in gamma-irradiated citrus peel. South African Journal of Science 83, 440-441.

Ehlting, J., Hamberger, B., Million-Rousseau, R., Werck-Reichhart, D., 2006. Cytochromes P450 in phenolic metabolism. Phytochemistry Reviews 5, 239-270.

Elliott, C. E., Gardiner, D. M., Thomas, G., Cozijnsen, Wouw, A, V. D., Howlett, B. J., 2007. Production of the toxin sirodesmin PL by *Leptosphaeria maculans* during infection of *Brassica napus*. Molecular Plant Pathology 8, 791-802.

El-Sharkawy, S. H., 1989. Microbial transformation of zearalenone .3. Formation of 2,4-*O*-β-diglucoside. Acta Pharmaceutica Jugoslavica 39, 303-310.

El-Sharkawy, S.H., Abul-Hajj, Y. J., 1988a. Microbial cleavage of zearalenone. Xenobiotica 18, 365-371.

El-Sharkawy, S. H., Abul-Hajj, Y. J., 1988b. Microbial transformation of zearalenone .2. Reduction, hydroxylation, and methylation products. Journal of Organic Chemistry 53, 515-519.

El-Sharkawy, S. H., Selim, M. I., Afifi, M. S., Halaweish, F. T., 1991. Microbial transformation of zearalenone to a zearalenone sulfate. Applied and Environmental Microbiology 57, 549-552.

El-Sharkawy, S., Abul-Hajj, Y., 1987. Microbial transformation of zearalenone .1. Formation of zearalenone-4-*O*-β-glucoside. Journal of Natural Products 50, 520-521.

Engelhardt, G., Zill, G., Wohner, B., Wallnöfer, P. R., 1988. Transformation of the *Fusarium* mycotoxin zearalenone in maize cell-suspension cultures. Naturwissenschaften 75, 309-310.

Fahey, J. W., Zalcmann, A. T., Talalay, P., 2001. The chemical diversity and distribution of glucosinolates and isothiocyanates among plants. Phytochemistry 56, 5-51.

Fallot, J., Deswarte, C., Dalmayrac, S., Colrat, S., Roustan, J. P., 1997. Eutypa dieback of grapevine: Isolation of a molecule synthesized by *Eutypa lata* and toxic for grapevine. Comptes Rendus De L Academie Des Sciences Serie Iii-Sciences De La Vie-Life Sciences 320, 149-158.

Férézou, J. P., Riche, C., Quesneauthierry, A., Pascardbilly, C., Barbier, M., Bousquet, J. F., Boudart, G., 1977. Structures of 2 toxins isolated from fungus cultures *Phoma lingam* tode-sirodesmin PL and deacetylsirodesmin PL. Nouveau Journal De Chimie-New Journal of Chemistry 1, 327-334.

Fitt, B. D. L., Brun, H., Barbetti, M. J., Rimmer, S. R., 2006. World-wide importance of phoma stem canker *Leptosphaeria maculans* and *L. biglobosa* on oilseed rape (*Brassica napus*). European Journal of Plant Pathology 114, 3-15.

Foroud, N. A., Eudes, F., 2009. Trichothecenes in cereal grains. International Journal of Molecular Sciences 10, 147-173.

Fruchter, R. G., Crestfield A.M. 1967. Specific alkylation by iodoacetamide of histidine-12 in active site of ribonuclease. Journal of Biological Chemistry 242, 5807-5812.

Fuchs, E., Binder, E. M., Heidler, D., Krska, R., 2002. Structural characterization of metabolites after the microbial degradation of type a trichothecenes by the bacterial strain BB SH 797. Food Additives and Contaminants 19, 379-386.

Gareis, M., Bauer, J., Thiem, J., Plank, G., Grabley, S., Gedek, B., 1990. Cleavage of zearalenone-glycoside, a "masked" mycotoxin, during digestion in swine. Journal of Veterinary Medicine Series B-Zentralblatt Für Veterinärmedizin Reihe B- 37, 236-240.

Glawischnig, E., Hansen, B. G., Olsen, C. E., Halkier, B. A., 2004. Camalexin is synthesized from indole-3-acetaidoxime, a key branching point between primary and secondary metabolism in *Arabidopsis*. Proceedings of the National Academy of Sciences of the United States of America 101, 8245-8250.

Goyer, C., Vachon, J., Beaulieu, C., 1998. Pathogenicity of *Streptomyces scabies* mutants altered in thaxtomin A production. Phytopathology 88, 442-445.

Graniti, A., 1991. Phytotoxins and their involvement in plant-diseases - introduction. Experientia 47, 751-755.

Grayer, R. J., Harborne, J. B., 1994. A survey of antifungal compounds from higher-plants, 1982-1993. Phytochemistry 37, 19-42.

Groves, J. T., 2005. Cytochrome P450: Structure, mechanism, and biochemistry new York : Kluwer academic/plenum publishers. Edited by P. R. Ortiz de Montellano 1-5.

Guan, D. L., Grau, B. L., Clark, C. A., Taylor, C. M., Loria, R., Pettis, G. S., 2012. Evidence that thaxtomin C is a pathogenicity determinant of *Streptomyces ipomoeae*, the causative agent of *streptomyces* soil rot disease of sweet potato. Molecular Plant-Microbe Interactions 25, 393-401.

Guillén, P., Guis, M., Martinez-Reina, G., Colrat, S., Dalmayrac, S., Deswarte, C., Bouzayen, M., Roustan, J. P., Fallot, J., Pech, J. C., Latché, A., 1998. A novel NADPH-dependent aldehyde reductase gene from *Vigna radiata* confers resistance to the grapevine fungal toxin eutypine. Plant Journal 16, 335-343.

Guo, M. Q., Zhang, L., Liu, Z. Q., 2009. Analysis of saponins from leaves of *Aralia elata* by liquid chromatography and multi-stage tandem mass spectrometry. Analytical Sciences 25, 753-758.

Hain, R., Reif, H. J., Krause, E., Langebartels, R., Kindl, H., Vornam, B., Wiese, W., Schmelzer, E., Schreier, P. H., Stocker, R. H., Stenzel, K., 1993. Disease resistance results from foreign phytoalexin expression in a novel plant. Nature 361, 153-156.

Halkier, B. A., Gershenzon, J., 2006. Biology and biochemistry of glucosinolates. Annual Review of Plant Biology 57, 303-333.

Han, F., Kleinhofs, A., Kilian, A., Ullrich, S. E., 1997. Cloning and mapping of a putative barley NADPH-dependent HC-toxin reductase. Molecular Plant-Microbe Interactions 10, 234-239.

Hansen, C. H., Wittstock, U., Olsen, C. E., Hick, A. J., Pickett, J. A., Halkier, B. A., 2001. Cytochrome P450 CYP79F1 from *Arabidopsis* catalyzes the conversion of dihomomethionine and trihomomethionine to the corresponding aldoximes in the biosynthesis of aliphatic glucosinolates. Journal of Biological Chemistry 276, 11078-11085.

Harris, L. J., Desjardins, A. E., Plattner, R. D., Nicholson, P., Butler, G., Young, J. C., Weston, G., Proctor, R. H., Hohn, T. M., 1999. Possible role of trichothecene mycotoxins in virulence of *Fusarium graminearum* on maize. Plant Disease 83, 954-960.

Hart-Davis, J., Battioni, P., Boucher, J. L., Mansuy, D., 1998. New catalytic properties of iron porphyrins: Model systems for cytochrome p450-catalyzed dehydration of aldoximes. Journal of the American Chemical Society 120, 12524-12530.

Healy, F. G., Krasnoff, S. B., Wach, D. M., Gibson, D. M., Loria, R., 2002. Involvement of a cytochrome P450 monooxygenase in thaxtomin A biosynthesis by *Streptomyces acidiscabies*. Journal of Bacteriology, 184, 2019-2029.

Healy, F. G., Wach, M., Krasnoff, S. B., Gibson, D. M., Loria, R., 2000. The *txtAB* genes of the plant pathogen *Streptomyces acidiscabies* encode a peptide synthetase required for phytotoxin thaxtomin A production and pathogenicity. Molecular Microbiology 38, 794-804.

Helmlinger, J., Rausch, T., Hilgenberg, W., 1985. Metabolism of ^{14}C-indole-3-acetaldoxime by hypocotyls of Chinese cabbage. Phytochemistry 24, 2497-2502.

Higa, A., Kimura, M., Mimori, K., Ochiai-Fukuda, T., Tokai, T., Takahashi-Ando, N., Nishiuchi, T., Igawa, T., Fujimura, M., Hamamoto, H., Usami, R., Yamaguchi, I., 2003. Expression in cereal plants of genes that inactivate Fusarium mycotoxins. Bioscience Biotechnology and Biochemistry 67, 914-918.

Higa-Nishiyama, A., Takahashi-Ando, N., Shimizu, T., Kudo, T., Yamaguchi, I., Kimura, M., 2005. A model transgenic cereal plant with detoxification activity for the estrogenic mycotoxin zearalenone. Transgenic Research 14, 713-717.

Hipskind, J. D., Paiva, N. L., 2000. Constitutive accumulation of a resveratrol-glucoside in transgenic alfalfa increases resistance to *Phoma medicaginis*. Molecular Plant-Microbe Interactions 13, 551-562.

Hofmeister, A. E., Grabowski, R., Linder, D., Buckel, W., 1993. L-Serine and L-threonine dehydratase from *Clostridium propionicum*. Two enzymes with different prosthetic groups. European Journal of Biochemistry 215, 341-349.

Howlett, B. J., Idnurm, A., Pedras, M. S. C., 2001. *Leptosphaeria maculans*, the causal agent of blackleg disease of Brassicas. Fungal Genetics and Biology 33, 1-14.

Huang, G., Zhang, L., Birch, R. G., 2000. Albicidin antibiotic and phytotoxin biosynthesis in *Xanthomonas albilineans* requires a phosphopantetheinyl transferase gene. Gene 258, 193-199.

Huang, G., Zhang, L., Birch, R. G., 2001. A multifunctional polyketide-peptide synthetase essential for albicidin biosynthesis in *Xanthomonas albilineans*. *Microbiology* 147, 631-642.

Ikunaga, Y., Sato, I., Grond, S., Numaziri, N., Yoshida, S., Yamaya, H., Hiradate, S., Hasegawa, M., Toshima, H., Koitabashi, M., Ito, M., Karlovsky, P., Tsushima, S., 2011. *Nocardioides* sp. strain WSN05-2, isolated from a wheat field, degrades deoxynivalenol, producing the novel intermediate 3-epi-deoxynivalenol. Applied Microbiology and Biotechnology 89, 419-427.

Inan, G., Zhang, Q., Li, P. H., Wang, Z. L., Cao, Z. Y., Zhang, H., Zhang, C. Q., Quist, T. M., Goodwin, S. M., Zhu, J. H., Shi, H. H., Damsz, B., Charbaji, T., Gong, Q. Q., Ma, S. S., Fredricksen, M., Galbraith, D. W., Jenks, M. A., Rhodes, D., Hasegawa, P. M., Bohnert, H. J., Joly, R. J., Bressan, R. A., Zhu, J. K., 2004. Salt cress. A halophyte and cryophyte *Arabidopsis* relative model system and its applicability to molecular genetic analyses of growth and development of extremophiles. Plant Physiology 135, 1718-1737.

Johal, G. S., Briggs, S. P., 1992. Reductase activity encoded by the *hm1* disease resistance gene in maize. Science 258, 985-987.

Kahn, R. A., Bak, S., Svendsen, I., Halkier, B. A., Møller, B. L., 1997. Isolation and reconstitution of cytochrome P450ox and in vitro reconstitution of the entire biosynthetic pathway of the cyanogenic glucoside dhurrin from *Sorghum*. Plant Physiology 115, 1661-1670.

Kahn, R. A., Fahrendorf, T., Halkier, B. A., Møller, B. L., 1999. Substrate specificity of the cytochrome P450 enzymes CYP79A1 and CYP71E1 involved in the biosynthesis of the cyanogenic glucoside dhurrin in *Sorghum bicolor* (L.) Moench. Archives of Biochemistry and Biophysics 363, 9-18.

Kakeya, H., Takahashi-Ando, N., Kimura, M., Onose, R., Yamaguchi, I., Osada, H., 2002. Biotransformation of the mycotoxin, zearalenone, to a non-estrogenic compound by a fungal strain of *Clonostachys* sp. Bioscience, Biotechnology and Biochemistry 66, 2723-2726.

Kamimura, H., 1986. Conversion of zearalenone to zearalenone glycoside by *Rhizopus* sp. Applied and Environmental Microbiology 52, 515-519.

Karlovsky, P., 1999. Biological detoxification of fungal toxins and its use in plant breeding, feed and food production. Natural Toxins 7, 1-23.

Kato, Y., Asano, Y., 2003. High-level expression of a novel FMN-dependent heme-containing lyase, phenylacetaldoxime dehydratase of *Bacillus* sp. strain OXB-1, in heterologous hosts. Protein Expression and Purification 28, 131-139.

Kato, Y., Asano, Y., 2005. Purification and characterization of aldoxime dehydratase of the head blight fungus, *Fusarium graminearum*. Bioscience Biotechnology and Biochemistry 69, 2254-2257.

Kato, Y., Asano, Y., 2006. Molecular and enzymatic analysis of the "aldoxime-nitrile pathway" in the glutaronitrile degrader *Pseudomonas* sp K-9. Applied Microbiology and Biotechnology 70, 92-101.

Kato, Y., Nakamura, K., Sakiyama, H., Mayhew, S. G., Asano, Y., 2000. Novel heme-containing lyase, phenylacetaldoxime dehydratase from *Bacillus* sp, strain OxB-1: Purification, characterization, and molecular cloning of the gene. Biochemistry 39, 800-809.

Kato, Y., Ooi, R., Asano, Y., 1998. Isolation and characterization of a bacterium possessing a novel aldoxime-dehydration activity and nitrile-degrading enzymes. Archives of Microbiology 170, 85-90.

Kato, Y., Ooi, R., Asano, Y., 1999. A new enzymatic method of nitrile synthesis by *Rhodococcus* sp. strain yh3-3. Journal of Molecular Catalysis B: Enzymatic 6, 249-256.

Kato, Y., Ooi, R., Asano, Y., 2000. Distribution of aldoxime dehydratase in microorganisms. Applied and Environmental Microbiology 66, 2290-2296.

Kato, Y., Yoshida, S., Xie, S. X., Asano, Y., 2004. Aldoxime dehydratase co-existing with nitrile hydratase and amidase in the iron-type nitrile hydratase-producer *Rhodococcus* sp. N-771. Journal of Bioscience and Bioengineering 97, 250-259.

Kawakishi, S., Muramatsu, K., 1966. Studies on the decomposition of sinalbin. Part i. The decomposition products of sinalbin. Agricultural and Biological Chemistry 30, 688-692.

Kawakishi, S., Namiki, M., Watanabe, H., Muramatsu, K., 1967. Studies on the decomposition of sinalbin. Part ii. The decomposition products of sinalbin and their degradation pathways. Agricultural and Biological Chemistry 31, 823-830.

Kimura, M., Kaneko, I., Komiyama, M., Takatsuki, A., Koshino, H., Yoneyama, K., Yamaguchi, I., 1998. Trichothecene 3-*O*-acetyltransferase protects both the producing organism and transformed yeast from related mycotoxins - cloning and characterization of *tri101*. Journal of Biological Chemistry 273, 1654-1661.

King, R. R., Calhoun, L. A., 2009. The thaxtomin phytotoxins: Sources, synthesis, biosynthesis, biotransformation and biological activity. Phytochemistry 70, 833-841.

King, R. R., Lawrence, C. H., 1996. Characterization of new thaxtomin A analogues generated in vitro by *Streptomyces scabies*. Journal of Agriculture and Food Chemistry 44, 1108-1110.

King, R. R., Lawrence, C. H., Calhoun, L. A., 1992. Chemistry of phytotoxins associated with *Streptomyces scabies*, the causal organism of potato common scab. Journal of Agriculture and Food Chemistry 40, 834-837.

King, R. R., Lawrence, C. H., Calhoun, L. A., 2000. Microbial glucosylation of thaxtomin A, a partial detoxification. Journal of Agriculture and Food Chemistry 48, 512-514.

King, R. R., Lawrence, C. H., Calhoun, L. A., Ristaino, J. B., 1994. Isolation and characterization of thaxtomin-type phytotoxins associated with *Streptomyces ipomoeae*. Journal of Agriculture and Food Chemistry 42, 1791-1794.

King, R. R., Lawrence, C. H., Clark, M. C., Calhoun, L. A., 1989. Isolation and characterization of phytotoxins associated with *Streptomyces scabies*. Journal of the Chemical Society-Chemical Communications 849-850.

Kobayashi, K., Pal, B., Yoshioka, S., Kato, Y., Asano, Y., Kitagawa, T., Aono, S., 2006. Spectroscopic and substrate binding properties of heme-containing aldoxime dehydratases, OxdB and OxdRE. Journal of Inorganic Biochemistry 100, 1069-1074.

Kobayashi, K., Yoshioka, S., Kato, Y., Asano, Y., Aono, S., 2005. Regulation of aldoxime dehydratase activity by redox-dependent change in the coordination structure of the aldoxime-heme complex. Journal of Biological Chemistry 280, 5486-5490.

Konishi, K., Ishida, K., Oinuma, K., Ohta, T., Hashimoto, Y., Higashibata, H., Kitagawa, T., Kobayashi, M., 2004. Identification of crucial histidines involved in carbon-nitrogen triple bond synthesis by aldoxime dehydratase. Journal of Biological Chemistry 279, 47619-47625.

Konishi, K., Ohta, T., Oinuma, K., Hashimoto, Y., Kitagawa, T., Kobayashi, M., 2006. Discovery of a reaction intermediate of aliphatic aldoxime dehydratase involving heme as

an active center. Proceedings of the National Academy of Sciences of the United States of America 103, 564-568.

Kumar, S. A., Mahadevan, S., 1963. 3-Indoleacetaldoxime hydro-lyase - a pyridoxal-5'-phosphate activated enzyme. Archives of Biochemistry and Biophysics 103, 516-518.

Langevin, F., Eudes, F., Comeau, A., 2004. Effect of trichothecenes produced by *Fusarium graminearum* during Fusarium head blight development in six cereal species. European Journal of Plant Pathology 110, 735-746.

Lawrence, C. H., Clark, M. C., King, R. R., 1990. Induction of common scab symptoms in aseptically cultured potato tubers by the vivotoxin, thaxtomin. Phytopathology 80, 606-608.

Lazarovits, G., Hill, J., King, R. R., Calhoun, L. A., 2004. Biotransformation of the *Streptomyces scabies* phytotoxin thaxtomin A by the fungus *Aspergillus niger*. Canadian Journal of Microbiology 50, 121-126.

Legrand, V., Dalmayrac, S., Latché, A., Pech, J. C., Bouzayen, M., Fallot, J., Torregrosa, L., Bouquet, A., Roustan, J. P., 2003. Constitutive expression of *Vr-ERE* gene in transformed grapevines confers enhanced resistance to eutypine, a toxin from *Eutypa lata*. Plant Science 164, 809-814.

Lemmens, M., Scholz, U., Berthiller, F., Dall'Asta, C., Koutnik, A., Schuhmacher, R., Adam, G., Buerstmayr, H., Mesterházy, A., Krska, R., Ruckenbauer, P., 2005. The ability to detoxify the mycotoxin deoxynivalenol colocalizes with a major quantitative trait locus for Fusarium head blight resistance in wheat. Molecular Plant-Microbe Interactions 18, 1318-1324.

Liao, R. Z., Thiel, W., 2012. Why is the oxidation state of iron crucial for the activity of heme-dependent aldoxime dehydratase? A QM/MM study. The Journal of Physical Chemistry B 116, 9396-9408.

Lin, F. Y., Lu, Q. X., Xu, J. H., Shi, J. R., 2008. Cloning and expression analysis of two salt and *Fusarium graminearum* stress associated UDP-glucosyltransferases genes in wheat. Yi Chuan 30, 1608-1614.

Loria, R., Bukhalid, R. A., Creath, R. A., Leiner, R. H., Olivier, M., Steffens, J. C., 1995. Differential production of thaxtomins by pathogenic *Streptomyces* species in vitro. Phytopathology 85, 537-541.

Lu, Y., Sun, X., Ji, S. Y., Wang, J. F., Huang, Y. J., Zhao, Y. F., Xu, P. X., 2007. Application of (^{31}P) NMR in analyzing the degradation efficiency of organic phosphorus degrading-bacteria. Environmental Monitoring and Assessment 130, 281-287.

Ludwig-Müller, J., Hilgenberg, W., 1988. A plasma membrane-bound enzyme oxidizes L-tryptophan to indole-3-acetaldoxime. Physiologia Plantarum 74, 240-250.

Ludwig-Müller, J., Hilgenberg, W., 1990. Conversion of indole-3-acetaldoxime to indole-3-acetonitrile by plasma-membranes from Chinese-cabbage. Physiologia Plantarum 79, 311-318.

Lykkesfeldt, J., Møller, B. L., 1993. Synthesis of benzylglucosinolate in *Tropaeolum majus* L. (isothiocyanates as potent enzyme-inhibitors). Plant Physiology 102, 609-613.

Mahadevan, S., 1963. Conversion of 3-indoleacetaldoxime to 3-indoleacetonitrile by plants. Archives of Biochemistry and Biophysics 100, 557- 558.

Mahuku, G. S., Goodwin, P. H., Hall, R., Hsiang, T., 1997. Variability in the highly virulent type of *Leptosphaeria maculans* within and between oilseed rape fields. Canadian Journal of Botany 75, 1485-1492.

Mansfield, J. W., Bailey, J. A., 1982. In phytoalexins, John Wiley, New York, 319-323.

Maor, R., Shirasu, K., 2005. The arms race continues: Battle strategies between plants and fungal pathogens. Current Opinion in Microbiology 8, 399-404.

Mathews, J. M., Black, S. R., Burka, L. T., 1998. Disposition of butanal oxime in rat following oral, intravenous and dermal administration. Xenobiotica 28, 767-777.

Meeley, R. B., Johal, G. S., Briggs, S. P., Walton, J. D., 1992. A biochemical phenotype for a disease resistance gene of maize. Plant Cell 4, 71-77.

Meeley, R. B., Walton, J. D., 1991. Enzymatic detoxification of HC-toxin, the host-selective cyclic peptide from *Cochliobolus carbonum*. Plant Physiology 97, 1080-1086.

Mikkelsen, M. D., Hansen, C. H., Wittstock, U., Halkier, B. A., 2000. Cytochrome P450 CYP79B2 from *Arabidopsis* catalyzes the conversion of tryptophan to indole-3-acetaldoxime, a precursor of indole glucosinolates and indole-3-acetic acid. Journal of Biological Chemistry 275, 33712-33717.

Möbius, N., Hertweck, C., 2009. Fungal phytotoxins as mediators of virulence. Current Opinion in Plant Biology 12, 390-398.

Monde, K., Takasugi, M., 1991. Studies on stress metabolites .14. Biosynthesis of cruciferous phytoalexins - the involvement of a molecular rearrangement in the biosynthesis of brassinin. Journal of the Chemical Society-Chemical Communications 1582-1583.

Morais, R. P., Lira, S. P., Seleghim, M. H. R., Berlinck, R. G. S., 2010. A method for destruxin analysis by HPLC-PDA-ELSD-MS. Journal of the Brazilian Chemical Society 21, 2262-2271.

Morant, A. V., Jørgensen, K., Jørgensen, C., Paquette, S. M., Sánchez-Pérez, R., Møller, B. L., Bak, S., 2008. β-glucosidases as detonators of plant chemical defense. Phytochemistry 69, 1795-1813.

Muhitch, M. J., McCormick, S. P., Alexander, N. J., Hohn, T. M., 2000. Transgenic expression of the *TRI*101 or *PDR*5 gene increases resistance of tobacco to the phytotoxic effects of the trichothecene 4,15-diacetoxyscirpenol. Plant Science 157, 201-207.

Műller, K., Bőrger, H., 1940. Experimentelle untersuchungen über die phytophthora resistenz der kartoffel. Arbeiten aus der Biologischen Reichsasnstalt Land Forstwirtsch 23, 189 - 231.

Multani, D. S., Meeley, R. B., Paterson, A. H., Gray, J., Briggs, S. P., Johal, G. S., 1998. Plant-pathogen microevolution: Molecular basis for the origin of a fungal disease in maize. Proceedings of the National Academy of Sciences of the United States of America 95, 1686-1691.

Nafisi, M., Goregaoker, S., Botanga, C. J., Glawischnig, E., Olsen, C. E., Halkier, B. A., Glazebrook, J., 2007. *Arabidopsis* cytochrome P450 monooxygenase 71A13 catalyzes the conversion of indole-3-acetaldoxime in camalexin synthesis. Plant Cell 19, 2039-2052.

Ngoka, L. C. M., Gross, M. L., 1999. Multistep tandem mass spectrometry for sequencing cyclic peptides in an ion-trap mass spectrometer. Journal of the American Society for Mass Spectrometry 10, 732-746.

Ohsato, S., Ochiai-Fukuda, T., Nishiuchi, T., Takahashi-Ando, N., Koizumi, S., Hamamoto, H., Kudo, T., Yamaguchi, I., Kimura, M., 2007. Transgenic rice plants expressing trichothecene 3-*O*-acetyltransferase show resistance to the *Fusarium* phytotoxin deoxynivalenol. Plant Cell Reports 26, 531-538.

Oinuma, K. I., Hashimoto, Y., Konishi, K., Goda, M., Noguchi, T., Higashibata, H., Kobayashi, M., 2003. Novel aldoxime dehydratase involved in carbon-nitrogen triple bond synthesis of *Pseudomonas chlororaphis* B23 - sequencing, gene expression, purification, and characterization. Journal of Biological Chemistry 278, 29600-29608.

Oinuma, K. I., Kumita, H., Ohta, T., Konishi, K., Hashimoto, Y., Higashibata, H., Kitagawa, T., Shiro, Y., Kobayashi, M., 2005. Stopped-flow spectrophotometric and resonance Raman analyses of aldoxime dehydratase involved in carbon-nitrogen triple bond synthesis. FEBS Letters 579, 1394-1398.

Oinuma, K., Ohta, T., Konishi, K., Hashimoto, Y., Higashibata, H., Kitagawa, T., Kobayashi, M., 2004. Heme environment in aldoxime dehydratase involved in carbon-nitrogen triple bond synthesis. FEBS Letters 568, 44-48.

Osbourn, A. E., 1996. Preformed antimicrobial compounds and plant defense against fungal attack. Plant Cell 8, 1821-1831.

Osbourn, A. E., Clarke, B. R., Lunness, P., Scott, P. R., Daniels, M. J., 1994. An oat species lacking avenacin is susceptible to infection by *Gaeumannomyces graminis* var tritici. Physiological and Molecular Plant Pathology 45, 457-467.

Pan, X. L., Cui, F. C., Liu, W., Liu, J. Y., 2012. QM/MM study on the catalytic mechanism of heme-containing aliphatic aldoxime dehydratase. The Journal of Physical Chemistry B.

Pan, Z. Z., Raftery, D., 2007. Comparing and combining NMR spectroscopy and mass spectrometry in metabolomics. Analytical and Bioanalytical Chemistry 387, 525-527.

Panaccione, D. G., Scott-Craig, J. S., Pocard, J. A., Walton, J. D., 1992. A cyclic peptide synthetase gene required for pathogenicity of the fungus *Cochliobolus carbonum* on maize. Proceedings of the National Academy of Sciences of the United States of America 89, 6590-6594.

Parada, R. Y., Oka, K., Yamagishi, D., Kodama, M., Otani, H., 2007. Destruxin B produced by *Alternaria brassicae* does not induce accessibility of host plants to fungal invasion. Physiological and Molecular Plant Pathology 71, 48–54.

Parada, R. Y., Sakuno, E., Mori, N., Oka, K., Egusa, M., Kodama, M. and Otani, H., 2008. *Alternaria brassicae* produces a host-specific protein toxin from germinating spores on host leaves. Phytopathology 98, 458-63.

Parry, D. W., Jenkinson, P., Mcleod, L., 1995. Fusarium ear blight (scab) in small-grain cereals - a review. Plant Pathology 44, 207-238.

Pedras, M. S. C., 1996. The chemistry of cyclohexenediones produced by the blackleg fungus. Canadian Journal of Chemistry 74, 1597-1601.

Pedras, M. S. C., Abrams, S. R., Séguin-Swartz, G., 1988. Isolation of the first naturally-occurring epimonothiodioxopiperazine, a fungal toxin produced by *phoma lingam*. Tetrahedron Letters 29, 3471-3474.

Pedras, M. S. C., Adio, A. M., 2008. Phytoalexins and phytoanticipins from the wild crucifers *Thellungiella halophila* and *Arabidopsis thaliana*: Rapalexin A, wasalexins and camalexin. Phytochemistry 69, 889-893.

Pedras, M. S. C., Ahiahonu, P. W. K., 2004. Phytotoxin production and phytoalexin elicitation by the phytopathogenic fungus *Sclerotinia sclerotiorum*. Journal of Chemical Ecology 30, 2163-2179.

Pedras, M. S. C., Ahiahonu, P. W. K., 2005. Metabolism and detoxification of phytoalexins and analogs by phytopathogenic fungi. Phytochemistry 66, 391-411.

Pedras, M. S. C., Biesenthal, C. J, 2000. Vital staining of plant cell suspension cultures: evaluation of the phytotoxic activity of the phytotoxins phomalide and destruxin B. Plant Cell Reports 19:1135–1138.

Pedras, M. S. C., Biesenthal, C. J., 1998. Production of the host-selective phytotoxin phomalide by isolates of *Leptosphaeria maculans* and its correlation with sirodesmin PL production. Canadian Journal of Microbiology 44, 547-553.

Pedras, M. S. C., Biesenthal, C. J., 2000. HPLC analyses of cultures of *phoma* spp.: Differentiation among groups and species through secondary metabolite profiles. Canadian Journal of Microbiology 46, 685-691.

Pedras, M. S. C., Biesenthal, C. J., 2001. Isolation, structure determination, and phytotoxicity of unusual dioxopiperazines from the phytopathogenic fungus *Phoma lingam*. Phytochemistry 58, 905-909.

Pedras, M. S. C., Biesenthal, C. J., Zaharia, I. L., 2000. Comparison of the phytotoxic activity of the phytotoxin destruxin B and four natural analogs. Plant Science 156, 185-192.

Pedras, M. S. C., Chumala, P. B., 2005. Phomapyrones from blackleg causing phytopathogenic fungi: Isolation, structure determination, biosyntheses and biological activity. Phytochemistry 66, 81-87.

Pedras, M. S. C., Chumala, P. B., 2011. Maculansins, cryptic phytotoxins from blackleg fungi. Natural Product Communications 6, 617-620.

Pedras, M. S. C., Chumala, P. B., Quail, J. W., 2004. Chemical mediators: The remarkable structure and host-selectivity of depsilairdin, a sesquiterpenic depsipeptide containing a new amino acid. Organic Letters 6, 4615-4617.

Pedras, M. S. C., Chumala, P. B., Venkatesham, U., 2005. New sesquiterpenic phytotoxins establish unprecedented relationship between different groups of blackleg fungal isolates. Bioorganic and Medicinal Chemistry 13, 2469-2475.

Pedras, M. S. C., Erosa-López, C. C., Quail, J. W., Taylor, J. L., 1999. Phomalairdenone: A new host-selective phytotoxin from a virulent type of the blackleg fungus *Phoma lingam*. Bioorganic and Medicinal Chemistry Letters 9, 3291-3294.

Pedras, M. S. C., Khallaf, I., 2012. Molecular interactions of the phytotoxins destruxin B and sirodesmin PL with crucifers and cereals: Metabolism and elicitation of plant defenses. Phytochemistry 77, 129-139.

Pedras, M. S. C., Minic, Z., Thongbam, P. D., Bhaskar, V., Montaut, S., 2010. Indolyl-3-acetaldoxime dehydratase from the phytopathogenic fungus *Sclerotinia sclerotiorum*: Purification, characterization, and substrate specificity. Phytochemistry 71, 1952-1962.

Pedras, M. S. C., Montaut, S., 2003. Probing crucial metabolic pathways in fungal pathogens of crucifers: Biotransformation of indole-3-acetaldoxime, 4-hydroxyphenylacetaldoxime, and their metabolites. Bioorganic and Medicinal Chemistry 11, 3115-3120.

Pedras, M. S. C., Montaut, S., Suchy, M., 2004. Phytoalexins from the crucifer rutabaga: Structures, syntheses, biosyntheses, and antifungal activity. Journal of Organic Chemistry 69, 4471-4476.

Pedras, M. S. C., Montaut, S., Xu, Y. M., Khan, A. Q., Loukaci, A., 2001. Assembling the biosynthetic puzzle of crucifer metabolites: Indole-3-acetaldoxime is incorporated efficiently into phytoalexins but glucobrassicin is not. Chemical Communications 1572-1573.

Pedras, M. S. C., Montaut, S., Zaharia, I. L., Gai, Y., Ward, D. E., 2003. Transformation of the host-selective toxin destruxin B by wild crucifers: Probing a detoxification pathway. Phytochemistry 64, 957-963.

Pedras, M. S. C., Morales, V. M., Taylor, J. L., 1993. Phomaligols and phomaligadiones - new metabolites from the blackleg fungus. Tetrahedron 49, 8317-8322.

Pedras, M. S. C., Nycholat, C. M., Montaut, S., Xu, Y. M., Khan, A. Q., 2002. Chemical defenses of crucifers: Elicitation and metabolism of phytoalexins and indole-3-acetonitrile in brown mustard and turnip. Phytochemistry 59, 611-625.

Pedras, M. S. C., Okinyo-Owiti, D. P., Thoms, K., Adio, A. M., 2009. The biosynthetic pathway of crucifer phytoalexins and phytoanticipins: De novo incorporation of deuterated tryptophans and quasi-natural compounds. Phytochemistry 70, 1129-1138.

Pedras, M. S. C., Séguin-Swartz, G., Abrams, S. R., 1990. Minor phytotoxins from the blackleg fungus *Phoma lingam*. Phytochemistry 29, 777-782.

Pedras, M. S. C., Smith, K. C., 1997. Sinalexin, a phytoalexin from white mustard elicited by destruxin B and *Alternaria brassicae*. Phytochemistry 46, 833-837.

Pedras, M. S. C., Smith, K. C., Taylor, J. L., 1998. Production of 2,5-dioxopiperazine by a new isolate type of the blackleg fungus *Phoma lingam*. Phytochemistry 49, 1575-1577.

Pedras, M. S. C., Suchy, M., Ahiahonu, P. W. K., 2006. Unprecedented chemical structure and biomimetic synthesis of erucalexin, a phytoalexin from the wild crucifer *Erucastrum gallicum*. Organic and Biomolecular Chemistry 4, 691-701.

Pedras, M. S. C., Taylor, J. L., 1993a. A novel chemical signal from the “blackleg” fungus: beyond phytotoxins and phytoalexins. Journal of Organic Chemistry 58, 4778-4780.

Pedras, M. S. C., Taylor, J. L., 1993b. Metabolism of the phytoalexin brassinin by the blackleg fungus. Journal of Natural Products 56, 731-738.

Pedras, M. S. C., Taylor, J. L., Morales, V. M. 1995. Phomalingin A and other yellow pigments in *Phoma lingam* and *P. wasabiae*. Phytochemistry 38, 1215-1222.

Pedras, M. S. C., Yaya, E. E., 2013. Dissecting metabolic puzzles through isotope feeding: a novel amino acid in the biosynthetic pathway of the cruciferous phytoalexins rapalexin A and isocyalexin A. Organic and Bimolecular Chemistry 11, 1149-1166

Pedras, M. S. C., Yaya, E. E., Glawischnig, E., 2011. The phytoalexins from cultivated and wild crucifers: Chemistry and biology. Natural Product Reports 28, 1381-1405.

Pedras, M. S. C., Yaya, E. E., Hossain, S., 2010. Unveiling the phytoalexin biosynthetic puzzle in salt cress: Unprecedented incorporation of glucobrassicin into wasalexins A and B. Organic and Biomolecular Chemistry 8, 5150-5158.

Pedras, M. S. C., Yu, Y., 2008a. Stress-driven discovery of metabolites from the phytopathogenic fungus *Leptosphaeria maculans*: Structure and activity of leptomaculins A-E. Bioorganic and Medicinal Chemistry 16, 8063-8071.

Pedras, M. S. C., Yu, Y., 2008b. Structure and biological activity of maculansin A, a phytotoxin from the phytopathogenic fungus *Leptosphaeria maculans*. Phytochemistry 69, 2966-2971.

Pedras, M. S. C., Yu, Y., 2009. Phytotoxins, elicitors and other secondary metabolites from phytopathogenic "blackleg" fungi: Structure, phytotoxicity and biosynthesis. Natural Product Communications 4, 1291-1304.

Pedras, M. S. C., Zaharia, I. L., 2000. Sinalbins A and B, phytoalexins from *Sinapis alba*: Elicitation, isolation, and synthesis. Phytochemistry 55, 213-216.

Pedras, M. S. C., Zaharia, I. L., Gai, Y. Z., Smith, K. C., Ward, D. E., 1999. Metabolism of the host-selective toxins destruxin B and homodestruxin B: Probing a plant disease resistance trait. Organic Letters 1, 1655-1658.

Pedras, M. S. C., Zaharia, I. L., Gai, Y., Zhou, Y., Ward, D. E., 2001. In planta sequential hydroxylation and glycosylation of a fungal phytotoxin: Avoiding cell death and overcoming the fungal invader. Proceedings of the National Academy of Sciences of the United States of America 98, 747-752.

Pedras, M. S. C., Zaharia, L. I., Ward, D. E., 2002. The destruxins: Synthesis, biosynthesis, biotransformation, and biological activity. Phytochemistry 59, 579-596.

Pedras, M. S. C., Zheng, Q. A., Schatte, G., Adio, A. M., 2009. Photochemical dimerization of wasalexins in UV-irradiated *Thellungiella halophila* and in vitro generates unique cruciferous phytoalexins. Phytochemistry 70, 2010-2016.

Pedras, M. S. C., Zheng, Q. A., Strelkov, S., 2008. Metabolic changes in roots of the oilseed canola infected with the biotroph *Plasmodiophora brassicae*: Phytoalexins and phytoanticipins. Journal of Agricultural and Food Chemistry 56, 9949-9961.

Perrin, D.R., Bottomley, W., 1962. Studies on phytoalexins .5. Structure of pisatin from *Pisum sativum* L. Journal of the American Chemical Society 84, 1919-1922.

Plasencia, J., Mirocha, C. J., 1991. Isolation and characterization of zearalenone sulfate produced by *Fusarium* spp. Applied and Environmental Microbiology 57, 146-150.

Poppenberger, B., Berthiller, F., Bachmann, H., Lucyshyn, D., Peterbauer, C., Mitterbauer, R., Schuhmacher, R., Krska, R., Glössl, J., Adam, G., 2006. Heterologous expression of *Arabidopsis* UDP-glucosyltransferases in *Saccharomyces cerevisiae* for production of zearalenone-4-*O*-glucoside. Applied and Environmental Microbiology 72, 4404-4410.

Poppenberger, B., Berthiller, F., Lucyshyn, D., Sieberer, T., Schuhmacher, R., Krska, R., Kuchler, K., Glössl, J., Luschnig, C., Adam, G., 2003. Detoxification of the *Fusarium* mycotoxin deoxynivalenol by a UDP-glucosyltransferase from *Arabidopsis thaliana*. Journal of Biological Chemistry 278, 47905-47914.

Proctor, R. H., Hohn, T. M., McCormick, S. P., 1995. Reduced virulence of *Gibberella zeae* caused by disruption of a trichothecene toxin biosynthetic gene. Molecular Plant-Microbe Interactions 8, 593-601.

Rajagopa, R., Larsen, P., 1972. Metabolism of indole-3-acetaldoxime in plants. Planta 103, 45-54.

Ramón, R. S., Bosson, J., Deíz-González, S., Marion, N., Nolan, S. P., 2010. Au/Ag-Cocatalyzed aldoximes to amides rearrangement under solvent- and acid-free conditions. Journal of Organic Chemistry 75, 1197–1202.

Richardson, K. E., Hagler, W. M., Mirocha, C. J., 1985. Production of zearalenone, α-zearalenol and β-zearalenol, and α-zearalenol and β-zearalanol by *Fusarium* spp in rice culture. Journal of Agriculture and Food Chemistry 33, 862-866.

Rocha, O., Ansari, K., Doohan, F. M., 2005. Effects of trichothecene mycotoxins on eukaryotic cells: A review. Food Additives and Contaminants 22, 369-378.

Rosenthal, G. A., Berge, M. A., Bleiler, J. A., 1989. A novel mechanism for detoxification of L-canaline. Biochemical Systematics and Ecology 17, 203-206.

Saharan, G. S., in Breeding Oilseed Brassicas, ed. K. S. Labana, S. S. Banga, and S. K. Banga. Springer, Berlin, 1993, p. 181.

Sawai, H., Sugimoto, H., Kato, Y., Asano, Y., Shiro, Y., Aono, S., 2009. X-ray crystal structure of Michaelis complex of aldoxime dehydratase. Journal of Biological Chemistry 284, 32089-32096.

Scalbert, A., Brennan, L., Fiehn, O., Hankemeier, T., Kristal, B. S., Ommen, B.V., Pujos-Guillot, E., Verheij, E., Wishart, D., Wopereis, S., 2009. Mass-spectrometry-based metabolomics: Limitations and recommendations for future progress with particular focus on nutrition research. Metabolomics 5, 435-458.

Schäfer, W., 1994. Molecular mechanisms of fungal pathogenicity to plants. Annual Review of Phytopathology 32, 461-477.

Schäfer, W., Straney, D., Ciuffetti, L., Van Etten, H. D., Yoder, O. C., 1989. One enzyme makes a fungal pathogen, but not a saprophyte, virulent on a new host plant. Science 246, 247-249.

Scheffer, R. P., Nelson, R. R., Ullstrup, A. J., 1967. Inheritance of toxin production and pathogenicity in *Cochliobolus carbonum* and *Cochliobolus victoriae*. Phytopathology 57, 1288-1293.

Scheffer, R. P., Ullstrup, A. J., 1965. A host-specific toxic metabolite from *Helminthosporium carbonum*. Phytopathology 55, 1037-1038.

Scheible, W. R., Fry, B., Kochevenko, A., Schindelasch, D., Zimmerli, L., Somerville, S., Loria, R., Somerville, C. R., 2003. An *Arabidopsis* mutant resistant to thaxtomin A, a cellulose synthesis inhibitor from *Streptomyces* species. Plant Cell 15, 1781-1794.

Schlaich, N. L., 2007. Flavin-containing monooxygenases in plants: Looking beyond detox. Trends in Plant Science 12, 412-418.

Schmidt, T. J., Alfermann, A. W., Fuss, E., 2008. High-performance liquid chromatography/mass spectrometric identification of dibenzylbutyrolactone-type lignans: Insights into electrospray ionization tandem mass spectrometric fragmentation of lign-7-eno-9,9'-lactones and application to the lignans of *Linum usitatissimum* (L.) (Common flax). Rapid Communications in Mass Spectrometry 22, 3642-3650.

Schweiger, W; Berthiller, F; Fischer, A; Erhart, C; Bicker, W; Shams, M; Schuhmacher, R; Krska, R; Wiesenberger, G; Mitterbauer, R; Glatt, H; Adam, G. 2008: Formation of zearalenone-4-sulfate by yeast cells expressing sulfotransferase genes.Cereal Research Communications 36, 385-389.

Seger, C., Sturm, S., Stuppner, H., Butt, T. M., Strasser, H., 2004. Combination of a new sample preparation strategy with an accelerated high-performance liquid chromatography assay with photodiode array and mass spectrometric detection for the determination of destruxins from *Metarhizium anisopliae* culture broth. Journal of Chromatography A 1061, 35-43.

Sewald, N., von Gleissenthall, J. L., Schuster, M., Müller, G., Aplin, R. T., 1992. Structure elucidation of a plant metabolite of 4-desoxynivalenol. Tetrahedron-Asymmetry 3, 953-960.

Shima, J., Takase, S., Takahashi, Y., Iwai, Y., Fujimoto, H., Yamazaki, M., Ochi, K., 1997. Novel detoxification of the trichothecene mycotoxin deoxynivalenol by a soil bacterium isolated by enrichment culture. Applied and Environmental Microbiology 63, 3825-3830.

Shivanna, K. R. and Sawhney, V. K, 1993. Pollen selection for *Alternaria* resistance in oilseed brassicas: responses of pollen grains and leaves to a toxin of *A. brassicae*. Theoretical and Applied Genetics 86:339-344

Shukla, P. S., Mahadevan, S., 1968. Indoleacetaldoxime hydro-lyase. II. Purification and properties. Archives of Biochemistry and Biophysics 125, 873-883.

Shukla, P. S., Mahadevan, S., 1970. Indoleacetaldoxime hydro-lyase (4.2.1.29). 3. Further studies on the nature and mode of action of the enzyme. Archives of Biochemistry and Biophysics 137, 166-174.

Stark-Lorenzen, P., Nelke, B., Hänbler, G., Mühlbach, H. P., Thomzik, J. E., 1997. Transfer of a grapevine stilbene synthase gene to rice (*Oryza sativa* L). Plant Cell Reports 16, 668-673.

Strange, R. N., 2007. Phytotoxins produced by microbial plant pathogens. Natural Product Reports 24, 127-144.

Strobel, G. A., 1982. Phytotoxins. Annual Review of Biochemistry 51, 309-333.

Sugawara, S., Hishiyama, S., Jikumaru, Y., Hanada, A., Nishimura, T., Koshiba, T., Zhao, Y., Kamiya, Y., Kasahara, H., 2009. Biochemical analyses of indole-3-acetaldoxime-dependent auxin biosynthesis in *Arabidopsis*. Proceedings of the National Academy of Sciences of the United States of America 106, 5430-5435.

Takabayashi, J., Dicke, M., Maarten, A., Posthumus, A., 1991. Variation in composition of predator- attracting herbivore-infested plants: Relative influence of plant and herbivore. Chemoecology 2, 1-6.

Takabayashi, J., Dicke, M., Takahashi, S., Posthumus, M. A., Van Beek, T. A., 1994. Leaf age affects composition of herbivore-induced synomones and attraction of predatory mites. Journal of Chemical Ecology 20, 373-386.

Takahashi-Ando, N., Kimura, M., Kakeya, H., Osada, H., Yamaguchi, I., 2002. A novel lactonohydrolase responsible for the detoxification of zearalenone: Enzyme purification and gene cloning. Biochemical Journal 365, 1-6.

Takahashi-Ando, N., Ohsato, S., Shibata, T., Hamamoto, H., Yamaguchi, I., Kimura, M., 2004. Metabolism of zearalenone by genetically modified organisms expressing the detoxification gene from *Clonostachys rosea*. Applied and Environmental Microbiology 70, 3239-3245.

Takahashi-Ando, N., Tokai, T., Hamamoto, H., Yamaguchi, I., Kimura, M., 2005. Efficient decontamination of zearalenone, the mycotoxin of cereal pathogen, by transgenic yeasts through the expression of a synthetic lactonohydrolase gene. Applied Microbiology and Biotechnology 67, 838-844.

Tang, C. S., 1974. Benzyl isothiocyanate as a naturally occurring papain inhibitor. Journal of Food Science 39, 94-96.

Tey-Rulh, P., Philippe, I., Renaud, J. M., Tsoupras, G., De Angelis, P., Fallot, J., Tabacchi, R., 1991. Eutypine, a phytotoxin produced by *Eutypa lata* the causal agent of dying-arm disease of grapevine. Phytochemistry 30, 471-473.

Thomzik, J. E., Stenzel, K., Stocker, R., Schreier, P. H., Hain, R., Stahl, D. J., 1997. Synthesis of a grapevine phytoalexin in transgenic tomatoes (*Lycopersicon esculentum* Mill.) conditions resistance against *Phytophthora infestans*. Physiological and Molecular Plant Pathology 51, 265-278.

Tront, J. M., Saunders, F. M., 2007. Sequestration of a fluorinated analog of 2,4-dichlorophenol and metabolic products by l. Minor as evidenced by ^{19}F NMR. Environmental Pollution 145, 708-714.

Tsuji, J., Jackson, E. P., Gage, D. A., Hammerschmidt, R., Somerville, S. C., 1992. Phytoalexin accumulation in *Arabidopsis thaliana* during the hypersensitive reaction to *Pseudomonas syringae* pv *syringae*. Plant Physiology 98, 1304-1309.

Urban, M., Daniels, S., Mott, E., Hammond-Kosack, K., 2002. *Arabidopsis* is susceptible to the cereal ear blight fungal pathogens *Fusarium graminearum* and *Fusarium culmorum*. Plant Journal 32, 961-973.

Van Etten, H. D., Mansfield, J. W., Bailey, J. A., Farmer, E. E., 1994. 2 classes of plant antibiotics - phytoalexins versus phytoanticipins. Plant Cell 6, 1191-1192.

Van Etten, H. D., Matthews, D. E., Matthews, P. S., 1989. Phytoalexin detoxification - importance for pathogenicity and practical implications. Annual Review of Phytopathology 27, 143-164.

Van Etten, H. D., Pueppke, S. G., Kelsey, T. C., 1975. 3,6a-dihydroxy-8,9-methylenedioxypterocarpan as a metabolite of pisatin produced by *Fusarium solani* f. sp. *pisi*. Phytochemistry 14, 1103-1105.

VanEtten, H. D., Sandrock, R. W., Wasmann, C. C., Soby, S. D., McCluskey, K., Wang, P., 1995. Detoxification of phytoanticipins and phytoalexins by phytopathogenic fungi. Canadian Journal of Botany-Revue Canadienne De Botanique 73, S518-S525.

VanEtten, H. D., Straney, D. C., Covert, S. F., Kistler, H. C., Corby, H. 2001. The genetics of *Nectria haematococca* mating population VI with special emphasis on its conditionally dispensable (cd) chromosomes: A source of habitat specific genes. Fusarium: Paul E. Nelson Memorial Symposium 97-112.

Vig, A. P., Rampal, G., Thind, T. S., Arora, S., 2009. Bio-protective effects of glucosinolates - A review. LWT-Food Science and Technology 42, 1561-1572.

Völkl, A., Vogler, B., Schollenberger, M., Karlovsky, P., 2004. Microbial detoxification of mycotoxin deoxynivalenol. Journal of Basic Microbiology 44, 147-156.

Walker, M. J., Birch, R. G., Pemberton, J. M., 1988. Cloning and characterization of an albicidin resistance gene from *Klebsiella oxytoca*. Molecular Microbiology 2, 443-454.

Walton, J. D., 1987. 2 enzymes involved in biosynthesis of the host-selective phytotoxin HC-toxin. Proceedings of the National Academy of Sciences of the United States of America 84, 8444-8447.

Walton, J. D., 2006. HC-toxin. Phytochemistry 67, 1406-1413.

Walton, J. D., Earle, E. D., 1983. The epoxide in HC-toxin is required for activity against susceptible maize. Physiological Plant Pathology 22, 371-376.

Walton, J. D., Panaccione, D. G., 1993. Host-selective toxins and disease specificity - perspectives and progress. Annual Review of Phytopathology 31, 275-303.

Wang, D. W., Liu, Z. Q., Guo, M. Q., Liu, S. Y., 2004. Structural elucidation and identification of alkaloids in *Rhizoma coptidis* by electrospray ionization tandem mass spectrometry. Journal of Mass Spectrometry 39, 1356-1365.

Wang, Y. Z., Miller, J. D., 1988. Effects of *Fusarium graminearum* metabolites on wheat tissue in relation to Fusarium head blight resistance. Journal of Phytopathology 122, 118-125.

Wasmann, C. C., VanEtten, H. D., 1996. Transformation-mediated chromosome loss and disruption of a gene for pisatin demethylase decrease the virulence of *Nectria haematococca* on pea. Molecular Plant-Microbe Interactions 9, 793-803.

Williams, R. H., Fitt, B. D. L., 1999. Differentiating A and B groups of *Leptosphaeria maculans*, causal agent of stem canker (blackleg) of oilseed rape. Plant Pathology 48, 161-175.

Wittstock, U., Halkier, B. A., 2000. Cytochrome P450 CYP79A2 from *Arabidopsis thaliana* L. catalyzes the conversion of L-phenylalanine to phenylacetaldoxime in the biosynthesis of benzylglucosinolate. Journal of Biological Chemistry 275, 14659-14666.

Xie, S. X., Kato, Y., Asano, Y., 2001. High yield synthesis of nitriles by a new enzyme, phenylacetaldoxime dehydratase, from *Bacillus* sp strain OxB-1. Bioscience Biotechnology and Biochemistry 65, 2666-2672.

Xie, S. X., Kato, Y., Komeda, H., Yoshida, S., Asano, Y., 2003. A gene cluster responsible for alkylaldoxime metabolism coexisting with nitrile hydratase and amidase in *Rhodococcus globerulus* A-4. Biochemistry 42, 12056-12066.

Young, M. R., Towers, G. H. N., Neish, A. C., 1966. Taxonomic distribution of ammonia-lyases for L-phenylalanine and L-tyrosine in relation to lignification. Canadian Journal of Botany 44, 341-349.

Zaharia, L. R., 2001. Alternaria blackspot phytotoxins: biotransformation and phytoalexin elicitation. Ph.D. thesis, University of Saskatchewan.

Zhang, L. H., Birch, R. G., 1997a. Mechanisms of biocontrol by *Pantoea dispersa* of sugar cane leaf scald disease caused by *Xanthomonas albilineans*. Journal of Applied Microbiology 82, 448-454.

Zhang, L. H., Birch, R. G., 1997b. The gene for albicidin detoxification from *Pantoea dispersa* encodes an esterase and attenuates pathogenicity of *Xanthomonas albilineans* to sugarcane. Proceedings of the National Academy of Sciences of the United States of America 94, 9984-9989.

Zhang, L. H., Xu, J. L., Birch, R. G., 1999. Engineered detoxification confers resistance against a pathogenic bacterium. Nature Biotechnology 17, 1021-1024.

Zhang, L. H., Birch, R. G., 1996. Biocontrol of sugar cane leaf scald disease by an isolate of *Pantoea dispersa* which detoxifies albicidin phytotoxins. Letters in Applied Microbiology 22, 132-136.

Zinedine, A., Soriano, J. M., Molto, J. C., Manes, J., 2007. Review on the toxicity, occurrence, metabolism, detoxification, regulations and intake of zearalenone: An oestrogenic mycotoxin. Food and Chemical Toxicology 45, 1-18.